

8-2021

IDENTIFICATION AND TARGETING OF DOWNSTREAM AR-CAMKK2-MEDIATED MECHANISMS FOR THE TREATMENT OF ADVANCED PROSTATE CANCER

Chenchu Lin

Follow this and additional works at: https://digitalcommons.library.tmc.edu/utgsbs_dissertations



Part of the [Medicine and Health Sciences Commons](#)

Recommended Citation

Lin, Chenchu, "IDENTIFICATION AND TARGETING OF DOWNSTREAM AR-CAMKK2-MEDIATED MECHANISMS FOR THE TREATMENT OF ADVANCED PROSTATE CANCER" (2021). *The University of Texas MD Anderson Cancer Center UTHealth Graduate School of Biomedical Sciences Dissertations and Theses (Open Access)*. 1130.

https://digitalcommons.library.tmc.edu/utgsbs_dissertations/1130

This Dissertation (PhD) is brought to you for free and open access by the The University of Texas MD Anderson Cancer Center UTHealth Graduate School of Biomedical Sciences at DigitalCommons@TMC. It has been accepted for inclusion in The University of Texas MD Anderson Cancer Center UTHealth Graduate School of Biomedical Sciences Dissertations and Theses (Open Access) by an authorized administrator of DigitalCommons@TMC. For more information, please contact digitalcommons@library.tmc.edu.

IDENTIFICATION AND TARGETING OF DOWNSTREAM AR-CAMKK2-MEDIATED
MECHANISMS FOR THE TREATMENT OF ADVANCED PROSTATE CANCER

by
Chenchu Lin, M.S.

APPROVED:

Daniel E. Frigo, Ph.D.
Advisory Professor

Nancy L. Weigel, Ph.D.

William Plunkett, Ph.D.

Jefferey A. Frost, Ph.D.

Shuxing Zhang, Ph.D.

APPROVED:

Dean, The University of Texas
MD Anderson Cancer Center UTHHealth Graduate School of Biomedical Sciences

IDENTIFICATION AND TARGETING OF DOWNSTREAM AR-CAMKK2-MEDIATED
MECHANISMS FOR THE TREATMENT OF ADVANCED PROSTATE CANCER

A

DISSERTATION

Presented to the Faculty of

The University of Texas

MD Anderson Cancer Center UTHealth

Graduate School of Biomedical Sciences

in Partial Fulfillment

of the Requirements

for the Degree of

Doctor of Philosophy

by

Chenchu Lin, M.S.

Houston, Texas

August 2021

Dedication

This dissertation is dedicated to my parents

Yong Lin

and

Dr. Jie Huang

Acknowledgements

First and foremost, I would like to express my deepest gratitude to my mentor Dr. Daniel Frigo, a smart scientist and kind leader. Thank you for incredible supportive of my study during my whole graduate school. Thank you for providing me numerous opportunities to learn new technique, to improve my public speaking and to touch with different projects. Sometimes, research is like an adventure without a map, and you are always the brightest North Star when the darkest night comes to me. Your passion for science, patience for students, and perseverance in overcoming difficulties always encourage me to be a better researcher. I am honored to be one of your students.

I would like to thank all my advisory committees. Thanks to Dr. William Plunkett for your invaluable help and support in science and graduate school. Your support, protection and encourage help me gain the confidence and enjoy a wonderful life in the Therapeutics and Pharmacology Program (TAP) family. I wish to whole-heartedly appreciate Dr. Nancy Weigel. Thank you for serving in my committee from my first committee meeting and contribute to my growth by your positive feedback and incredible support. I am appreciative to have Dr. Jeffrey Frost. Your knowledge and expertise are important to my progression. Thank you Dr. Shuxing Zhang for your support and guidance in both committee and TAP program. Thank you to provide such a knowledgeable and amazing therapeutic course to TAP students. I am truly grateful to Dr. Pratip Bhattacharya for agreeing to serve in my committee and helping me out for my defense in such a short notice. I would also like to thank all past members of my advisory committee: Drs. Geoffrey Bartholomeusz, Shaun Zhang, Gregg Roman, Sanghyuk Chung, Chin-Yo Lin and Yuhong Wang for your advice and encouragement during my graduate education. Especially during the challenging transferring time, thank you Dr. Shaun Zhang to be my co-mentor for one semester and provide me an endless patience and support to deal with the visa issue.

I would like to extend my appreciation to all current and past members of Frigo Lab for daily support, help and impact. I extremely appreciate Jenny Han. Your help has never been absent whenever I need. I would like to thank Drs. Yan Shi, Alicia Blessing, Mollianne Murray, Mark White, Efrosini Tsouko and Mingfei Yan. I have learned so much from you. I also want to thank Sandi Wilkenfeld, Dr. Thomas Pulliam, Dominik Awad, Dr. Elavarasan Subramani and Dr. Paul Viscuse, Alex Pham and Jiaqian Xu. The invaluable scientific discussions and unwavering support in the daily work are essential to my progression.

I am grateful to having all tremendous collaborators. Thanks to Drs. Michael Ittmann and Elizabeth Whitley for helping me with all histological analysis. Thanks to Dr. Nora Navone and Peter Shepherd for providing prostate cancer PDX samples. Thanks to Dr. Wenyi Wang, Carlos C Vera Recio, Feng Zhang and Dr. Jingjing Liu for teaching me the initial concept about big data analysis and the basic knowledge of programming. Thanks to Drs. Reuben J. Shaw and Sonja N. Brun for providing the ULK1 inhibitor and comments for ULK1 manuscript. Thanks to Dr. Seth Gammon for helping with imaging.

I am blessed to have all my friends in the department of Cancer Systems Imaging (CSI) and graduate school, especially Dr. Rao Yi, Dr. Qizhen Cao, Dr. Margie Sutton, Dr. Cong-Dat Pham, Knisha Arthur, Dr. Iman Sahnoune, Sunada Khadka, Mary Figueroa, Lon Fong and Jeffrey Ackroyd. Your generous help means a lot to me. I am so glad to have a friendship with all of you.

I am fortunate to meet all members of The University of Texas Graduate School of Biomedical Sciences, CSI and Department of Biology and Biochemistry (University of Houston), especially Dr. Michelle Barton, Dr. William Mattox, Brenda Gaughan, Dr. Natalie Sirisaengtaksin, Marcia Richards and Rosezelia Jackson. Thank you for helping me out my transferring process and supporting me during my graduate school. Without your help, it would be much more difficult to pursue my PhD.

Finally, I would like to like to express my sincere gratitude to my family. Thanks to my mom, dad and grandmas for unconditional love and support in every stage of my life. Thanks to my parents-in-law for supporting and cares. Thanks to my husband, Dr. Haopeng Yang, for endless love, support and companion in the past 10 years and the future journey of my life. I am indebted to everything that you've done and continue to do for me.

IDENTIFICATION AND TARGETING OF DOWNSTREAM AR-CAMKK2-MEDIATED MECHANISMS FOR THE TREATMENT OF ADVANCED PROSTATE CANCER

Chenchu Lin, M.S.

Advisory Professor: Daniel E. Frigo, Ph.D.

The androgen receptor (AR) is the primary driver of prostate cancer and, therefore, AR-regulated signaling events are essential for the development and progression of the disease. Despite their initial effectiveness, drugs targeting AR eventually fail as sustained inhibition of receptor activity remains a challenge. Previously, Ca²⁺/calmodulin-dependent protein kinase kinase 2 (CAMKK2) was identified as an essential downstream component of AR signaling in prostate cancer that correspondingly tracked with disease progression. While the importance of CAMKK2 in AR-mediated prostate cancer progression has been established, our understanding of the events downstream that promote the disease remains incomplete. Here, I elucidated two AR-CAMKK2-regulated kinase signaling cascades which are hypothesized to promote disease progression and therefore represent alternative therapeutic targets in castration-resistant prostate cancer (CRPC).

First, I identified Unc-51 like autophagy activating kinase 1 (ULK1), an important autophagic initiator, as one of downstream effectors regulated by AR-CAMKK2-5'-AMP-activated protein kinase (AMPK) signaling. CAMKK2-induced protective autophagy is partially dependent on the phosphorylation of ULK1 at serine 555, which is required for prostate cancer cell growth. Accordingly, inhibition of CAMKK2-AMPK-ULK1 signaling by molecular, genetic and/or pharmacological inhibitors decreased autophagy and cell growth in CRPC tumor growth.

Second, I investigated the role of AR-CAMKK2 on the activation of the transcription factor cyclic-AMP response element-binding protein (CREB). Cancer cell-intrinsic CAMKK2 signaling promoted CRPC in part through increasing the activity of CREB. Molecularly, this was shown to occur through the calcium/calmodulin-dependent protein kinase I-mediated phosphorylation of CREB on its serine 133 activation site. I also determined a functional redundancy between two CREB family members, CREB1 and Activating Transcription Factor 1. Deletion of both genes impaired transcriptional activity and maximal prostate cancer cell proliferation in tissue culture and tumor initiation as well as growth in CRPC. Therapeutically, pharmacological targeting of CREB by 666-15 effectively blocked cell cycle and inhibited cell/tumor growth without significant toxicity and was able to decrease the growth of CRPC tumors resistant to second-generation antiandrogens.

Collectively, I have leveraged orthogonal molecular, genetic and pharmacological approaches to delineate how AR-CAMKK2 signaling drives prostate cancer progression and define potential new therapeutic strategies for targeting this oncogenic cascade in CRPC.

Table of Contents

Approval Page.....	i
Title Page.....	ii
Dedication	iii
Acknowledgements	iv
Abstract.....	vii
List of Illustrations	xii
List of Tables.....	xv
Abbreviations	xvi
Chapter 1 Introduction.....	1
1.1 Current treatment to target AR.....	3
1.2 CAMKK2 and its downstream kinases in prostate cancer	7
1.2.1 Structure and regulation of CAMKK2.....	7
1.2.2 CAMKK2 in prostate cancer	8
1.2.3 Downstream targets of CAMKK2.....	10
1.3 ULK1 and autophagy	15
1.3.1 ULK1: structure, function and regulation.....	17
1.3.2 Controversial roles of autophagy in prostate cancer	20
1.4 CREB: function, regulation and role in cancer.....	21
1.4.1 The basic structure and functional activation of CREB	22
1.4.2 Signal-dependent post translational modification of CREB in cancer.....	25
1.4.3 CREB in prostate cancer	29

1.4.4 Targeting CREB in cancer.....	31
Chapter 2 Materials and Methods.....	34
Chapter 3 Inhibition of CAMKK2 Impairs Autophagy and Castration-Resistant Prostate Cancer via Suppression of AMPK-ULK1 Signaling.....	59
3.1 Introduction.....	60
3.2 Results.....	62
3.2.1 Chloroquine impairs CRPC xenograft growth	62
3.2.2 CAMKK2 promotes autophagy and autophagic flux in prostate cancer	65
3.2.3 CAMKK2 is required for CRPC cell growth <i>in vivo</i>	71
3.2.4 AR-CAMKK2-AMPK signaling enhances autophagy through phosphorylation of ULK1 at serine 555 independent of mTOR-mediated ULK1 phosphorylation of Ser757	74
3.2.5 ULK1 correlates with poor patient prognosis in men with prostate cancer	79
3.2.6 Pharmacological targeting of ULK1 inhibits prostate cancer cell growth	80
3.3 Discussion	83
Chapter 4 Identification of an AR-CAMKK2 Signaling Cascade that Promotes Prostate Cancer Progression through CREB activity.	89
4.1 Introduction.....	90
4.2 Results.....	91
4.2.1 Phosphorylation of CREB at serine 133 and CREB activity are positively correlated with AR-CAMKK2 signaling	91
4.2.2 CREB is a downstream target of the AR-CAMKK2-CAMKI signaling pathway.....	95

4.2.3 AR antagonists, in a CAMKK2-independent manner, paradoxically function as weak activators of CREB.....	103
4.2.4 CREB1 is required for prostate cancer cell growth, which is associated with alteration of CREB dependent transcription.....	104
4.2.5 CREB1 and ATF1 exhibit functional redundancy in prostate cancer.....	112
4.2.6 Pharmacologic targeting of CREB in prostate cancer	116
4.2.7 CREB is involved in prostate cancer metastasis through matrix metalloproteinase 16 (MMP16)	121
4.3 Discussion	125
Chapter 5 Discussion and Future Directions.....	133
Appendix	140
Bibliography	141
Vita.....	186

List of Illustrations

Figure 1. AR signaling pathway and current therapeutic strategies against AR.	6
Figure 2. <i>CAMKK2</i> KO cells are preferentially vulnerable to nutrient deficiency.	10
Figure 3. AR-CAMKK2-AMPK signaling in prostate cancer.*	14
Figure 4. Genomic organization and domain structure of human CREB family.....	24
Figure 5. The direct phosphorylation regulation of CREB.*	26
Figure 6. Chloroquine inhibits castration-resistant prostate cancer (CRPC) growth <i>in vivo</i> . ..	63
Figure 7. Histological staining of tumor samples from chloroquine treated mice.....	64
Figure 8. Overexpression of <i>CAMKK2</i> increases autophagy in LNCaP cells.	66
Figure 9. Knockout <i>CAMKK2</i> decreases autophagy in C4-2 cells.....	67
Figure 10. Knockdown of <i>CAMKK2</i> decreases autophagy in 22Rv1 cells.....	68
Figure 11. <i>CAMKK2</i> promotes autophagic flux.	70
Figure 12. <i>CAMKK2</i> is required for C4-2 tumor growth <i>in vivo</i>	72
Figure 13. <i>CAMKK2</i> is required for 22Rv1 tumor growth <i>in vivo</i>	73
Figure 14. AR-CAMKK2-AMPK signaling increases autophagy by phosphorylating ULK1 at serine 555.	77
Figure 15. AR-CAMKK2 mediated autophagy is independent on canonical mechanistic target of rapamycin (mTOR) activity.	78
Figure 16. High <i>ULK1</i> tumor expression predicts poor patient prognosis in independent clinical cohorts of men with prostate cancer.	79
Figure 17. The ULK1 inhibitor SBI-0206965 inhibits autophagy in prostate cancer cell.	81
Figure 18. The ULK1 inhibitor SBI-0206965 represses prostate cancer cell growth.....	832
Figure 19. Working model depicting how AR-CAMKK2-AMPK signaling regulates autophagy by ULK1 phosphorylation and activation in prostate cancer.....	88

* Figure 3 and Figure 5 were created by biorender.com.

Figure 20. Pathway enrichment analysis of <i>CAMKK2</i> KO versus Cas9 control C4-2 cells...	93
Figure 21. The expression of p-CREB (Ser133) in prostate cancer PDX, cell line and GEMM models.	94
Figure 22. AR increases p-CREB and CREB activity.....	96
Figure 23. <i>CAMKK2</i> contributes to p-CREB in both HSPC and CRPC cells.	98
Figure 24. p-CREB decreases in Pb-cre ^{Tg/+} <i>Camkk2</i> ^{ff} TRAMP ^{Tg/+} mice.	99
Figure 25. AMPK is not responsible for AR- <i>CAMKK2</i> mediated CREB phosphorylation....	100
Figure 26. <i>CAMK1α</i> is the predominant kinase for AR- <i>CAMKK2</i> mediated p-CREB in prostate cancer cells.	102
Figure 27. Exogenous PNCK can contribute to p-CREB expression.	103
Figure 28. <i>CAMKK2</i> is not involved in AR antagonist-mediated increase of p-CREB.	104
Figure 29. CREB1 is required for AR-dependent LNCaP cell growth.....	105
Figure 30. CREB1 is required for CRPCs cell growth.	107
Figure 31. CREB1 is required for CRPC progression in xenograft model.....	108
Figure 32. Deletion of <i>CREB1</i> leads to a transcriptional dependent cellular process alteration.	1110
Figure 33. ATF1 and CREB1 exhibit functional redundancy in CRPC.	113
Figure 34. CREB1/ATF1 DKO decreases CRPC cell growth.....	114
Figure 35. <i>CREB1 ATF1</i> DKO dramatically reduces tumor growth and prolongs survival in xenograft models of CRPC.....	115
Figure 36 . CREB inhibitor 666-15 blocks cell growth and cell cycle.....	117
Figure 37. The small molecule CREB inhibitor 666-15 decreased tumor growth without significant toxicity in xenograft models of CRPC.....	118
Figure 38. The efficacy of 666-15 in PDX models.....	119
Figure 39. PSMA is a potential biomarker for CREB activity/inhibitors.....	1210
Figure 40. CREB is involved in extracellular matrix regulation.....	123

Figure 41. The CREB inhibitor 666-15 decreases cell migration.....	124
Figure 42. <i>MMP16</i> is amplified in prostate cancer and predicts poor patient prognosis.	125
Figure 43. A schematic representation of AR-CAMKK2-AMPK-ULK1 and AR-CAMKK2-CAMKI-CREB signaling pathways.....	134
Figure 44. A mouse model of prostate cancer metastasis.	138

List of Tables

Table 1. Post-translational modification and function of ULK1.....	18
Table 2. CREB downstream targets in prostate cancer.....	30
Table 3. The source and concentration of antibodies.....	48
Table 4. Chemicals and commercial Kits.....	51
Table 5. Software.....	53
Table 6. The sequences of siRNAs, shRNAs, sgRNAs and primers.....	53
Table 7. Sanger sequence of WT and CRISPR-Cas9 KO cells.....	56
Table 8. CT values of CAMK1 and CAMK4 in prostate cancer cell lines	101

Abbreviations

ACC	Acetyl-CoA carboxylase
ADT	Androgen deprivation therapy
AKT	Protein kinase B
AML	Acute myeloid leukemia
AMPK	AMP-activated kinase
AR	Androgen receptor
ARE	Androgen response element
ATF1	Activating transcription factor 1
ATG13	Autophagy-related protein 13
BLI	Bioluminescence imaging
bZIP	Basic leucine zipper
CAM	Calmodulin
CAMKI	Calcium/calmodulin-dependent protein kinase I
CAMKK2	Calcium/calmodulin-dependent protein kinase kinase 2
CQ	Chloroquine
CREB	cAMP responsive element binding protein
CREBBP	CREB Binding Protein
CREM	cAMP responsive element modulator
CRPC	Castration resistant prostate cancer
CRTC	CREB regulated transcription coactivator
CS-FBS	Charcoal-stripping FBS
CYP17A1	Cytochrome P450 17A1
DHT	Dihydrotestosterone
DKO	Double knockout

DOX	Doxycycline
FBS	Fetal bovine serum
FDA	U.S. Food and Drug Administration
FIP200	FAK family kinase-interacting protein of 200 kDa
GSEA	Gene set enrichment analysis
GEMM	Genetic mouse model
H&E	Hematoxylin and eosin
IHC	Immunohistochemistry
IP	Intraperitoneal
KEGG	Kyoto Encyclopedia of Genes and Genomes
KID	Kinase inducible domain
KIX	Kinase inducible domain interacting domain
KM	Kaplan-Meier
LFC	Log fold change
LH	Luteinizing hormone
LHRH	Luteinizing hormone-releasing hormone
MAP3K	MAPK kinase kinase
MAP4K	MAPK kinase kinase kinase
MAPK	Mitogen-activated protein kinase
MAPKAPK	MAPK-activated protein kinases
MAPKK	MAPK kinase
MMP16	Matrix Metalloproteinase 16
mTOR	Mechanistic target of rapamycin
PDX	Patient derivative xenograft
PFA	Paraformaldehyde

PGC1 α	Peroxisome proliferator-activated receptor gamma coactivator 1-alpha
PI3K	Phosphatidylinositol 3-kinase
PKA	cAMP protein kinase A
PNCK	Pregnancy up-regulated nonubiquitous CaM kinase
PSA	Protein specific antigen
PSMA	Prostate-specific membrane antigen
RFP	Red fluorescent protein
ROS	Reactive oxygen species
SCID	Severe combined immunodeficient
siRNA	Small interfering RNA
SKO	Single knockout
TAK1	TGF-beta activated kinase 1
TBC1D4	TBC1 domain family member 4
TEM	Transmission electron microscopy
TRAMP	Transgenic adenocarcinoma mouse prostate
ULK1	Unc51-like kinase 1
UPR	Unfolded protein response
VPS34	Phosphatidylinositol 3-kinase catalytic subunit type 3

Chapter 1
Introduction

Prostate cancer is the second most commonly occurring cancer among men in the United States, with 24,8530 estimated new-diagnosed cases and 34,130 estimated death cases in 2021¹. In spite of advances in therapy, it remains a public health challenge and requires the development of novel therapeutics. Androgen receptor (AR) is a ligand dependent transcription factor and has been revealed to drive the initiation and progression of prostate cancer². Androgens, especially endogenous testosterone and dihydrotestosterone (DHT), play important roles to activate AR through binding to AR, assisting the translocation of AR to the nucleus and further triggering the transcription of AR target genes. In detail, testosterone synthesized in testes first circulates in serum and diffuses into targeted cells where it is converted to a more active derivative, DHT by 5 α -reductase. Once DHT binds to AR, AR releases from heat shock protein, changes its conformation to form a homodimer. and is subsequently translocated to the nucleus. The nuclear AR then binds to androgen response elements (AREs) in the promoter region and recruit cofactors to initiate the transcription of AR target genes, which ultimately regulates cell growth and survival (Figure 1). While androgen and the activated AR signaling pathway are required for the development and maintenance of normal prostate, the aberrant activation of AR could drive the malignancy of prostate and promote the progression of prostate cancer. Therefore, androgen deprivation therapy (ADT), including chemical or surgical castration, serve as a standard care in clinic. As its name indicates, the goal of ADT is to decrease the level of androgen produced from testicles, adrenal glands and even prostate cancer itself, and prevent the progression of prostate cancer³. Therefore, ADT is often applied to patients who cannot use or no longer respond to initial surgery or radiation therapy. It can also be combined with radiation if the diagnostic indicators like Gleason score and serum protein specific antigen (PSA) predict a high risk of relapse³. As a standard treatment for advanced and metastatic prostate cancer, ADT acts as an initial plan and displays effectiveness for a couple of years, however, most diseases relapse to an incurable and lethal stage termed castration-resistant prostate cancer (CRPC).

This is due to various mechanisms of resistance including increased intratumoral androgen synthesis, AR gene and enhancer amplifications, splice variants, cofactor dysregulation, and glucocorticoid receptor crosstalk etc.^{2, 4} Thus, looking for the therapeutic targets for CRPC becomes essential. Importantly, though a small population of CRPC is non-AR driven, for most circumstances, the AR signaling axis is still active and remains to fuel the progression of prostate cancer.

1.1 Current treatment to target AR

Apart from orchiectomy which removes the testicles directly to block androgen production (Figure 1A), the most common strategies to target AR are through directly targeting ligands for AR activation or AR receptor itself.

The physiological signal for androgen generation usually starts from the release of luteinizing hormone-releasing hormone (LHRH) by the hypothalamus. LHRH then promotes the release of follicle stimulating hormone and luteinizing hormone (LH) from the pituitary gland. In the testicles, LH binds to receptors on Leydig cells, driving the conversion of cholesterol to dehydroepiandrosterone and androstenedione, the latter of which is in turn converted to testosterone for AR activation⁵. Therefore, to reduce the serum level of androgen, LHRH agonists, antagonists and androgen synthesis inhibitors have been developed and applied in clinics. LHRH agonists, including leuprolide (Lupron, Eligard), goserelin (Zoladex), triptorelin (Trelstar) and histrelin (Vantas) are synthetic peptides which can bind to LHRH receptor and repress the release of LH³ (Figure 1B). As a result, the circulating androgens usually drop to castrate levels leading to tumor shrinkage. However, there are some disadvantages of LHRH agonists, especially the tumor flare after initial treatment. With a slightly different working mechanism, LHRH antagonists can also reduce

the serum androgens faster but with no tumor flare. There are two available LHRH antagonists degarelix (Firmagon) and relugolix (Orgovyx)³ (Figure 1B). Relugolix is the first oral LHRH antagonist for advanced prostate cancer approved by U.S. Food and Drug Administration (FDA) in 2020, which has shown improved medical castration effect with lower serious cardiac risks⁶. Although LHRH agonists and antagonists are able to maintain the low level of androgens from testicles, adrenal glands and prostate cancer itself became important resources for prostate cancer progression. Hence, androgen synthesis inhibitors have been used for second-line therapy against CRPC treatment. Abiraterone (Zytiga) is a selective and irreversible inhibitor of cytochrome P450 17A1 (CYP17A1), which inhibits the conversion from pregnane steroids into androgens⁷ (Figure 1C). Abiraterone can stop both intratumoral androgen synthesis and adrenal androgens but not androgens from testicles, thus patients without orchiectomy are required to continue LHRH agonist or antagonist treatment³. Moreover, prednisone is needed to combine with abiraterone treatment due to the side effect caused by adrenocorticotrophic hormone increase⁵.

Though the ligand-targeted therapies mentioned above displayed some effectiveness, their side effects as well as inevitable AR reactivation mechanisms, warranted the development of new therapeutic strategies directly targeting AR. Flutamide (Eulexin), bicalutamide (Casodex) and nilutamide (Nilandron) are the first generation non-steroid AR antagonists, which competitively interact with the ligand binding domain of AR (Figure 1D). Bicalutamide was also reported to transiently decrease AR expression and might switch to an agonist in some CRPCs⁵. In the clinic, these antiandrogens are mostly combined with surgical castration or a LHRH agonist or LHRH antagonist for the treatment of progressive prostate cancer or used to prevent the tumor flare because of LHRH agonists³. The second generation of AR antagonists includes enzalutamide (Xtandi), apalutamide (Erleada) and darolutamide (Nubeqa). Enzalutamide and apalutamide are very potent AR antagonists with high affinity to

the ligand binding domain of AR (Figure 1D). They are highly similar in structure and exhibit close clinical performances⁸. They have been approved by the FDA for treatment of CRPC and metastatic castration-sensitive prostate cancer. Compared with enzalutamide and apalutamide, darolutamide shows very similar clinical benefits but has a unique molecular structure. Therefore, they have been regarded as “apple (Enzalutamide and apalutamide)” and “banana (darolutamide)” by the principal investigator of ARAMIS trial Karim Fizazi at the 2019 ASCO Genitourinary Cancers Symposium^{8,9}. Since there is no available clinical data comparing the efficacy among these three AR antagonists, which one is better for individual patients might be more depending on safety reasons. For example, whether higher blood brain barrier penetration of enzalutamide would be considerable as an increased risk of central nervous system effect, and whether lack of CYP-inhibitor activity of darolutamide would benefit patients who need to take other drugs. Of note, darolutamide and its metabolite have been reported to be complete antagonists for both AR mutants F876L and W741L. The former mutant is linked to enzalutamide and apalutamide resistance while the latter one contributes to the turnover of bicalutamide to an AR agonist¹⁰, suggesting the potential function of darolutamide to overcome the resistance. The clinical benefit of darolutamide in these mutants has yet to be revealed.

Though abiraterone robustly reduces circulating androgen and the second-generation AR antagonists display the most potent inhibition on AR activity, they only alleviate prostate cancer to some extent. Resistance to AR inhibition therapies still exists and more mechanisms of CRPC further indicate it is urgent to development new treatment strategies. Admittedly, AR is still one of the best targets for prostate cancer therapy and thus multiple recent studies have aimed to develop novel AR inhibitors by obstructing required conformational changes of AR, blocking the interaction between AR and its cofactors and degrading AR^{7, 11, 12} (Figure 1E&F).

In addition to AR itself, aberrant AR-regulated signaling pathways have been considered as an alternative strategy for prostate cancer treatments. Emerging genomic and proteomics data from cell and clinical samples have rendered significant evidence for the essential role of kinases and phosphorylation events in prostate cancer progression¹³ (Figure 1G). From these kinases, calcium/calmodulin-dependent protein kinase kinase 2 (CAMKK2) stands out as a direct target of AR and its regulation on key phosphorylation events upon androgen stimulation, and has been identified as a promising therapeutic target in prostate cancer¹⁴. Therefore, a clear and thorough mechanism on studies derived from both the clinical side and bench side will be important for future drug development.

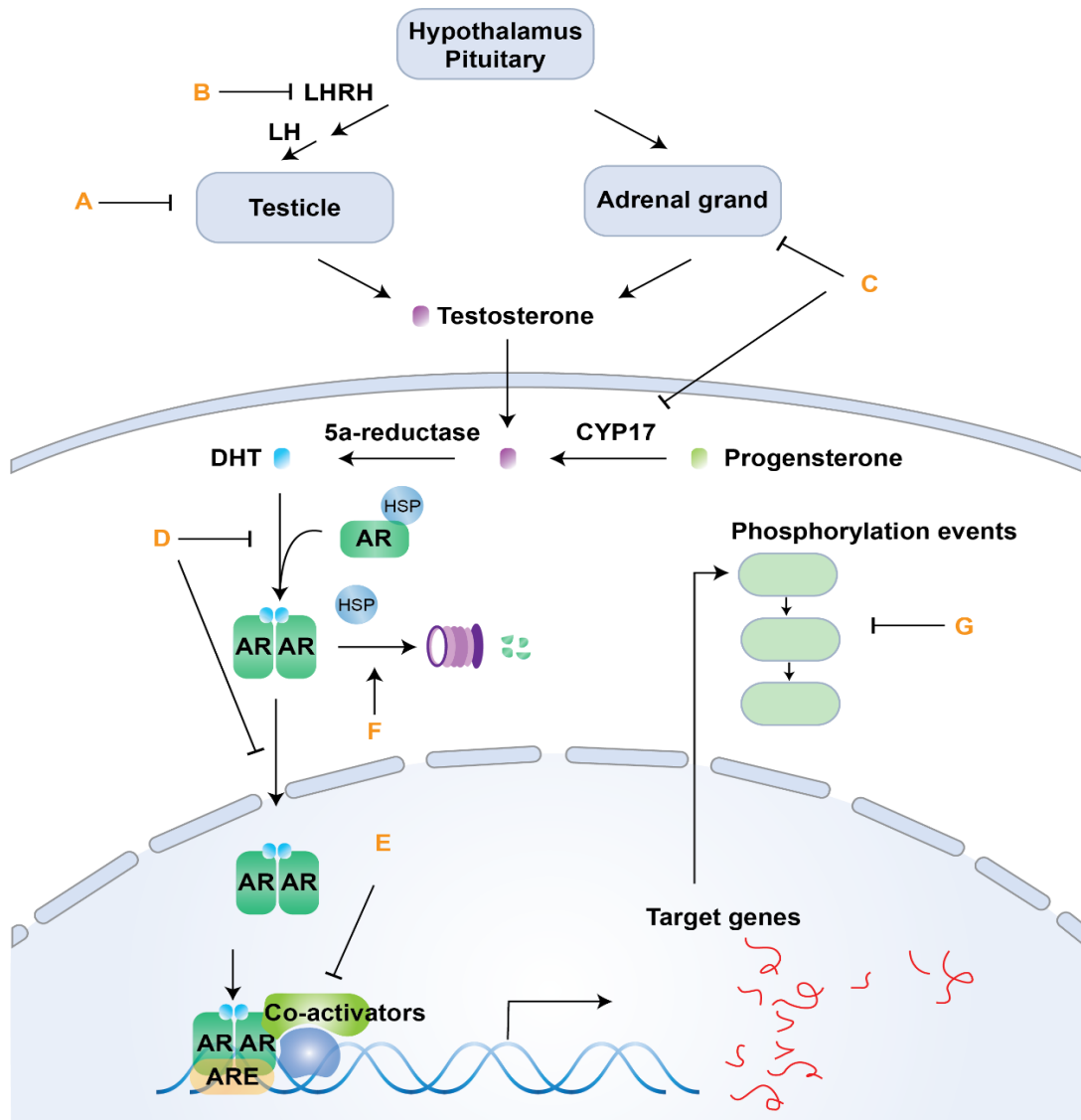


Figure 1. AR signaling pathway and current therapeutic strategies against AR.

Scheme of AR transcriptional activation is shown above, with capital letter (A-G) indicating the different therapeutic strategies against AR. Regulated by LH and LHRH, the androgens like testosterone are released from testicle and diffuse into targeting organs including prostate. In prostate cancer cells, 5 α -reductase catalyzes the reaction from testosterone to DHT, which can bind and activate AR. DHT stimulates AR to dissociate from HSP and undergo a conformational change. Then AR can form dimers and translocate to the nucleus where it binds to androgen response elements (AREs), recruits coregulators and starts targeted-gene transcription. The androgens are also created by the adrenal glands and peripheral tissues including prostate cancer. Per the AR activation signaling, current therapeutic strategies against AR includes: (A) surgical castration, a surgery to remove the testicles; (B) LHRH agonists and LHRH antagonist, reducing circulating androgens; (C) androgen synthesis inhibitors, inhibiting the formation of androgens by adrenal glands and prostate cancer; (D) AR antagonists, blocking androgen binding to AR. The second generation can also inhibit AR nuclear translocation; (E) AR degraders, repressing AR protein level; (F) targeting AR cofactors and AR-cofactor interaction; and (G) targeting AR downstream targets like kinases and phosphorylation events.

1.2 CAMKK2 and its downstream kinases in prostate cancer

1.2.1 Structure and regulation of CAMKK2

CAMKK2 is a Ca²⁺/Calmodulin (CAM)-dependent serine-threonine protein kinase, which was first identified in early 1990s. In humans, the *CAMKK2* gene consists of 18 exons and encodes 7 isoforms of CAMKK2 through alternative splicing and/or polyadenylation sites. The majority of the difference among different isoforms comes from the C-terminal variation¹⁵. Structure studies showed that CAMKK2 is composed of four domains: N-terminal domain, kinase domain, regulatory domain and C-terminal domain¹⁶. The kinase domain of CAMKK2 is located in the middle of CAMKK2, which is highly similar to other CAMK family members but with 22 exclusive Pro/Arg/Gly-rich residues in the ATP binding pocket. The Ser/Thr

catalytic activity of CAMKK2 is regulated by Ca^{2+} -CAM binding and autophosphorylation. Flanking the right side of the kinase domain, the regulatory domain is responsible for autoinhibition and CAM binding. Due to the overlapping between the autoinhibitory and CAM binding domain, the binding between the regulatory domain and Ca^{2+} /CAM brings about the release of the autoinhibitory domain from the catalytic pocket, leading to subsequent substrate access. Once activated by Ca^{2+} /CAM, autophosphorylation of CAMKK2 at Thr 85 and Thr 482 further promotes the activity of CAMKK2, which is required for lasting CAMKK2 activity without relying on Ca^{2+} signal^{17, 18}. Uniquely, a sequential phosphorylation event in the N-terminal region has been reported to affect the autonomous activity and stability of CAMKK2¹⁹. In the basal state, phosphorylation starting at Ser137 by CDK5 and then Ser129 and Ser137 by GSK3b maintains CAMKK2 at a considerably low level of autonomous activity but stabilizes the new synthesized CAMMK2, which might provide CAMKK2 a sufficient CAMKK2 response to calcium influx.

1.2.2 CAMKK2 in prostate cancer

CAMKK2 was first identified as a direct downstream target of AR in 2011 as demonstrated by the discovery of an ARE situated on *CAMKK2* promoter (~ 2.1 kb upstream of the *CAMKK2* transcriptional start site)¹⁴. A chromatin immunoprecipitation study on clinic samples confirmed the importance of this ARE in CRPC²⁰. In prostate cancer cells, androgen treatment activated AR and promoted AR binding to this region to start the transcription of CAMKK2. Therefore, mRNA and protein level of CAMKK2 were found to be positively correlated with prostate progression^{14, 21}. Compared to benign tissue, prostate cancer exhibited higher CAMKK2 expression in multiple patient tissue microarrays, which can immediately be downregulated by androgen deprivation therapy. In relapsed disease,

CAMKK2 was restored and thus can be tracked with PSA level and Gleason score. This transition has been further confirmed by the Transgenic Adenocarcinoma Mouse Prostate (TRAMP) genetic mouse model and xenograft mouse model which compared androgen sensitive cells (CWR22) to its corresponding castration-resistant derivative (22Rv1)²².

Since a close correlation between CAMKK2 and AR has been found, the functional role of CAMMK2 has been investigated in many prostate cancer studies. By using siRNA to knockdown CAMKK2 or applying a CAMKK2 inhibitor STO-609 to block CAMKK2 activity, Massie et al first revealed that the CAMKK2 is required for androgen mediated LNCaP cell proliferation²¹, which was later confirmed by showing that CAMKK2 can affect LNCaP cell growth through disrupting cell cycle progression^{22, 23}. Likewise, in a xenograft model, STO-609 can inhibit C4-2B tumor growth in castrated mice but show a minor benefit in intact mice²¹, in line with our unpublished data showing that *CAMKK2* KO cells grew slower in serum starvation medium compared to WT cells (Figure 2), both of which suggest that CAMKK2 plays important roles under certain stress. Moreover, in a genetic mouse model, elevated CAMKK2 levels have been observed in two well-established spontaneous prostate cancer models, TRAMP and Pb-Cre *Pten*^{fl/fl} mice^{22, 24}, while *Camkk2* deletion or STO-609 treatment prevented the tumor progression in *Pten* knockout mice through the regulation on cell cycle and cell death²⁴. Besides proliferation, CAMKK2 is also involved in cell migration and invasion¹⁴. In LNCaP and VCaP cells, STO-609 was able to inhibit androgen-increased migration and invasion while overexpression of CAMKK2 promoted migration. However, the role of CAMKK2 in prostate cancer migration and metastasis has not been studied as extensively as proliferation and we currently have few data of metastasis from xenograft or genetic mouse models.

Studies also found that CAMKK2's role in prostate cancer progression, in part, relies on cellular metabolism regulation. CAMKK2 is necessary for AR mediated glucose uptake.

Knockdown of *CAMKK2* or STO-609 treatment significantly decreased basal and AR-induced cellular glucose uptake and impaired lactate and citrate generation^{21, 25}. This function is mainly through the regulation of AMP-activated kinase (AMPK), a key metabolic sensor in homeostatic maintenance. The details will be discussed in section 1.2.3. Moreover, *CAMKK2* was found to be involved in lipogenesis. Deletion of *CAMKK2* reduced two essential lipogenic enzymes, acetyl-CoA carboxylase and fatty acid synthase expression, which, in turn, limited *de novo* lipogenesis in prostate cancer²⁴.

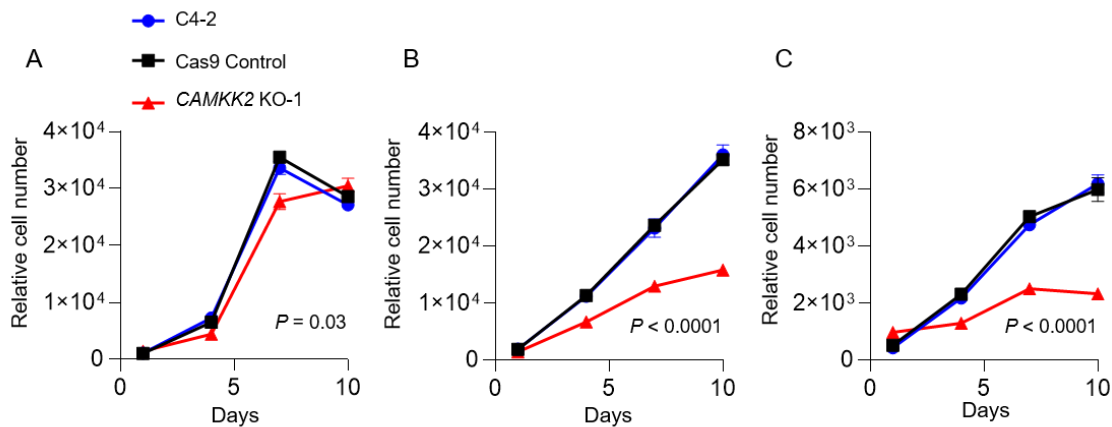


Figure 2. *CAMKK2* KO cells are preferentially vulnerable to nutrient deficiency.

Cell growth of C4-2, Cas9 control and C4-2 *CAMKK2* KO-1 cells in normal 5% FBS media (A), charcoal-stripping FBS media (B) and 0.5% FBS media (C).

1.2.3 Downstream targets of *CAMKK2*

Once activated, *CAMKK2* can phosphorylate and activate three major downstream substrates: Ca^{2+} /calmodulin-dependent protein kinase I (CAMKI), CAMK4 and AMPK.

CAMKI is one of the most well characterized downstream kinases of *CAMKK2* whose full activation is dependent on calcium stimulus and phosphorylation modification. The binding of Ca^{2+} -CAM induces a conformational change of CAMKI, which escapes from the intrasteric

autoinhibition and exposes the phosphorylation site to CAMKK^{26, 27}. Four members have been identified in CAMKI family: CAMKI α , CAMKI β /PNCK (Pregnancy up-regulated nonubiquitous CAM kinase), CAMKI γ , and CAMKI δ , which are encoded by *CAMK1*, *PNCK*, *CAMK1G* and *CAMK1D* respectively. Similar to CAMKK2, CAMKI bears a catalytic domain containing an ATP binding region and a regulatory domain containing overlapping autoinhibitory and CAM binding sequence. Within the activation loop, they can be phosphorylated at a threonine residue by CAMKK2 (CAMKI α : Thr177, PNCK: Thr174, CAMKI γ : Thr178, CAMKI δ : Thr180) to acquire the maximal activation^{26, 28-30}. Activated CAMKI further phosphorylates its substrates which contain the consensus substrate sequence (Hyd-x-R-x2-[S/T]-x3-Hyd)²⁸.

Emerging evidence has indicated that CAMKI has a close correlation with cancer. Overexpression of CAMKI has been observed in several cancers. High expression level of CAMKI has been detected in acute myeloid leukemia (AML) and was correlated with poor overall survival. Inhibition of CAMKI activity was found to block AML progression and decrease the AML stem cell activity³¹. Such high expression of CAMKI was also observed in pancreatic cancer, however, it was associated with a better overall survival and disease-free survival³². Moreover, the mRNA and protein levels of PNCK were elevated and highly correlated with clinical and pathologic factors in certain subtype of breast cancer, nasopharyngeal carcinoma, clear cell renal cell carcinoma and hepatocellular carcinoma³³⁻³⁷. Interestingly, a heterogeneous expression pattern of PNCK in breast cancer has been reported and proposed to be correlated with some cancer initiating genetic events. In murine mammary tumors, *c-myc* or *int-2/Fgf3* driven tumors appeared to have a higher *Pnck* expression compared with those from *neu* or *H-ras*³⁶. Despite the fact that there is still a lack of direct evidence demonstrating a correlation between PNCK and these oncogenes, it is worth determining whether patients with high PNCK expression have a different prognosis and drug response in breast cancer. Besides PNCK, CAMKI δ also increased in invasive breast cancer. In basal-

like breast cancer, the amplified CAMK1 δ significantly increased the tumor growth rate and epithelial-mesenchymal transition, indicating that CAMK1 δ is a potential therapeutic target³⁸. In addition to clinical correlation, many mechanism studies have endorsed the significance of CAMK1 in cancer biology. A variety of CAMK1 downstream targets are involved in tumor progression, metastasis and therapeutic resistance. CREB, as a classical CAMK1 substrate, has been profoundly correlated to cancer survival, cancer metabolism and cell cycle regulation. In AML, CAMK1/CREB signaling was required for cell survival and self-renewal of AML stem cells³⁹. In addition, the identification of Cdk4 and caspase as CAMK1 downstream targets suggested a potential effect of CAMK1 on cancer survival⁴⁰. Besides, CAMKK/CAMK1 cascade mediated phosphorylation of β PIX promoted the migration of basal medulloblastoma via Rac1, indicating the role of CAMK1 in metastasis⁴¹. CAMK1 was also implicated in tumor environment remodeling by phosphorylating and degrading I κ B α , which in turn resulted in the activation of NF- κ B signaling⁴². On the other hand, CAMK1 displays some influences on other essential cancer-related signaling pathways. Knockdown of PNCK slowed down nasopharyngeal carcinoma cell growth but raised apoptosis by reducing the activity of PI3K/AKT/mTOR signaling pathway³⁴. PNCK can also decrease mitogen-activated protein kinase (MAPK) signaling pathway through promoting ligand-independent EGFR degradation^{33, 43}. Finally, it is worth noting that recent studies have disclosed a potential role of CAMK1 in therapeutic resistance, especially for immunotherapy. In prostate cancer, the transition from androgen sensitive to castration resistance has been correlated with CAMK1 δ expression though the underlying mechanism is still unclear⁴⁴. Moreover, CAMK1 was identified as one of prognosis-associated genes for rituximab plus cyclophosphamide, doxorubicin, vincristine and prednisone (R-CHOP) immunochemotherapy in diffuse large B-cell lymphoma⁴⁵. Similarly, a genetic screen showed that CAMK1 δ was a key factor that triggered an immune resistance in anti-PD-L1 treatment. Through Fas-receptor, cytotoxic T

lymphocytes could activate CAMK1 δ followed by phosphorylation and suppression of caspase-3,-6,-7 in apoptosis, which eventually protected tumor cells from anti-PD-L1 treatment⁴⁰.

AMPK is a heterotrimeric complex containing a catalytic α subunit and two regulatory subunits β and γ ⁴⁶. The catalytic domain of AMPK is located in the N-terminus and contains a T-activation loop. In this loop, phosphorylation of Thr172 is necessary for full activation of AMPK and strongly mediated by upstream kinase including liver kinase B1 (LKB1), CAMKK2 and TGF- β activated kinase-1 (TAK1). In response to cellular stress, additional binding of AMP/ADP to the γ subunit induces an allosteric activation, working with N-terminal myristoylation in the β subunit, which in turn facilitates the exposure of the Thr172 site to upstream kinases. In the meantime, high AMP/ADP: ATP ratio is an essential factor to prevent the participation of dephosphorylase^{47, 48}. Once activated, AMPK is a master regulator to maintain energy homeostasis by phosphorylating its numerous targets.

In prostate cancer, AMPK is the most extensively investigated downstream target of CAMKK2 and its mediated-reprogramming of central carbon metabolism subsequently contributes to CAMKK2's pro-cancer activity^{21, 25, 49}. Knockdown of AMPK's catalytic subunits resulted in aberrant glucose and fatty acid oxidation, mechanistically through downregulating peroxisome proliferator-activated receptor gamma coactivator 1-alpha (PGC-1 α)-mediated mitochondrial biogenesis⁵⁰. Additionally, it has been revealed that AR-CAMKK2-AMPK signaling trigger the phosphorylation of TBC1 Domain Family Member 4 (TBC1D4) and facilitates the trafficking of the glucose transporter GLUT12 to the plasma membrane, leading to enhanced of glucose uptake and glycolysis²⁵. Moreover, AMPK can also phosphorylate 6-phosphofructo-2-kinase/fructose-2,6-biphosphatase 2/3, a rate-limiting step of glycolysis and thus positively regulating glycolysis^{51, 52}. In the clinic, increased phosphorylation of AMPK at

Thr172 and phosphorylation of its classical substrate Acetyl-CoA carboxylase (ACC) at Ser79 are observed in relapsed prostate cancer patients while benign samples have low phosphorylation levels^{50, 53}. Most recently, CAMKK2-AMPK-mediated p38 activation was

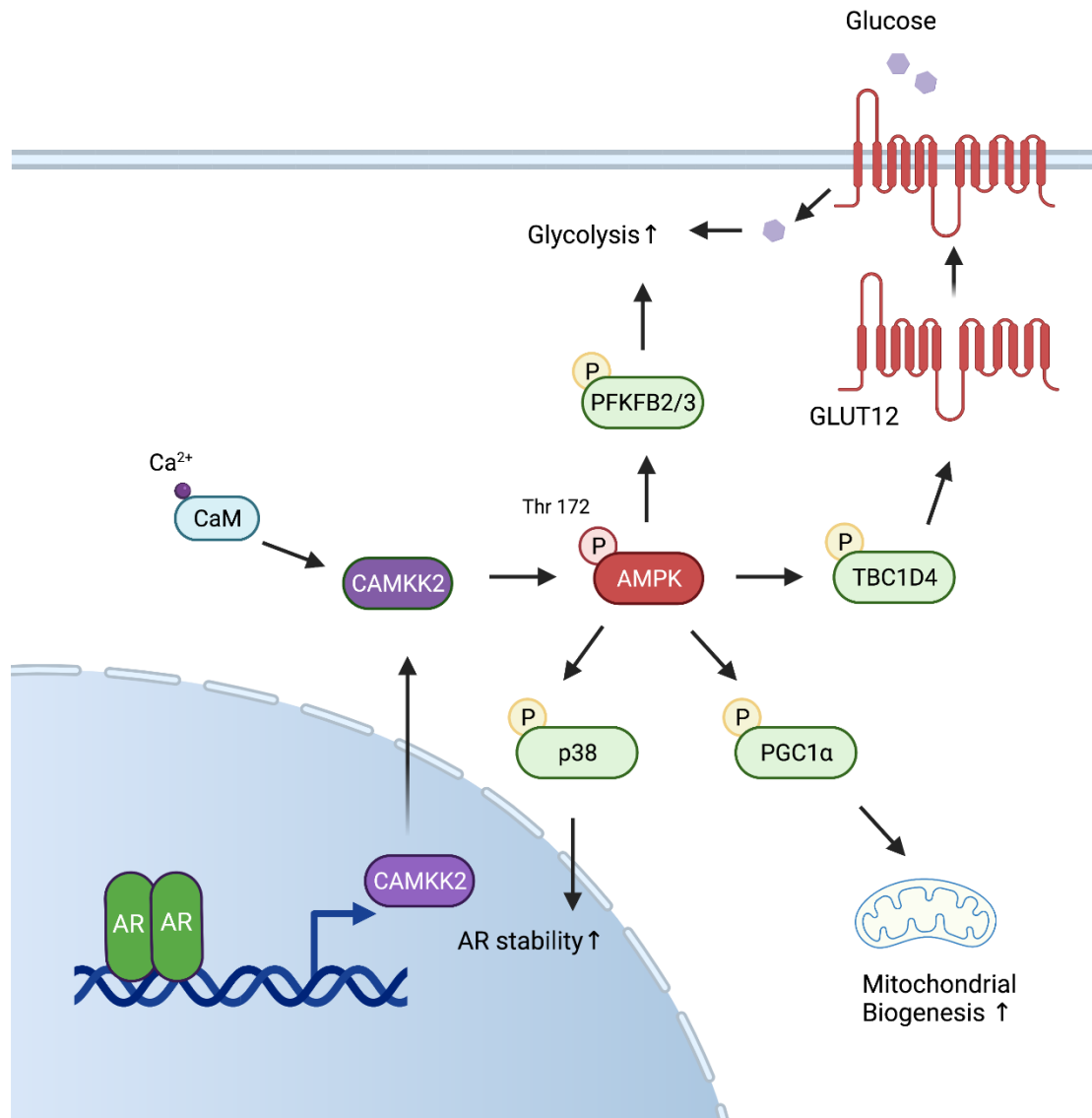


Figure 3. AR-CAMKK2-AMPK signaling in prostate cancer.

AR-induced CAMKK2 phosphorylates AMPK at Thr172, a major phosphorylation site for AMPK kinase activity. Activated AMPK is involved in metabolic alterations through TBC1D4, PGC1 α and PFKFB2/3 as well as maintains the stability of AR through p38.

shown to reactivate AR upon acute AR inhibition. In detail, AR inhibition decreased the expression of succinate dehydrogenase A/B, which converted succinate to fumarate. The accumulation of succinate promoted the release of calcium from endoplasmic reticulum to cytoplasm, leading to the activation of CAMKK2-AMPK-p38 signaling. p38 can further phosphorylate and activate HSP27 to stabilize and then translocate AR to nucleus⁴⁹.

CAMK4, highly similar to CAMKK2 and CAMK1, consists of a kinase domain for catalysis and a regulatory domain for intrasteric autoinhibition²⁶. Similarly, the activation of CAMK4 requires sequential Ca^{2+} /CAM binding and CAMKK-mediated phosphorylation at Thr200 in the activation loop. Interestingly, this phosphorylation stimulates a Ca^{2+} /CAM-independent activity which is essential for CAMK4 transcriptional function⁵⁴. In addition, CAMK4 has a second intrasteric autoinhibition mechanism which is regulated by two autophosphorylation sites Ser12 and Ser13. Moreover, CAM binding and activity can be blocked if Ser336 is phosphorylated²⁶. Although CAMKK2-CAMK4 signaling is important in hepatic cancer⁵⁵, CAMK4 cannot be detected in some prostate cancer cells. Details will be discussed in Chapter 4.

Besides these canonical targets, CAMKK2 has also been reported to phosphorylate SIRT1 at Ser27 and Ser47 to stabilize SIRT1 protein and facilitate its activity in endothelial cells⁵⁶ as well as phosphorylate AKT at Thr308 to support cell growth in ovarian cancer cells⁵⁷. Future studies will be required to investigate whether these events are universal in other cells.

1.3 ULK1 and autophagy

Macroautophagy, herein referred to as autophagy, is a self-degradative and recycling process whereby impaired, detrimental or excess components are engulfed by a double membrane vesicle called an autophagosome degraded by the lysosomal system and

ultimately recycled for cell reuse⁵⁸. It is a highly conserved homeostatic mechanism by which cells can process protein and organelle quality and quantity control, protect itself against internal and external toxins as well as survive energy stress. Thus, autophagy plays an essential role in physiological processes but numerous diseases including cancer can result if this process is abnormal. Several sequential steps make up the classical process of autophagy which include initiation of autophagy by unc-51-like kinase 1 (ULK1) complex, nucleation through class III phosphatidylinositol 3-kinase complex PI3K-III) complex, two ubiquitin-like conjugation systems: mediated-elongation and maturation, lysosomal fusion and cargo degradation⁵⁹⁻⁶¹. The ULK1 complex consists of ULK1/2, autophagy-related protein 13 (ATG13), focal adhesion kinase family interacting protein of 200 kDa (FIP200), and ATG101. When autophagy is initially triggered by intracellular and extracellular stimuli like nutrient deficiency, dephosphorylated and inactive mTORC1 will be released from the ULK1 complex and ULK1/2 and ATG13 will be dephosphorylated at certain residues. These dephosphorylations, in turn, leads to boosting the ULK1/2 kinase activity and rapidly phosphorylating its substrates including ATG13, FIP200 and ULK1/2, and eventually promoting the translocation of ULK1 complex to autophagy initiation sites. In addition, ATG101 also contributes to the phosphorylation of ATG13 to stabilize the ULK1 complex⁶¹. In the autophagosome assembly and formation step, Beclin1 gets rid of the sequestration from Bcl2, concomitant with the formation of PI3K III complex. This complex is comprised of vacuolar protein sorting 34 (VPS34), Beclin1, VPS15, ATG14L, and p150, which is in charge of phospholipid phosphatidylinositol 3-phosphate (PI3P) generation and phagophore forming. After that, ATG12 conjugation and LC3-phosphatidylethanolamine conjugation machineries are involved in expansion and final autophagosome closure. As a result, a conversion from LC3 I to LC3 II is frequently applied to serve as a readout of autophagy occurrence.

1.3.1 ULK1: structure, function and regulation

ULK1 is a serine/threonine protein kinase containing an N-terminal kinase domain, a serine-proline rich region and a C-terminal interacting domain. The kinase domain is responsible for catalysis and LC3 binding. Many autophagy related proteins are substrates of ULK1. The ULK1 complex itself is the first identified ULK1 substrate and most all components in this complex can be phosphorylated. The autophosphorylation of ULK1 occurs at Thr180, Ser1042 and Thr1046. Thr180 is located in the kinase domain whose phosphorylation propels the activation of ULK1. The other two phosphorylation sites are in the interacting domain and associated with ULK1 ubiquitination-mediated degradation. ULK1 can also phosphorylate ATG13 at Ser318 when chaperone complex Hsp90-Cdc3 binds to ULK1. This phosphorylation releases ATG13 from ULK1 and anchors ATG13 to impaired mitochondria for clearance⁶². In addition, ULK1 has been reported to phosphorylate PI3K-III complex members such as VPS34, Beclin1 and ATG14L. Phospho-VPS34 at Ser249 was recently found to increase the binding ability of LC3-interacting region domain⁶³. Phospho-Beclin1 at Ser14 and phospho-ATG14L at Ser29 showed a similar function to promote VPS34 complex activity for autophagosome biogenesis^{64, 65}. Moreover, ULK1 can also regulate autophagy trafficking through ATG9 (Ser14) and LC3 related conjugation processes through ATG4B (Ser316)⁶⁶. In addition to autophagy, the phosphorylation of some metabolic proteins like hexokinase 1, phosphofructokinase 1 and enolase 1 are dependent on ULK1 regulation for cellular homeostasis maintenance under stress conditions⁶⁷.

The serine-proline rich region of ULK1 sits next to the catalytic domain and it contains many post-modification sites for regulation. mTORC1 is one of the key regulators for ULK1, which maintains the phosphorylation of ULK1 at Ser757 and Ser637 to repress autophagy in nourishment condition. However, in acute starvation stimulus, phospho-Ser638 is first removed from ULK1 to facilitate the dephosphorylation of Ser757 and disrupt AMPK and ULK1

interaction⁶⁸. Additionally, in starvation or upon genotoxic stress, Ser638 can be dephosphorylated by protein phosphatase 2A or protein phosphatase 1D respectively. A stressful environment can also activate AMPK to initiate autophagy. Indirectly, AMPK-mediated phosphorylation of raptor serves as an important factor for mTORC1 inactivation. Importantly, there is a direct regulation between AMPK and ULK1 through multiple serine residues (Ser317, Ser467, Ser555, Ser637 and Ser777) at ULK1 that are phosphorylated by AMPK⁶¹. Of interest, ULK1 can also mediate both AMPK and mTORC1 inversely, suggesting complicated feedbacks among mTOR, AMPK and ULK1. Besides the negative regulation between AMPK and mTOR, during starvation, activated ULK1 is able to elevate the phosphorylation levels of raptor at Ser855, Ser859 and Ser792 to further repress mTOR kinase activity⁶¹. On the contrary, ULK1 seems to inhibit AMPK phosphorylation at Thr172 for autophagy termination by an unknown mechanism⁶⁹. However, a recent study showed a dissimilar observation that ULK1 boosts AMPK signaling by direct phosphorylating AMPK β 1 at Ser108 independent of Thr172⁷⁰, indicating timing or context variations might determine the observations of autophagy status. Recently, through theoretical and molecular biological techniques, a study confirmed the existence of period autophagy during prolonged cellular stress. Such oscillation can only be observed at a certain level of cellular stress, indicating a fine-tune regulation of autophagy in response to a harsh environment⁶⁹. Additionally, acetylation and ubiquitylation are associated with ULK1 activity and expression. Table 1 summarize the regulation of ULK1 by different post-translational modification.

Table 1. Post-translational modification and function of ULK1

Residues	Modification	Kinase	Function	Ref
Thr180	Phosphorylation	ULK1	Increase ULK1 kinase activity and autophosphorylation activity	⁷¹

Ser317	Phosphorylation	AMPK	Increase ULK1 kinase activity	72
Ser467	Phosphorylation	AMPK	Promote mitophagy and cell survival upon nutrient deprivation	73
Ser555	Phosphorylation	AMPK	Promote 14-3-3 binding/YWHAZ-binding, Increase ULK1 kinase activity, facilitate mitochondrial translocation,	71, 73-75
Thr574	Phosphorylation	AMPK	Promote mitophagy and cell survival upon nutrient deprivation	73
Ser637	Phosphorylation	mTOR/ AMPK	Promote ULK1 AMPK interaction	68
	Phosphorylation	AMPK		73, 74
Thr659	Phosphorylation	AMPK	Promote YWHAZ-binding	74
Ser757	Phosphorylation	mTOR	Disrupt ULK1 and AMPK binding	68, 72
Ser777	Phosphorylation	AMPK	Increase ULK1 kinase activity	72
Ser1042, Thr1046	Phosphorylation	ULK1	Recruit to the KLHL20-associated E3 ligase for ubiquitination and degradation	76
Ser774	Phosphorylation	AKT	Insulin inhibited autophagy	71
Lys162, Lys606	Acetylation	TIP60	Serum starvation induced autophagy	77
Unknown	Poly-Ub	NEDD4L	Control oscillatory activation of autophagy	78
Unknown	Poly-Ub	Cul3- KLHL20	Autophagy termination	76
Lys63	Poly-Ub	TRAF6	Enhance ULK1 stability and activity	79

1.3.2 Controversial roles of autophagy in prostate cancer

Although the concept of autophagy has been introduced since 1963 and autophagy has been studied in cancer for decades, the role of autophagy in cancer is still not fully elucidated. It appears that the function of autophagy during cancer development is dependent on many contexts including cancer type, genetic alteration, treatment condition and stage of disease. In prostate cancer, autophagy was characterized as a tumor suppressor due to the *PTEN* deletion or *BECN1* monoallelic loss⁸⁰. *PTEN* loss has been observed in many prostate cancers and serves as an important event for abnormal PI3K/AKT/mTOR signaling activation. Upregulated mTOR is no doubt associated with aberrant cell proliferation and malignant behavior. Meanwhile, mTOR negatively regulates ULK1 activation and leads to the repression of autophagy. Therefore, autophagy deficiency is linked to *PTEN* loss-driven cancer progression. Besides *PTEN*, *BECN1* is another key gene for autophagosome formation and its allelic loss also often occurs in prostate cancer. Moreover, autophagy inactivation has been correlated with therapeutic resistance. Prostate leucine zipper protein mediated autophagy deactivation serves as a survival mechanism by which CRPC cells protect themselves against docetaxel induced apoptosis⁸¹. Similarly, autophagy stimulation by Atorvastatin seems to further expand the ionizing radiation induced cell death in AR negative PC3 cells⁸². However, emerging studies have conferred contrasting evidence suggesting that autophagy can serve as a tumor promoter in prostate cancer. Although *PTEN* KO was thought to indicate high mTOR and low autophagy activity, genetic mice with prostate-specific *Atg7* and *Pten* double deletion significantly suppressed *Pten* deficiency induced tumor progression through the production of endoplasmic reticulum stress and impairing autophagy dependent protein homeostasis⁸³. Combination of an autophagy inhibitor, chloroquine (CQ), with AKT inhibitor (AZD5363) has been demonstrated to be effective in PC-3 prostate cancer xenograft model⁸⁴. Importantly, autophagy has been associated with AR mediated prostate cancer progression.

Yan *et al.* indicated that autophagy induction is one of survival mechanisms by which androgen can enhance prostate cancer growth. Correspondingly, knockdown of *ATG7* or treatment cells with CQ can block androgen-mediated prostate cancer proliferation⁸⁵. To date, several mechanisms have been elucidated to explain how AR promotes autophagy. For instance, androgen-induced reactive oxygen species partly resulted in the elevation of autophagy⁸⁵. Moreover, some autophagy and lysosomal genes such as *ATG4B*, *ATG4D*, *ULK1/2*, and *TFEB* are direct targets of AR. These genes are required for maximal androgen-mediated prostate cancer growth^{86, 87}. Of interest, a recent study showed that an AR co-regulator, lysine demethylase 4B, not only stabilizes and activates AR, but enhances autophagy by Wnt/ β -catenin signaling⁸⁸. While mechanisms underlying AR and autophagy regulation is still yet to be completely clarified, a synergistic lethal effect has been disclosed when ADT treatment is combined with autophagy inhibitors like CQ and 3MA, providing an insight into autophagy as a promising therapeutic target for prostate cancer⁸⁹⁻⁹¹.

1.4 CREB: function, regulation and role in cancer

cAMP responsive element binding protein (CREB), since being discovered in 1987, acts as a well-characterized transcription factor in the basic leucine zipper (bZIP) superfamily and is known for its phosphorylation-dependent activation in response to diverse signals and its contribution to various stimulus-induced cellular processes including proliferation, differentiation, survival and homeostasis in both physiological and disease states^{92, 93}. Despite the critical roles of CREB in many neurological disorders⁹⁴, emerging evidence has revealed the strong correlation of CREB with cancer by showing its abnormal overexpression in many primary and metastatic tumors, as well as identifying its downstream targets that participate in cancer initiation, progression and metastasis⁹⁵⁻⁹⁷. Therefore, CREB is a promising candidate to exploit as a prognostic biomarker and therapeutic target in cancer.

1.4.1 The basic structure and functional activation of CREB

CREB comprises four major functional domains, and the most important one for its transcriptional function is the kinase-inducible-domain (KID) that is located in the middle of protein. The KID domain contains many serine residues which can be phosphorylated by upstream kinases to further respond to different stimuli. Among nine identified phosphorylation sites, serine 133 is the most characterized one and is frequently involved in the downstream signaling cascades induced by the activation of CREB. Phosphorylation of Ser133 facilitates the interaction between KID and KIX (KID interacting domain) of CREB binding protein (CBP)/P300, not only affecting the dimerization and DNA binding of CREB but promoting the recruitment of the transcriptional machinery to the promoters of its substrates, consequently initiating CREB dependent gene transcription^{92, 93}. In addition to Ser133, Ser129 is another phosphorylation site devoted to inducing CREB transcriptional activity. In response to parathyroid hormone and epidermal growth factor, the full transcriptional function of CREB depends on both Ser133 and Ser129^{98, 99}. However, other phosphorylation sites (Ser108, Ser111, Ser114, Ser117, Ser121, Ser142 and Ser143) are negative regulators for CREB function. On one hand, these phosphorylations disrupt the interaction between KID and KIX domain^{100, 101}. On the other hand, phosphorylation at residues 108-117 (CK cassette) blocks the interaction between DNA and bZIP domain due to more intramolecular binding (between KID and bZIP domain)¹⁰². Therefore, the activity of CREB largely depends on the phosphorylation status in the KID domain. Flanking on each side of the KID domain, two hydrophobic glutamine-rich domains (Q1 and Q2) are associated with CREB basal transcription activity. Through an interaction with the transcription factor TAFII130/135, Q1 and Q2 domains stabilize CREB by directly binding to chromatin and recruiting the RNA polymerase II complex to maintain the constitutive activity of CREB¹⁰³⁻¹⁰⁶. A structure study has shown that Q2 domain is sufficient for basal transcription activity while Q1 domain is

needed for complete constitutive function¹⁰⁴. Following Q2 domain, the C-terminal bZIP domain denotes a central core for DNA binding and dimerization. In the bZIP domain, the basic region has a high affinity to a conserved palindromic cAMP response element 5'-TGACGTCA-3' or half-site 5'-TGACG-3', which is usually located several kb of the upstream of a transcription start site^{93, 107}. Although 10,447 full and 740,390 half CREs have been identified from the human genome, in most scenarios, CREB cannot access to most of them because of the methylation status of the CpG island¹⁰⁸. This partly explains the different CREB behavior in different contexts. Besides, the bZIP domain plays an important role in dimerization. CREB with its family members, even with other proteins in the bZIP superfamily (c-jun, c-fos), has been observed to form homo- or heterodimers. CREB1-CREB1 dimers show the most potent CRE binding ability while some heterodimers work as CREB inhibitors. Interestingly, the bZIP domain also serves as a transactivation domain in response to stimulus owing to its interaction with the CREB-regulated transcriptional coactivators (CRTC). CRTC is sequestered in cytoplasm by 14-3-3 with high phosphorylation. The increase of cAMP or calcium signals allows the dissociation of CRTC from 14-3-3 and promotes its nucleus translocation and formation of the CRTC (the N-terminal CREB binding domain), CREB (bZIP domain) and DNA (CRE) ternary complex¹⁰⁹. This structure diminishes the dissociation kinetics and thus stabilizes the binding between CREB and DNA. On some promoters, CRTC has been found to cooperate with CBP/p300 to synthetically facilitate CREB function¹¹⁰.

In mammalian cells, the CREB family includes three members: CREB1, ATF1 (activating transcription factor 1) and CREM (cAMP responsive element modulator), which are encoded by *CREB1*, *ATF1* and *CREM* respectively (Figure 4). They share an extensive degree of identity especially in the bZIP domain. CREB1 and ATF1 are very similar, sharing 65% structure identity. They are ubiquitously expressed in tissues and mostly play as activators. CREM, though it is largely identical to CREB, exhibits a cell-specific and inducible expression

pattern depending on various isoforms. On account of alternative promoter control or alternative exon splicing, CREM gene can produce activators or repressors. CREM isoforms with deletion of transactivation regions or/and using the alternative bZIP domain are able to behave as endogenous antagonists. They either directly bind to mono-activated CREB or form a homodimeric repressor by competing with other activated CREB dimers to transiently block

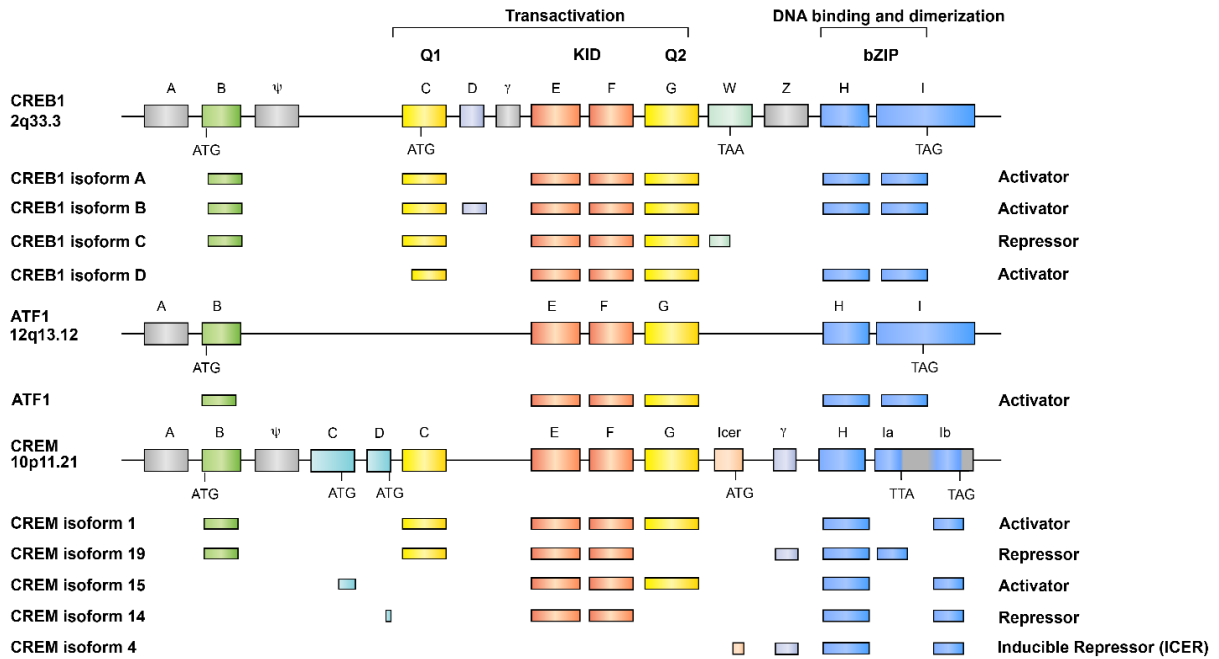


Figure 4. Genomic organization and domain structure of human CREB family.

The genomic organization of human CREB family were based on Mayr et. al 2001 and NCBI gene database (<https://www.ncbi.nlm.nih.gov/gene/1385>, 5-9-2021). Human ATF1 gene encodes one major protein product while CREB and CREM gene encode many products. In general, CREB, from N-terminus, to C-terminus, is consisted of Q1 (Glu-rich) domain, Kinase-inducible domain, Q2 (Glu-rich) domain and bZIP (basic Leucine zipper) domain. There are 4 isoforms of CREB1 and more than 50 isoforms of CREM that are generated as the result of alternative splicing. All available human CREB1 alternative splice products and representative human CREM alternative splice products with different transcriptional activity are presented. Majority CREB1 and ATF1 are activator while CREM are cell type specific and context dependent.

expression of CRE-containing genes expression¹¹¹⁻¹¹³. This regulation has been linked to CREB-dependent spatial and temporal transcriptional regulation.

1.4.2 Signal-dependent post translational modification of CREB in cancer

The stimulus-elicited activation of CREB is highly regulated by the post-transcriptional modification of CREB, majorly by phosphorylation at Ser133. Diverse signals, through various kinases, transmit to and converge on CREB by distinct phosphorylation events, resulting in a fine-tuning of the augment and endurance of the transcriptional activity (Figure 5). In past decades, CREB signaling pathway has been profoundly correlated with cancer initiation, progression, metastasis and drug resistance. In most contexts, CREB and its downstream targets serve as tumor promoters to propel cancer development.

The first and the best-characterized CREB upstream signal is cAMP-protein kinase A (PKA) signaling. In fact, the initial identification of the interaction between CRE and CREB originates from the studies of cAMP-dependent hormone biosynthesis. cAMP is an intracellular second messenger that can be triggered by hormones, neurotransmitters and other signaling molecules. Neurotransmitters and hormones depend on G-protein coupled receptors to activate adenylyl cyclase and trigger a conversion from ATP to cAMP while bicarbonate and calcium ions directly stimulate soluble adenylyl cyclase to generate cAMP¹¹⁴. The primary cAMP actions were executed by PKA dependent phosphorylation. In the basal state, inactive PKA is a heterotetrameric kinase complex composed of two regulatory subunits and two catalytic subunits when inactive. Once binding to accumulated cAMP, a conformational change of the regulatory subunits drives the release of the catalytic subunits from the inactive complex, resulting in the phosphorylation of CREB at Ser133. Aberrant PKA-CREB signaling has been often been correlated with tumor growth, metabolic alteration and therapy resistance¹¹⁵. Activated PKA-CREB can regulate cell cycle and promote tumor

progression in lung, liver and prostate cancer¹¹⁶⁻¹¹⁸. PKA-CREB pathway is also involved in the Warburg effect by regulating glycolysis related genes like Hexokinase 2^{52, 119}. In breast cancer, estrogen induced cAMP-PKA-CREB activation can stimulate glycolysis in cancer associated fibroblasts to provide extra pyruvate and lactate for tumor energetic requirement¹²⁰. In addition, by activating EZH2, PKA-CREB signaling pathway partially

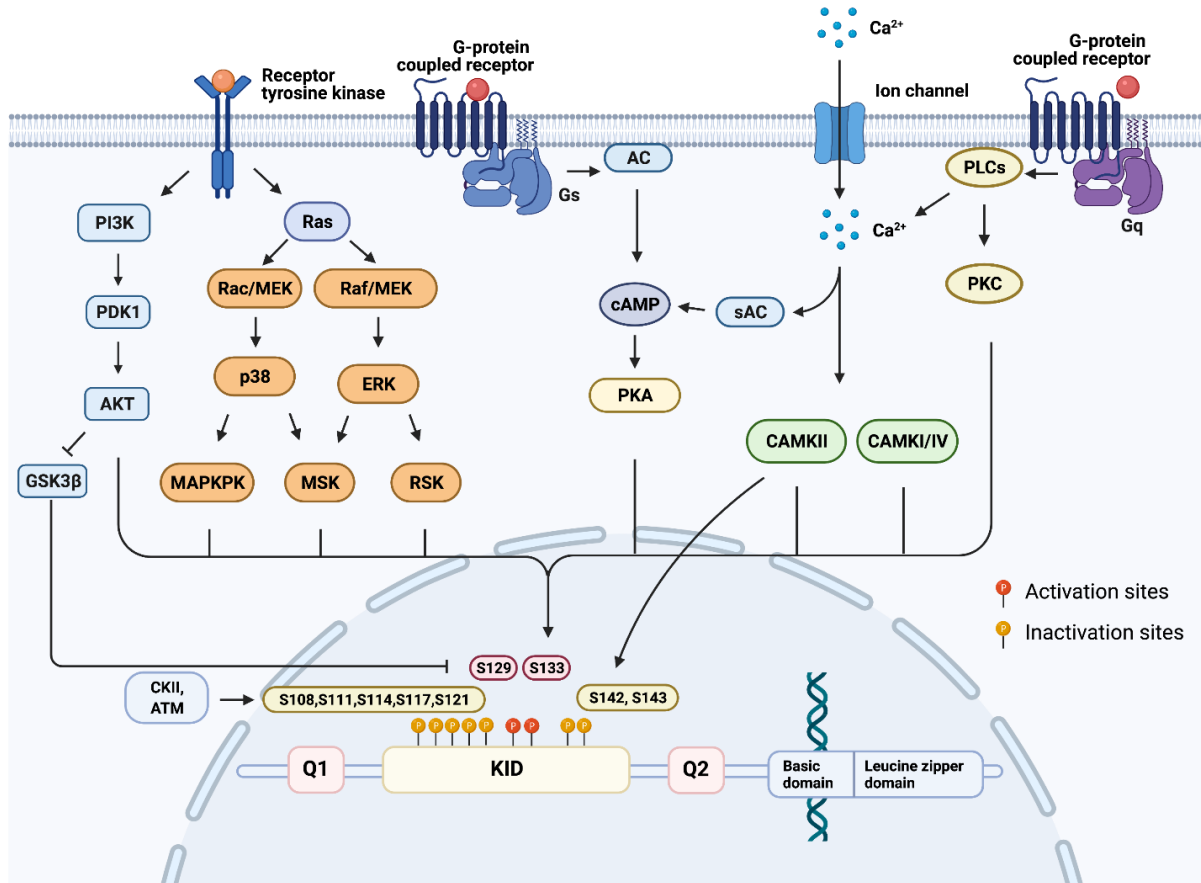


Figure 5. The direct phosphorylation regulation of CREB.

Several phosphorylation sites locate in the KID domain. Among them, Ser133 is the most important activation site and regulated by multiple upstream kinases (PKA, AKT, CAMK, MAPKPK, RSK, MSK, PKC, etc.) for CREB transcriptional activity. Ser129 is the other activation site but can be inhibited by GSK3 β . On the flanking of activation residues, two clusters of a sequential serine residues are inactivation sites. N-terminal clusters (Ser108, 111, 114, 117, 121) are regulated by CKII and ATM while C-terminal Ser142/143 are phosphorylated by CAMKII.

mediates androgen deprivation induced neuroendocrine differentiation and angiogenesis¹²¹. Similar to CREB, ATF1 is also responsive to cAMP-PKA signaling with the phosphorylation at Ser63, but may be more sensitive when it responds to cAMP¹²².

Besides PKA, mitogen-activated protein kinase (MAPK) cascade is of importance to regulate Ser133 CREB phosphorylation in many types of cancer. To date, four MAPK signaling pathways have been identified: ERK, JNK/stress-activated protein kinase, p38 MAPK and ERK5. Sequential kinases (MAPK kinase kinase kinase (MAP4K), MAPK kinase kinase (MAP3K), MAPK kinase (MAPKK), MAPK and MAPK-activated protein kinases (MAPKAPK)) drive the cascade, which can be further activated and eventually phosphorylate the downstream target like CREB^{123, 124}. Activation of ERK-CREB by Hepatitis B virus X protein has been shown to escalate the expression of FoxM1 which promotes hepatocellular carcinoma metastasis and is associated with a poor prognosis. Moreover, ERK-CREB has been linked to castration-resistant prostate cancer growth as a downstream signal of arginine vasopressin receptor 1a¹²⁵. Of interest, ERK-CREB signaling also displayed an influence on tumor microenvironment by controlling the expression and secretion of IL4 and IL10, which bring about the M2 macrophage polarization and colon cancer cell growth¹²⁶. ERK also contributes to phosphorylation of CREB at Ser129, but little is known about its role in cancer¹²⁷.

Similar to ERK, p38 MAPK pathway can regulate cancer progression partly through phosphorylation of CREB. In hepatocellular carcinoma, CD13 induced p38 signaling activation is required for CREB activation and subsequently autophagy occurrence, eventually leading to a resistance to 5-fluorouraci therapy¹²⁸. By contrast, inhibition of the p38/CREB axis has anti-proliferative and anti-migrative effects¹²⁹⁻¹³².

Importantly, the MAPK-CREB cascade is also activated in response to the accumulation of intracellular calcium. Ca²⁺ signals are able to activate the MAPK cascade by different

kinases. First, ras, as a classical regulator, has been linked between Ca^{2+} and MAPK. Stimulation of PYK2, Ras-GRF and CAMK but inhibition of Ras-GAPs seems to be the mechanism that by which Ca^{2+} induces ras¹³³. Secondly, PKA appears to be involved in MAPK activation by promoting the nuclear translocation of ERK¹³⁴. Also, protein kinase C can affect Ser133 phosphorylation through MAPK¹³⁵. In fact, PKC/MAPK/CREB signal pathway has been associated with Trichosanthen repressed HeLa cell proliferation through cell cycle arrest¹³⁶. Moreover, PKC ϵ siRNA reduces constitutive CREB1(Ser133) phosphorylation and Bcl-2 expression in breast cancer¹³⁷.

The other more closely cascade that responds to Ca^{2+} influx is CAMK signaling pathways. How Ca^{2+} activates CAMKs have been discussed in the previous section. Activated CAMKs has been demonstrated to significantly influence CREB phosphorylation by multiple knockdown and overexpression studies¹³⁸. Specifically, CAMKI and CAMK4 play their major roles on phosphorylation of Ser133. Two studies in acute myeloid leukemia have reported the contribution of CAMKI and CAMK4 on Ser133 phosphorylation, resulting in disease development^{31, 39}. The CAMKI/CREB axis is also found to promote lung and endometrial cancer cell proliferation^{139, 140}. CAMK2, however, seems to be more complicated. Though some researches have indicated that CAMK2 exerts its function on Ser133¹⁴¹, another study suggested that it has dual functions on both active site Ser133 and inactive site Ser142¹⁴². Moreover, in certain contexts, CAMK2 phosphorylates ATF1 at Ser63 instead of CREB¹⁴³. Interestingly, γ CAMK2 shuttles Ca^{2+} /CAM to the nucleus to trigger phosphorylation of CREB at Ser133¹⁴⁴. Although CAMK2 was shown to promote cell migration and proliferation, the underlined mechanism, especially whether it depends on CREB transcriptional activity, has yet to be fully explored.

In addition, phosphoinositide 3-kinase (PI3K)-Protein kinase B (AKT) signaling, one of the most recurrently aberrant pathways in human cancers, has been shown to directly

phosphorylate CREB at Ser133, and helps recruit CBP to regulate transcription for cancer survival and growth¹⁴⁵⁻¹⁴⁷. In tamoxifen resistant breast cancer, AKT-dependent CREB activation is necessary for aromatase synthesis, acting as an important enzyme for the biosynthesis of estrogens and breast cancer progression¹⁴⁸. Also, EGFR/AKT/CREB is involved in favorable changes in the pancreatic cancer microenvironment. AKT and CREB activation induced by tumor secreted REG4 triggered the polarization of tumor-associated macrophages to M2 phenotype¹⁴⁹.

Taken together, CREB can be regulated by a wide range of upstream kinases dependent on time, context, cell type and stimulus (Figure 5). While Ser133 has been intensively studied, other phosphorylation sites also play their important roles on CREB's functions. Beside phosphorylation, CREB can also be ubiquitinated, acetylated, glycosylated and SUMOylated. The crosstalk between these post-modifications contribute together to the fine-tune regulation of CREB expression and activity.

1.4.3 CREB in prostate cancer

The close correlation between CREB and prostate cancer progression, metastasis and drug resistance has been discussed over the years. In the clinic, an increased level of p-CREB has been observed in poorly-differentiated and bone metastatic prostate cancer patient samples compared with normal and benign prostate glands, indicating the correlation between the malignant level and CREB activity¹⁵⁰. Beyond the clinical evidence, the TRAMP mice and fetal globin-SV40/T-antigen mice have emphasized the potential role of CREB in tumor development. With the purpose to elucidate the mechanism of Nexrutine in prostate cancer, the reduction of AKT/CREB/cyclin D1 level was found to significantly attenuate the tumor development rate in TRAMP mice¹⁵¹. Moreover, in globin-SV40/T-antigen mice, CREB was

identified as one of the important transcription factors for carcinogenesis by putative binding site enrichment analysis¹⁵². Notably, emerging studies have suggested a fascinating connection between CREB and neuroendocrine differentiation prostate cancer. Emerging studies highlighted the role of CREB in promoting neuroendocrine differentiation phenotypic change under stimulus and treatment including IL6, epinephrine, AR antagonist, and radiation therapy^{121, 153-155}. Furthermore, this transformation is clearly correlated with therapeutic failure and drug resistance. Mechanically, CREB in prostate cancer can be regulated by many important oncogenic proteins like PKA, PAK4, AKT and HIF1^{151, 156-158}. Also, multiple proliferation, survival, anti-apoptosis, and angiogenesis related genes such as Bcl2, cyclinA1, GRK3, and TSP1 are identified as the downstream targets of CREB. Table 2 shows the full list of CREB downstream targets in prostate cancer.

Table 2. CREB downstream targets in prostate cancer.

Targets	Cell or animal model	Upstream signaling	Function	Ref
ABCG4	DU-145, PC3	Glutathione depletion-NFkb-cMyc	Doxorubicin resistance	159
Bcl2	PC3 xenograft	PAK4	Neuroendocrine differentiation and chemoresistance	156
	LNCaP, PC3	AKT	Apoptosis, PTEN induces chemosensitivity	160-162
GRK3	RWPE1, PC3	PKA	Neuroendocrine phenotype	163
PAI-1	PC3		MnTE-2-PyP reduced growth and metastasis	158

Pinin	PC3, DU145	PI3K/AKT, ERK/MAPK	Cell growth, invasion, migration and EMT	164
cyclinD1	TRAMP, PC3	AKT	Nexrutine related cancer progression	151
CYP27B1	PZHPV-7	PKA, MAPK	Vitamin D autocrine system	165
HDAC2	PC3, DU-145	PKA	Tumor angiogenesis	166
CYP11A1/ CYP17A1	PTEN null cell and mouse model	AKT-RUNX2- osteocalcin (OCN)- GPRC6A	Intratumoral androgen synthesis and tumor microenvironment remodeling	167
Cox 2	LNCaP, PC3	AKT	Nexrutine related anti- proliferative effect	168
IGF-IR	LNCaP		Proliferation	169
HK2	LNCaP	PKA	<i>De novo</i> lipid synthesis	52
EZH2 TSP1	LNCaP, NEPC	PKA	Neuroendocrine differentiation and angiogenesis	121

1.4.4 Targeting CREB in cancer

Given the potential important function of CREB in the progression of multiple cancer types, CREB represents a promising therapeutic target for drug development. Although CREB was initially thought to be a challenging target due to a transcription factor, the CREB: CRE-DNA interaction surface, the CREB: coactivator interaction surface and CREB upstream kinases have been applied to the discovery of small molecules for treatment.

One of strategies to diminish CREB function is to perturb the interaction between CREB and DNA through the disruption of the bZIP: CRE binding. Using the National Cancer Institute diversity set of 1990 compounds, a high-throughput fluorescence anisotropy screening has

identified 12 active compounds repressing the DNA binding of CREB¹⁷⁰. Among them, NSC 12155 (surfen) has been shown to not only slow the proliferation by affecting G1 to S phase transition but also alter cellular metabolism in HER-2/neu⁺ cells. In addition, NSC 13778 and its derivatives NSC 13748 and P6981 (arylstibonic acids), despite not being specific, have potent inhibitions on CREB-DNA binding. As a result, it is very effective in clear cell sarcoma cells with EWS-ATF1 without toxicity¹⁷¹⁻¹⁷³.

2-naphthol-AS-E-phosphate (KG-501) represents another strategy which inhibits the interaction between CREB and CBP¹⁷⁴. Through an NMR-based medium-throughput screening, KG501 was identified from a preselected small molecule library containing 762 compounds. Through the structural studies of the CREB-CBP complex, a three-helix structure with a shallow hydrophobic groove was identified from the KIX domain. Notably, KG-501 interferes with the interface required for KID: KIX domain interaction by targeting the CBP KIX domain including residues that are mainly in helices $\alpha 1$ and $\alpha 2$, and a few in helix $\alpha 3$, which eventually diminishes the cAMP-CREB dependent transcription activity. Subsequent studies also found that cellular activity of KG-501 is attributed to its dephosphorylation to Naphthol AS-E, which is a cell permeable CREB:CBP inhibitor¹⁷⁵. Naphthol AS-E and its derivatives are effective for various cancer cells proliferation without toxicity to normal cells in low micromolar concentration¹⁷⁶. To get better aqueous solubility compounds, a series of compounds were designed and modified from Naphthol AS-E. Among them, 666-15 exhibits a potent inhibition on CREB transcriptional activity despite a weak ability in CREB:CBP interaction disruption¹⁷⁷. 666-15 inhibited breast cancer growth in the xenograft without significant toxicity. To date, many groups have confirmed the antitumor effect of 666-15 on various cancers. In acute myeloid leukemia, activation of CREB is required for cancer survival and treatment with 666-15 decreased the CREB phosphorylation and cell growth in colony formation assay³⁹. 666-15 also has a profound influence on tobacco exposure-induced tumor associated macrophage

recruitment and Treg expansion and activation, which in turn restricted pancreatic tumor progression¹⁷⁸. Additionally, a recent study corroborated that mutant p53 and KRAS induced CREB1 contribute together for FOXA1 activation. As a result, 666-15 robustly lessened FOXA1 and b-catenin expression and obstructed PDAC metastasis¹⁷⁹. More interestingly, an enhancer compound 653-47 has been identified to boost the activity of 666-15¹⁸⁰.

Regarding the essential role of p-CREB in CREB transcriptional activity, depression of the upstream pathway (kinases) became the third promising pharmacological strategy to inhibit CREB function, especially aberrant CREB upstream kinases, like PKA, AKT, MAPK, AMPK and CAMK which are often observed in cancer development.

Recently, CJMJD3/UTX demethylase inhibitor GSK-J4 has been shown to impede CREB activity by affecting CREB protein stability, which might represent a novel strategy for CREB inhibitor design⁹⁵.

Chapter 2

Materials and Methods

In this chapter, material was in part from “Lin, C., Blessing, A. M., Pulliam, T. L., Shi, Y., Wilkenfeld, S. R., Han, J. J., ... & Frigo, D. E. (2021). Inhibition of CAMKK2 impairs autophagy and castration-resistant prostate cancer via suppression of AMPK-ULK1 signaling. *Oncogene*, 40(9), 1690-1705.”, with permission from Nature Publishing Group.

Mouse models and strains

The conditional *Camkk2* floxed and *Pten* floxed, TRAMP and *Pb-Cre4* mouse models have been previously described¹⁸¹⁻¹⁸⁴. TRAMP, *Pten*^{fl/fl}, *Pb-Cre4* mice were purchased from Jackson Laboratories (stock number: 003135, 004597, 026662). *Camkk2*^{fl/fl} mice are gifted from Dr. Anthony Means (Baylor College of Medicine). Deletion of *Camkk2* was directed to prostate by breeding *Camkk2*^{fl/fl} mice with *Pb-Cre4* mice. *Pb-Cre4*, *Camkk2*^{fl/fl} mice were then crossed with TRAMP to acquire *Pb-Cre4*, *Camkk2*^{fl/fl}, TRAMP^{Tg/+} mice. In the experiment, *Pb-Cre4*, *Pten*^{+/+} littermates were used as controls for *Pb-Cre4*, *Pten*^{fl/fl} mice; and *Pb-Cre4*, *Camkk2*^{+/+}, TRAMP^{Tg/+} littermates were used as controls for *Pb-Cre4*, *Camkk2*^{fl/fl}, TRAMP^{Tg/+} mice. All these mouse strains were generated in a C57BL/6 background and backcrossed into C57BL/6 background for 3 generations to attain the genetic identity of offspring. All genotyping was performed by PCR/qPCR analysis, and the protocol has been reported^{181, 184, 185}. All experimental mice were males, and mouse prostate glands or tumors were harvested at 15 and 40 weeks after birth, as indicated in the corresponding legend. NSG mice used in chapter 3 were purchased from either The Jackson Laboratory (stock number: 005557) or the University of Texas MD Anderson Cancer Center Experimental Radiation Oncology Breeding Core. Nude and NSG mice used for chapter 4 were purchased from the University of Texas MD Anderson Cancer Center Experimental Radiation Oncology Breeding Core. Fox Chase severe combined immunodeficient (SCID) mice were purchased from Charles River (strain code: 236). All mice were born (transgenic mice) and maintained (both transgenic and

experimental mice) in a dedicated pathogen-free environment. All animal experiments were approved by and conducted under the Institutional Animal Care and Use Committee (IACUC) at the University of Texas MD Anderson Cancer Center and the University of Houston according to NIH and institutional guidelines.

Xenografts

Xenografts were performed on 6-8 weeks old male NSG/Nude mice. Castrations were conducted one week before injections (7 weeks). 1×10^6 cells in 200 μ l DPBS: Matrigel® (1:1 vol/vol) were injected subcutaneously into flanks (8 weeks). When tumors were palpable, tumor size was measured by calipers. Tumor volume was calculated by the formula: length x width²/2.

In Chapter 3, castrated NSG mice bearing 22Rv1-sh*CAMKK2* cells were randomized into normal/control or doxycycline-containing (625 mg/kg, Envigo) diet groups. Then, shRNA expression with surrogate red fluorescent protein (RFP) was tracked by fluorescence (IVIS Spectrum In Vivo Imaging System). For chloroquine xenograft experiments, mice were randomly grouped into vehicle control or chloroquine intraperitoneal (IP) treatment when the tumor volume reached 100 mm³. All mice in Chapter 3 were sacrificed when tumor lengths in the control group reached 1.5 cm or signs of morbidity were observed.

In Chapter 4, castrated nude mice with C4-2 cells were randomly grouped into vehicle control (5% Tween 80 and 1% N-methylpyrrolidone in PBS), 2 mg/kg and 10 mg/kg 666-15 IP treatment groups when the tumor volume reached 100 mm³. Mice were treated five days on and two days off a week (treated from Monday to Friday) and tumor size were measured three times a week (Monday, Wednesday and Friday). Tumors and major organs (heart, liver, spleen, lung and kidney) were collected when tumor lengths in the control group reached 1.5

cm or signs of morbidity were observed. For the *CREB* KO/DKO experiment, castrated mice were injected with corresponding cells and tumor sizes were monitored one time a week after cell injection. The observation of 0.5 cm tumor lengths was recorded as “tumor start”. When tumor lengths reached 1.5 cm, mice were recorded as “death” and tumors were harvested.

Patient-derived Xenograft (PDX)

All PDX models (180-30 and 274-2) were gifted from Dr. Nora Navone. PDX seeds from Dr. Nora Navone lab (F1 in Frigo lab) ¹⁸⁶ were implanted subcutaneously into the flank pocket of 7 weeks old SCID mice to generate the F2 PDX model. Specifically, mice were weighed and anesthetized with isoflurane inhalation, followed by being shaved to expose a large area across their back and wiped with 70% isopropanol and chlorhexidine scrub at implantation site. A small nick incision (~0.6 cm) in the back area was made and subsequently applied a glass micro-dissector to make a pocket. PDX seed (~0.5 cm) was then placed in the pocket as far down as possible to ensure it did not pop out of the pocket. After implantation, 1~2 wound clips were applied on the incision. Depending on the growth rate and the viability of the seeds, F2 PDXs were generally palpable for 2~4 weeks and then tumors were monitored weekly by caliper. Once F2 tumor is generated (tumor length ~1.5 cm), tumor was harvested fresh and sequentially passaged to five mice. Depending on the number of F1 seeds and the required number of experimental mice, F2 or F3 PDXs were used for the final experiments. For PDXs 180-30 and 166-1, mice were randomly grouped into vehicle control (5% Tween 80 and 1% N-methylpyrrolidone in PBS) and 10mg/kg 666-15 IP treatment. For PDX 274-2, mice were randomly grouped into vehicle control (5% DMSO, 30% PEG 400 and 10% Tween-80 in PBS), 10mg/kg enzalutamide and 10mg/kg 666-15 IP treatment. Mice were treated five times a week (Monday to Friday) and tumor sizes were measured twice a week. Tumors as

well as major organs (heart, liver, spleen, lung and kidney) were collected when tumor lengths in the control group reached 1.5 cm or signs of morbidity were observed.

Histology and immunostaining

One hour before harvesting the tumor, mice were intraperitoneally injected with 100 mg/kg BrdU. Half of the tumor sample was snap frozen while the other half was immediately fixed in 4% paraformaldehyde (PFA) overnight at 4°C. Following 3 times PBS wash after overnight fixation, tissue/tumor samples were then transferred and stored in 70% ethanol until paraffin processing. Paraffin processing of tissue was conducted by the University of Texas MD Anderson Cancer Center Department of Veterinary Medicine and Surgery Research Animal Support Facility. When staining, paraffin slides were rehydrated and further processed with antigen retrieval in citrate buffer for immunohistochemistry (IHC) staining. Peroxidase blocking was performing in 1% H₂O₂ plus 10% MeOH solution. Slides were then blocked with goat serum and incubated overnight with primary antibody. The catalog number and dilution strategy of primary antibodies were listed in Table 3. After washing with PBST (PBS with 0.02% Tween 20), the corresponding secondary antibodies were incubated for 30 minutes. Sections were developed by DAB. For hematoxylin and eosin staining (H&E staining), rehydrated sections were stained with hematoxylin solution first. After “blued” by rinsing in tap water, slides were destained with 1% acid alcohol. Subsequently, sections were washed and stained with eosin (mostly performed by the University of Texas MD Anderson Cancer Center Department of Veterinary Medicine and Surgery Research Animal Support Facility). Both IHC and H&E stained slides were dehydrated (ethanol), cleared (xylene) and mounted before imaging. Images were collected by a Nikon ECLIPSE Ci-L or Olympus BX51 microscope and staining intensity was scored by Pathologists Dr. Michael Ittmann, Dr. Elizabeth Whitley or Image J software (Plugin: Colour Deconvolution¹⁸⁷).

Apoptotic cells were detected by TUNEL staining using the *In Situ* Cell Death Detection Kit, Fluorescein following the manufacturer's instructions. In detail, rehydrated tissue sections (same as IHC) were incubated with Proteinase K solution for 30 min at 37°C. After PBS wash, sections were incubated with TUNEL reaction mixture for 60min at 37°C and then analyzed by a fluorescence microscope (Olympus BX51 microscope). Analysis was done on 3-6 acquired fields per section and data were averaged.

Cell lines

LNCaP, VCaP, 22Rv1, RWPE1 and HEK293T cell lines were obtained from American Type Culture Collection (CRL-1740, CRL-2876, CRL-2505, CRL-11609 and CRL-3216). C4-2 and LNCaP-ARV7 cells were obtained from Dr. Nancy Weigel (Baylor College of Medicine). LNCaP-42DENZR and 16DCRPC cells were obtained from Dr. Amina Zoubeidi (Vancouver Prostate Centre, Vancouver, British Columbia, Canada). C4-2B cells were obtained from Dr. Sue-Hwa Lin. LNCaP cells were routinely cultured in RPMI-1640 supplemented with non-essential amino acids solution (1X), sodium pyruvate solution (1X) and fetal bovine serum (10%). VCaP cells were cultured in DMEM supplemented with non-essential amino acids solution (1X), sodium pyruvate solution (1X) and fetal bovine serum (10%). LNCaP-ARV7, LNCaP-42DENZR, 16DCRPC cells, and C4-2B cells were cultured in RPMI-1640 supplemented with fetal bovine serum (10%). HEK293T cells were cultured in DMEM supplemented with fetal bovine serum (10%). C4-2 cells were cultured in IMEM supplemented with fetal bovine serum (5%). RWPE1 cells were cultured in Keratinocyte Serum Free Medium (K-SFM). Mycoplasma-free tests were routinely performed by MycoAlert Mycoplasma Detection Kit. In all experiments, cells were steroid-starved in corresponding phenol red-free medium containing 10% charcoal stripped-FBS (5% CS-FBS for C4-2 cells, RWPE1 cells

were switched to 10% CS-FBS + phenol red-free RPMI-1640 medium) for 72 hours before treatment unless otherwise noted.

Expression vectors and sgRNA design

pcDNA4-VPS34-Flag was a gift from Dr. Qing Zhong (Addgene plasmid #: 24398). pcDNA3.1-hULK1 and 4SA mutant were gifts from Dr. Mondira Kundu (St. Jude Children's Research Hospital). Enhanced GFP-LC3 and mCherry-GFP-LC3B constructs have been previously described⁸⁵. pDONR221-CREB1 plasmid was obtained from DNASU plasmid repository (HsCD00040022) and used to generate CREB^{WT} with PAM sequence mutant and CREB^{S133A} mutant plasmids by Q5® Site-Directed Mutagenesis Kit (primers were listed in table 5). Modified targets of interest (CREB1^{WT} or CREB1^{S133A} mutant) were transformed from pDONR-221 to MSCV-IRES-GFP by gateway cloning strategy. pcDNA3.1-CAMKI construct was generated by pDONR221-CAMKI (DNASU plasmid repository, HsCD00296769) and pcDNA3.1-nv5-DEST by gateway cloning strategy. pCMV6-PNCK plasmid was purchased from OriGene (RC229215). GIPZ Lentiviral shRNA targeting empty vector, *CAMKK2* and *CREB1* were purchased from Baylor College of Medicine cell-based assay screening service. shRNAs were then cloned to pINDUCER10 plasmid (gifted from Dr. Stephen J. Elledge, Baylor College of Medicine) to generate pINDUCER10-CAMKK2 plasmid and pINDUCER10-*CREB1* plasmids as previously described^{58, 188}. To generate PGL 4.26-CRE-luc construct, 4xCRE fragments (TGACGTCA, gBlocks from IDT, sequence was list in table 5) was cloned to pGL4.26 vector (Promega, E8441) by NheI and HindIII restriction sites.

The pCW-Cas9 and pLX-sgRNA were gifts from Drs. Eric Lander & David Sabatini (Addgene; plasmids numbers: 50661, 50662)¹⁸⁹. pLX-sgRNA plasmid was modified to remove the extra Esp3I restriction site, which enables flanking corresponding gRNAs into it by simple

restriction digestion and ligation. Oligos of sgRNAs targeting *CAMKK2/CREB1/ATF1* were designed by <http://crispor.tefor.net/> and synthesized by Sigma (listed in Table 3). SgRNAs of *CAMKK2* were designed to target the conserved exon of the human *CAMKK2* gene and sgRNAs of *CREB1/ATF1* were designed to target exon 2 or 3 of the human *CREB1/ATF1* genes.

Generation of overexpression CRISPR/Cas9 knockout (KO) cells

pCW-Cas9 was co-transfected with lentiviral packaging plasmids into actively growing HEK293T cells using Lipofectamine 2000 transfection reagent. After 48 hours, medium containing virus was collected, filtered and added to the target cells with 8 µg/ml polybrene. Virus-medium was replaced by fresh medium with 1 µg/ml puromycin after 48 hours, which was used to select doxycycline-inducible Cas9 expressing target cells. Cas9 expression was then validated by western blot following doxycycline treatment (200~1000ng/ml) and the optimal concentration of doxycycline was determined. pLX-*CAMKK2* sgRNAs. pLX-*CREB1* sgRNAs and pLX-*ATF1* sgRNAs were transfected into Cas9-inducible cells by the same lentiviral transduction strategy before selection with 10 µg/ml blasticidin. Cells expressing inducible Cas9 and sgRNAs were first treated with doxycycline for 7 days. After, single clones were isolated and screened to establish knockout cells. Each clone was validated by sanger sequencing of the Cas9 edited region and western blotting of protein of interest. Double knockout (DKO) cells were established by sequential transduction method. In detail, C4-2 and 22Rv1 *CREB1* single KO (SKO) cells were first established and validated. Coincidentally, sanger sequence results showed that one C4-2 *CREB1* KO subclone has the same genotype as one 22Rv1 *CREB1* KO subclone. Therefore, the SKO subclones with the same genotype (one from C4-2 and one from 22Rv1) were selected to transfect with two sgRNAs targeting *ATF1* respectively. Single clones of the DKO were selected and validated same as the SKO.

Generation of knockdown and overexpression cells

Lentiviral transduction strategy was used to generate LNCaP-sh*CREB1*, C4-2 sh*CAMKK2* and 22Rv1 sh*CAMKK2* cells. Briefly, the target plasmid was cotransfected with lentiviral packaging plasmids pMDL-G/P-RRE, pCMV-VSVG and pRSV-REV in a 5:2.5:1.5:1 ratio to activate HEK293T cells to acquire viral particles. 48 hours post transfection, medium containing virus was collected, filtered through 0.45 µm syringe filter and added to the target cells with 8 µg/ml polybrene in regular growth medium. After another 48 hours, successfully transduced cells were selected with corresponding antibiotics (puromycin: 1 µg/ml for shRNA; G418: 1400 µg/ml for LNCaP overexpression, 800 µg/ml for VCaP overexpression). Various concentrations of doxycycline were tested (200-1600 ng/ml for shRNA, 20-100 ng/ml for overexpression) to select the optimal induction condition for experiments.

Retroviral transduction strategy was used to establish *CREB1* WT/S133A add back cells. The MSCV-IRES-GFP-*CREB1*/S133A construct was cotransfected with PCL10A in 1:1 ratio by FuGENE® transfection reagent and the viral supernatant was collected as in the lentiviral method. After 48 hours, yield sorting and purity sorting were performed to get GFP positive cells by BD FACS Aria™ Fusion Cell Sorter at the University of Texas MD Anderson Cancer Center Flow Cytometry and Cellular Imaging Core Facility.

Small interfering RNA (siRNA) and transient plasmid transfections

All transfections were conducted as previously described^{25, 85}. In brief, plasmids were transfected using Lipofectamine® 2000 transfection reagent according to the manufacturer's instructions. For siRNA transfection, siRNAs were purchased from Thermo Fisher Scientific or Sigma. siRNA duplex (final concentration 50 nM) and 2.5 µl Lipofectamine™ 2000 or 5ul DharmaFECT 1 transfection reagent was diluted to 100 µl Opti-MEM® I Medium separately

for 5 min. Then, the siRNA and transfection reagent were mixed together for 15 min. siRNA duplex/plasmid- transfection reagent complexes were added to 30-50% confluence cells with 800 µl experimental medium for 4-6 hours. After 72 hours, cells were collected for subsequent experiments. For CAMKI or PNCK overexpression, 1 µg of pcDNA3.1-nv5-DEST or pCMV6-PNCK plasmid was transfected into LNCaP cells after 12 hours of corresponding siRNA treatment. Cells were collected after 48 hours after overexpression plasmid transfection. All dual transfections were conducted using Lipofectamine 2000 transfection reagent.

Western blot

After the indicated treatments, cells were washed with PBS twice and protein was extracted by RIPA lysis buffer (50 mM Tris HCl pH 8, 150 mM NaCl, 1% NP-40, 0.5% sodium deoxycholate, 0.1% SDS, 1% glycerol, 5mM EDTA) supplemented with Complete Protease Inhibitor Cocktail and phosphatase inhibitor (PhosSTOP or NaF+Na₃VO₄). Lysates were incubated on ice for 30 minutes followed by centrifuging 10 minutes at 4°C. Supernatants were subsequently collected and protein concentration was determined by Bio-Rad protein assay dye reagent concentrate. 30µg of protein were subjected to gel-electrophoresis. Then, proteins were transferred onto a nitrocellulose membrane and then blocked with 5% non-fat milk in TBST (TBS+0.1% Tween-20) for 1 hour at room temperature. Membranes were then incubated with the primary antibody in blocking buffer (Table 3) overnight at 4°C. The next day, the membranes were washed with TBST for 10 minutes three times before being incubated with the corresponding secondary antibody in blocking buffer for 1 hour at room temperature. Following with three times wash, the signal was visualized with Enhance Chemiluminescent Reagents with a film developer.

RNA preparation and real-time PCR

After the indicated treatment, cells were washed with PBS twice and total RNA was isolated by Aurum™ Total RNA Mini Kit and cDNAs were synthesized by SuperScript™ III First-Strand Synthesis System according to the manufacturer's instructions. Real-time PCR samples were prepared by SYBR Green Master Mix and conducted by CFX96 Touch Deep Well Real-Time PCR System (Biorad). All primers were purchased from Sigma/IDT and listed in Table 5. The expression of target genes was normalized to RPLP0/36b4.

RNA-sequencing

RNAs for RNA-sequencing (RNA-seq) were isolated by RNeasy Plus Kits according to the manufacturer's instructions. After extraction, RNA quality and quantity were determined by Tapestation 4200 (Agilent) with High Sensitivity RNA ScreenTape Assay (Agilent) and Qubit fluorometer with Qubit RNA HS Assay Kit respectively. The RNA integrity number (RIN) for all RNA-seq samples was greater than 8. RNA-seq libraries were prepared using KAPA RNA HyperPrep Kits with Ribo Erase (Roche). Total RNA input for each library preparation was 500 ng quantified by Qubit, and PCR amplification was set with 8 cycles. The quality control of each RNA-seq library was tested by Qubit fluorometer and Tapestation 4200 before pooling. 9 libraries with different KAPA dual-indexed adaptor were multiplexed as one pool and sequenced on one lane of the Illumina HiSeq 4000 sequencing platform (Illumina) at Advanced Technology Genomics Core (ATGC) at the University of Texas MD Anderson Cancer Center, with 5% PhiX spike-in and read format of 76-8-8-76, paired-end.

RNA-sequencing analysis

Fastq files were trimmed by Trimmomatic (0.39)¹⁹⁰ and then aligned to the GRCh38 assembly using STAR (2.7.0f) two-pass alignment¹⁹¹. The transcripts abundance was counted by HT-seq (0.11.0)¹⁹². Differentially expressed genes were determined using the R package DESeq2 (1.30.1) with the following filters: absolute log fold change (LFC) ≥ 1 and adjust p value (padj) ≤ 0.01 unless otherwise noted¹⁹³. R package biomaRT was used for ID conversion and annotation. R package NMF, RColorBrewer and Venn were used for visualization.

Gene set enrichment analysis

Gene set enrichment analysis (GSEA) analysis was performed on the pre-ranked RNA-seq data generated by DESeq2 using the GSEA software tool 4.1.0 with default setting¹⁹⁴. V7.4 Hallmark, C2, C3, and C5 MSigDb collections were selected as genesets database. Significant pathways were set at p values < 0.05 and false discovery rate $q < 0.25$.

Proliferation assays

Cell proliferation assays were performed by measuring the cellular double-stranded DNA content using Hoechst 33342. Briefly, cells were plated in at least triplicates in 96 well plates at 2000~10000 cells/well. After treatment (if required), plates were collected as indicated days for DNA staining. The staining intensity was determined by at Synergy H4 microplate reader (Biotech) at Ex/Em 350/461. For the IC50 curve, the test sample data were normalized to corresponding vehicle treatment.

Clonogenic assays

Cells were plated at 5000 (LNCaP) or 1000 (C4-2 and 22Rv1) cells/well in 6-well plates. Colonies were formed for 3-4 weeks. Media and treatments were refreshed every week. Cells were fixed with acetic acid/methanol 1:7 (vol/vol) and then stained with 0.5% crystal violet. The number of visible colonies were counted. The data were representative of three independent experiments with similar results.

Immunofluorescence microscopy

For LC3 assays, GFP-LC3/mCherry-GFP-LC3 fusion constructs were expressed in cells as previously described^{85, 86}. Following treatments, cells were fixed with 4% PFA for 15 min at RT and DAPI was used as a counterstain.

Images were captured using the Olympus BX51 fluorescence microscope and cellSense imaging software. For LC3 quantification, samples were analyzed by Image J where LC3 puncta per cell were counted for 50 cells per cell line and averaged.

Transmission electron microscopy (TEM)

Cells were plated at 100,000 cells/well in 6-well plates and treated as indicated in figures/figure legends. Samples were fixed with Karnovsky's fixative solution (3% glutaraldehyde plus 2% paraformaldehyde in 0.1 M cacodylate buffer, pH 7.3) at 4 °C. Samples were further processed by the University of Texas MD Anderson Cancer Center High Resolution Electron Microscopy Core Facility.

BrdU cell cycle analysis

Cells were treated as indicated and labeled with 10 μ M BrdU 1 hour prior to collection. Cells were fixed with 70% ethanol at 4 °C overnight. After fixation, 2N HCl with 0.5% Triton-100 was used to carry out permeabilization and DNA hydrolysis. Following 1% BSA blocking, cells were stained with BrdU antibody for 1 hour followed by 30 min FITC anti-mouse secondary antibody FITC. Before measurement, cell pellets were resuspended with PI/RNase solution for 30 min. To quantify the phases of cell cycle, cells were subjected to BD LSRFortessa™ Flow Cytometer (BD) analysis (at the University of Texas MD Anderson Cancer Center Flow Cytometry and Cellular Imaging Core Facility) and gated for BrdU-FITC and PI staining populations.

Flow cytometric analysis

Cells were treated as indicated and disassociated by Accutase to generate single cell suspension. After two times PBS wash, cells were blocked with 2% FBS. And then, cells were incubated with PE anti-human PSMA (FOLH1) antibody for 1 hour. Data were collected by BD LSRFortessa™ Flow Cytometer (BD) and analyzed by FlowJo software.

Luciferase reporter assays.

To assess CREB transcriptional activity, cells were transfected with pGL4.26-CRE-luciferase reporter and β -galactosidase control vector and then treated as indicated in figures/figure legends. Before measurement, cells were lysed (25mM Tris Phosphate, 2mM EDTA, 10% Glycerol, 0.5% Triton X-100 and 2mM DTT) and the supernatant was transferred to a white plate. Luciferase activity was measured by Synergy H4 microplate reader and

normalized to β -galactosidase activity¹⁹⁵.

Statistical analysis

Statistical analyses were performed using Microsoft Excel 2013 and GraphPad Prism 8. ULK1 and MMP16 related bioinformatic analyses were generated from cBioPortal^{196, 197}. One-way or two-way ANOVAs and Student *t*-tests were used to determine the significance among groups as indicated in the figures or figure legends. Log-rank test was used to determine the significance of Kaplan-Meier curves. Grouped data were presented as mean \pm SEM unless otherwise noted. *P* values were indicated in figures or figure legends.

Table 3. The source and concentration of antibodies

Antibodies	Company	Cat. Number	Dilution
Rabbit polyclonal anti-CAMKK2	Sigma	HPA017389	1:2000
Rabbit monoclonal anti-phosphorylated AMPK(T172) (40H9)	Cell Signaling Technology	2535	1:1000
Rabbit monoclonal anti-AMPK α (D5A2)	Cell Signaling Technology	5831	1:1000
Rabbit monoclonal anti-phosphorylated CREB (Ser133) (87G3)	Cell Signaling Technology	9198	1:1000 WB 1: 500 IHC
Mouse monoclonal anti-CREB (86B10)	Cell Signaling Technology	9104	1:1000

Mouse monoclonal anti-ATF1 (25C10G)	Santa Cruz Biotechnology	sc-270	1:1000
Mouse monoclonal anti-AR (441)	Santa Cruz Biotechnology	Sc-7305	1:1000
Rabbit monoclonal anti-CAMK1 alpha (EPR2217Y)	Abcam	ab68234	1:1000
Rabbit polyclonal anti-phosphorylated CAMK1 (Thr177)	Santa Cruz Biotechnology	sc-28438-R	1:1000
Rabbit polyclonal anti PNCK	Novus Biologicals	NBP1-86652	1:1000
Mouse monoclonal anti-CAMK1 delta (C9)	Santa Cruz Biotechnology	sc-374028	1:1000
Rabbit monoclonal anti-PSMA (D7I8E)	Cell Signaling Technology	12815	1:1000 WB 1: 200 IHC
Rabbit polyclonal anti-LC3B	Cell Signaling Technology	2775	1:1000
Rabbit polyclonal anti-p62	Enzo Life Sciences	BML-PW9860-0100	1:200
Rabbit monoclonal anti-LC3A/B (D3U4C)	Cell Signaling Technology	12741	1:200 IHC
Rabbit monoclonal anti-GAPDH	Sigma	G8795	1:10000
Mouse monoclonal anti-BrdU	Calbiochem (Part of Millipore Sigma)	NA61	1:100 IHC 1:200 F
Rabbit monoclonal anti-phosphorylated ULK1 (S555) (D1H4)	Cell Signaling Technology	5869	1:1000
Rabbit polyclonal anti-ULK1 (D8H5)	Cell Signaling Technology	4773	1:1000

Rabbit monoclonal anti-ULK1 (JA58-36)	Novus Biologicals	NBP2-66765	1:1000
Rabbit polyclonal anti-phosphorylated ULK1 (S556)	Abcam	Ab203207	1:1000
Rabbit monoclonal anti-ULK1 (JA58-36)	Thermo Fisher Scientific	MA532699	1:1000
Rabbit polyclonal anti-phosphorylated PI3K Class III (S249)	Cell Signaling Technology	13857	1:200
Mouse monoclonal anti-Flag	Sigma	F1804	1:5000
PE anti-human PSMA (FOLH1) antibody	Biolegend	342504	1:200
Goat anti-rabbit IgG (H + L)-HRP Conjugate	Bio-Rad	1706515	1:2000- 1:10000
Goat anti-mouse IgG (H + L)-HRP Conjugate	Bio-Rad	1706516	1:2000- 1:5000
Mouse-on-mouse HRP polymer	Biocare Medical	MM620	1X
Goat anti-rabbit IgG secondary antibody, poly HRP conjugate	Invitrogen	B40962	1X
Donkey anti-mouse IgG (H+L) highly cross-adsorbed secondary antibody, Alexa Fluor 488	Invitrogen	A-21202	1:200
Goat anti-rabbit IgG (H+L) cross-adsorbed secondary antibody, Alexa Fluor 594	Invitrogen	A-11012	1:200

Table 4. Chemicals and commercial Kits

Chemicals	Company	Cat. Number
Chloroquine	Sigma-Aldrich	C6628
Methyltrienolone (R1881)	PerkinElmer	NLP005005MG
Doxycycline hyclate	Sigma-Aldrich	D9891
Puromycin	Sigma-Aldrich	P8833
BrdU (5-bromo-2'-deoxyuridine)	Sigma-Aldrich	B5002
Polybrene	Sigma-Aldrich	TR-1003
G418 sulfate	Gold Biotechnology	G-418-25
Blasticidin	Millipore Sigma	203350
666-15	Selleckchem	S8846
	TOCRIS	5661
Enzalutamide	Selleckchem	S2840
Apalutamide	Selleckchem	S2840
Darolutamide	Selleckchem	S7559
Matrigel® Matrix	Corning	356231
D-luciferin, sodium salt	Gold Biotechnology	103404-75-7
STO-609 acetate	TOCRIS	1551
Hoechst 33342 solution (10mg/ml)	Invitrogen	H3570
Goat serum	Dako	X090710-8
Target retrieval solution in citrate buffer	Dako	S169984-2
Lipofectamine® 2000 Transfection Reagent	Thermo Fisher Scientific	11668019
DharmaFECT 1	Horizon	T-2001

FuGENE® HD Transfection Reagent	Promega	E2311
iTaq Universal SYBR Green Supermix	Bio-rad	1725121
Global 18% Protein Rodent Diet-Control	Envigo	TD.00588
Rodent Diet (2018, 625 Doxycycline)	Envigo	TD. 01306
Commercial kits		
<i>In Situ</i> Cell Death Detection Kit, Fluorescein	Roche	11684795910
RNeasy Mini Plus Kits	Qiagen	74014
KAPA RNA HyperPrep Kit with RiboErase (HMR)	Roche	08098131702
KAPA Dual-Indexed Adapter Kit Illumina® Platforms	Roche	KK8722
NEBNext® Ultra™II RNA Library Prep with Sample Purification Beads	New England Biolabs	E7775S
NEBNext® Poly(A) mRNA Magnetic Isolation Module	New England Biolabs	E7490S
Aurum™ Total RNA Mini Kit	Bio-rad	7326820
SuperScript™ III First-Strand Synthesis System	Thermo Fisher Scientific	18080051
Q5® Site-Directed Mutagenesis Kit	New England Biolabs	E0554S
MycoAlert™ Mycoplasma Detection Kit	Lonza	LT07-118
K-SFM	Thermo Fisher Scientific	17005-042
ImmPACT® DAB Substrate, Peroxidase (HRP)	Vector Laboratories	SK-4105
DAB Quanto	Thermo Scientific	TA-060-QHDX
Qubit™ RNA HS Assay Kit	Invitrogen	Q32852

Table 5. Software

Software	Developer	Download resource
GraphPad Prism 8	GraphPad	https://www.graphpad.com/
Flowjo 10.7.1	BD	https://www.flowjo.com/solutions/flowjo/downloads
ImageJ	NIH	https://imagej.nih.gov/ij/
GSEA 4.1.0	Broad Institute	http://www.gsea-msigdb.org/gsea/downloads.jsp
R	R Core Team	https://cran.r-project.org/bin/windows/base/
Trimmomatic (0.39)	Bolger et al., 2014	http://www.usadellab.org/cms/?page=trimmomatic
STAR (2.7.0f)	Dobin et al., 2012	https://github.com/alexdobin/STAR
HT-seq ((0.11.0)	Anders et al., 2014	https://htseq.readthedocs.io/en/master/install.html
DESeq2 1.30.1	Love et al., 2014	https://www.bioconductor.org/packages/release/bioc/html/DESeq2.html
	Zhu et al., 2018 (apeglm)	https://bioconductor.org/packages/release/bioc/html/apeglm.html
cBioPortal	Memorial Sloan Kettering Cancer Center	https://www.cbioportal.org/

Table 6. The sequences of siRNAs, shRNAs, sgRNAs and primers.

Oligonucleotides	Sequence
<i>siRNAs</i>	
AR siRNA-1	5'- CCCUUUCAAGGGAGGUUACACCAAA -3'

AR siRNA-2	5'- GACUCCUUUGCAGCCUUGCUCUCUA -3'
AMPK siRNA-1	5'- CACAGAAGGAUUUAAAUAUUGAGGG -3'
AMPK siRNA-2	5'- ACCAUGAUUGAUGAUGAAGCCUUA -3'
AMPK siRNA-3	5'- UUAAGGCUUCAUCAUCAUCAUGGU -3'
CAMK1 α siRNA-1	5'- GAGAAUGAGAUUGCUGUCCUGCACA -3'
CAMK1 α siRNA-2	5'- UGGGCAUUGUACACCGGGAUCUCAA -3'
CAMK1 α siRNA-3	5'- AUACAGCUCUAGAUAAAGAAtt -3'
CAMK1 α siRNA-4	5'- AGAUUUUGAAGGCCGAGUAAtt -3'
PNCK siRNA-1	5'- CGAAGAUCAUCAUGGUCUCUGA -3'
PNCK siRNA-3	5'- GAGGACAUCAGCAGCGUCUACGAGA -3'
PNCK siRNA-4	5'- GAAGAUCAUGGUCUCUGACUUUGGA -3'
CAMK1 δ siRNA-1	5'- CAGGCUAUGUCGCUCCUGA -3'
CAMK1 δ siRNA-2	5'- CUGUGGAACUCCAGGCUAU -3'
ULK1 siRNA-1	5'- GCAUCGGCACCAUCGUCUtt -3'
ULK1 siRNA-2	5'- GCAUGGACUUCGAUGAGUUtt -3'
<i>shRNAs</i>	
CAMKK2 shRNA	5'- GGCATCGAGTACTTACACT -3'
CREB1 shRNA-1	5'- ATTCTTTCTTCTTTCTACG -3'
CREB1 shRNA-1	5'- ATTTTGTCTTTCAGGTTGT -3'
<i>sgRNAs</i>	
CAMKK2 sgRNA	5'- TGGAAGGTTTGATGTCACGG -3'
CREB1 sgRNA-1	5'- CAGCTGTACTAGAGTTACGG -3'
CREB1 sgRNA-2	5'- GTTCTCGGCTCCAGATTCCA -3'

ATF1 sgRNA-1		5'- CTCTGACGTGGTACTCTTGT -3'
ATF1 sgRNA-2		5'- GCGCCGTGCTAGGATCCCGT -3'
<i>Primers (qPCR)</i>		
CAMK1 α	Forward	5'- TGCTGTCCTGAACAAGATCAA -3'
	Reverse	5'- AGCCTTTTTCCACAATACGGT -3'
PNCK	Forward	5'- TGCTCCGTAGGATCAGTCACC -3'
	Reverse	5'- GCGTGGCATAACAGGAGGTT -3'
CAMK1 γ	Forward	5'- CAATGGGTGCGAAAGGAAGAA -3'
	Reverse	5'- GCTTCCCAGTCAGTCTTTGC -3'
CAMK1 δ	Forward	5'- GGGCAAAGGAGATGTGATGT -3'
	Reverse	5'- CAGTCAACGGCTTTGCTGTA -3'
CAMK4	Forward	5'- CTTCTTCGCCTCTCACATCCA -3'
	Reverse	5'- CATCTCGCTCACTGTAATATCCC -3'
36b4	Forward	5'- GGACATGTTGCTGGCCAATAA -3'
	Reverse	5'- GGGCCCGAGACCAGTGTT -3'
FOLH1	Forward	5'- CAAGCAGCCACAACAAGTATGC -3'
	Reverse	5'- GAAGGGTCCACTTTGCTTTCAA -3'
MMP16	Forward	5'- CGGAACGGAGCAGTATTTCAA -3'
	Reverse	5'- CGCAGCACTGACATTCTGG -3'
<i>Primers (molecular cloning)</i>		
S133A mutation	Forward	5'- AAGGAGGCCTGCCTACAGGAA -3'
	Reverse	5'- GAAAGAATTTCCCTTCGCTTTTG -3'
PAM mutation (CREB1 sgRNA-2)	Forward	5'- CCACCATGACTATGGAATCTG -3'

	Reverse	5'- AGCCTGCTTTTTTGTACAAAG -3'
gBlock-4xCRE	5'- CAGTGAGCTAGCGTCGACAGCCTGACGTCAGAGAGCCTGACGT CAGAGAGCCTGACGTCAGAGAGCCTGACGTCA-3'	
<i>Primers (Genotyping)</i>		
CREB1 KO-1 cells	Forward	5'- CTTGGGAAGAGCTGAAAAGGATAGGG -3'
	Reverse	5'- CAAACCCAAAGGAAAGATCTCTCCAAAGA -3'
CREB1 KO-2 cells	Forward	5'- GAGGCGGGAGGATCACTTGAGC -3'
	Reverse	5'- CTCTTGGAACGTATTCCTCTAGGAAGAG -3'
ATF1 KO-1 cells	Forward	5'- GCCTGGCCTTTGCTTGTTTTGT -3'
	Reverse	5'- CCATTGCTACCAGTTCTTTTCCATTGA -3'
ATF1 KO-2 cells	Forward	5'- CTTGGGAAGAGCTGAAAAGGATAGGG -3'
	Reverse	5'- CTCATCCAGTCTCATGGCTTTAAGGAC -3'
CAMKK2 KO cells	Forward	5'- TCCCTGCCTGTCACATAGGATG -3'
	Reverse	5'- GCCTGTGTGCGTTGGGTTTCT -3'

Table 7. Sanger sequence of WT and CRISPR-Cas9 KO cells.

Cells	Sequence
C4-2	
CAMKK2 WT	5'- CCGTGACATCAAACCTTCCA -3'
CAMKK2 KO-1	5'- CCG—ACATCAAACCTTCCA -3' (deletion)
(Heterozygous)	5'- CCG G TGACATCAAACCTTCCA -3' (insertion)
CAMKK2 KO-2 (Homozygous)	5'- CCG I TGACATCAAACCTTCCA-3' (insertion)
CREB1 WT (exon2)	5'- TGGAATCTGGAGCCGAGAAC -3'
CREB1 KO-1	5'- TGG-ATCTGGAGCCGAGAAC -3' (deletion)

(Homozygous)	
CREB1 WT (exon3)	5'- CCGTAACTCTAGTACAGCTG -3'
CREB1 KO-2 (Homozygous)	5'- CCG-AACTCTAGTACAGCTG -3' (deletion)
ATF1 WT (exon3)	5'- CTCTGACGTGGTACTCTTGT -3'
ATF1 KO-1 (Homozygous)	5'- CTCTGACGTGGTACTCTT T GT -3' (insertion)
ATF1 WT (exon2)	5'- GCGCCGTGCTAGGATCCCGT -3'
ATF1 KO-2 (exon2) (Heterozygous)	5'- GCGCCGTGCTAGGATCC G CGT -3' (insertion)
	5'- GCGCCGTGCTAGGAT GGG CGT -3' (insertion)
CREB1 ATF1 DKO-1 (CREB1 exon 2 Homozygous ATF1 exon 3 Heterozygous)	CREB1: 5'- TGG-ATCTGGAGCCGAGAAC -3' (deletion)
	ATF1: 5'- GCGCCGTGCTAGGAT-CCGT -3' (deletion)
	5'- GCGCCGTG-----CGT -3' (deletion)
CREB1 ATF1 DKO-2 (CREB1 exon 2 Homozygous ATF1 exon 2 Heterozygous)	CREB1: 5'- TGG-ATCTGGAGCCGAGAAC -3' (deletion)
	ATF1: 5'- CTCTGACGTGGTACTCTTGT (WT)
	5'- CTCTGACGTG----- TCC CACG TCAACT-3' (deletion+substitution)
22Rv1	
CREB1 KO-1 (Homozygous)	5'- TGG-ATCTGGAGCCGAGAAC -3' (deletion)
CREB1 KO-2 (Heterozygous)	5'- CCG G TAACTCTAGTACAGCTG -3' (insertion)

5'- CCGG-----CTG -3' (deletion)

Red dashes and letters indicate the identified mutations.

Chapter 3

Inhibition of CAMKK2 Impairs Autophagy and Castration-Resistant Prostate Cancer via Suppression of AMPK-ULK1 Signaling

In this chapter, material was from “Lin, C., Blessing, A. M., Pulliam, T. L., Shi, Y., Wilkenfeld, S. R., Han, J. J., ... & Frigo, D. E. (2021). Inhibition of CAMKK2 impairs autophagy and castration-resistant prostate cancer via suppression of AMPK-ULK1 signaling. *Oncogene*, 40(9), 1690-1705.”, with permission from Nature Publishing Group.

3.1 Introduction

Macroautophagy, herein referred to as autophagy, is a highly conserved process whereby cellular components are captured and delivered to a double membrane vesicle known as an autophagosome, and subsequently degraded by the lysosomal system¹⁹⁸. Autophagy can function as a survival mechanism in response to stress by recycling the lysosomal breakdown products towards essential processes. Autophagy can also serve as a cellular quality control mechanism by removing damaged organelles and toxins. Therefore, autophagy is of importance in physiological processes as well as diseases such as cancer¹⁹⁹. However, the role of autophagy in cancer is complicated and context dependent²⁰⁰⁻²⁰³. For example, autophagy can protect cells and tissues from damage and impair malignant transformation^{204, 205}. Conversely, in more advanced cancers, autophagy can enable cells to evade apoptosis in hypoxic and nutrient-deficient environments as well as promote drug resistance²⁰⁶⁻²⁰⁹. In prostate cancer, studies from our laboratory and others using cell lines, xenografts and genetic mouse models indicate that autophagy can promote disease progression^{83-86, 89-91, 210}. This included various studies demonstrating that chloroquine could inhibit prostate cancer progression^{85, 90, 91, 211}. These preclinical data provided the rationale for a series of clinical trials (NCT04011410, NCT00726596, NCT00786682, NCT03513211, NCT01828476, NCT02421575, NCT01480154) that

tested the efficacy of chloroquine derivatives such as hydroxychloroquine in men with prostate cancer²¹². Chloroquine and hydroxychloroquine were chosen because they 1) are already FDA-approved for the treatment of malaria and rheumatological disorders and 2) have been demonstrated to impair autophagic flux by increasing lysosomal pH and decreasing autophagosome-lysosome fusion^{213, 214}. Hence, chloroquine and hydroxychloroquine represented potential clinical grade inhibitors of autophagy that could be rapidly repurposed for the treatment of cancer. To date, however, these trials, as well as similar trials in other tumors types, have yielded mixed results²⁰¹. To that end, a major challenge has been achieving high enough concentrations of chloroquine or hydroxychloroquine in patients to consistently block autophagy without major side effects²⁰². The chloroquine-mediated side effects may in part be due to the mechanism of action of this drug. Chloroquine-like compounds inhibit autophagy by blocking the late lysosomal step. Since lysosomal function is required for processes beyond autophagy, this indicates that chloroquine is not specific for autophagy. Hence, I speculate that targeting other steps in autophagy could provide an improved therapeutic window.

We previously demonstrated that androgens, in an AR-dependent manner could increase autophagy and autophagic flux through multiple mechanisms^{85, 86}. These included indirect activation of autophagy through increases in reactive oxygen species (ROS) and the expression of several core components of the autophagic machinery. Given AMPK's known link to autophagy^{72, 215, 216} and our previous findings that AR could increase AMPK activity in a CAMKK2-dependent manner^{14, 25}, I sought to

determine whether the increased CAMKK2 observed in AR+ prostate cancer could be driving disease progression in part through activating autophagy. I also reasoned that delineation of this signaling cascade, combined with the restricted expression profile of CAMKK2 and tolerance for its systemic inhibition in mice^{15, 217}, could nominate alternative ways to safely block autophagy in men with prostate cancer.

3.2 Results

3.2.1 Chloroquine impairs CRPC xenograft growth

To initially assess the effect of chloroquine in a preclinical model of CRPC, castrated NSG mice were injected with CRPC 22Rv1 cells stably expressing firefly luciferase (22Rv1-fLuc). When tumors became palpable, mice were randomized to PBS/control and chloroquine treatment groups (Figure 6A). The tumors were monitored by bioluminescence imaging (BLI) and caliper measurements until the maximum allowable size. In the first two weeks, the BLI clearly showed inhibition of tumor growth by chloroquine (Figure 6B). However, the bioluminescence intensity lost its sensitivity once the tumors grew large (data not shown), which likely resulted from a lack of oxygen or necrosis in the center of the large tumors. Despite this, the tumor volume demonstrated that chloroquine treatment as expected decreased tumor growth rate (Figure 6C). The decreased tumor growth rate corresponded to a prolonged survival (Figure 6D). Compared to the vehicle group, fewer cell nuclei were stained, suggesting the breakdown of chromatin and therefore fewer viable cells (Figure 7 H&E). As expected, chloroquine treatment increased both p62 and LC3B accumulation (Figure 7), indicating impaired autophagic flux. The reduced tumor growth appeared to be a product of reduced proliferation and increased cell death as assessed by BrdU and TUNEL staining, respectively (Figure 7). These observations suggest that inhibiting autophagy using

chloroquine can reduce proliferation and increase cell death, ultimately decreasing CRPC growth and prolonging survival.

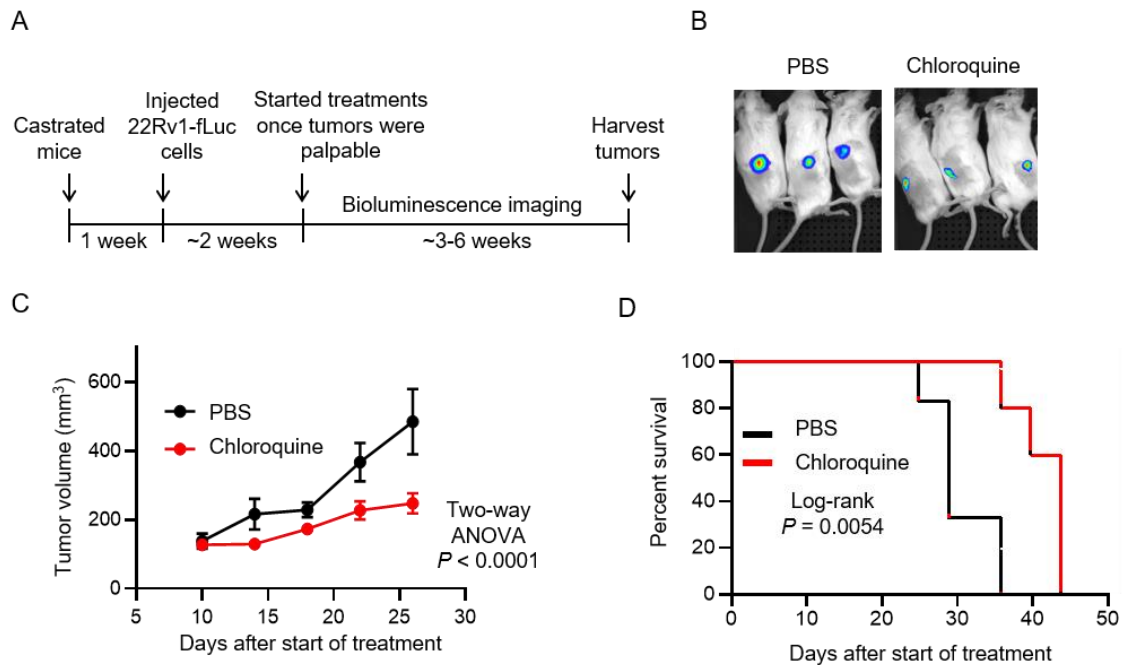


Figure 6. Chloroquine inhibits castration-resistant prostate cancer (CRPC) growth *in vivo*.

(A) Schematic of xenograft study using CRPC 22Rv1-fLuc cells in castrated NSG mice treated via vehicle (PBS) or 60 mg/kg/day chloroquine (PBS: n=6, chloroquine: n=7). (B) Bioluminescence imaging of six representative mice bearing tumors. PBS = vehicle. (C) Tumor growth curves of 22Rv1-fLuc xenograft mice treated with vehicle (PBS) or chloroquine. (D) Kaplan-Meier survival curve of 22Rv1-luc xenograft mice following chloroquine treatment.

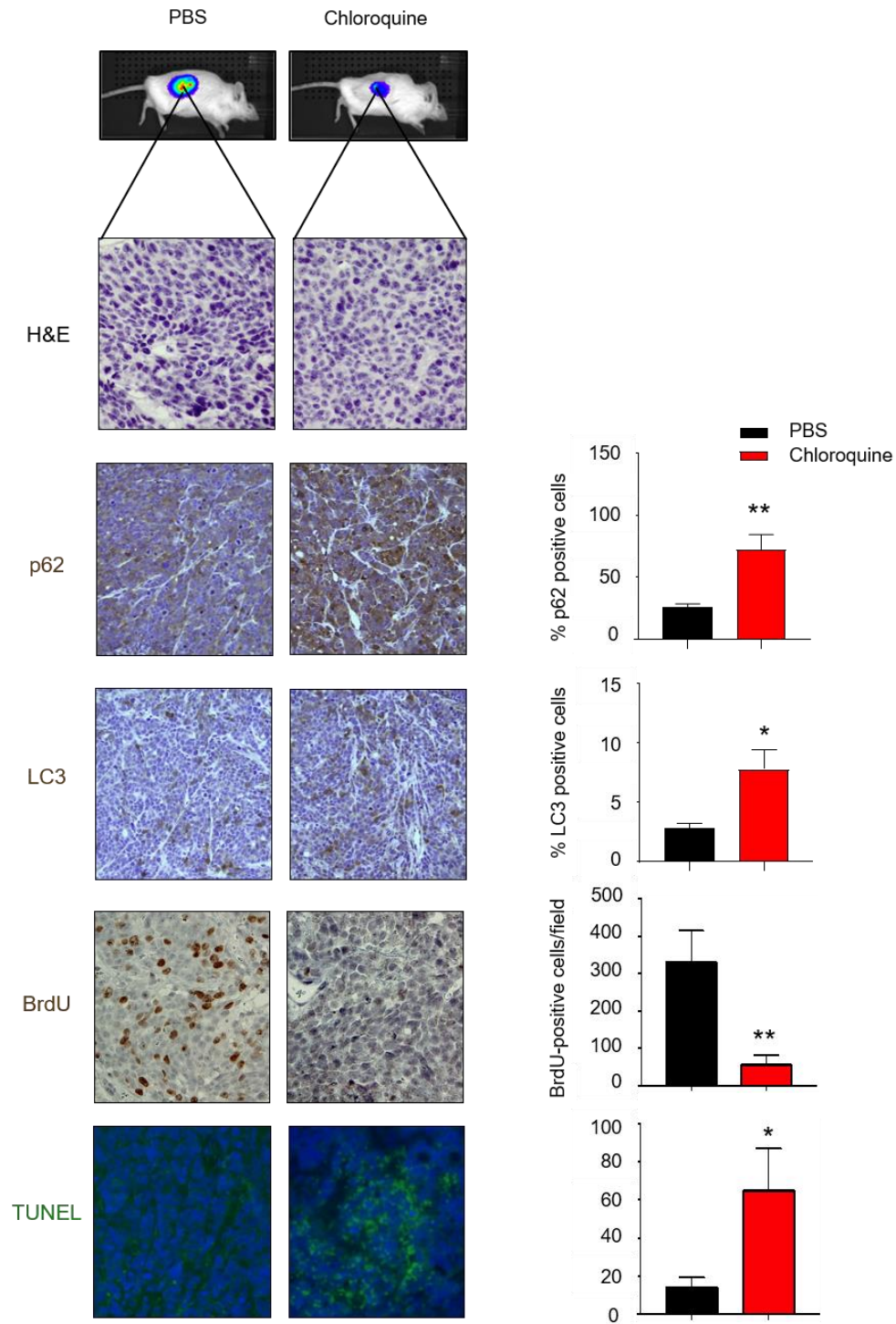


Figure 7. Histological staining of tumor samples from chloroquine treated mice.

H&E, p62, LC3, BrdU and TUNEL staining in the xenograft tumors (*left*). Quantification of p62, LC3, BrdU and TUNEL staining (*right*). * $P < 0.05$, ** $P < 0.01$.

3.2.2 CAMKK2 promotes autophagy and autophagic flux in prostate cancer

Although chloroquine derivatives have been tested in cancer clinical trials, the high dosage needed in patients to maintain autophagy inhibition remains a challenge that limits the therapeutic window of this class of compounds. I propose that targeting upstream regulators of autophagy may offer safer, alternative options for inhibiting autophagy. *CAMKK2* has previously been shown to be a direct transcriptional target of AR in prostate cancer that promotes the phosphorylation and activation of AMPK^{14, 50}. Given the critical role of AMPK in autophagy^{72, 73, 216, 218}, I investigated whether *CAMKK2* augmented autophagy in prostate cancer. To do this, I first engineered hormone-sensitive LNCaP cells to inducibly express *CAMKK2* in the presence of doxycycline (DOX) (LNCaP-*CAMKK2*). I then examined via immunoblot the effect of *CAMKK2* overexpression on AMPK phosphorylation and the accumulation of phosphatidylethanolamine-conjugated LC3B (LC3BII), a marker of autophagy (Figure 8A). *CAMKK2* overexpression increased p-AMPK and conversion of LC3BI to LC3BII (Figure 8A). Likewise, *CAMKK2* overexpression increased GFP-LC3 puncta formation, indicative of increased autophagosome formation (Figure 8B). To further confirm the effects on autophagy, TEM was used to verify the increased number of autophagic vesicles (autophagosomes and autophagolysosomes) following *CAMKK2* expression (Figure 8C). Given the high expression of *CAMKK2* in AR+ CRPC^{14, 20, 21, 219}, I next knocked out *CAMKK2* in C4-2 cells, an LNCaP-derived CRPC model, using CRISPR-Cas9 to assess the effects of *CAMKK2* disruption in CRPC. Two *CAMKK2* knockout (KO) clones were selected and compared to control (Cas9 only) cells to examine effects on autophagy (Figure 9A-C). Both *CAMKK2* KO clones exhibited substantially reduced AMPK phosphorylation and LC3B conversion (Figure 9A) as well as decreased LC3 puncta (Figure 9B). Compared to control C4-2 Cas9 cells, it was difficult to find autophagic vesicles in *CAMKK2* knockout cells by TEM (Figure 9C). However, apoptotic bodies were clearly detectable (Figure 9C). I confirmed the

effects of CAMKK2 inhibition on autophagy using an independent model of CRPC, 22Rv1 cells, in which I created a stable derivative that could express shRNA targeting *CAMKK2* in the presence of DOX. Similar to *CAMKK2* genetic KO in C4-2 cells, the inducible knockdown of *CAMKK2* in 22Rv1 cells inhibited autophagy (Figure 10).

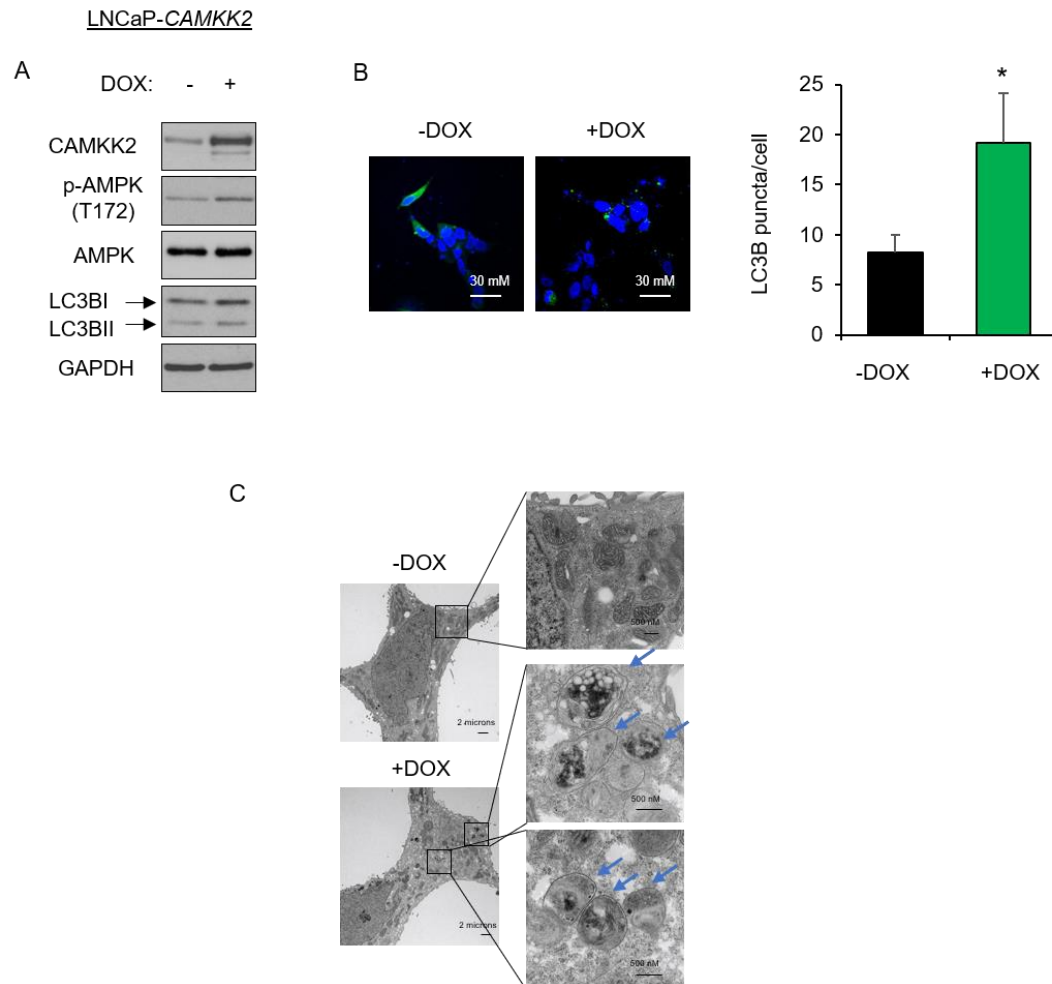


Figure 8. Overexpression of CAMKK2 increases autophagy in LNCaP cells.

(A) Immunoblot analysis of doxycycline (DOX)-inducible LNCaP stable cells (LNCaP-CAMKK2) that express CAMKK2 upon addition of 50 ng/ml DOX for 48 hours. (B) LNCaP-CAMKK2 cells were transiently transfected with GFP-LC3 (green) and then treated \pm 50 ng/ml DOX for 48 hours. Representative images (*left*). GFP-LC3 puncta (green) were quantified as the average number of GFP-LC3 puncta per cell \pm SEM (*right*). The nuclei are stained with DAPI (blue) for reference. * $P < 0.05$. (C) LNCaP-CAMKK2 cells were treated \pm 50 ng/ml DOX for 48 hours and imaged using TEM. Two magnifications of ultrastructures are shown. Blue arrows indicate autophagosomes and autolysosomes.

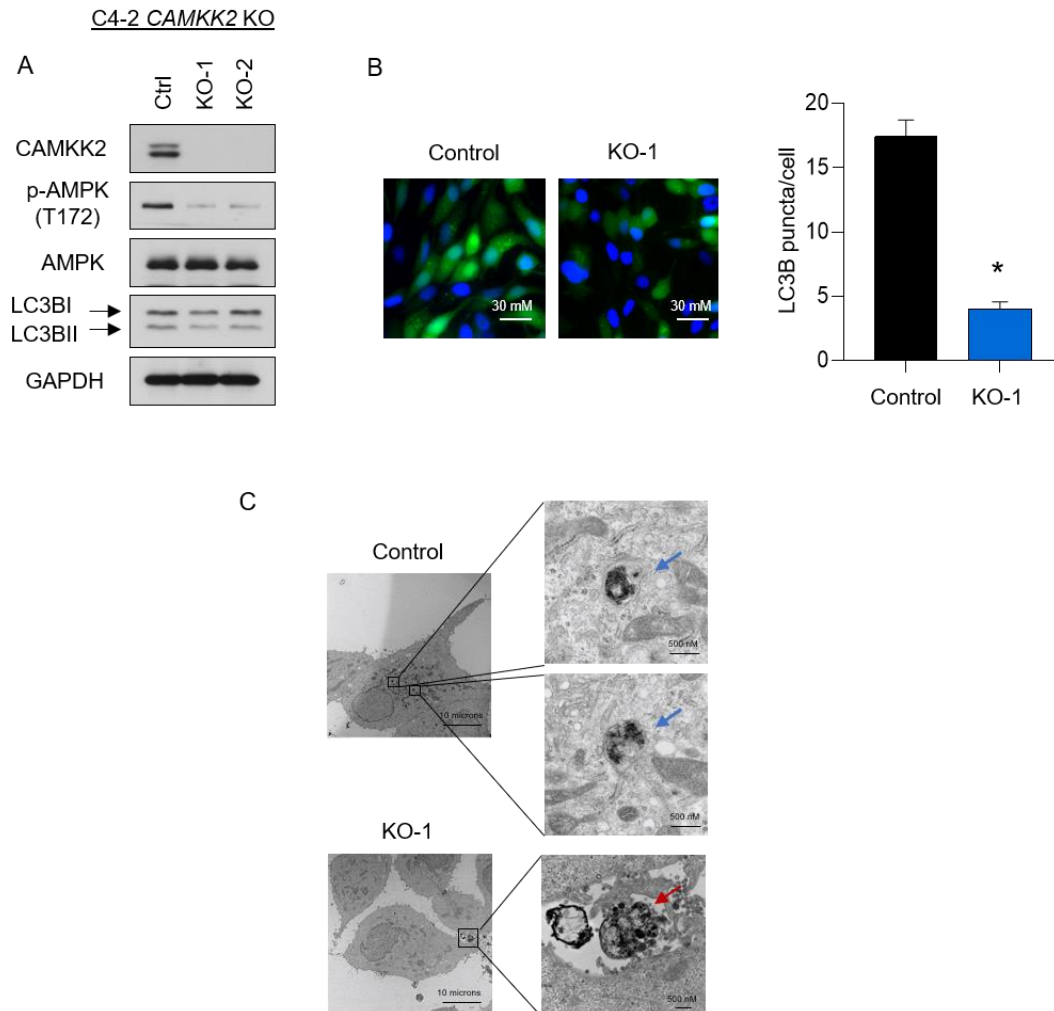


Figure 9. Knockout *CAMKK2* decreases autophagy in C4-2 cells.

(A) Immunoblot analysis of two independent clones of CRISPR-modified C4-2 *CAMKK2* knockout (KO) cells compared with their parental C4-2 Cas9 control cells (Ctrl). (B) GFP-LC3 was expressed in C4-2 Cas9 control and *CAMKK2* KO-1 cell derivative. GFP-LC3 puncta (representative images; *left*) and quantification (*right*) are shown as in Figure 8B. (C) C4-2 control and C4-2 *CAMKK2* KO-1 cells were imaged using TEM as in Figure 8C. Red arrows indicate apoptotic bodies.

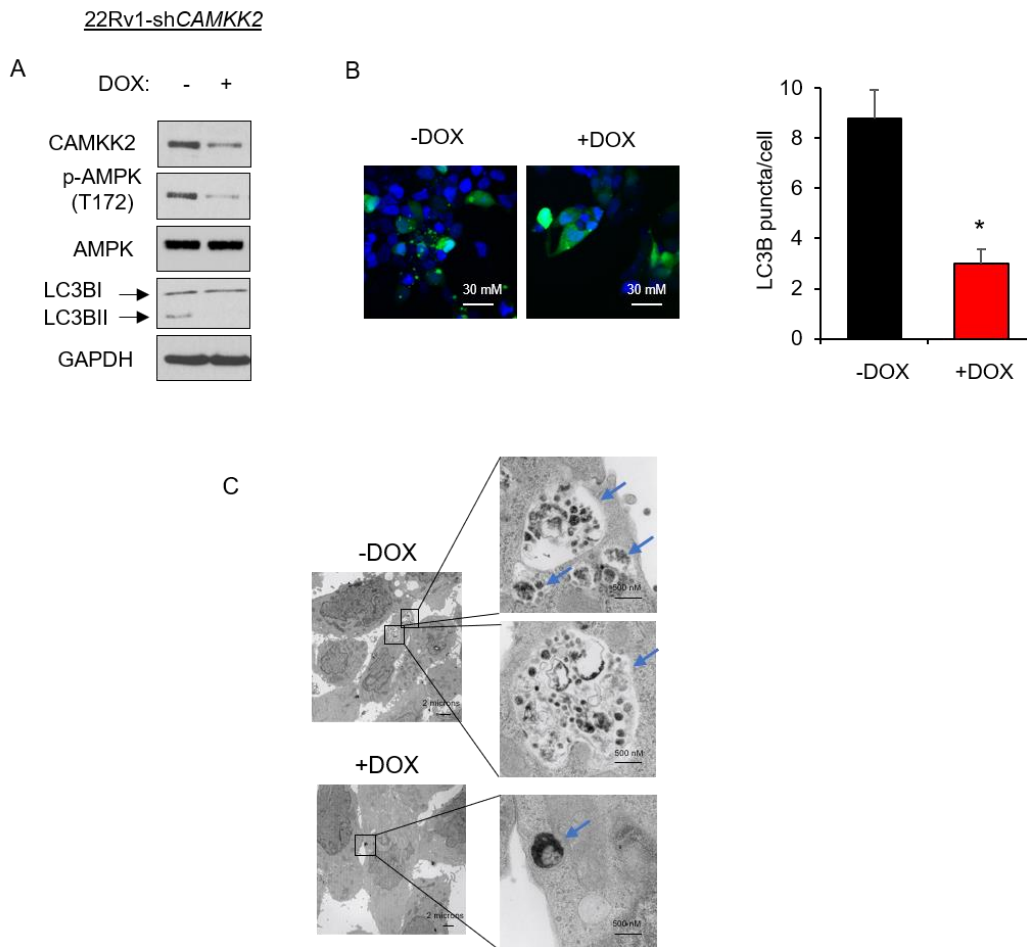


Figure 10. Knockdown of *CAMKK2* decreases autophagy in 22Rv1 cells.

(A) Immunoblot analysis of DOX-inducible 22Rv1 stable cells that express shRNA targeting *CAMKK2* (22Rv1-sh*CAMKK2*) with 800 ng/ml DOX treatment for 72 hours. (B) 22Rv1-sh*CAMKK2* cells were transiently transfected with GFP-LC3 and then treated \pm 800 ng/ml DOX for 72 hours. GFP-LC3 puncta (representative images; *left*) and quantification (*right*) are shown as in Figure 8B. (C) 22Rv1-sh*CAMKK2* cells were treated \pm 800 ng/ml DOX for 72 hours and imaged with TEM as in Figure 8C.

There are several sequential steps involved in autophagy, including initiation, autophagosome formation, autolysosome fusion and degradation. Hence, CAMKK2-mediated increases in LC3 lipidation and relocalization could result from either increased autophagic entry or decreased autophagic flux⁸⁵. I therefore used a tandem mCherry-GFP-LC3B fusion protein to evaluate CAMKK2's role in autophagic flux. LC3B fusion protein is represented as a yellow signal due to the equal expression of both mCherry and GFP basally (diffuse signal) and during early autophagy/prelysosomal fusion (puncta). However, after lysosomal fusion (late autophagy), the acidic environment of the lysosome quenches the GFP signal but retains mCherry, resulting in the colorimetric shift from yellow to red. Consistent with our previous studies^{85, 86}, androgens increased overall LC3B puncta and GFP⁺mCherry⁺ LC3B puncta (red) (Figure 11A). I also observed that *CAMKK2* overexpression has a similar result as androgen treatment, which significantly elevated total and red puncta (Figure 11A). This indicates that CAMKK2, an AR target, can promote autophagic flux similar to androgen treatment. To further validate these findings, I used a lysosomal block assay^{85, 220}. As described above, chloroquine is a lysosomotropic agent that can block the lysosomal turnover of LC3B. Therefore, in the presence of chloroquine, LC3BII would only be increased if there was greater entry into autophagy. I observed androgens or CAMKK2 expression further increased LC3BII levels in the presence of a lysosomal block, while knockdown of *CAMKK2* decreased LC3B conversion (Figure 11B&C), suggesting that CAMKK2 enhanced autophagic flux by increasing autophagy initiation.

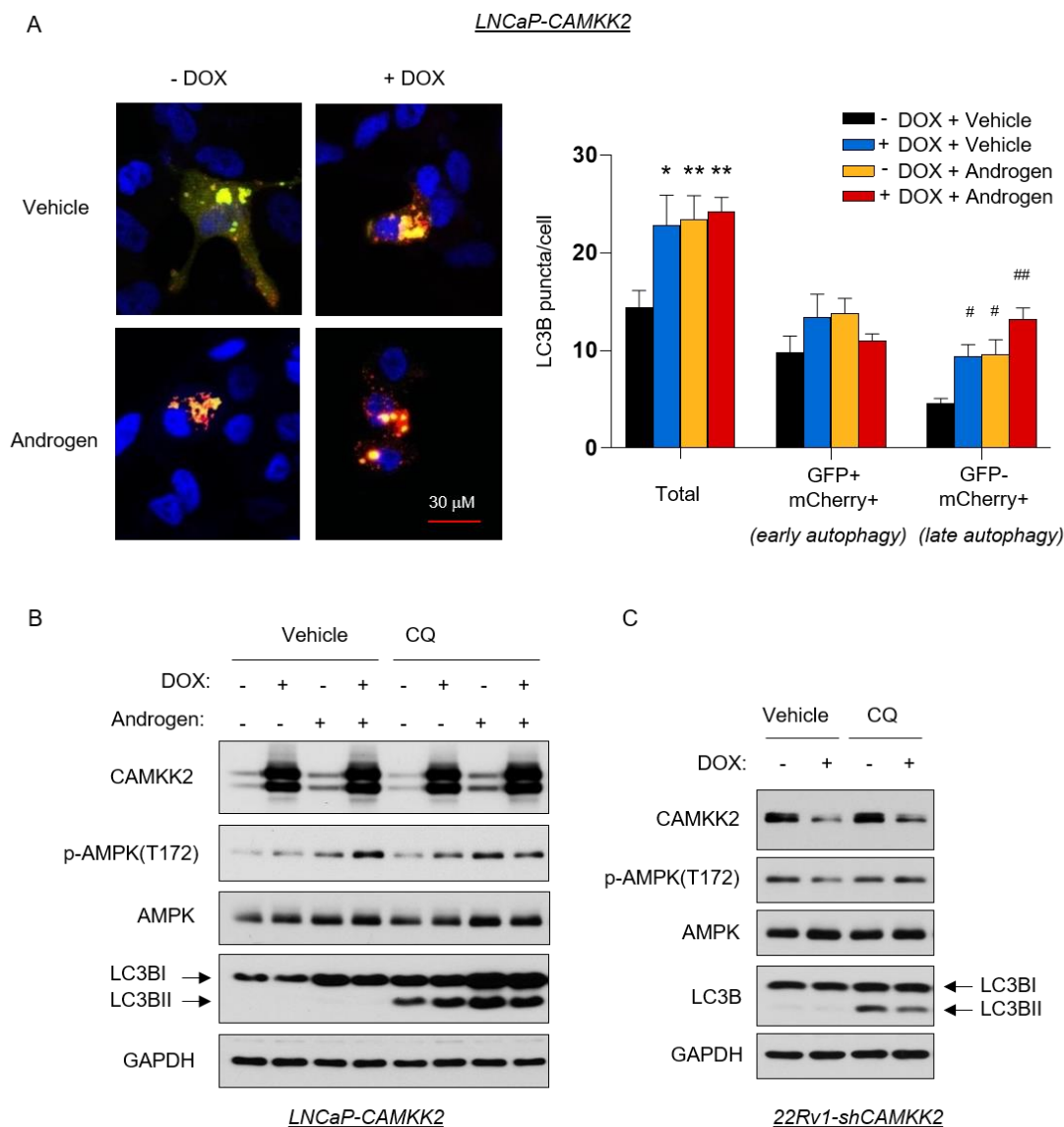


Figure 11. CAMKK2 promotes autophagic flux.

(A) LNCaP-CAMKK2 cells were transfected with an mCherry-GFP-LC3 plasmid and treated \pm 10 nM R1881 (androgen) \pm 50 ng/ml DOX. Representative fluorescence images of the cellular localization of autophagic puncta (*top*) and quantification (*bottom*). * P < 0.05, ** P < 0.01, compared to vehicle group in total. # P < 0.05, ## P < 0.01, compared to vehicle group in GFP-mCherry+. (B) LNCaP-CAMKK2 cells were treated \pm 10 nM R1881 (androgen) \pm 50 ng/ml DOX \pm 20 μ M chloroquine (lysosomal block/inhibitor of autophagic flux) for 72 hours. Cell lysates were then subjected to immunoblot analysis. (C) Immunoblot analysis of 22Rv1-shCAMKK2 cells \pm 800 ng/ml DOX \pm 20 μ M chloroquine treatment for 72 hours.

3.2.3 CAMKK2 is required for CRPC cell growth *in vivo*

Previous studies using the pharmacological inhibitor STO-609 have suggested the potential role of CAMKK2 in CRPC growth²¹. However, STO-609 has multiple kinase targets²²¹⁻²²³. Here, I used a genetic approach to assess the role of CAMKK2 in CRPC tumorigenesis and progression *in vivo*. Castrated NSG mice were subcutaneously injected with C4-2 Cas9 control and C4-2 *CAMKK2* KO cells (Figure 12A). *CAMKK2* ablation had a profound effect on CRPC tumor growth (Figure 12B). In fact, when the average tumor size of the control group was ~500 mm³, no tumors could even be detected in the KO groups. Accordingly, *CAMKK2* KO also dramatically prolonged survival (Figure 12C). Immunohistochemical (IHC) analysis of tumor tissues determined both a reduction in proliferation and increase in cell death in *CAMKK2* KO groups compared to control (Figure 12D). To validate my findings in a second model of CRPC and test what would happen if I decreased CAMKK2 after tumor implantation, I leveraged my DOX-inducible 22Rv1-sh*CAMKK2* cell model (Figure 13A). Consistent with the C4-2 *CAMKK2* KO xenograft results, knockdown of *CAMKK2* in 22Rv1 tumors decreased tumor burden over time and consequently increased overall survival (Figure 13B-C). Moreover, *CAMKK2* knockdown-mediated tumor growth reduction was again correlated to lower proliferation (BrdU) and more cell death (TUNEL) (Figure 13D). Consistent with a pro-survival role of CAMKK2-mediated autophagy, I also observed inducible *CAMKK2* knockdown tumors displayed increased necrosis, but clear regions of perivascular tumor sparing (Figure 13D, +DOX H&E (high magnification)). Collectively, these data suggest that CAMKK2 is required for maximum CRPC tumorigenesis and progression *in vivo*, potentially by enabling cells to withstand the harsh, nutrient-deficient tumor microenvironment.

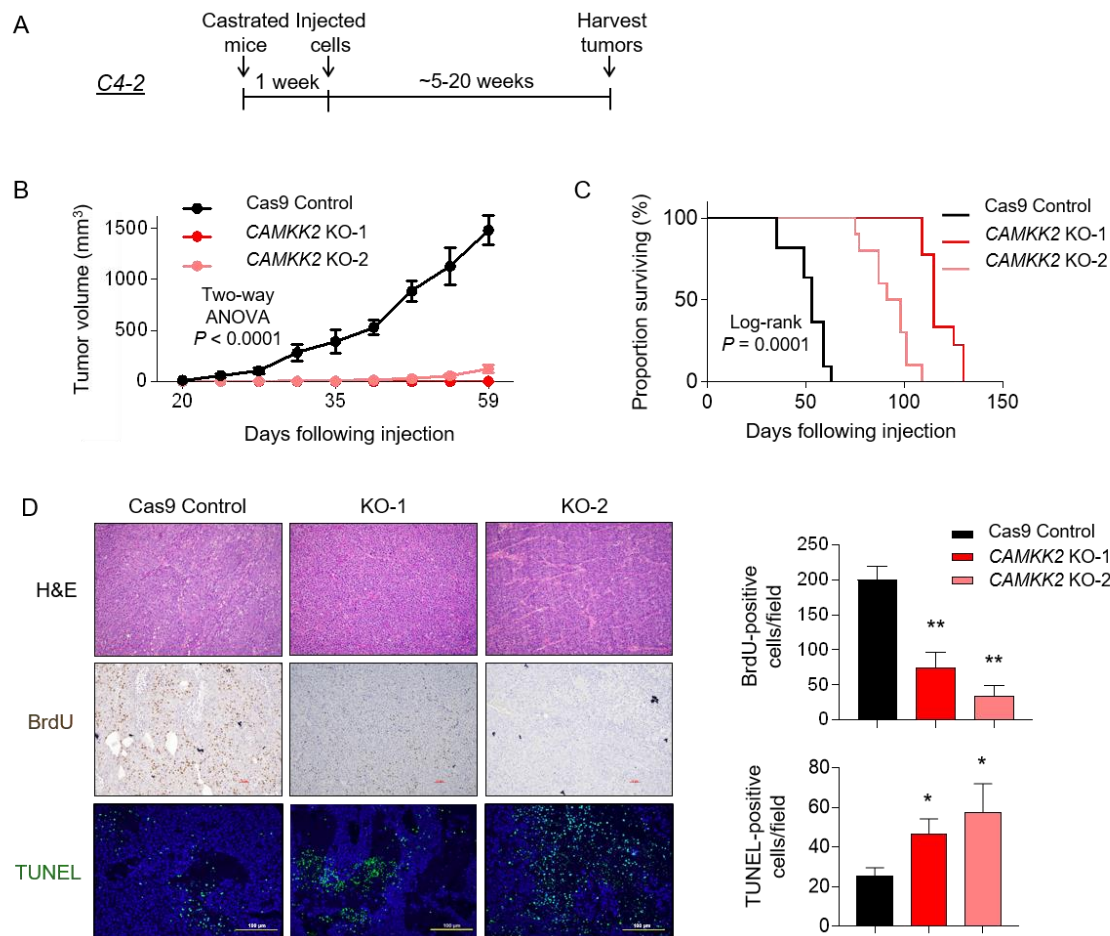


Figure 12. CAMKK2 is required for C4-2 tumor growth *in vivo*.

(A) Schematic of xenograft study using CRPC C4-2 Cas9 control and *CAMKK2* CRISPR knockout (KO) cell derivatives in castrated NSG mice. (B) Tumor growth curves of C4-2 Cas9 control and C4-2 *CAMKK2* KO xenografts in castrated NSG mice ($n = 10/\text{group}$). (C) Kaplan-Meier survival curve of C4-2 Cas9 control and C4-2 *CAMKK2* KO xenograft mice. (D) C4-2 xenograft tumor samples were stained with H&E, BrdU and TUNEL. Representative images (*left*) and quantifications of BrdU and TUNEL staining (*right*). * $P < 0.05$, ** $P < 0.01$.

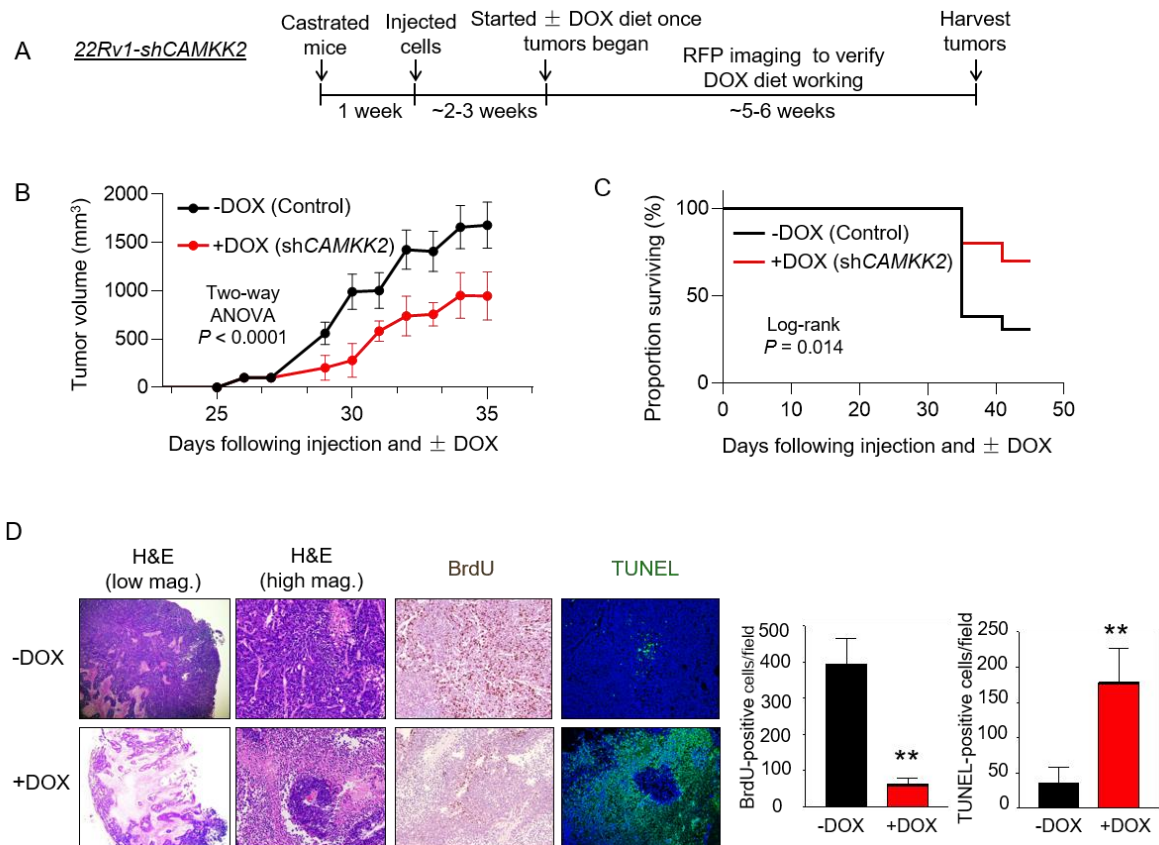


Figure 13. CAMKK2 is required for 22Rv1 tumor growth *in vivo*.

(A) Schematic of xenograft study using DOX-inducible CRPC 22Rv1-shCAMKK2 cells in castrated NSG mice. (B) Tumor growth curves of 22Rv1-shCAMKK2 xenografts in castrated NSG mice fed control or DOX-enriched (625 mg/kg) chow. (C) Kaplan-Meier survival curve of 22Rv1-shCAMKK2 xenograft mice ± DOX. (D) 22Rv1-shCAMKK2 xenograft tumor samples were stained with H&E, BrdU and TUNEL. Representative images (*left*) and quantifications of BrdU and TUNEL staining (*right*). Note, evidence of perivascular tumor sparing in DOX-treated tumors (H&E high magnification (mag.)). ** $P < 0.01$.

3.2.4 AR-CAMKK2-AMPK signaling enhances autophagy through phosphorylation of ULK1 at serine 555 independent of mTOR-mediated ULK1 phosphorylation of Ser757

Since AR-CAMKK2 signaling promotes autophagic flux, I further explored the mechanism by which it initiated autophagy. A key protein involved in autophagy initiation is the serine/threonine protein kinase Unc-51 like autophagy activating kinase 1 (ULK1), which functions as part of a complex to transduce upstream signals to the downstream core autophagy machinery⁶¹. AMPK is a known ULK1 upstream regulator by phosphorylating and activating ULK1 at multiple sites in a context dependent-manner^{73, 224, 225}. Thus, I speculated that AR-CAMKK2 activated autophagy through ULK1 in prostate cancer. To explore this possibility, I co-treated LNCaP cells with androgens and the CAMKK2 inhibitor STO-609. Androgens increased the levels of CAMKK2, p-AMPK and LC3BII, an effect that could be abrogated by STO-609 (Figure 14A). Androgens also increased ULK1 phosphorylation at serine 555, an effect that was again reversed by STO-609 (Figure 14A). This was of interest because serine 555 has been shown to be a critical phosphorylation site necessary for AMPK-mediated autophagy *in vitro* and *in vivo*^{71, 73, 75, 226}. To exclude the non-specific effects of STO-609, I next tested p-ULK1(Ser555) status in cells following genetic or molecular modification of CAMKK2 and AMPK. In LNCaP-CAMKK2 cells, DOX alone increased CAMKK2 expression level, resulting in a similar increase in p-AMPK, p-ULK1 and LC3BII levels compared to androgen treatment alone (Figure 14B). These increases could be reversed upon knockdown of AMPK α 1, the predominant AMPK α catalytic subunit in prostate cancer^{14, 46, 50, 227}. The requirement for AMPK was confirmed with three independent siRNAs (Figure 14C). To verify that ULK1 phosphorylation was necessary for CAMKK2-mediated autophagy, I transfected LNCaP-CAMKK2 cells with constructs expressing vector control, WT ULK1 or ULK1 4SA mutant, an AMPK non-phosphorylatable ULK1⁷³. Cells treated with DOX (CAMKK2 expression) and expressing WT ULK1 had increased LC3BII levels, indicating an increase of

autophagy, while 4SA mutant blocked CAMKK2-mediated autophagy (Figure 14D). The requirement of CAMKK2 for AMPK-ULK1-mediated autophagy was confirmed in both the C4-2 and 22Rv1 CRPC models (Figure 14E-F). Notably, phosphorylation of Ser757, previously shown to be the major mTOR inhibitory target site on ULK1²²⁸, was unchanged following modulation of CAMKK2-AMPK signaling (Figure 15). Moreover, mTOR signaling remained largely intact in my models suggesting that in prostate cancer, AMPK and mTOR may be able to coexist. In fact, in 22Rv1 cells, knockdown of *CAMKK2* even decreased p-S6 levels (Figure 15C), suggesting that under some contexts CAMKK2 may even promote mTOR activity. Whether this is due to the PTEN intact status of these cells (LNCaP and C4-2 are PTEN mutated) is unknown. Together, these findings demonstrated that AR-CAMKK2 triggers AMPK phosphorylation and activation, and in turn phosphorylates ULK1 at serine 555, which ultimately stimulates autophagy independent of mTOR regulation.

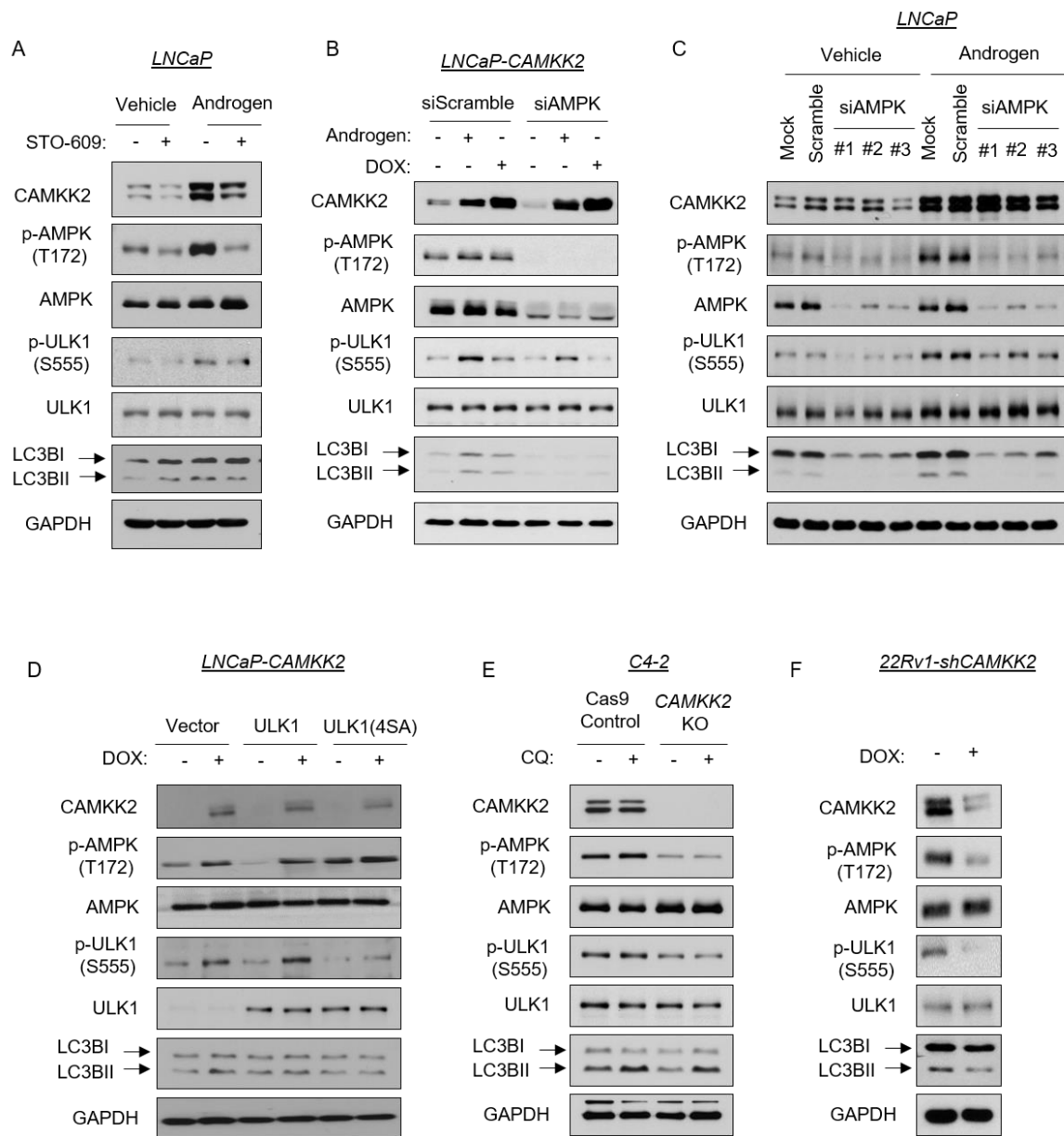


Figure 14. AR-CAMKK2-AMPK signaling increases autophagy by phosphorylating ULK1 at serine 555.

(A) LNCaP cells were treated \pm 10 nM R1881 (androgen) \pm 30 μ M STO-609 for 72 hours. Cell lysates were subjected to immunoblot analysis. (B) LNCaP-*CAMKK2* cells were transfected with siRNAs targeting scramble control or the α 1 catalytic subunit of AMPK (*siAMPK*) and then treated with androgen for 72 hours or DOX (50 ng/ml) for 48 hours. Cell lysates were subjected to immunoblot analysis. (C) Parental LNCaP cells were transfected with siRNAs targeting scramble control or three different regions of the α 1 catalytic subunit of AMPK (*siAMPK*) and then treated with vehicle or androgen for 72 hours. Cell lysates were subjected to immunoblot analysis. (D) LNCaP-*CAMKK2* cells were transfected with empty vector, ULK1 or ULK1 (4SA) expression constructs and then treated \pm DOX for 48 hours. Cell lysates were subjected to immunoblot analysis. (E) Immunoblot analysis of C4-2 Cas9 control and *CAMKK2* KO derivative cells treated with vehicle or chloroquine (20 μ M). (F) Immunoblot analysis of 22Rv1-sh*CAMKK2* cells \pm 800 ng/ml DOX treatment for 72 hours.

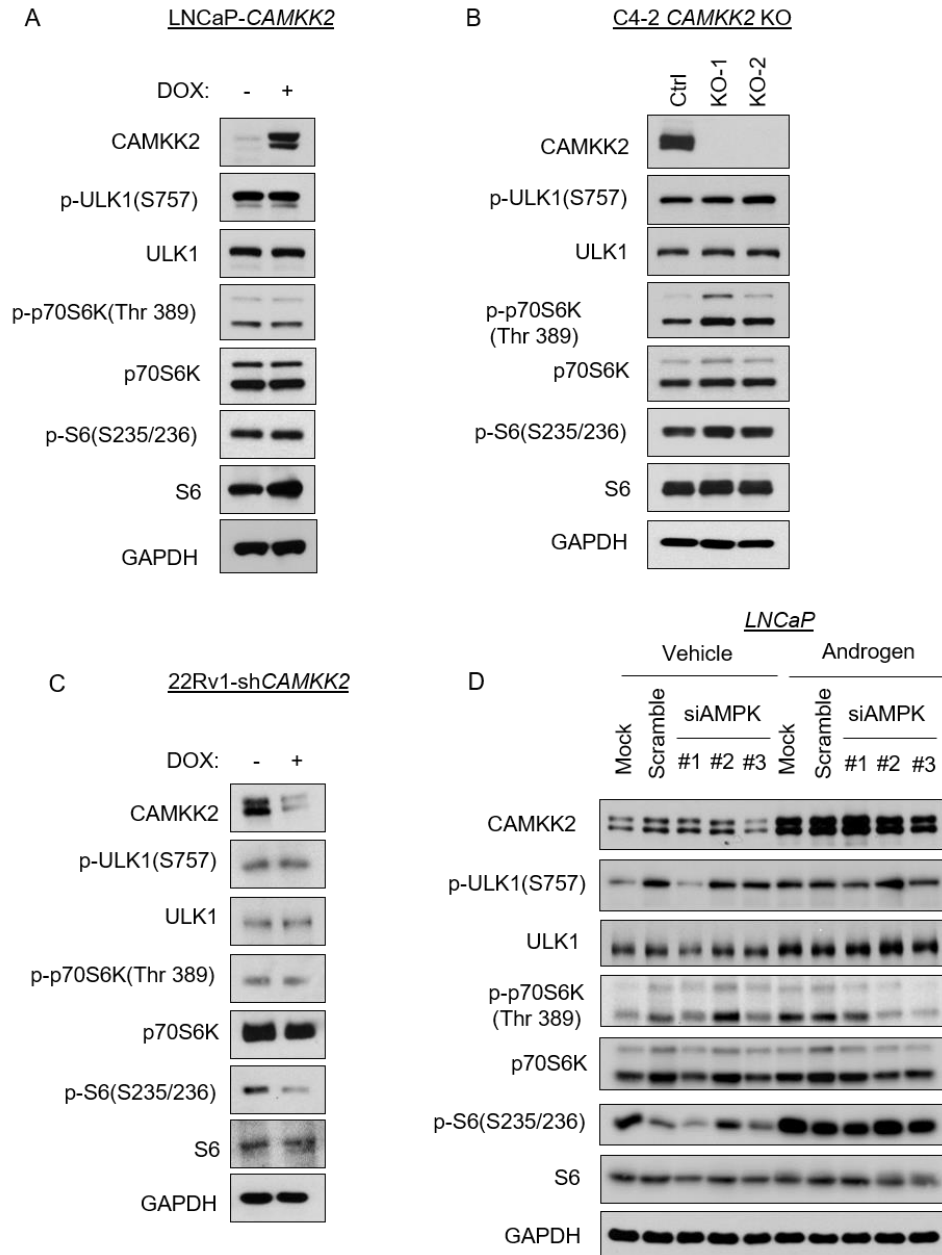


Figure 15. AR-CAMKK2 mediated autophagy is independent on canonical mechanistic target of rapamycin (mTOR) activity.

(A) LNCaP-CAMKK2 cells treated with DOX (50 ng/ml) for 48 hours. Cell lysates were subjected to immunoblot analysis. (B) Immunoblot analysis of C4-2 Cas9 control and CAMKK2 knockout (KO) cells. (C) 22Rv1-shCAMKK2 cells treated with DOX (800 ng/ml) for 48 hours. Cell lysates were subjected to immunoblot analysis. (D) Parental LNCaP cells treated with siRNAs targeting either scramble or AMPK +/- R1881 for 72 hours. Cell lysates were subjected to immunoblot analysis.

3.2.5 ULK1 correlates with poor patient prognosis in men with prostate cancer

To examine the clinical association between ULK1 and patient prognosis, I analyzed two well-annotated, publicly available patient databases. The expression level of *ULK1* mRNA was inversely correlated with disease-free survival in both TCGA²²⁹ (Figure 16A) and Taylor *et al.* 2010²³⁰ (Figure 16) clinical cohorts. Consistent with these clinical correlations, previous histological studies have linked high ULK1 levels to biochemical recurrence and PSA levels^{231, 232}.

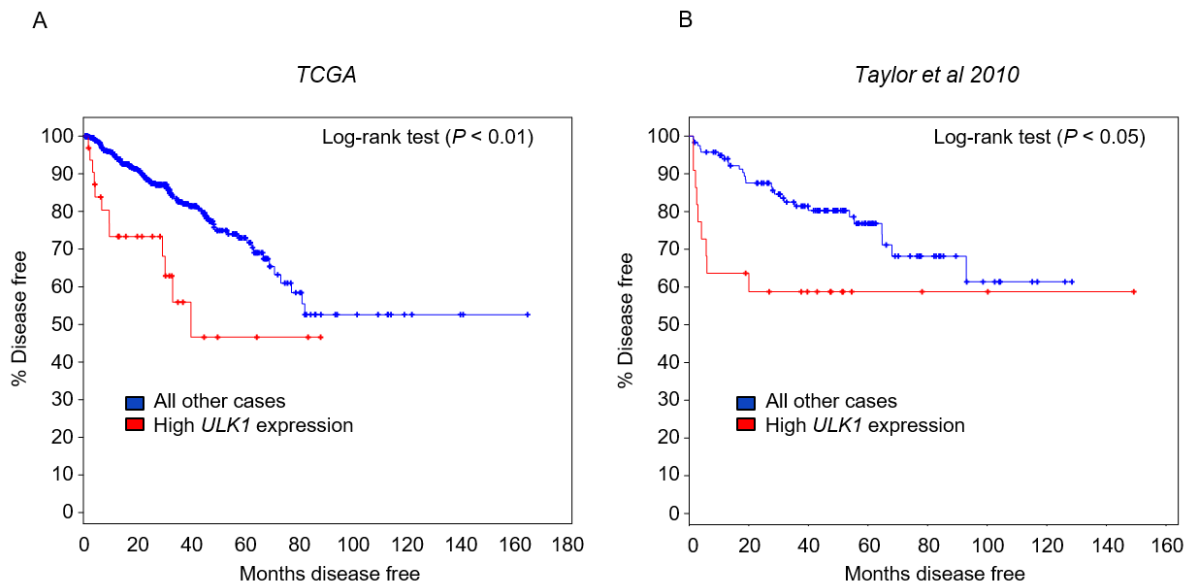


Figure 16. High *ULK1* tumor expression predicts poor patient prognosis in independent clinical cohorts of men with prostate cancer.

Kaplan-Meier estimates of disease-free survival in The Cancer Genome Atlas (TCGA) and Taylor *et al.* 2010 clinical cohorts based on *ULK1* expression. Data were generated from cBioPortal. The high expression ULK1 group was defined by ULK1 mRNA expression > 2 SD above the mean.

3.2.6 Pharmacological targeting of ULK1 inhibits prostate cancer cell growth

I next wanted to determine if ULK1 was a potential therapeutic target in prostate cancer. To test this, I leveraged SBI-0206965 (6965), a recently described ULK1 inhibitor that has shown anti-cancer effects in lung cancer cells under nutrient deprivation (Figure 17A)²³³. To validate 6965's antagonistic effects in prostate cancer cells, I first used the known ULK1 substrate VPS34 to determine whether 6965 could block ULK1 activity. 6965 decreased both basal and androgen-induced phosphorylation of VPS34 at serine 249, in alignment with the reduction of LC3BII (Figure 17B). In 22Rv1 cells, 6965 also resulted in inhibition of p-VPS34 and LC3BII accumulation (Figure 17C). Interestingly, I noticed an increase of p-AMPK after 6965 treatment, consistent with the previously described negative feedback loop that exists between ULK1 and AMPK²³⁴. Next, to assess the efficacy of 6965 on prostate cancer cell growth, I treated LNCaP-CAMKK2 cells with androgens, DOX and/or 6965 for 7 days. Although 6965 did not significantly inhibit basal LNCaP cell growth, it blocked androgen- and/or DOX-mediated LNCaP cell growth (Figure 18A), consistent with our previous findings that siRNA-mediated knockdown of ULK1 blocked androgen-mediated cell growth⁸⁶. Interestingly, the LNCaP-derived CRPC derivative C4-2 cells were more sensitive to 6965 treatment, showing a ~70% reduction in growth (Figure 18B). In 22Rv1 cells, ~50% growth inhibition was observed (Figure 18C). To evaluate the long-term effects of 6965 on cell proliferation, I performed clonogenic assays. All three cells were very sensitive to prolonged 6965 treatment with almost 100% inhibition in clonogenic potential (Figure 18D-F). Collectively, these data indicate that ULK1 is a potentially druggable target for the treatment of prostate cancer. Future studies would need to explore the safety of such an approach *in vivo*.

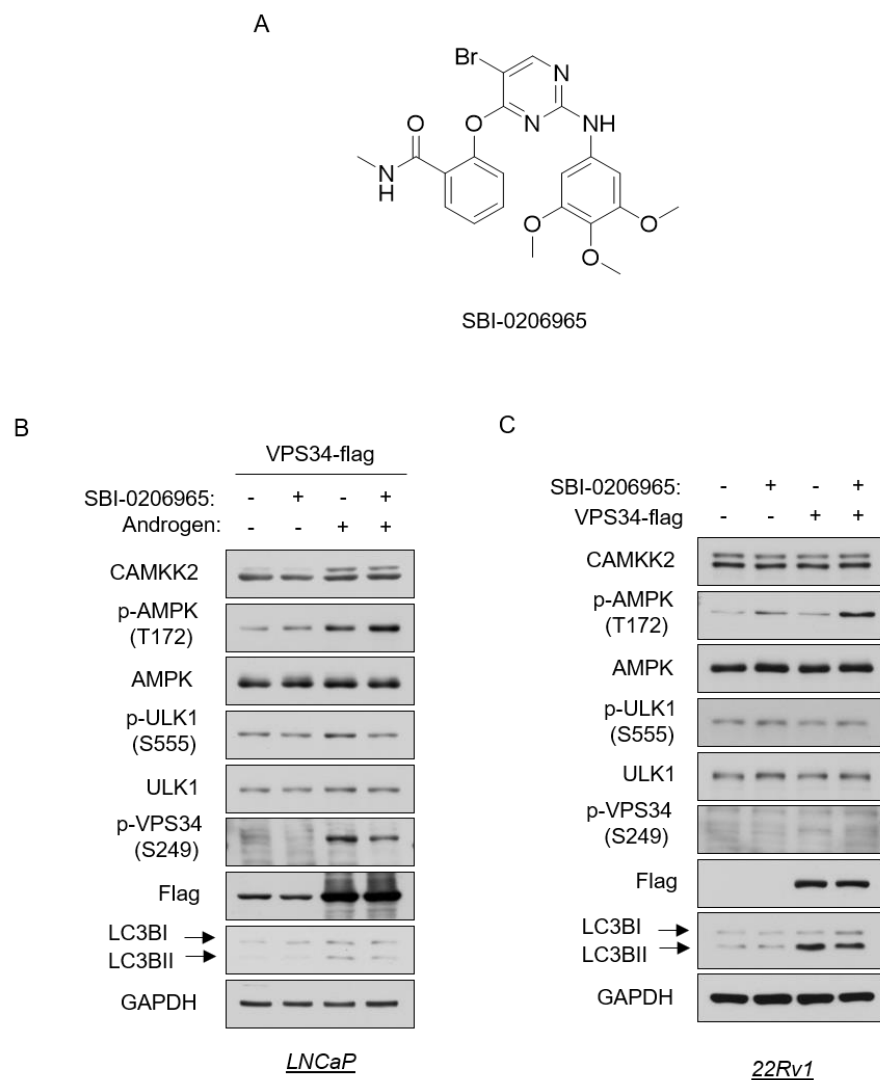
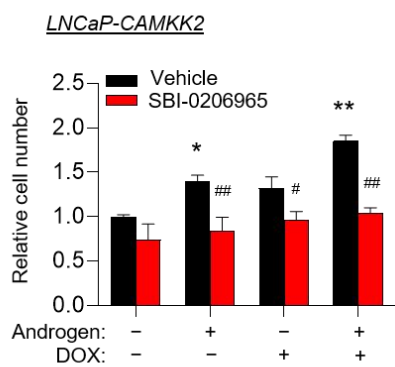


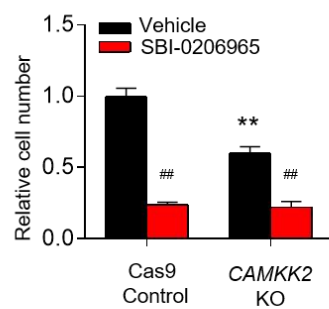
Figure 17. The ULK1 inhibitor SBI-0206965 inhibits autophagy in prostate cancer cell.

(A) Chemical structure of the ULK1 inhibitor SBI-0206965. (B) LNCaP cells were transfected with VPS34-FLAG following 72 hours 10 nM R1881 (androgen) treatment. Cell lysates were collected 2 hours after vehicle or SBI-0206965 (10 μ M) treatment and subjected to immunoblot analysis. (C) 22Rv1 cells were transfected \pm VPS34-FLAG for 48 hours. Immunoblot analysis of transfected cells with 2 hours SBI-0206965 (10 μ M) treatment.

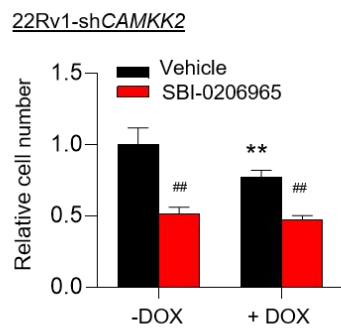
A



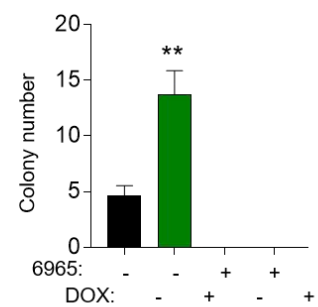
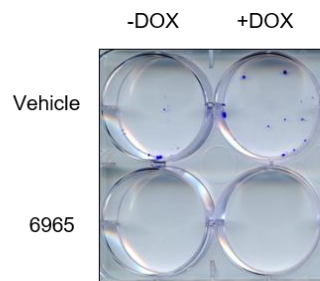
B



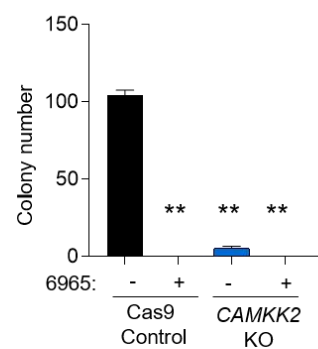
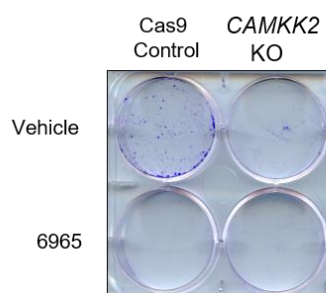
C



D



E



F

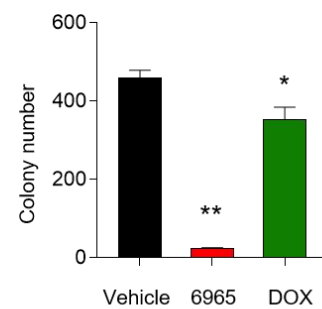
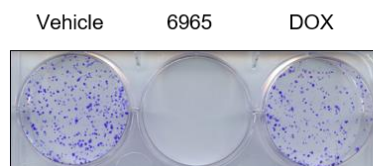


Figure 18. The ULK1 inhibitor SBI-0206965 represses prostate cancer cell growth.

(A) Cell growth of LNCaP-CAMKK2 cells following 7 days R1881 (androgen, 10 nM), DOX (50 ng/ml) and/or SBI-0206965 (10 μ M) treatment. * P < 0.05, ** P < 0.01 compared to no androgen/DOX/SBI-0206965 treatment group. # P < 0.05, ## P < 0.01, compared to corresponding vehicle (SBI-0206965) treatment group. (B) Cell growth of C4-2 Cas9 control and C4-2 CAMKK2 KO derivative cells \pm SBI-0206965 (10 μ M). ** P < 0.01 compared to C4-2 control cells. ### P < 0.01, compared to vehicle treatment group. (C) Cell growth of 22Rv1-shCAMKK2 cells treated for 7 days \pm DOX (800 ng/ml) \pm SBI-0206965 (10 μ M). * P < 0.05, ** P < 0.01 compared to no DOX treatment group. ### P < 0.01, compared to corresponding vehicle (SBI-0206965) treatment group. (D) Colony formation assay of LNCaP-CAMKK2 cells following 28-day DOX and/or SBI-0206965 (10 μ M) under 100 pM R1881 (androgen) treatment (required for LNCaP colony formation). Representative image (*left*). Quantification of three independent experiments (*right*). ** P < 0.01, compared to double-vehicle treatment group. (E) Colony formation assay of C4-2 Cas9 control and C4-2 CAMKK2 KO derivative cells \pm SBI-0206965 (10 μ M) for 21 days. Representative image (*left*). Quantification of three independent experiments (*right*). ** P < 0.01, compared to C4-2 control vehicle treatment group. (F) Colony formation assay of 22Rv1-shCAMKK2 cells treated for 21 days \pm DOX (800 ng/ml) or SBI-0206965 (10 μ M). Representative image (*left*). Quantification of three independent experiments (*right*). * P < 0.05, ** P < 0.01, compared to vehicle treatment group.

3.3 Discussion

Although autophagy has context-dependent roles in cancer^{203, 235-238}, our data support a pro-cancer role for this cellular process in prostate cancer. These findings are consistent with our previous work^{85, 86} and the work of others in the field^{83, 88, 90, 91, 211, 237, 239, 240}. As presented in our previous reports, blocking autophagy by molecular or pharmacological approaches resulted in decreased androgen-mediated prostate cancer cell growth^{85, 86}. Mechanistically, androgens stimulate AR to promote autophagy through multiple mechanisms including the indirect accumulation of intracellular ROS and more directly through the transcription of several core autophagy genes^{85, 86}. In this study, I revealed a novel mechanism underlying how AR regulates autophagy. My data demonstrated that an AR-CAMKK2-AMPK signaling

cascade can drive autophagy through the phosphorylation of ULK1, an important initiator of autophagy, at serine 555. This phosphorylation activates the ULK1 complex and ultimately initiates autophagy and autophagic flux in an mTOR-ULK1(Ser757)-independent manner for prostate cancer cell proliferation and survival *in vitro* and *in vivo*, promoting CRPC progression (Figure 19). My finding not only provides a novel mechanistic insight into AR's regulation of autophagy, but highlights potential new avenues for therapeutic targeting of autophagy in prostate cancer. A non-AR-mediated regulation of autophagy has been reported as a resistance mechanism to treatment with the anti-tumor compound triptolide in prostate cancer²⁴¹. As a result, chloroquine was applied to overcome triptolide resistance, enhancing the anti-tumor effect of triptolide in much the same way chloroquine enhanced the effect of hormone ablation in our own CRPC models (Figure 6). Despite differences identified in the ULK1 phosphorylation sites, my results agree with the overall concept that CAMKK2-AMPK-induced ULK1 activation and autophagy provides an important survival mechanism for prostate cancer cell growth. Likewise, in a genetic mouse model of *Pten*- and *Tp53*-deficient prostate cancer or AR-indifferent prostate cancer cells, ULK1-mediated autophagy (ULK1 phosphorylation was not examined) inhibited apoptosis²¹⁰. However, unlike these prior studies, my data suggest that AR signaling can promote CAMKK2-AMPK-mediated ULK1 activation and autophagy independent of any inhibition of mTOR activity. Moreover, my data directly demonstrate key roles for CAMKK2 and ULK1 not only in cell survival, but also in proliferation.

Despite agreement that autophagy promotes prostate cancer progression, how this process is regulated by AR is still debated^{46, 85, 86, 90, 203, 211, 215, 237, 240, 242}. These discrepancies may be attributable to differences in the duration of upstream signals, reliance on indirect or nonselective modulators of autophagy or treatment conditions. As we and others have shown, androgens, in an AR-dependent mechanism, can directly and indirectly increase autophagy through a variety of mechanisms including elevating intracellular ROS levels and transcription

of core autophagy genes^{83, 85, 86, 237}. As shown here, there is also a clear, direct AR regulation of AMPK-mediated autophagy through the expression of *CAMKK2*. The mechanism underlying how antiandrogens can, like androgens, paradoxically also can increase autophagy is less clear. But these different observations may speak to the potential benefit of targeting downstream effector processes like autophagy that can be activated under a variety of conditions to drive disease progression. my data presented here provides evidence that targeting CAMKK2-AMPK-ULK1 signaling may be an effective, alternative strategy to block protective autophagy in advanced prostate cancer.

Under glucose or amino acid starvation, ULK1 is well characterized to be regulated by AMPK. AMPK binds to the serine/proline-rich domain and can phosphorylate ULK1 at multiple sites (Ser317, Ser467, Ser555, Thr575, Ser637 and Ser777) which subsequently change ULK1 conformation and enhance its kinase activity. In addition, AMPK can indirectly promote ULK1 activity through the inhibition of mTOR and subsequent decrease of mTOR-mediated ULK1 phosphorylation on Ser757—an inhibitory posttranslational modification²²⁸. These phosphorylation events, in turn, promote the formation of the ULK1 complex (ULK1, ATG13, ATG101, and FIP200)^{61, 228}. Activated ULK1 can further phosphorylate downstream VPS34 complex members to induce autophagic entry⁶¹. In this study, I first demonstrated the Ser555 site of ULK1 as a downstream target of AMPK in response to androgen treatment. Ser555 was increased under androgen treatment but could not be activated when cells were subjected to *AMPK* siRNA (Figure 14B&C). When cells were reconstituted with a non-phosphorylatable ULK1 mutant (4SA), they were defective in autophagy following AMPK activation (Figure 13D). Surprisingly, the AR-CAMKK2-AMPK activation of ULK1-mediated autophagy was independent of any inhibition of mTOR signaling and subsequent ULK1(Ser757) phosphorylation (Figure 15)²²⁸. Although I cannot exclude contributions from other phosphorylation sites, these findings together suggest the importance of ULK1 Ser555

phosphorylation by AMPK in AR-mediated autophagy induction and support prior reports that Ser555 is functionally one of the most important AMPK target sites on ULK1^{73, 75, 226}.

Interestingly, I observed a negative feedback loop between AMPK and ULK1 similar to what has been described before in HEK293 cells under starvation²³⁴. While non-phosphorylatable ULK1 mutants impaired autophagy, they significantly increased p-AMPK (Thr172) (Figure 14D). Likewise, when cells were treated with the ULK1 inhibitor SBI-0206965, a robust enhancement of p-AMPK was detected (Figure 17B&C). It is unclear at this time if this translates to other AMPK-mediated processes being hyperactivated and therefore influencing prostate cancer cell pathobiology.

The efficacy of autophagy inhibition in preclinical models of cancer has paved the way for new clinical trials investigating the efficacy of autophagy inhibition in patients, particularly in combination with traditional anti-cancer treatments. Chloroquine and its derivative hydroxychloroquine, as FDA-approved drugs, have been favored and repurposed in prostate cancer. Previous studies indicated that chloroquine in combination with other therapeutic agents including anti-androgens, chemotherapy and kinase inhibitors can induce greater cytotoxicity than single agent treatment alone^{90, 91, 201, 211, 240, 243-245}. Likewise, our data indicate anti-cancer effects for chloroquine in combination with androgen deprivation therapy *in vivo* (Figure 6). Although a series of clinical trials in prostate cancer have been started to test the efficacy of chloroquine analogs, thus far, limited clinical efficacy has been observed. This is believed to be due in large part to an inability to achieve the drug concentration needed for sustained inhibition of autophagy within tumors prior to the onset of significant side effects²⁰². Despite the fact that hydroxychloroquine is safer than chloroquine, micromolar concentrations are required to maintain autophagy inhibition in patients²⁴³. Even so, variable effects on autophagy are still being observed, possibly due to inconsistencies in cell penetration that are in part dependent on the individual's tumor microenvironment²⁰¹. Thus, long-term and high-dosage treatments will inevitably reduce the therapeutic window. Given the potential

challenges in the use of lysosomotropic agents, which are not even specific for autophagy, targeting other steps in autophagy, such as ULK1, may provide alternative solutions.

ULK1 expression is highly correlated with patient disease-free time, biochemical recurrence, Gleason score, and metastasis (Figure 16 & ^{231, 232}). Currently, three studies have investigated the ULK1 inhibitor SBI-0206965 and showed potent and selective inhibition on ULK1 activity^{233, 246, 247}. In agreement with other reports, my data showed that SBI-0206965 inhibited ULK1 activity as evidenced by the reduction of p-VPS34 (Ser249) (Figures 16B&C). Moreover, SBI-0206965 exhibited its anti-growth activity in both hormone-sensitive and CRPC cells (Figure 18). A recent study suggested that SBI-0206965 is a dual inhibitor of AMPK and ULK1 ²⁴⁸. While this would potentially be beneficial for blocking two important nodes of AR-CAMKK2-AMPK-ULK1 signaling, I did not observe a consistent decrease of p-ULK1 after SBI-0206965 treatment, suggesting SBI-0206965 may not function as an AMPK inhibitor in my models. However, I acknowledge that this interpretation may be convoluted due to the above-described feedback mechanism between AMPK and ULK1²³⁴. In addition, the efficacy and pharmacokinetic profile of SBI-0206965 *in vivo* are still largely unknown.

Given that systemic blocking or genetic ablation of CAMKK2 appears well-tolerated in mouse models and CAMKK2 has a more restricted expression profile but is elevated in prostate cancer, I propose targeting CAMKK2 may be a viable alternative. Unfortunately, the use of STO-609 as used in this study is likely not a clinically viable option due to its off-target effects on other kinases and pharmacokinetic limitations²²¹⁻²²³. There are, however, ongoing efforts to develop next-generation CAMKK2 inhibitors^{222, 249-251}.

In summary, my results provide a novel mechanism that links AR signaling and protective autophagy in prostate cancer. Targeting CAMKK2 decreases the AMPK-mediated phosphorylation of ULK1 at serine 555, which in turn stalls the initiation of autophagy and impairs prostate cancer cell growth. These findings not only add a mechanistic layer of complexity to shed light on AR's regulation of autophagy, but also provides new opportunities

for inhibiting autophagy in prostate cancer that I postulate warrant being tested to determine if they can overcome the existing limitations of chloroquine.

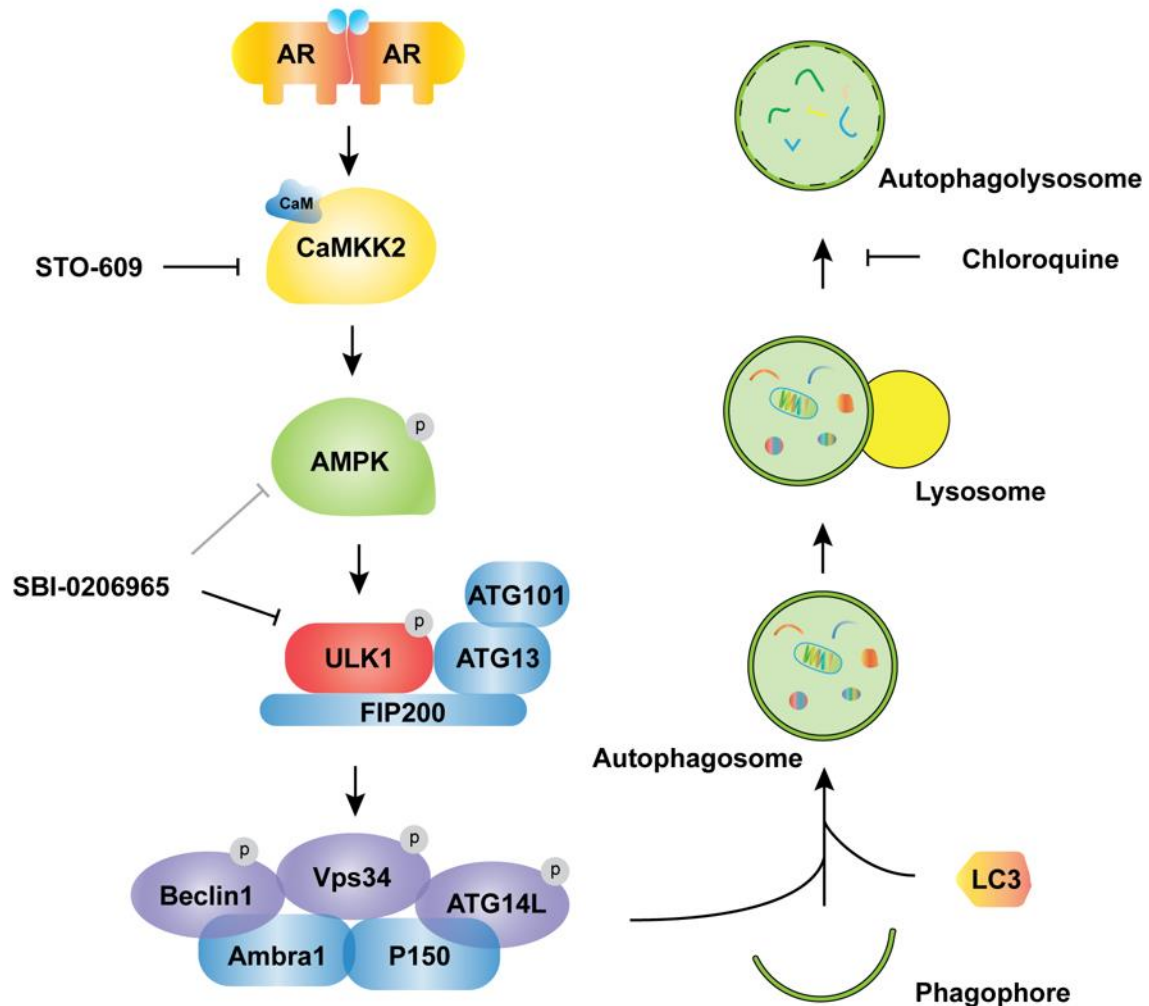


Figure 19. Working model depicting how AR-CAMKK2-AMPK signaling regulates autophagy by ULK1 phosphorylation and activation in prostate cancer.

AR increases the expression of *CAMKK2* which in turn phosphorylates and activates AMPK at threonine 172. As a result, AMPK phosphorylates ULK1 at serine 555 which activates the ULK1 complex and initiates autophagy in an mTOR-independent manner, supporting prostate cancer growth. This growth and survival mechanism can be blocked at several steps and as such, offers alternative strategies for targeting autophagy in prostate cancer.

Chapter 4

**Identification of an AR-CAMKK2 Signaling Cascade that Promotes Prostate Cancer
Progression through CREB activity.**

4.1 Introduction

CREB is a transcription factor that includes three members: CREB1, ATF1 and CREM. They share high sequence similarity and are conserved from *Drosophila* to humans²⁵². The primary function of the CREB family is to integrate signals from intra- and extracellular stimuli and mediate transcriptional activity. It has been well-known that Ser133 is the most important phosphorylation site on CREB as it is required for signaling convergence on CREB and maximal transcriptional activity⁹³. Ser133 can be activated by a variety of serine-threonine kinases, including AMPK, CAMKI and CAMK4, CAMKK2's three primary substrates^{31, 39, 46, 253, 254}. Thus, I hypothesized that AR-CAMKK2 activated CREB indirectly through Ser133 phosphorylation.

Emerging studies have linked CREB overexpression and overactivation (primarily through Ser133 phosphorylation) to cancer development and progression. In liver, melanoma, prostate and stomach cancers, high mRNA levels of CREB have been correlated with worse 5-year overall survival⁹⁵. In prostate cancer, increased phosphorylation of CREB has been observed within poorly differentiated tumors and metastasis⁹⁷. Functionally, deletion or inactivation of CREB increased chemotherapy and radiation-induced cell apoptosis as well as repressed neuroendocrine differentiation and angiogenesis^{121, 154, 159, 163}. These findings indicate important roles for CREB in the progression of prostate cancer. Mechanistically, a large number of identified CREB targets are involved in aberrant cell proliferation, apoptotic resistance, angiogenesis and drug resistance, suggesting phospho-Ser133 dependent transcriptional activity is of importance for cancer initiation, progression and metastasis¹⁴⁷. While several studies have demonstrated the pro-oncogenic role of CREB in hormone-sensitive and neuroendocrine prostate cancer, CREB remains largely unexplored in CRPC progression.

Here, I tested the hypothesis that activation of CREB-dependent transcription by the AR-CAMKK2 signaling plays a key role in prostate cancer progression. More specifically, I investigated the upstream regulators and downstream effectors of CREB through multiple *in vitro* and *in vivo* prostate cancer models. I also revealed a functionally redundancy between *CREB1* and *ATF1* in CRPC using RNA sequencing on CRISPR-modified prostate cancer cell lines. Finally, I tested the efficacy of a small molecule inhibitor of CREB in diverse preclinical mouse models of CRPCs.

4.2 Results

4.2.1 Phosphorylation of CREB at serine 133 and CREB activity are positively correlated with AR-CAMKK2 signaling

To identify the downstream targets of the AR-CAMKK2 signaling pathway, I analyzed the RNA-seq data from C4-2 cells following *CAMKK2* knockout. GSEA revealed that genes downregulated in *CAMKK2* KO cells were significantly enriched in CREB activity related genesets, including genes having at least one occurrence of the transcription factor binding site (CREB_Q2, CREB_Q2_1 and CREB_Q4) and genes involved in the cAMP pathway (WANG_RESPONSE_TO_FORSKOLIN_UP) (Figure 20A). KEGG and Reactome pathway analysis displayed similar results (Figure 20B), indicating a potential link between CAMKK2 and CREB-dependent transcriptional activity. As an orthogonal approach, I performed western blots to assess the expression of AR, CAMKK2 and phosphorylation of CREB (p-CREB (Ser133)) in eleven prostate cancer patient-derived xenograft (PDX) models (Figure 21A). These data further indicated that 1) CAMKK2 levels were significantly correlated with AR and 2) both AR and CAMKK2 positively correlated with p-CREB (Figure 21). In addition, p-CREB, like CAMKK2, increased in an isogenically matched HSPC-CRPC-mCRPC model

of prostate cancer progression (Figure 21B), mirroring what has been reported in separate clinical cohorts^{150, 255}. Moreover, p-CREB staining was increased in prostate tissues, especially in dorsal-lateral lobes, of conditional *Pten* deletion mice and TRAMP mice (Figure 21C). These genetic mouse models (GEMM) are well-established prostate cancer preclinical models that were previously reported to express high levels of CAMKK2 in prostate epithelial-specific, *Pten*-deleted and TRAMP mice compared to WT control mice^{22, 24}. Together, these data suggest a high correlation between AR-CAMKK2 signaling and, phosphorylation of CREB, CREB activity, and prostate cancer progression.

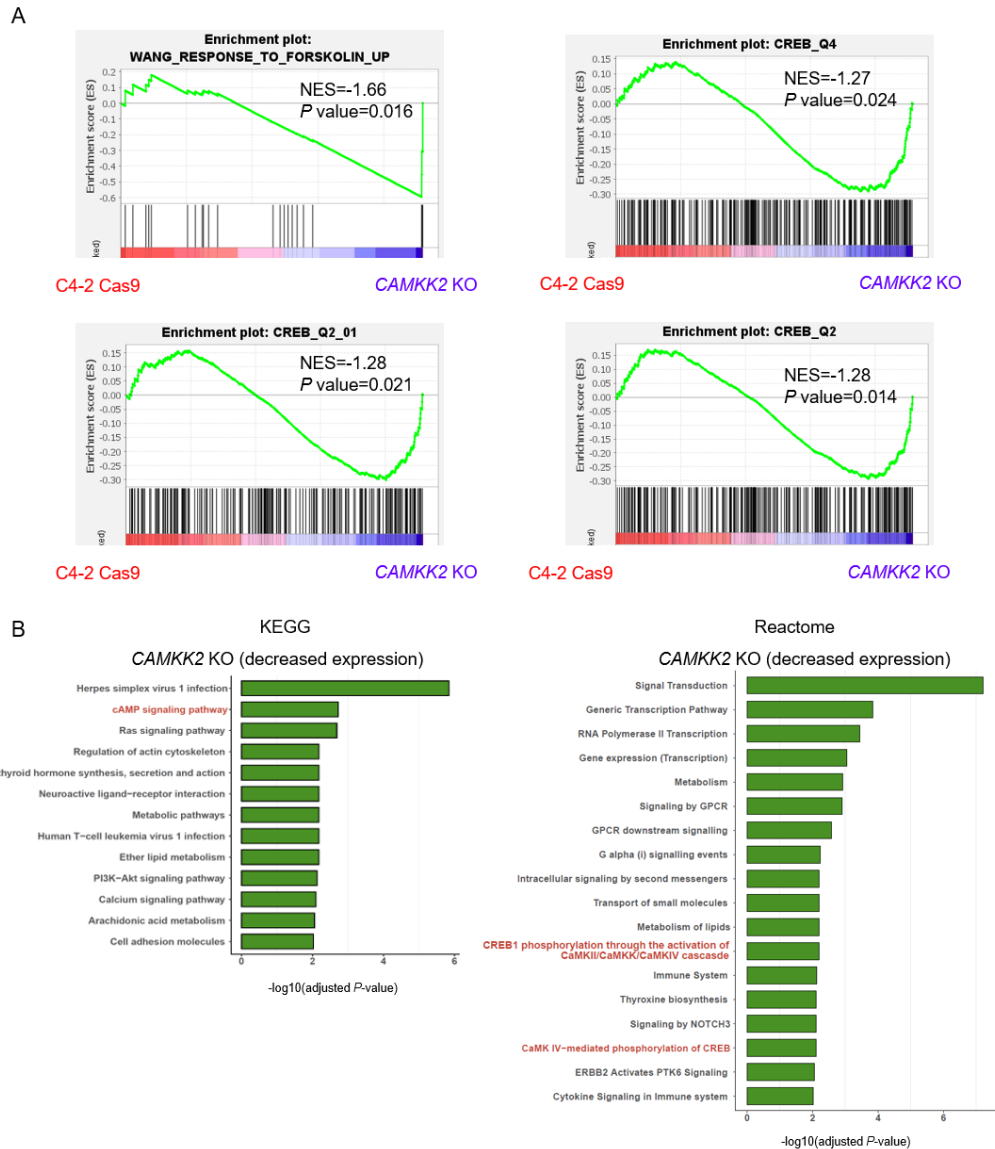


Figure 20. Pathway enrichment analysis of *CAMKK2* KO versus Cas9 control C4-2 cells.

(A) GSEA analysis of cAMP pathway and CREB motif signatures along the stat score rank of transcripts expressed in *CAMKK2* KO compared to Cas9 control C4-2 cells. (B) KEGG (*left*) and Reactome (*right*) pathway analysis of significant downregulated genes in *CAMKK2* KO compared to Cas9 control C4-2 cells.

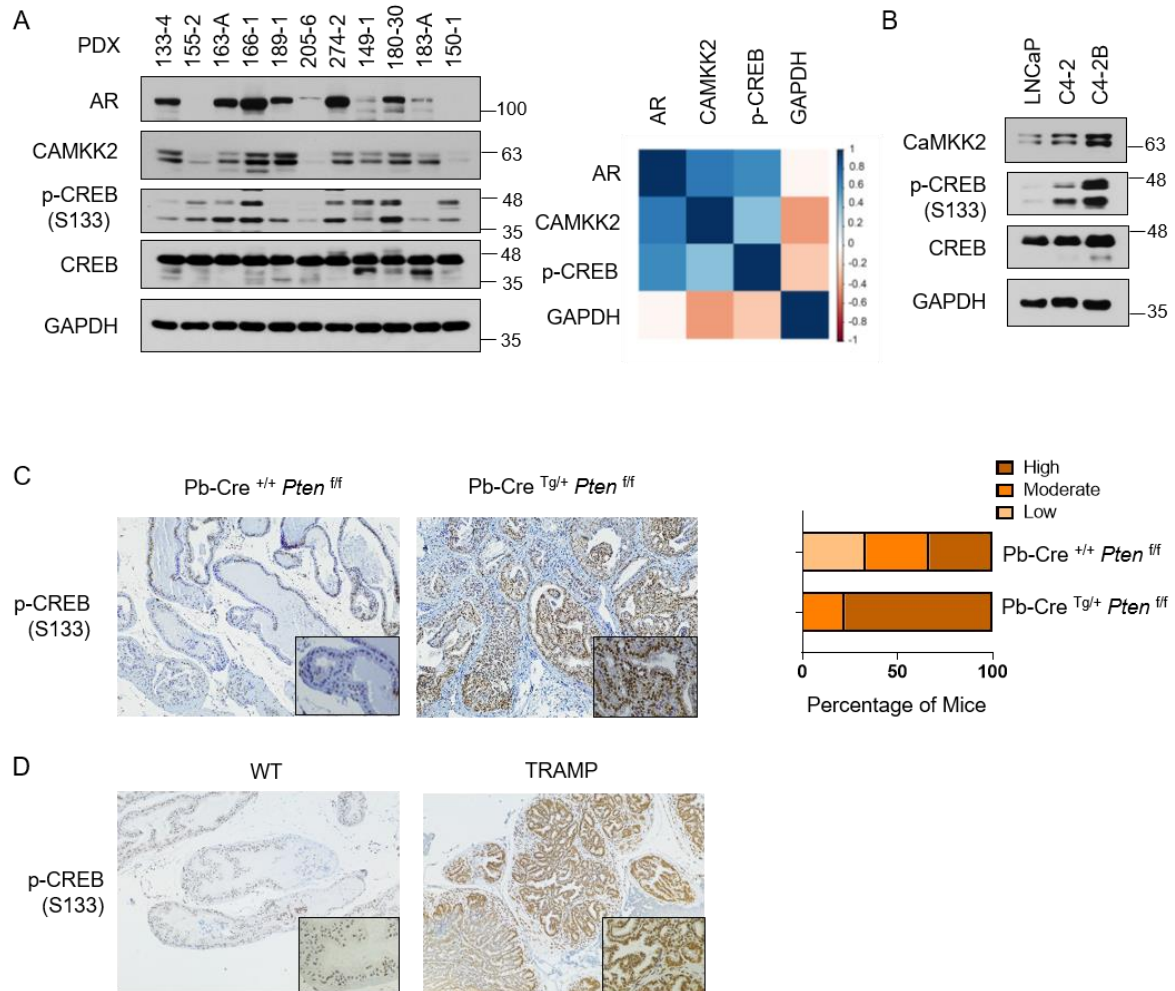


Figure 21. The expression of p-CREB (Ser133) in prostate cancer PDX, cell line and GEMM models.

(A) Immunoblot (*left*) and densitometry (*right*) analysis of AR, CAMMK2 and p-CREB (Ser133) in 11 prostate cancer PDX models. (B) Immunoblot analysis of LNCaP, LNCaP-derived CRPC cells (C4-2 and C4-2B). (C) IHC staining of p-CREB (representative prostate staining: left, 100X; quantification: right) in 40-week old Pb-cre^{+/+} *Pten*^{fl/fl} and Pb-cre^{Tg/+} *Pten*^{fl/fl} mice. (D) IHC staining of p-CREB (representative prostate staining: 100X) in 30-week old WT and TRAMP mice.

4.2.2 CREB is a downstream target of the AR-CAMKK2-CAMKI signaling pathway

Since p-CREB levels positively correlated with AR-CAMKK2 in prostate cancer and the primary CAMKK2 downstream targets have been reported to serve as the upstream kinases of CREB^{253, 254}, I sought to determine whether p-CREB and CREB transcriptional activity are regulated by AR-CAMMK2 signaling pathway. To explore whether AR can activate p-CREB, I treated hormone-sensitive LNCaP cells with the synthetic androgen R1881 to test if p-CREB responded to the activation of AR in prostate cancer cells. Western blot analysis showed that p-CREB at Ser133 was significantly elevated upon R1881 treatment while enzalutamide, an AR antagonist, blocked the R1881-augmented p-CREB increase (Figure 22A). Since Ser133 is responsible for CREB transcriptional activity, a luciferase reporter containing 3x cAMP response elements (CREs) was created and used to measure the CREB-dependent transcription in cells. Similar to p-CREB, androgen treatment increased CRE-mediated expression while enzalutamide resulted in a decrease (Figure 22B). To further confirm AR's role, I used two separate siRNAs to deplete *AR* expression. Similar to enzalutamide treatment, siRNAs targeting *AR* reversed R1881-induced p-CREB levels (Figure 22C). Taken together, these findings indicate that AR promotes the phosphorylation of CREB at Ser133 and downstream CREB activity in prostate cancer cells.

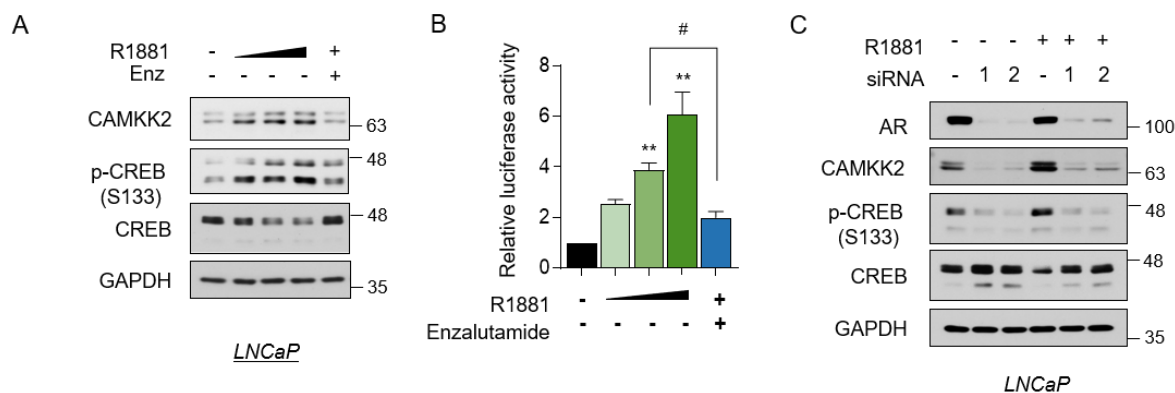


Figure 22. AR increases p-CREB and CREB activity.

Immunoblot analysis of LNCaP cells treated with R1881 alone (100 pM, 1 nM, and 10 nM) or combination (1 nM) with enzalutamide (Enz, 10 μ M, 1hr pretreatment) for 72 hours. (B) CRE-luciferase activity of LNCaP cells transfected with pGL4.23-CRE-luc plasmid and treated with R1881 alone (100 pM, 1 nM, and 10 nM) or combination (1 nM) with enzalutamide (10 μ M, 1hr pretreatment) for 72 hours. $**P < 0.01$, compared to vehicle treatment group. $\#P < 0.05$. (C) LNCaP cells were transfected with siRNAs targeting scramble control or *AR* and immunoblot analysis of transfected cells that were treated \pm 10 nM R1881 for 72 hours.

Next, I sought to investigate whether CAMKK2 mediated AR-induced CREB phosphorylation and activity. STO-609, a pharmacological inhibitor of CAMKK2, was used to inhibit the activity of CAMKK2. In both LNCaP and VCaP cells, p-CREB was increased after androgen treatment, while STO-609 blocked the androgen-mediated increase of p-CREB in both cell lines (Figure 23A-C), indicating that CAMKK2 is required for the androgen-mediated CREB phosphorylation. Interestingly, when treated with the same amount of androgen, p-CREB levels not altered by STO-609 in RWPE-1 non-transformed prostate epithelial cells (Figure 23D). As STO-609 has been reported to target multiple kinases ²²¹⁻²²³, I next sought to confirm CAMKK2's role in AR-induced CREB phosphorylation using molecular and genetic approaches. First, I established doxycycline-inducible, CAMKK2-overexpressing LNCaP and VCaP cells. Doxycycline-mediated CAMKK2 expression increased p-CREB levels in both LNCaP and VCaP cells (Figure 23E-F). Because CRPC cells showed higher p-CREB levels, I then reduced CAMKK2 expression using doxycycline-inducible shRNAs in C4-2 and 22Rv1 cells to validate CAMKK2's regulation of CREB phosphorylation/activity in models of CRPC. Doxycycline-induced knockdown of CAMKK2 decreased both p-CREB levels and CREB activity (Figure 23G-I). Consistent with the human prostate cancer cell models, conditional KO of *Camkk2* in prostate epithelial cells of TRAMP mice impaired disease progression and decreased p-CREB levels (Figure 24). Together, these results demonstrate that AR-CAMKK2 pathway promotes CREB(Ser133) phosphorylation and activity in both human HSPC and CRPC cells and *in vivo* mouse models of prostate cancer.

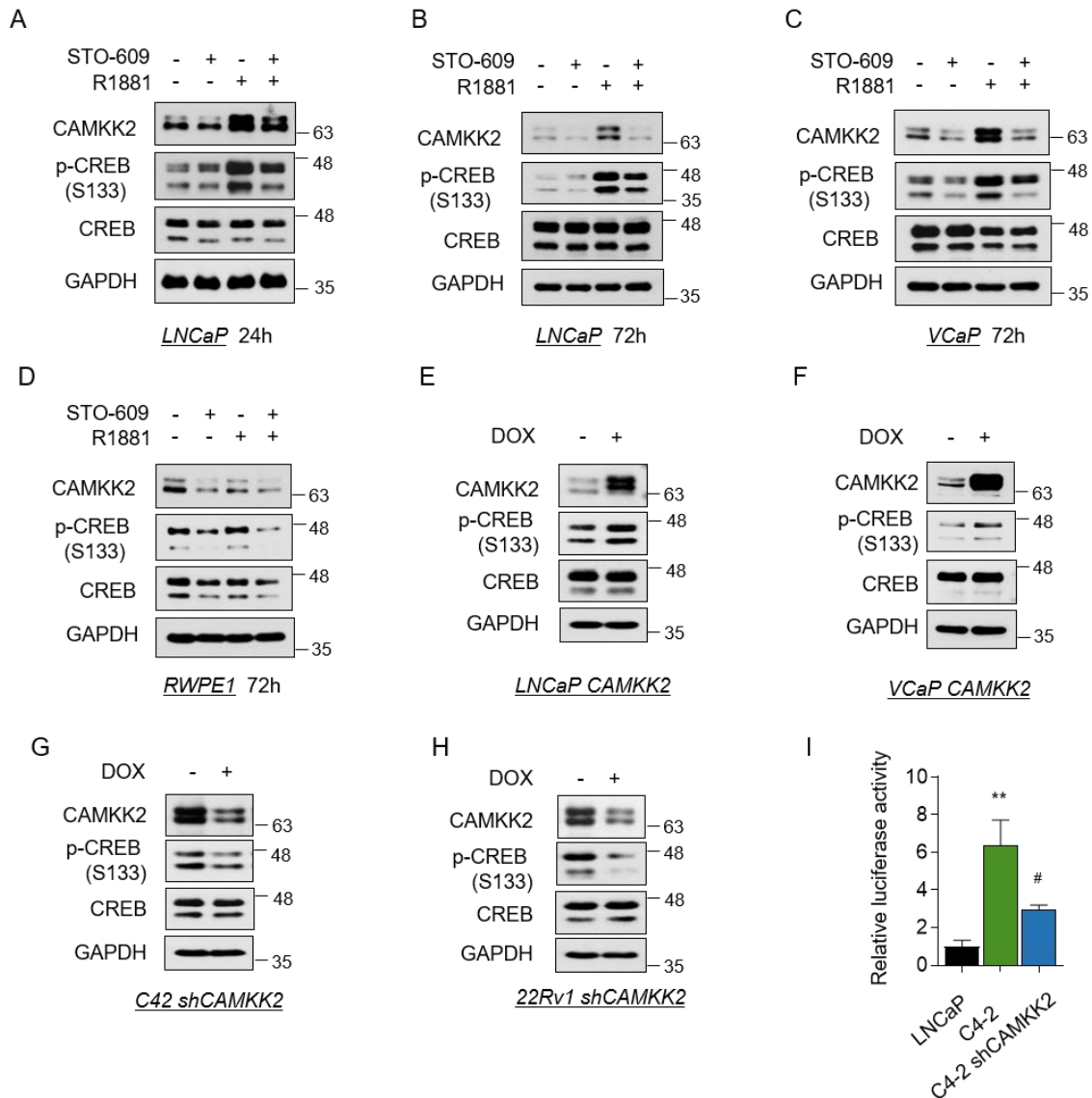


Figure 23. CAMKK2 contributes to p-CREB in both HSPC and CRPC cells.

(A-B) Immunoblot analysis of LNCaP cells treated \pm STO-609 and \pm R1881 for 24 (A) and 72 hours (B). (C-D) Immunoblot analysis of VCaP (C) and RWPE1 (D) cells treated \pm STO-609 and \pm R1881 for 72 hours. (E-F) Immunoblot analysis of inducible CAMKK2 overexpression LNCaP (E) and VCaP (F) cells treated with 20 nM doxycycline (DOX) for 48 hours. (G-H) Immunoblot analysis of inducible CAMKK2 knockdown C4-2 and 22Rv1 cells treated with 800 nM doxycycline for 72 hours. (G) CRE-luciferase activity of LNCaP, C4-2 and C4-2 shCAMKK2. ** $P < 0.01$, C4-2 compared to LNCaP. # $P < 0.05$, C4-2 shCAMKK2 compared to C4-2.

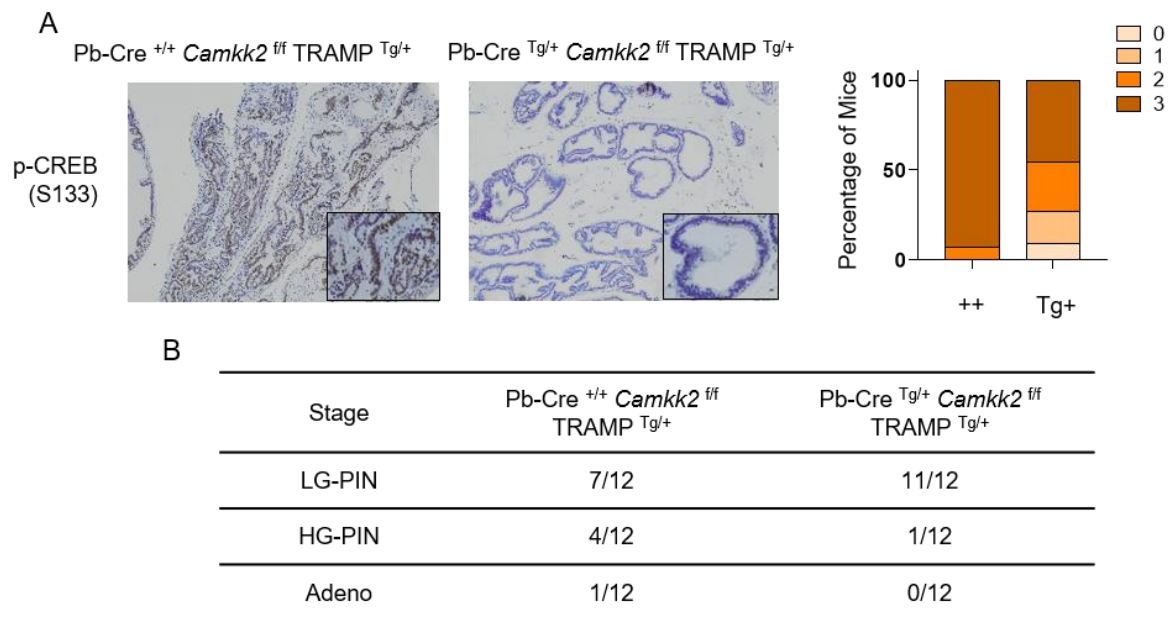


Figure 24. p-CREB decreases in Pb-cre^{Tg/+} *Camkk2*^{fl/fl} TRAMP^{Tg/+} mice.

(A) IHC staining of p-CREB (representative prostate staining: *left*, 100X; quantification: *right*) in 15-week old Pb-cre^{+/+} *Camkk2*^{fl/fl} TRAMP^{Tg/+} and Pb-cre^{Tg/+} *Camkk2*^{fl/fl} TRAMP^{Tg/+} mice. (B) Pathology report of 15-week old Pb-cre^{+/+} *Camkk2*^{fl/fl} TRAMP^{Tg/+} and Pb-cre^{Tg/+} *Camkk2*^{fl/fl} TRAMP^{Tg/+} mice.

The majority of CAMKK2's oncogenic effects in prostate cancer have, to date, been attributed to AMPK⁴⁶. Moreover, AMPK was identified as a CREB kinase *in vitro*²⁵⁴. Thus, I initially hypothesized that the AR-CAMMK2 increased p-CREB through AMPK. Using siRNAs targeting *PRKAA1*, which encodes the predominant AMPK α catalytic subunit in prostate cancer^{46, 227}, I observed that while p-AMPK and total AMPK was robustly silenced, p-CREB levels were unaltered in both HSPC and CRPC cells(Figure 25A&B), implying that AMPK does not facilitate AR-CAMKK2-mediated CREB phosphorylation. Next, I investigated the possible regulation of the remaining known CAMKK2 substrates, CAMKI (isoform $\alpha, \beta, \delta, \gamma$) and CAMK4, by the AR-CAMKK2 pathway. Using RT-qPCR, I examined the expression status of CAMKI and CAMK4 in prostate cancer cells. In some cell lines in which I observed robust CAMKK2 regulation of CREB, CAMKI γ and CAMK4 could not even be detected, indicating

they were not involved (Table 7). I then used siRNAs to knockdown CAMK1 α , β (PNCK) and δ . Only knockdown of CAMK1 α diminished AR-induced p-CREB levels (Figure 26). Of note, although endogenous CAMK1 β /PNCK was difficult to detect by western blot, p-CREB could be increased following exogenous CAMK1 β /PNCK overexpression. Conversely, knockdown of exogenous CAMK1 β /PNCK reversed AR mediated p-CREB expression (Figure 27). These data suggest that CAMK1 α , and under some contexts CAMK1 β , is the relay kinase that mediates AR-CAMKK2-induced CREB(Ser133) phosphorylation.

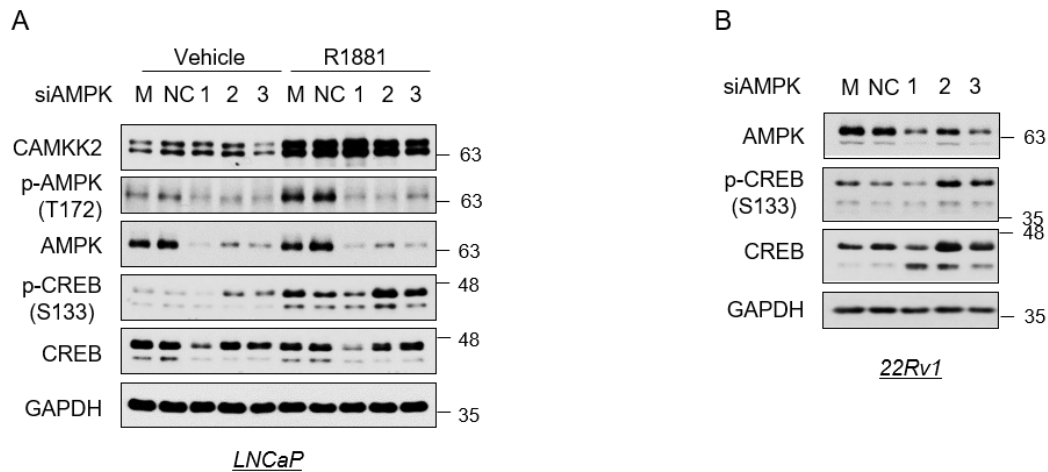


Figure 25. AMPK is not responsible for AR-CAMKK2 mediated CREB phosphorylation.

(A) LNCaP cells were transfected with mock (M) or siRNAs targeting scramble control (NC) or *PRKAA1* and immunoblot analysis was performed on transfected cells that were treated \pm 10 nM R1881 for 72 hours. (B) 22Rv1 cells were transfected with siRNAs targeting scramble control or *PRKAA1* and subjected to immunoblot analysis after 72 hours.

Table 8. CT values of CAMKI and CAMK4 in prostate cancer cell lines.

CT value (Target/36b4)	LNCaP	VCaP	22Rv1	C4-2
CAMKI-alpha	24.2/16.98	25.31/15.7	26.86/17.33	26.52/18.96
CAMKI- beta(PNCK)	31.84/16.98	27.87/15.7	35.68/17.33	34.34/18.96
CAMKI-gamma	Undetermined	Undetermined	Undetermined	Undetermined
CAMKI-delta	27/16.98	26.91/15.7	26.98/17.33	32.03/18.96
CAMK4	Undetermined	Undetermined	26.74/17.33	Undetermined

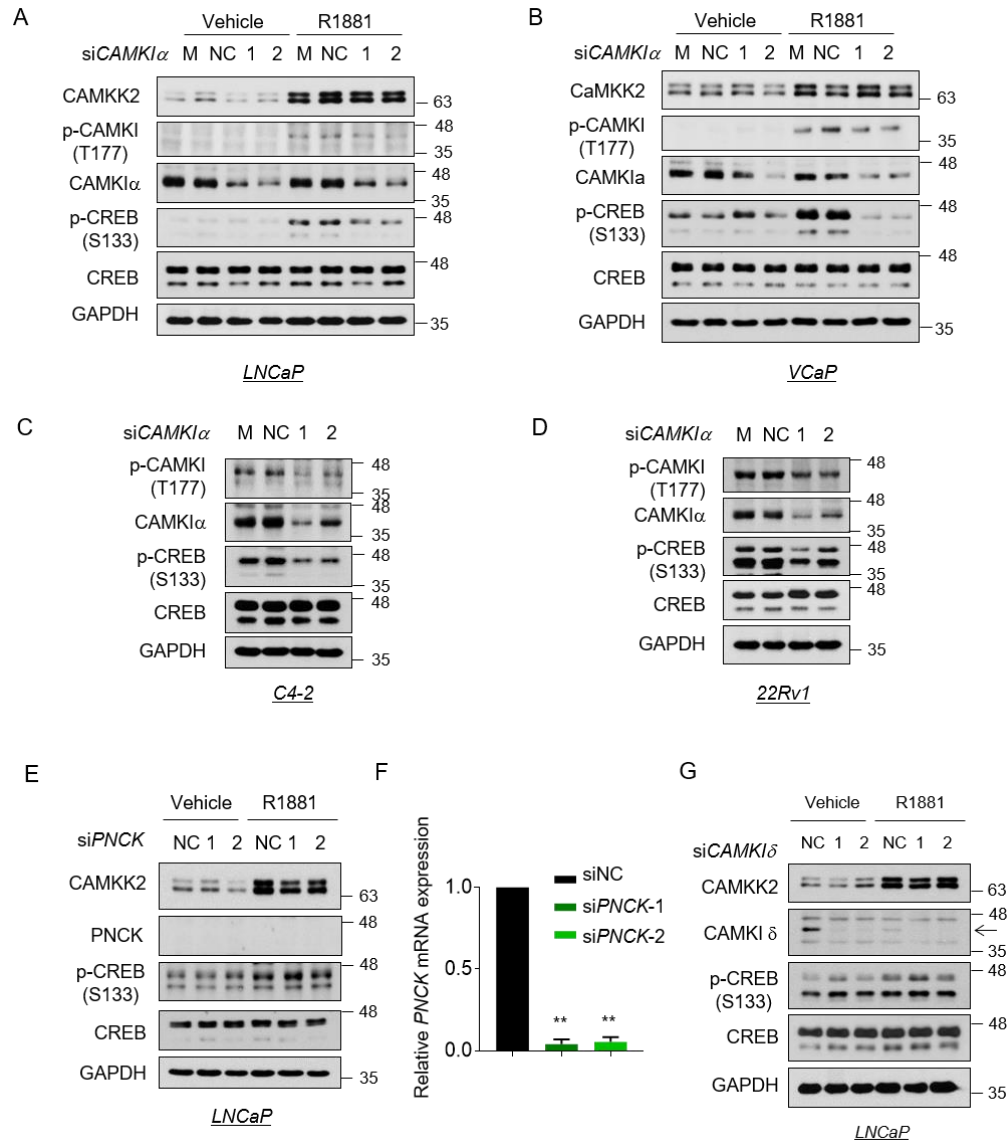


Figure 26. CAMK1α is the predominant kinase for AR-CAMKK2 mediated p-CREB in prostate cancer cells.

(A-B) LNCaP (A) and VCaP (B) cells were transfected with siRNAs targeting scramble control or *CAMK1α* and immunoblot analysis of transfected cells that were treated \pm 10 nM R1881 for 72 hours. (C-D) C4-2 (C) and 22Rv1 (D) cells were transfected with siRNAs targeting scramble control or *CAMK1α* and subjected to immunoblot analysis after 72 hours. (D) LNCaP cells were transfected with siRNAs targeting scramble control or *PNCK* and immunoblot analysis of transfected cells that were treated \pm 10 nM R1881 for 72 hours (*left*). Since the endogenous *PNCK* expression is difficult to detect by western blot, mRNA level of *PNCK* was shown. $**P < 0.01$, compared to negative control (*right*). (E) LNCaP cells were transfected with siRNAs targeting scramble control or *CAMK1δ* and immunoblot analysis of transfected cells that were treated \pm 10 nM R1881 for 72 hours.

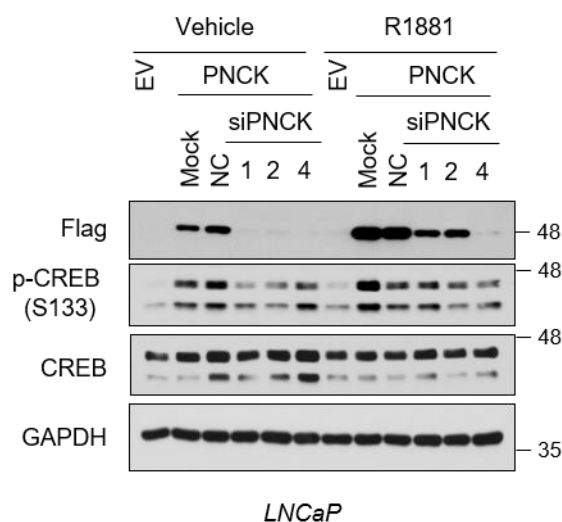


Figure 27. Exogenous PNCK can contribute to p-CREB expression.

LNCaP cells were transfected with PNCK-Flag and siRNAs targeting scramble control or *PNCK* and immunoblot analysis was performed on transfected cells that were treated \pm 10 nM R1881 for 72 hours.

4.2.3 AR antagonists, in a CAMKK2-independent manner, paradoxically function as weak activators of CREB

A previous study suggested that enzalutamide was able to increase p-CREB levels and thus, CREB activation was proposed as a mechanism of resistance to enzalutamide¹²¹. Given my findings that androgens were robust inducers of p-CREB, I wanted to further explore this seemingly paradoxical situation. To first identify whether this phenomenon was specific to enzalutamide or more broadly applicable to other AR antagonists, I treated LNCaP cells with different next-generation AR antagonists including enzalutamide and darolutamide alone and in combination with androgens. The results demonstrated that androgens were stronger inducers of CREB phosphorylation compared to AR antagonists alone but that the antagonists were able to decrease androgen-mediated p-CREB to some extent (Figure 28). Importantly, CAMKK2 was not changed when treating cells with AR antagonists alone (Figure 28), suggesting that while AR antagonists do activate CREB to an extent, this occurs via a CAMKK2-independent mechanism.

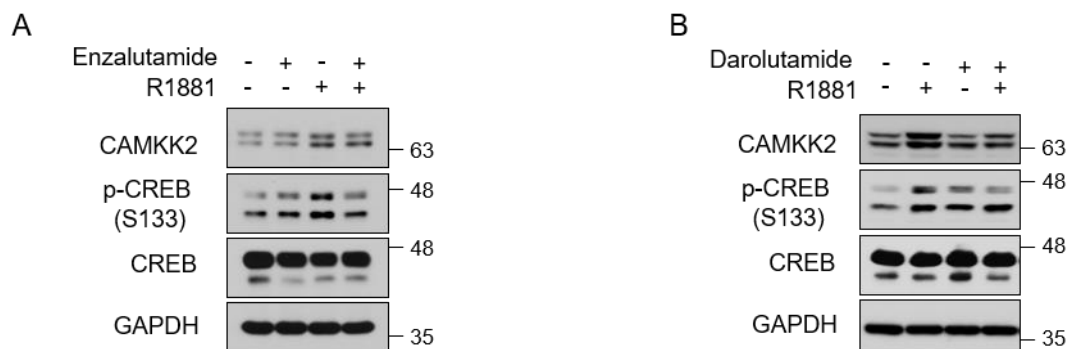


Figure 28. CAMKK2 is not involved in AR antagonist-mediated increase of p-CREB.

Immunoblot analysis of LNCaP cells pretreated \pm 10 μ M enzalutamide (A) or darolutamide (B) and \pm 1 nM R1881 for 72 hours.

4.2.4 CREB1 is required for prostate cancer cell growth, which is associated with alteration of CREB dependent transcription.

Prior studies have described the function of CREB in maintaining the malignant behavior in other cancer types^{96,97}. Considering work from our laboratory and others that demonstrated AR-CAMKK2 signaling promotes prostate cancer progression^{14, 21, 50, 256}, I hypothesized CREB was required for maximal AR-CAMKK2-mediated prostate cancer progression. To test this, lentiviral-mediated, doxycycline-inducible shRNAs and CRISPR-Cas9 system were used to generate CREB1 KD/KO cells to determine the role of CREB in cell growth. Doxycycline-inducible KD of CREB1 by two distinct shRNAs in LNCaP cells was sufficient to inhibit androgen-mediated cell growth and colony formation (Figure 29). Compared to corresponding control cells, CREB KD colonies showed both smaller size and substantially lower numbers (Figure 29F&G). Since I was unable to achieve sustainable shRNA-mediated KD of *CREB1* in C4-2 cells (not shown), I used CRISPR-Cas9 to KO *CREB1* in these cells. *CREB1* deletion in C4-2 and 22Rv1 cells both abrogated cell growth, but to different extents with C4-2 cells being more sensitive to *CREB1* KO than 22Rv1 cells (Figure 30A&B). In C4-2 cells, the *CREB1* KO cells were barely able form colonies (Figure 30A). To assess the role of CREB in

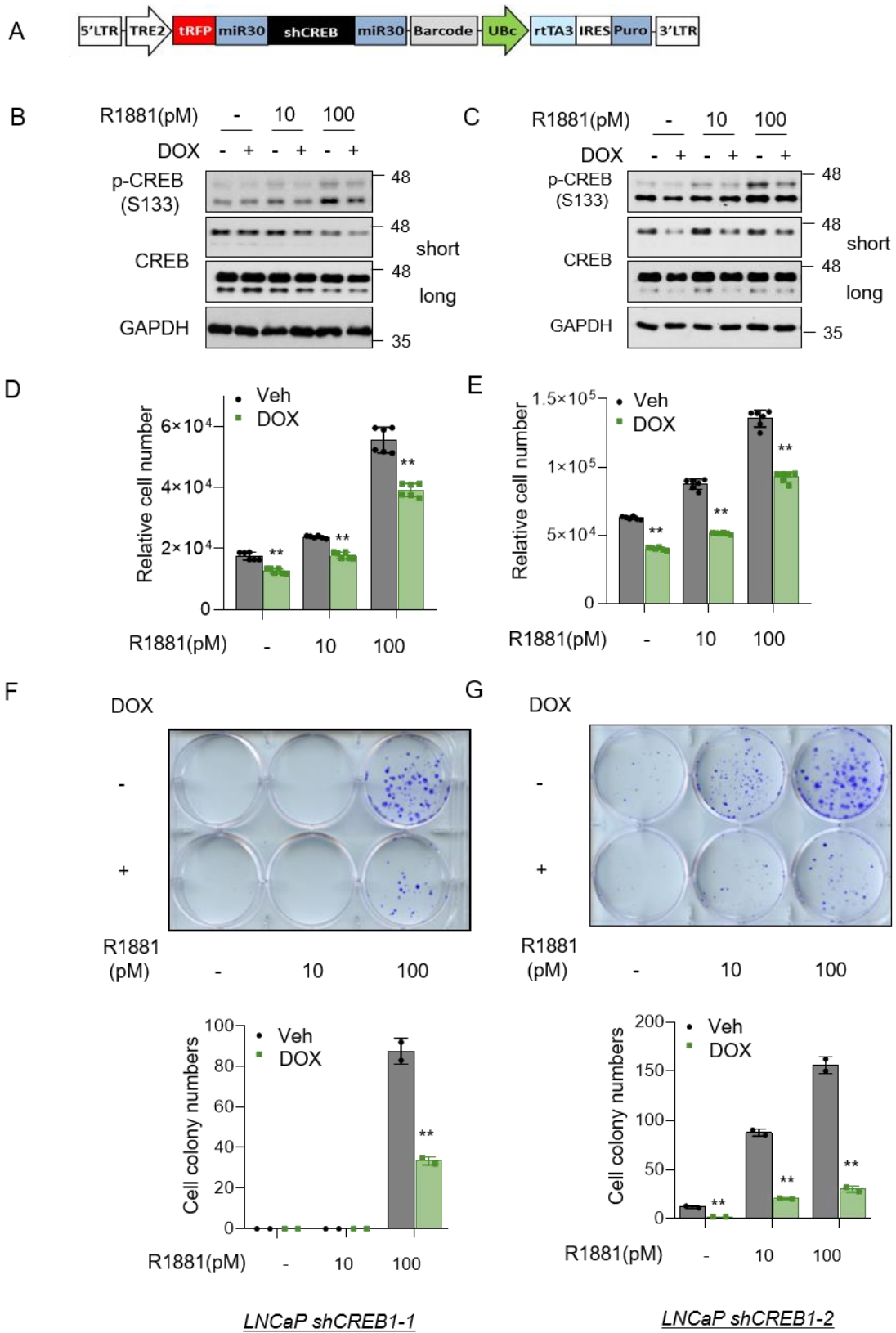


Figure 29. CREB1 is required for AR-dependent LNCaP cell growth.

(A) Construct used to create a doxycycline (Dox)-inducible shCREB1 LNCaP cell line. (B-C) Immunoblot analysis of shCREB1-1 (B) and shCREB1-2 (C) knockdown efficiency. (D-E) Cell growth of LNCaP shCREB1-1 (D) and LNCaP shCREB1-2 (E) cells following 7 days DOX and/or R1881 treatment. $**P < 0.01$, compared to corresponding vehicle treatment. (F-G) Colony formation assay of LNCaP shCREB1-1 (F) and LNCaP shCREB1-2 (G) cells following 28-day DOX and/or R1881 treatment. Representative images (*top*). Quantifications of two independent experiments (*bottom*). $**P < 0.01$, compared to corresponding vehicle treatment.

prostate cancer further, complementation studies were done by exogenously expressing CREB1-WT and CREB1-S133A in CREB1 KO C4-2 cells. While CREB1-WT partially rescued the anti-growth effects of CREB1 KO, equivalent expression of the CREB1(S133A) mutant had no rescue effect (Figure 30C), indicating that the phosphorylation of CREB at Ser133 is required for maximal prostate cancer cell proliferation. Importantly, the impact of CREB1 on CRPC tumorigenesis and progression were further confirmed in castrated mice xenograft models. CREB1 deletion not only had a profound effect on CRPC tumor growth but largely delayed initial tumor formation and extended overall survival of the tumor-bearing mice (Figure 31A-C). Consistent with my *in vitro* data, tumor growth was partially restored following re-expression of WT CREB1, but not the S133A mutant (Figure 31A-C), confirming the requirement of both CREB1 and in particular, Ser133 phosphorylation in CRPC tumor growth *in vivo*. Of note, I speculate that the reason for the partial and not full rescue of CREB1 may be attributable to exogenous CREB1 levels being unable to achieve endogenous CREB1 levels in the WT cells/tumors (Figure 31D). Regardless, these results together support a functional role for CREB Ser133 phosphorylation in CRPC both in culture and *in vivo*.

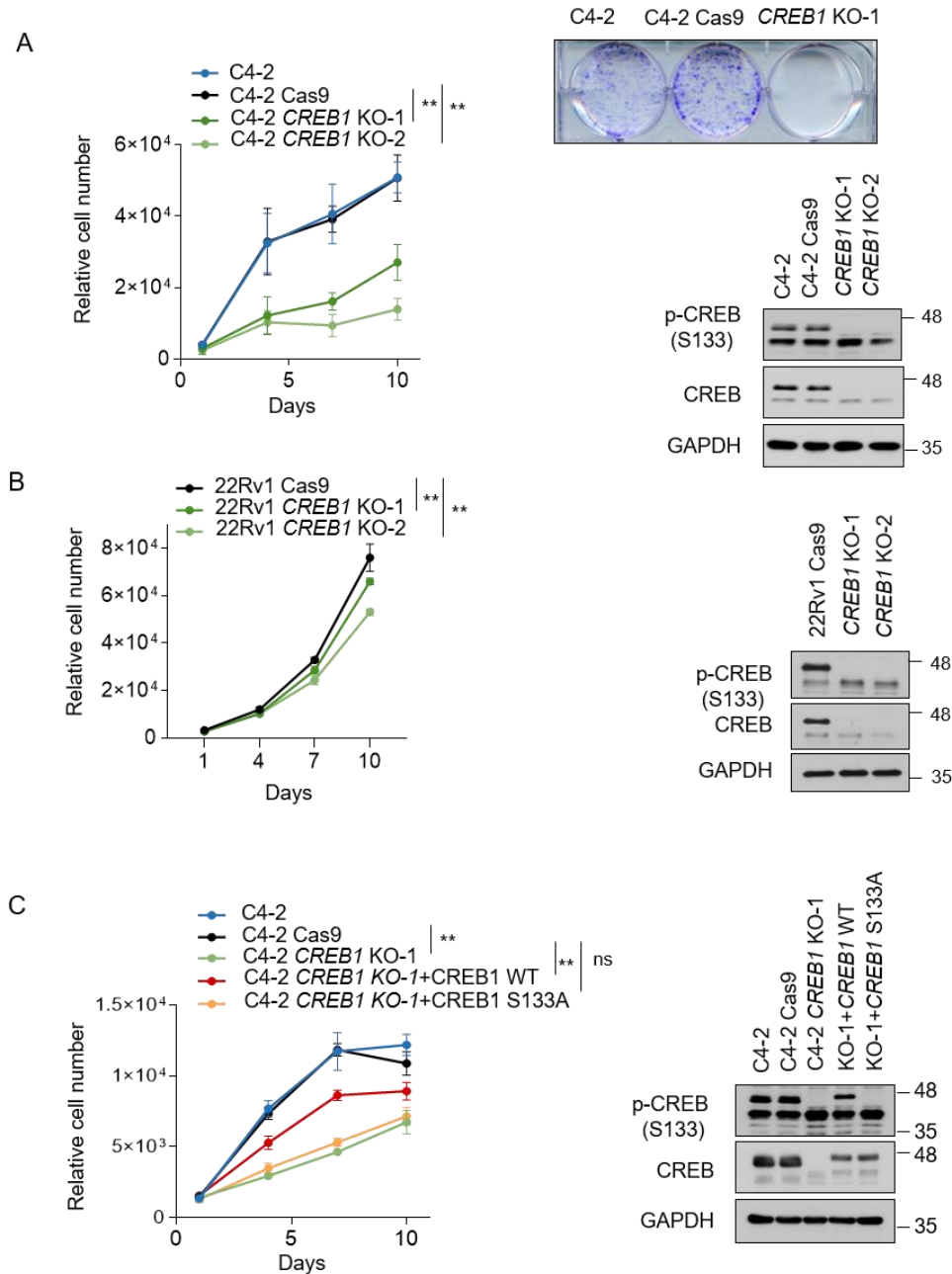


Figure 30. CREB1 is required for CRPCs cell growth.

(A-B) Cell growth curve (*left*) and Immunoblot analysis (*right*) of CRISPR-modified C4-2 cells with *CREB1* KO compared to parental C4-2 and C4-2 Cas9 cells. $**P < 0.01$, compared to Cas9 control. (B) Cell growth curve (*left*) and Immunoblot analysis (*right*) of CRISPR-modified 22Rv1 cells with *CREB1* KO compared to control 22Rv1 Cas9 cells. $**P < 0.01$, compared to Cas9 control. (C) Cell growth curve (*left*) and Immunoblot analysis (*right*) CRISPR-mediated C4-2 cells with *CREB1* KO and WT or S133A CREB1 addback compared to control C4-2 Cas9 cells. $**P < 0.01$.

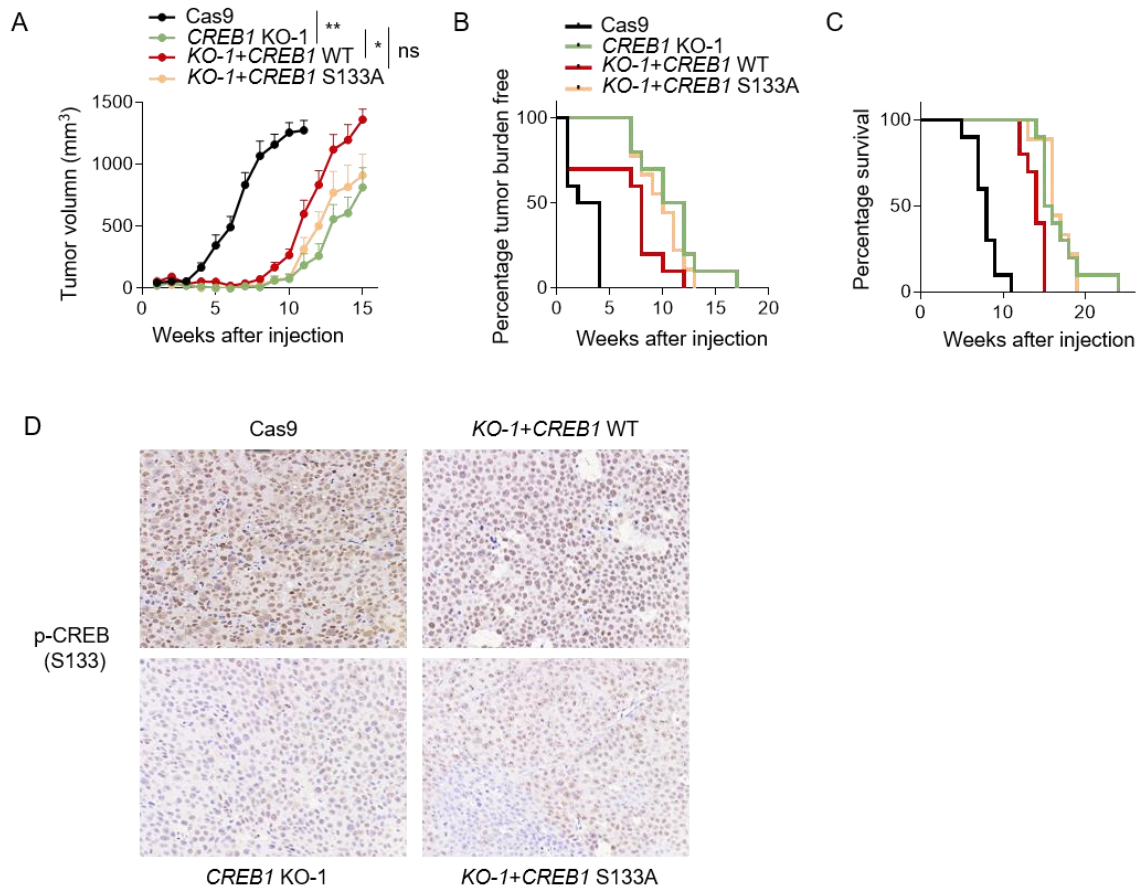


Figure 31. CREB1 is required for CRPC progression in xenograft model.

CRISPR-mediated *CREB1* deletion in C4-2 CRPC cells (*CREB1* KO) and WT or S133A *CREB1* addback subclones were subcutaneously injected into castrated NSG mice (n=10/group) and tumors were monitored every week. (A) tumor growth, ** $P < 0.01$, * $P < 0.05$. (B) KM plot of tumor incidence. (C) KM plot of survival. (D) IHC staining of p-CREB for tumor samples (100X).

Given the functional importance of CREB phosphorylation and activity contributing to CRPC cell growth, I next performed transcriptomic profiling to characterize how CREB promotes CRPC. To do this, I analyzed RNA isolated from C4-2 Cas9 control, C4-2 *CREB1* KO, C4-2 *CREB1* KO+WT CREB1, and C4-2 *CREB1* KO+Ser133A CREB1 cells using RNA-Seq. My analysis revealed that 2703 genes were significantly downregulated while only 179 genes were upregulated in CREB KO cells compared to C4-2 Cas9 cells ($|\text{LFC}| \geq 1$ and $|\text{padj}| < 0.01$). Such biased gene expression alteration in the CREB KO group strongly supported key roles of CREB1 during transcriptional activation in CRPC. Unsupervised hierarchical clustering of these downregulated genes further corroborated the requirement of CREB(Ser133) phosphorylation for maximal CREB-mediated transcription since CREB1 WT addback is clustered with Cas9 control while Ser133A and KO were clustered together (Figure 32A). Similar to the effects observed on cell proliferation and tumor growth, a large proportion of altered genes were restored in add-back cells re-expressing WT CREB1, unlike in cells expressing Ser133A mutant (Figure 32A). GSEA analysis of KEGG, Reactome, Hallmark, and GO gene sets comparing the isogenic models revealed that gene signatures related to cell growth, steroid-cholesterol metabolism, protein trafficking, the unfolded protein response, extracellular matrix organization and lipid metabolism related signatures were downregulated in CREB1-null cells, but could be restored in CREB1-WT. However, this was not observed in Ser133A expressing cells (Figure 32B-D). Collectively, these data demonstrate that CREB1 is required for cell proliferation *in vitro* and CRPC tumor growth *in vivo* and modulated many important cellular processes.

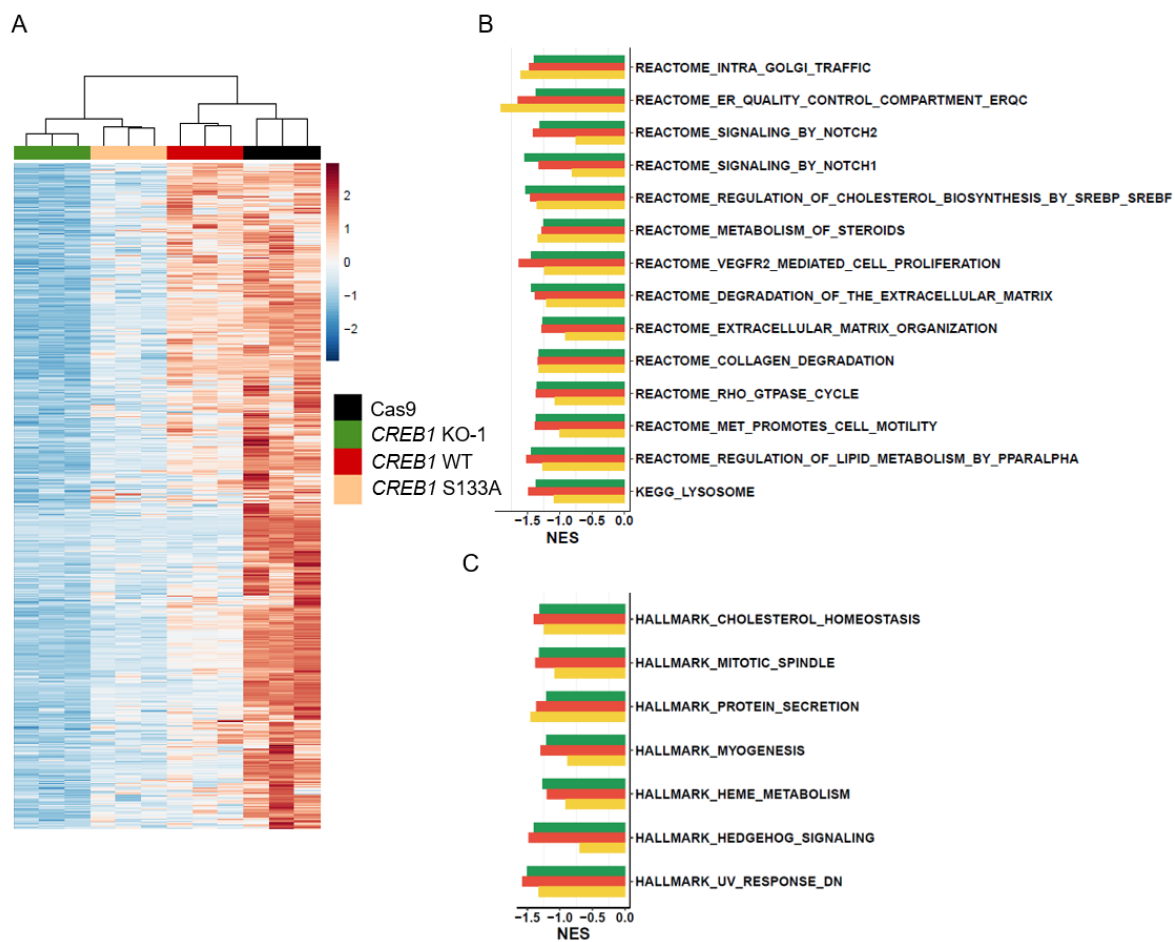




Figure 32. Deletion of *CREB1* leads to a transcriptional dependent cellular process alteration.

(A) Heatmap of RNA-seq data from C4-2 Cas9, *CREB1* KO and WT or S133A *CREB1* addback cells. Genes with significant changed (LFC) ≥ 1 and [padj <0.01] comparing *CREB* KO1 versus Cas9 control were considered for the clustering. The color scale bar indicated the Z score (blue, decreased expression, red, increased expression). (B-D) GSEA analysis of KEGG, Reactome (B), Hallmark (C), and GO (D) gene sets comparing C4-2 Cas9, *CREB1* KO-1, *CREB1* WT and *CREB1* S133A mutant addback cells. Normalized enrichment scores (NES) for gene sets 1) with $p<0.05$ and FDR $q<0.25$ in *CREB* KO1 versus Cas9 and *CREB* KO1 versus WT, 2) occurred in at least two databases are shown.

4.2.5 CREB1 and ATF1 exhibit functional redundancy in prostate cancer

CREB1 and its family member ATF1 are almost identical, sharing similar domain structures and exhibiting 69% amino acid homology overall and as high as 93% in their bZIP DNA-binding domains (Figure 33A). To investigate whether ATF1 has a shared or unique function in prostate cancer, I performed proliferation and transcriptomic analyses to compare the effects of CREB1 KO (2 sgRNAs) and ATF1 KO (2 sgRNAs) in C4-2 cells. Similar to CREB1 KO, ATF1 KO alone led to a comparable reduction in cell growth (Figure 33B). Compared to Cas9 control cells, ATF1 KO also led to primarily decreased gene expression (ATF1 KO-1, 1865 genes with decreased expression:145 genes with increased expression; ATF1 KO-2, 581 genes with decreased expression:100 genes with increased expression), suggesting ATF1, like CREB1, was primarily involved in transcriptional activation in prostate cancer. Moreover, genes that were dramatically decreased in CREB1 KO cells were also largely decreased in ATF1 KO cells (84.5% in ATF1 KO-1; 94.05% in ATF1 KO-2) and vice versa (93.68% in CREB1 KO-1, 72.99% in CREB1 KO-2) (Figure 33C). This data indicated that CREB1 and ATF1 might have redundant functions in CRPC, in line with proliferation data previously reported in this research. However, when comparing the most significantly changed genes in CREB1 KO cells to those in ATF1 KO cells, only 9.2% of the genes showed overlap between the two genetic backgrounds, indicating their own preferential regulation on gene expression intensity despite their similar substrate pools. For example, CREB KO is able to decrease *FOLH1* and *GIRK2* expression to a greater extent than ATF1 KO while ATF1 KO can promote *CDKN1A* gene expression which was not observed in CREB KO cells. To address the possibility of redundancy, I established CREB1/ATF1 double KO models. Proliferation assays showed that DKO exhibited greater growth impairment compared to either *CREB1* or *ATF1* single KO (SKO) in both C4-2 and 22Rv1 cells (Figure 34A&B). Cell-cycle analysis upon DKO revealed a significant reduction in the S-phase in comparison to

control cells and single KO cells (Figure 34C). I also observed that DKO cells had more extensive transcriptomic alterations than single KOs (Figure 34D). The number of downregulated genes in DKO was >500% than that in SKOs, highlighting the functional redundancy between CREB1 and ATF1. In xenograft mice, DKO led to a profound impairment in tumor growth (Figure 35A) which corresponded to dramatic increases in time to tumor formation time and overall survival (Figure 35B&C). Nine out of ten mice were even tumor free at 11 weeks when all mice in the control arm were sacrificed. Moreover, three mice harboring DKO tumors survived >32 weeks. Accordingly, DKO mice also displayed significantly decreased proliferation, as detected by BrdU staining (Figure 35D).

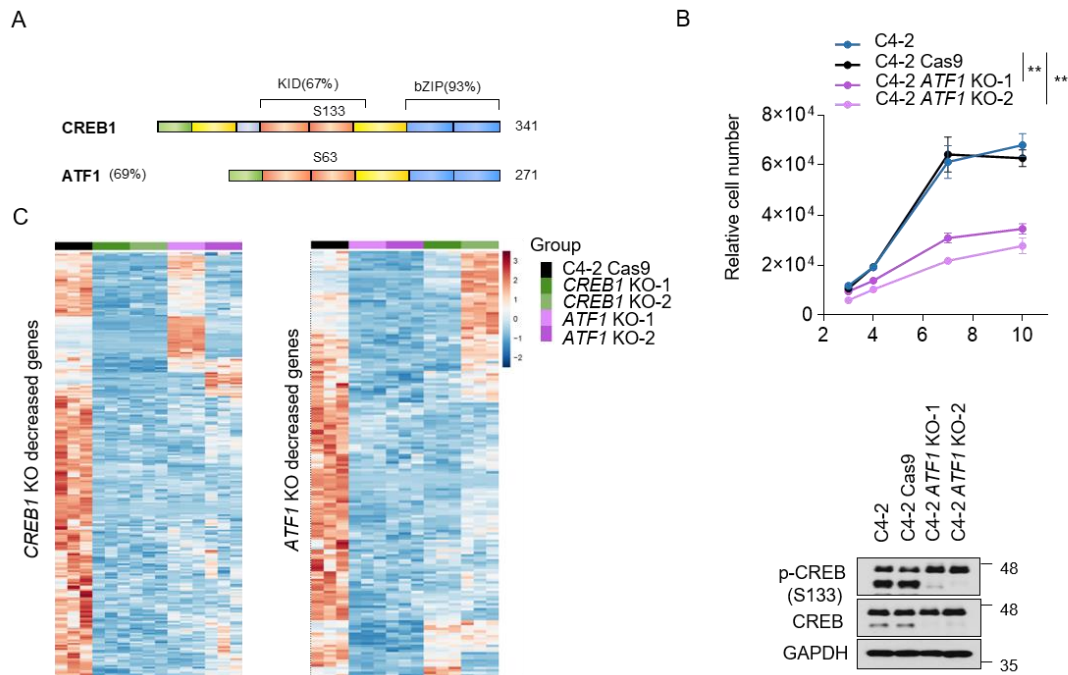


Figure 33. ATF1 and CREB1 exhibit functional redundancy in CRPC.

(A) Alignment of human CREB1 and ATF1 protein. Percentages denote the amino acid homology between CREB1 and ATF1 in KID and bZIP domain. (B) Cell growth curve (top) and Immunoblot analysis (bottom) of CRISPR-modified C4-2 cells with *ATF1* KO compared to parental C4-2 and C4-2 Cas9 cells. ** $P < 0.01$. (C) Heatmaps of differentially expressed genes in *CREB1* KO (left) and *ATF1* KO (right) cells, compared with Cas9 control ($\text{LFC} \geq 1$ and $\text{padj} < 0.01$). The color scale bar indicated the Z score (blue, decreased expression, red, increased expression).

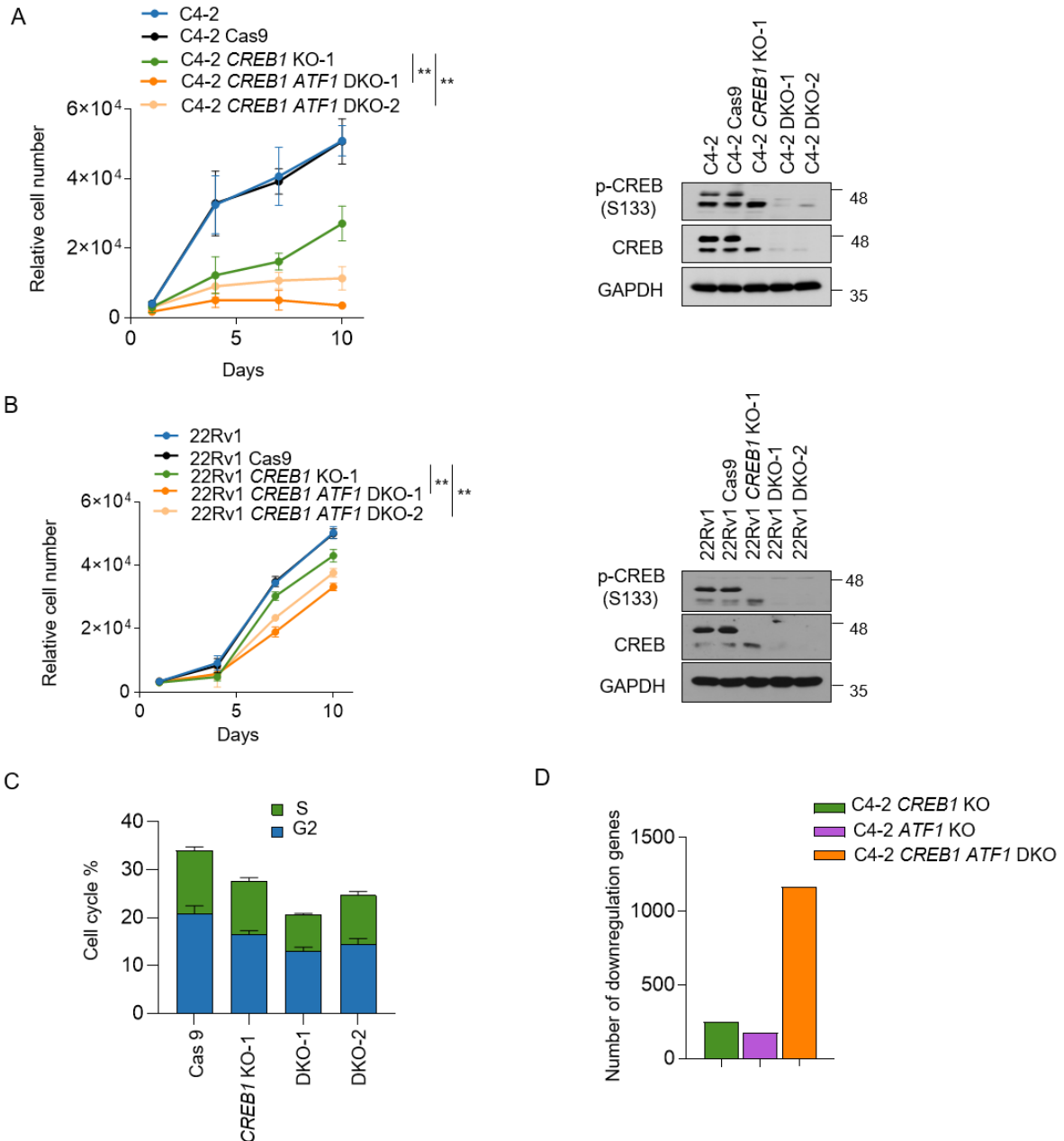


Figure 34. CREB1/ATF1 DKO decreases CRPC cell growth.

(A) Cell growth curve (left) and Immunoblot analysis (right) of CRISPR-modified C4-2 cells with *CREB1* KO and *CREB1 ATF1* DKO compared to parental C4-2 and C4-2 Cas9 cells. $**P < 0.01$. (B) Cell growth curve (left) and Immunoblot analysis (right) of CRISPR-modified 22Rv1 cells with *CREB1* KO and *CREB1 ATF1* DKO compared to parental 22Rv1 and 22Rv1 Cas9 cells. $**P < 0.01$. (C) Cell cycle analysis of SKO and DKO cells. (D) The number of downregulation genes in SKO and DKO. The result shows the overlap gene list from two sgRNA.

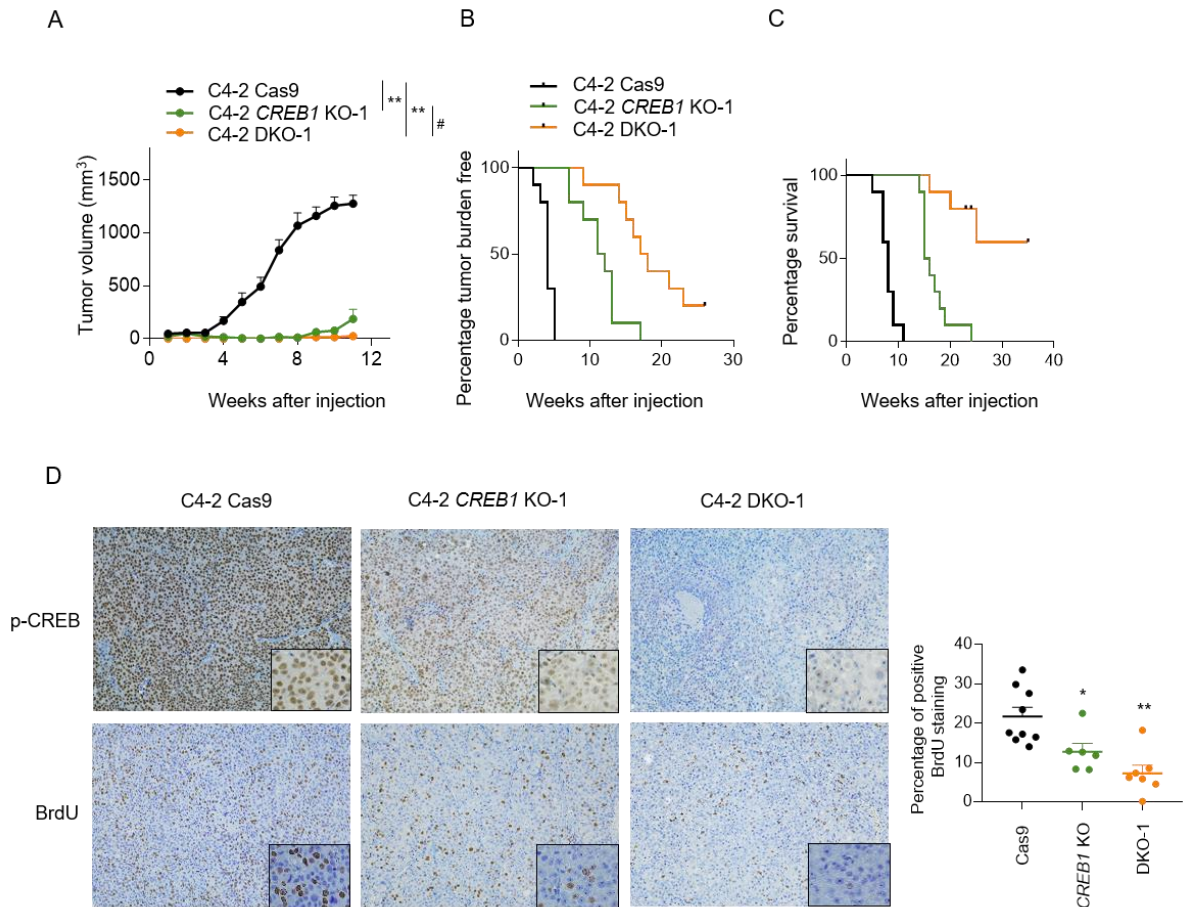


Figure 35. *CREB1 ATF1* DKO dramatically reduces tumor growth and prolongs survival in xenograft models of CRPC.

CRISPR-mediated *CREB1* deletion and *CREB1 ATF1* double deletion C4-2 cells were subcutaneously injected into castrated NSG mice (n=10/group) and tumors were monitored every week. (A) Tumor growth. (B) KM plot of tumor incidence. (C) KM plot of survival. Three of DKO mice survived more than 8 months. (D) IHC staining of p-CREB and BrdU for tumor samples (100X). ** $P < 0.01$, * $P < 0.05$, compared with Cas9 control. # $P < 0.05$, compared with *CREB1* KO-1.

4.2.6 Pharmacologic targeting of CREB in prostate cancer

The observed functional redundancy between CREB1 and ATF1 suggested that from a therapeutic perspective, small molecule inhibitors capable of targeting both CREB family members could be highly efficacious for the treatment of CRPC. 666-15 is a recently developed small molecular inhibitor of CREB (Figure 36A) which can block CREB dependent transcriptional activity²⁵⁷. 666-15 has been successfully demonstrated to inhibit tumor growth and metastasis in breast cancer and pancreatic cancer^{179, 257}. Various prostate cancer cell lines I tested including HSPC, CRPC and enzalutamide-resistant cells all exhibited sensitivity to 666-15 with IC50s ranging from 100 nM ~ 1 μ M (Figure 36B). Notably, compared with corresponding control, CREB1 and ATF1 single KO showed modestly reduced sensitivity upon 666-15 treatment, while a significantly right-shifted IC50 was found in the DKO cells (Figure 36B). This data not only further confirmed the redundancy of CREB1/ATF1 but demonstrated the selectivity of 666-15 towards both CREB1 and ATF1 (Figure 36C&D). Interestingly, C4-2 cells exhibited increased sensitivity to 666-15 relative to isogenically matched, hormone-sensitive LNCaP cells, further suggesting an increased dependence on CREB during the transition from HSPC to CRPC (Figure 36E). BrdU cell cycle analysis showed that 666-15 treatment exhibited a dose-dependent G1/S cell cycle arrest (Figure 36F), consistent with what I observed in DKO cells (Figure 34). I then tested the efficacy of 666-15 *in vivo* in C4-2 CRPC xenograft models (Figure 37A). Even the lowest dose of 666-15 (2mg/kg) exhibited dramatic inhibition of established C4-2 tumors propagated in castrated mice (Figure 37B&C). Similar to a previous report²⁵⁸, I observed no obvious toxicities at the highest dose tested (10 mg/kg) (Figure 37D&F). In line with my finding that 666-15 displayed G1/S cell cycle arrest *in vitro*, reduced BrdU staining was also observed in 666-15 treated mice compared to the vehicle control group (Figure 37E). I then selected two PDX tumors for

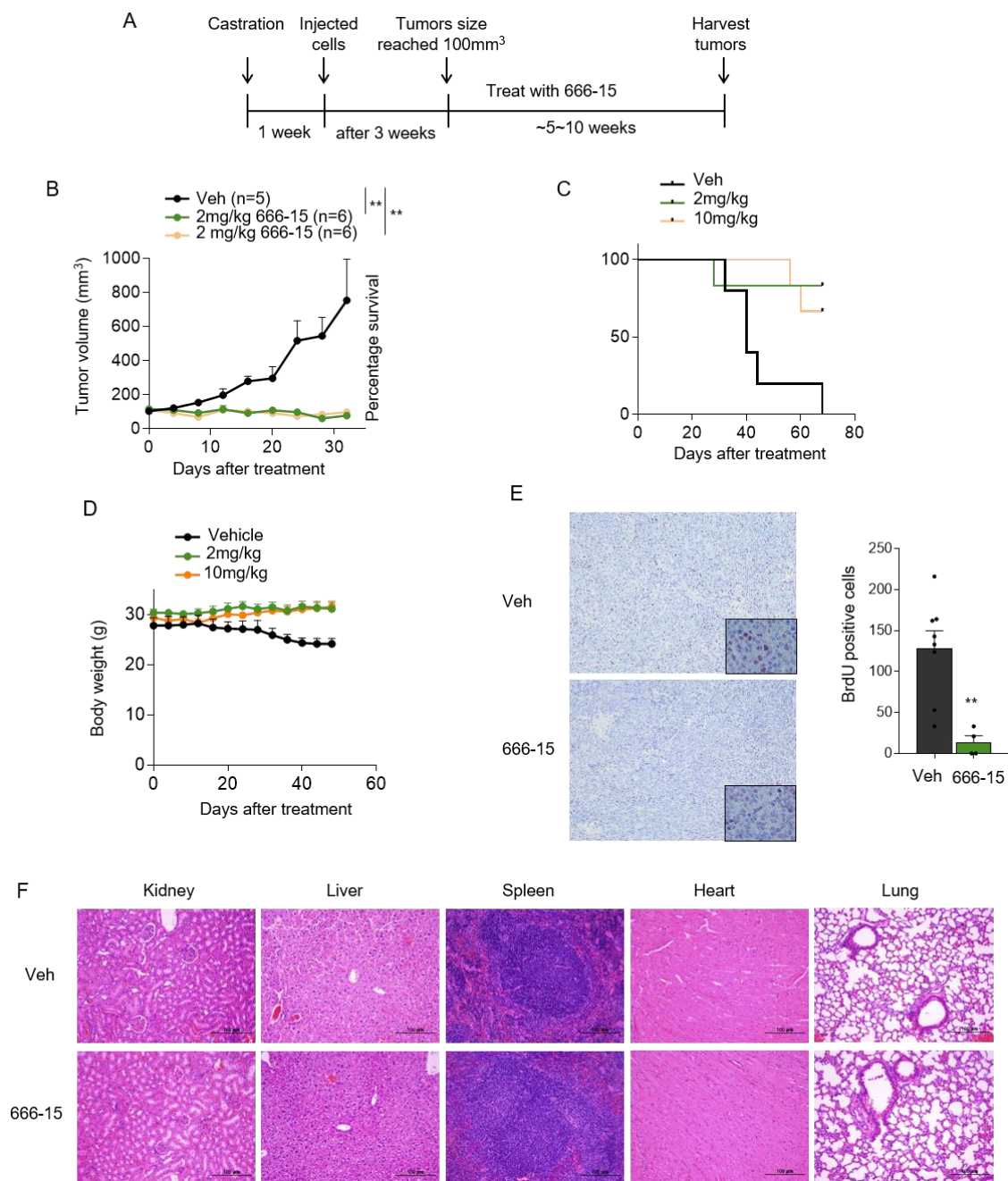


Figure 37. The small molecule CREB inhibitor 666-15 decreased tumor growth without significant toxicity in xenograft models of CRPC.

(A) Schematic of 666-15 treatment in xenograft study. (B-C) The tumor growth (** $P < 0.01$) (B) and survival curves (C) of C4-2 xenograft mice with treated 666-15. (D) The body weight change curve of xenograft mice treated with 666-15. (E) IHC staining of BrdU for tumor samples. *Left*, representative staining (100X); *right*, quantification. ** $P < 0.01$, compared to vehicle treatment. (F) H&E staining of major organs (200X).

further testing that I identified as having high p-CREB expression (Figure 21A). Tumor growth curves showed that 666-15 led to a significant reduction in tumor growth of enzalutamide-resistant PDX 274-2 while 180-30 had no response to 666-15 (Figure 38). This data suggested inhibition of CREB by 666-15 may be a potential therapeutic strategy for enzalutamide-resistant prostate cancers. However, the response was not directly correlated with p-CREB level, indicating a better biomarker for patient selection is likely needed.

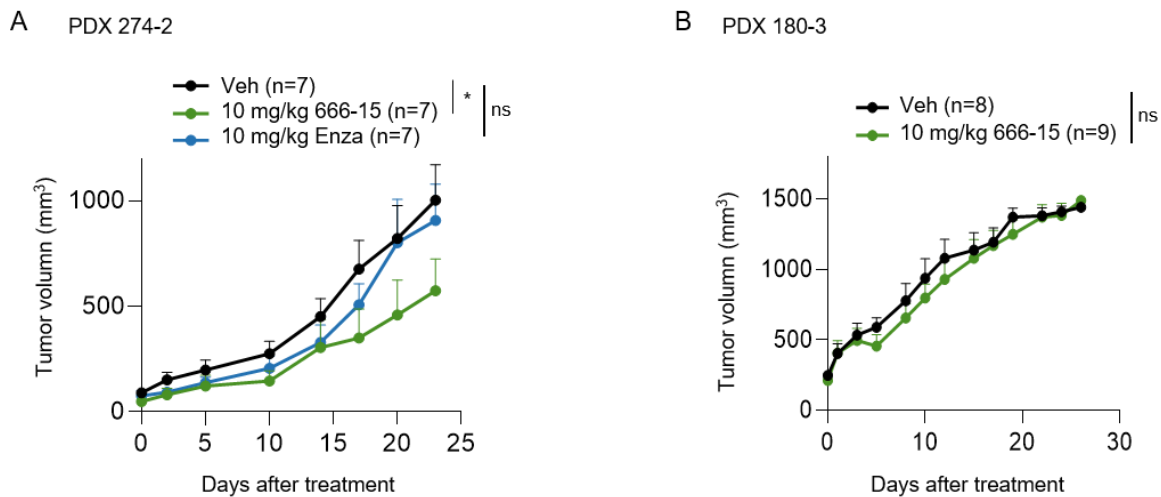


Figure 38. The efficacy of 666-15 in PDX models.

Tumor growth curves of PDX models 274-2 (A) and 180-30 (B) with 666-15 treatment. * $P < 0.05$

In addition to evaluating the efficacy of 666-15, I also conducted molecular analysis for downstream effectors of CREB inhibition in prostate cancer. Interestingly, *FOLH1*, the gene encoding prostate-specific membrane antigen (PSMA), was identified to be regulated by CREB based on RNA-seq analysis of CREB SKO and DKO CRISPR models. These data were further confirmed by qPCR, immunoblot and flow cytometry (Figure 39A-E). As PSMA-PET has been recently approved by FDA for the detection of recurrent and metastatic prostate cancer, there is ongoing work to investigate whether PSMA can be used as a predictive and pharmacodynamic biomarker for 666-15 treatment/CREB targeting. When comparing with

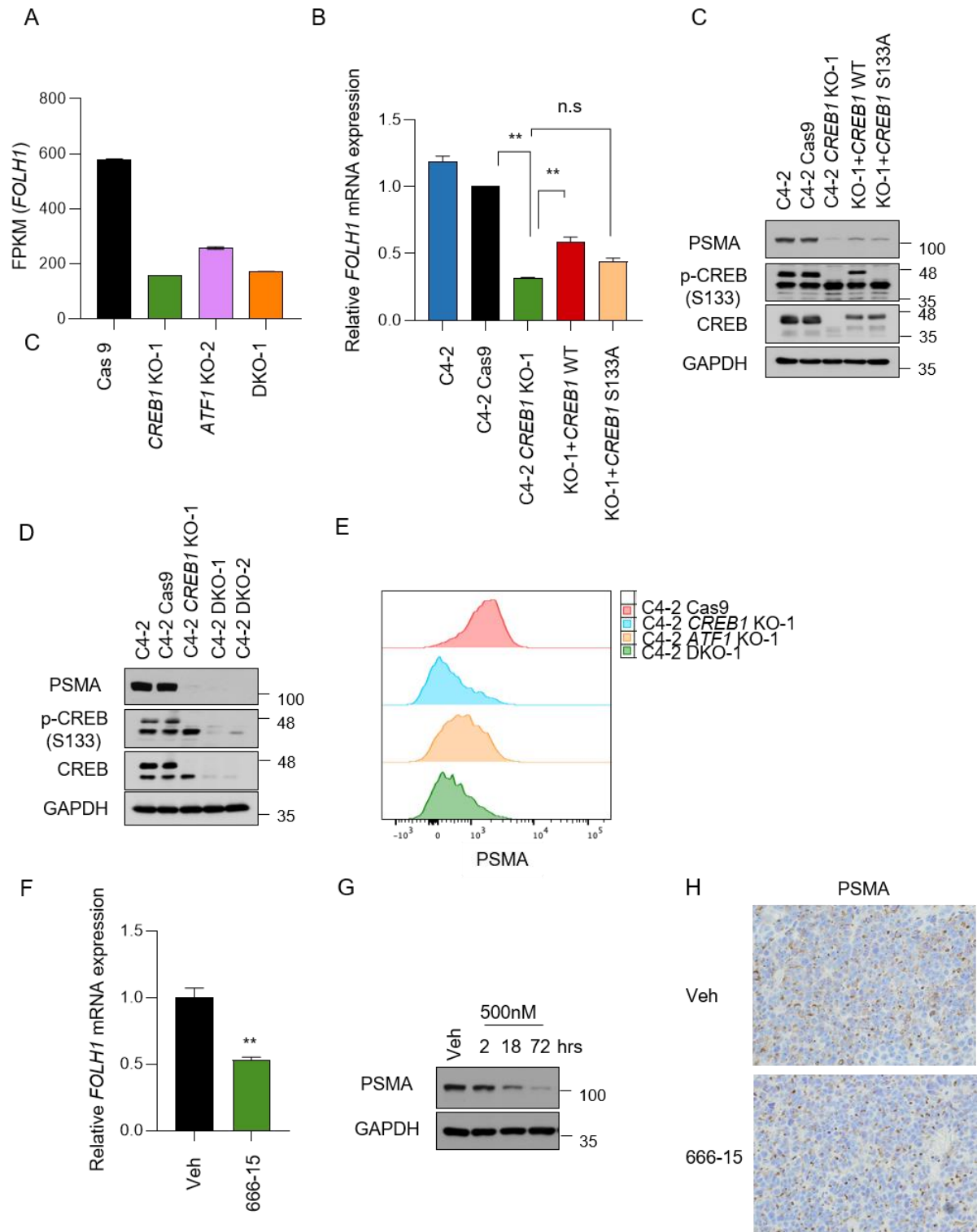


Figure 39. PSMA is a potential biomarker for CREB activity/inhibitors.

(A) FPKM of *FOLH1* in C4-2 Cas9, *CREB1* KO, *ATF1* KO and *CREB1 ATF1* DKO cells. (B) qPCR analysis *FOLH1* in C4-2 Cas9, *CREB1* KO and WT or S133A CREB1 addback cells. (C) Immunoblot analysis of PSMA in C4-2 Cas9, *CREB1* KO and WT or S133A CREB1 addback cells. (D) Immunoblot analysis of PSMA in C42 Cas9, *CREB1* KO and *CREB1 ATF1* DKO cells. (E) Flow cytometry analysis of PSMA in C42 Cas9, *CREB1* KO, *ATF1* KO and *CREB1 ATF1* DKO cells. (F) qPCR analysis of *FOLH1* in C4-2 cells treated with 500 nM 666-15 for 72 hours. $**P < 0.01$. (G) Immunoblot analysis of PSMA in C4-2 cells treated with 500 nM 666-15 for indicated time. (H) IHC staining of PSMA for PDX 274-2 tumor samples (200X).

vehicle control, *FOLH1* was significantly downregulated in 666-15 treated C4-2 cells, as shown by decreased mRNA levels from RNA-seq and RT-qPCR, as well as protein levels from western blot and IHC staining (Figure 39F-H), indicating the potential application of PSMA-PET to monitor the efficacy of CREB inhibitors in prostate cancer patients.

4.2.7 CREB is involved in prostate cancer metastasis through matrix metalloproteinase 16 (MMP16)

When performing my prior GSEA analysis to look for CREB-regulated processes (Figure 32), a significant enrichment in the extracellular matrix organization was observed (Figure 40A&B). Further analysis of RNA-seq data of CREB inhibition revealed that one of the leading-edge genes in related processes was MMP16, an endopeptidase involved in extracellular matrix degradation, suspected to contribute to metastasis. RNA-Seq data indicated that MMP16 expression was strongly decreased by *CREB1* or *ATF1* SKO and was further decreased in DKO cells (Figure 40C&D), which was confirmed by RT-qPCR analysis (Figure 40E). Accordingly, the CREB inhibitor 666-15 also inhibited MMP16 expression (Figure 40F). Wound healing assays showed that 666-15 treatment can block C4-2 cell migration, consistent with a potential role for CREB in metastasis (Figure 41). Consistent with this, *MMP16* gene amplifications are frequently observed in human prostate cancer and

particularly in metastatic samples (Figure 42A&B). *MMP16* amplifications are inversely correlated with disease-free survival in both TCGA and Taylor *et al.* 2010 clinical cohorts (Figure 42C&D). Overall, these findings suggest a potential additional role for CREB in cancer metastasis through the induction of *MMP16*.

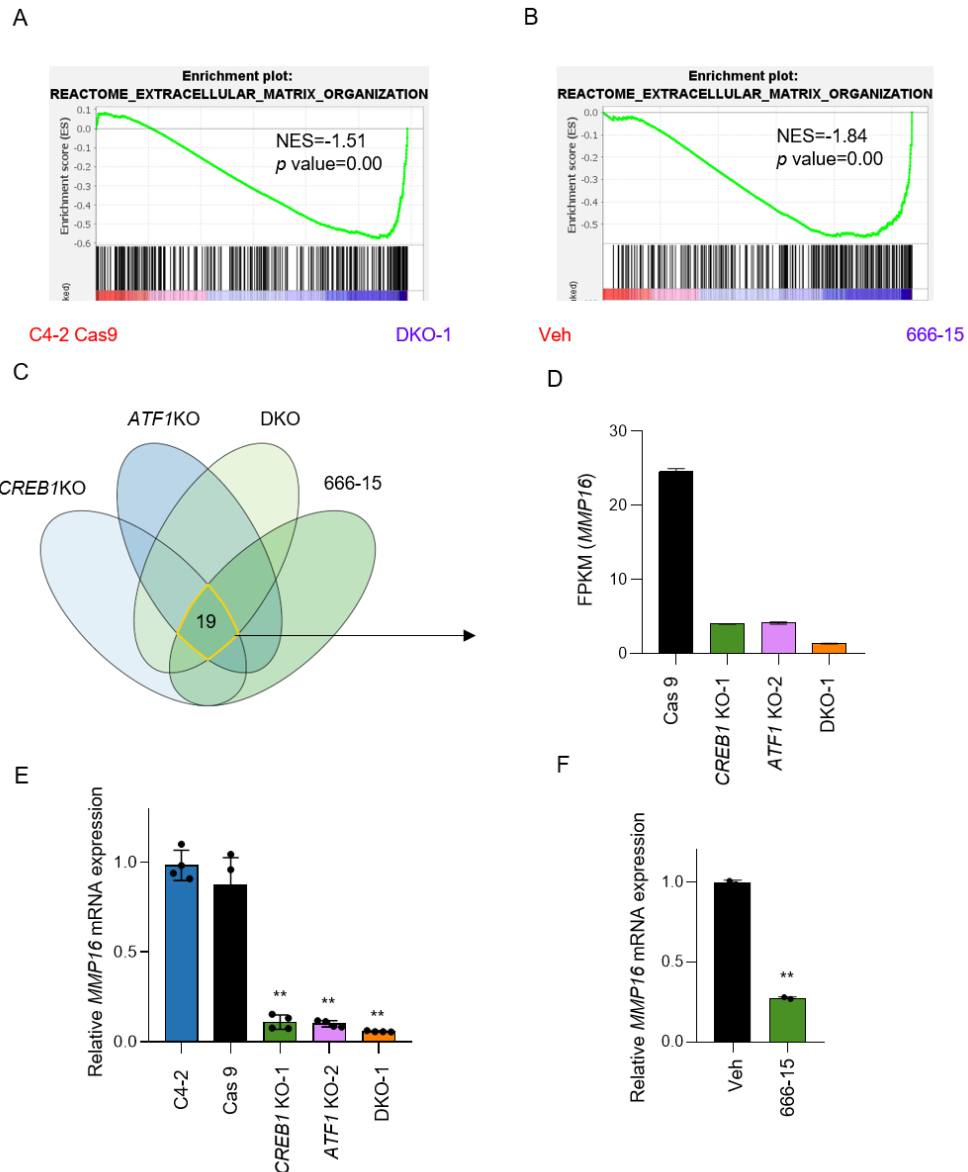


Figure 40. CREB is involved in extracellular matrix regulation.

(A-B) GSEA analysis of Reactome_extracellular_matrix_organization signatures along the stat score rank of transcripts expressed in DKO compared to C4-2 Cas9 cells (A) and 500 nM 666-15 treatment for 72 hours compared to vehicle in C4-2 cells (B). (C) Venn diagrams of genes differentially expressed in *CREB1* KO, *ATF1* KO, DKO compared with Cas9 control respectively and 666-15 treatment compared with vehicle. (D) FPKM of *MMP16* in Cas9, *CREB1* KO, *ATF1* KO and DKO cells. (E) qPCR analysis of *MMP16* in C4-2, Cas9, *CREB1* KO, *ATF1* KO and DKO cells. ** $P < 0.01$, compared to Cas9 control. (F) qPCR analysis of *MMP16* in vehicle and 500 nM 666-15 treatment for 72 hours. ** $P < 0.01$, compared to vehicle treatment.

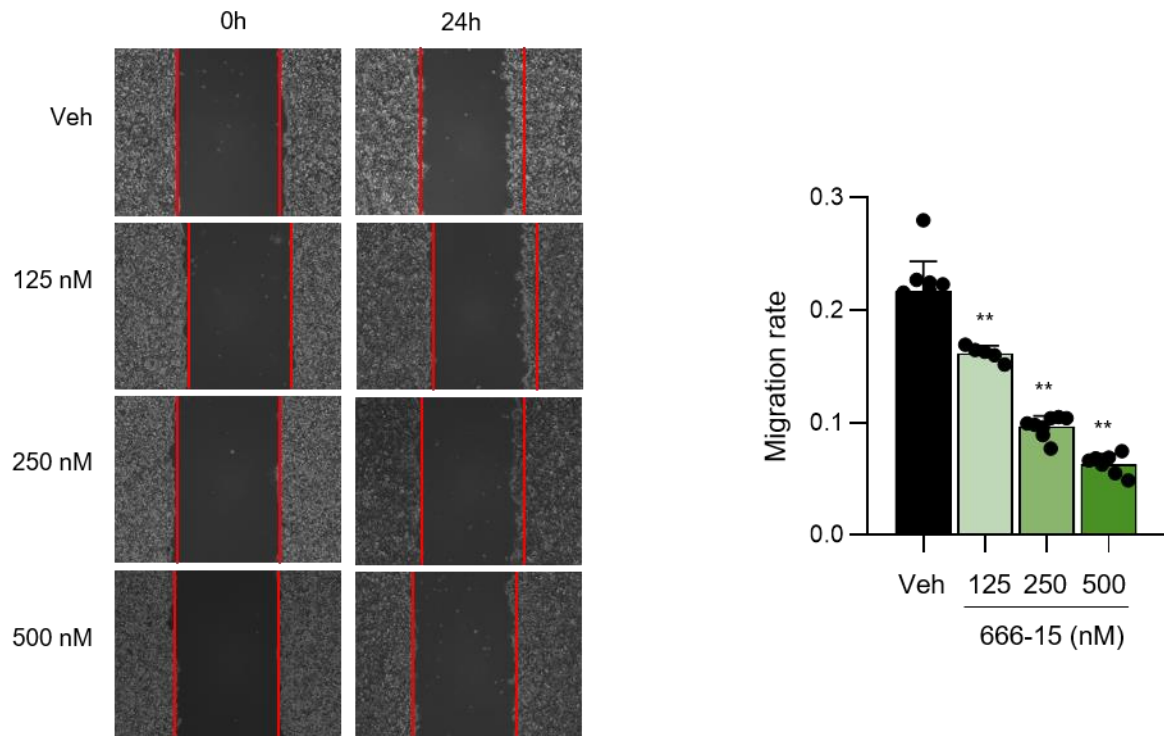


Figure 41. The CREB inhibitor 666-15 decreases cell migration.

Representative phase-contrast images (*left*) and quantification (*right*) of the inhibition of cell migration after 24 hours 666-15 treatment. ** $P < 0.01$, compared to vehicle treatment.

Moreover, consistent with previous studies^{52, 121, 169}, downregulation of CREB1 expression by shRNA decreased AR-induced LNCaP cell growth and colony formation. I further elucidated the proliferative role of CREB1 and ATF1 in CRPC via CRISPR-Cas9 mediated knock-out models. Both proliferation assays and xenograft experiments indicated that CRPC is vulnerable to CREB1 or ATF1 SKO, but even more sensitive to CREB1/ATF1 DKO (Figures 31-31,33-34). Of note, CREB activity was highly dependent on Ser133 phosphorylation (Figure 32). Together, these data support an essential role for the CREB family in prostate cancer progression.

Although PKA is the most commonly studied upstream kinase of CREB, here I investigated the regulation of CREB by AR-CAMKK2-CAMKI signaling given the central role of AR in prostate cancer. Several previous studies have reported that p-CREB at Ser133 is positively regulated by androgen treatment or correlates with AR expression in prostate cancer and even hepatocellular carcinoma^{52, 119, 259, 260}. Interestingly, a divergent study recently revealed that p-CREB was increased by the treatment of the antiandrogen enzalutamide in the absence of androgen, whereas, when combined with androgen, it suppressed the activation of CREB¹²¹. However, they failed to show the status of p-CREB when androgen treatment alone in the same study. In the present study, I found that androgen treatment robustly increased p-CREB levels in a dose- and AR-dependent manner in multiple prostate cancer cell models (Figure 22). In agreement with the previous study, I also found AR antagonists including enzalutamide and darolutamide had similar but weaker effects on p-CREB expression when used alone, although in the presence of androgen, the antiandrogens showed obvious inhibition of androgen-increased p-CREB (Figure 28). Together, these findings indicate that both androgens and antiandrogens can enhance p-CREB but to different extents, and such increase could be impaired by mutual interaction. However, the mechanisms underlying these observations, which seem to run counter to each other, remain

to be fully elucidated. This may be in part due to the complexity of dual regulations from both AR and PKA. To that end, previous studies attributed the androgen-or antiandrogen-mediated upregulation of p-CREB to PKA^{52, 114, 121}. Here, I demonstrated that AR-mediated CAMKK2 clearly represents another robust CREB regulatory mechanism (Figure 23). This not only adds to our understanding of how AR mediates p-CREB enhancement, but provides an alternative strategy for CRPC treatment. Unlike PKA, CAMKK2 levels were unaltered by AR antagonists when treated alone, suggesting that antiandrogens increased p-CREB in a CAMKK2-independent manner. Of note, CREB has been identified as a substrate of many kinases including ERK, AKT and PAK4²⁶¹. These kinases have discrete responses to AR activation and AR inhibition, which underscore the complex upregulation of p-CREB observed following androgen or antiandrogen treatments^{52, 121, 261-264}. Moreover, the crosstalk among these kinases, such as PKA deactivating CAMKK2, adds an additional layer of regulation on p-CREB²⁶⁵⁻²⁶⁷. Therefore, it is highly possible that the final status of p-CREB is determined by the integrated signals from many kinases that function in a context-dependent manner. Regardless, my data support that AR-mediated CREB has an oncogenic function in prostate cancer progression: AR promoted p-CREB is positively correlated with prostate cancer growth while AR antagonist induced p-CREB has been reported as a mechanism of resistance by which NEPC cells survive hostile conditions¹²¹. These data converge to highlight the potential of targeting CREB, which functions as a downstream effector of both AR agonist- and antagonist-mediated pro-cancer signals.

Although the majority identified CAMKK2's pro-cancer role was through AMPK, previous study has suggested that CAMKK2 has AMPK-independent oncogenic function²⁴. Interestingly, my data here revealed that CAMK1 but not AMPK, mediates phosphorylation of p-CREB downstream of AR-CAMKK2 signaling (Figures 25&26). Endogenously, only CAMK1 α was responsible for AR-mediated p-CREB increase (Figure 26). However, I cannot

not rule out that under some contexts CAMK1 β /PNCK may also phosphorylate/activate CREB since overexpression of PNCK increased CREB phosphorylation while KD of exogenously expressed PNCK by siRNA could reverse it (Figure 27), indicating PNCK can function similar to CAMK1 α but that the levels of CAMK1 isoforms might ultimately determine the primary kinase that regulates CREB phosphorylation. Little is known about the role of CAMK1 in prostate cancer. This is the first time CAMK1 has been linked to CAMKK2 oncogenic functions in prostate cancer. These findings are in agreement with a previous study in AML reporting that CAMK1-mediated CREB activation is required for cancer survival³⁹. Overall, I extended our knowledge on AR-CAMKK2 signaling in prostate cancer and addressed the endogenous downstream kinase that facilitates CREB activity.

In addition to elucidating the upstream mechanism of CREB regulation, I also demonstrated the central role of CREB as a transcription factor and the downstream processes it modulates. Transcriptomic analysis revealed that in prostate cancer cells, CREB controls the expression of many important cellular processes including steroid-cholesterol metabolism, protein trafficking, the unfolded protein response (UPR) and lipid metabolism, which are all needed for cell growth (Figure 32). The rewiring of cholesterol metabolism may contribute essential membrane constituents and metabolites for tumorigenesis, as well as steroid hormone precursors, consistent with ongoing work focused on interfering with cholesterol metabolism to inhibit cancer progression²⁶⁸. Also, the inhibition of cholesterol biosynthesis was believed to be a strategy to overcome CRPC²⁶⁹. Although, cholesterol biosynthesis has not been linked to CREB in cancer, the deregulation of sterol biosynthesis and cholesterol biosynthesis upon CREB and CREM deficiency has previously been reported in synaptic plasticity study of neurons²⁷⁰. The importance of both lipid metabolism and the UPR have also been reported as key pro-cancer elements for tumor cells to accommodate key metabolic requirements and adapt to the harsh tumor microenvironment. CREB-mediated

lipid metabolism via PPAR γ , FAS, and ATP citrate lyase (ACLY) has been demonstrated in many liver disease as well as hepatic carcinoma²⁷¹. It was also shown in low vertebrates that CREB is required for UPR-mediated lipid metabolic reprogramming, supporting a central role for CREB metabolism²⁷². Moreover, by elucidating the CREB-mediated cellular processes in prostate cancer, I also provide a therapeutic basis for targeting CREB as 666-15-treated C4-2 cells exhibited broad inhibition at the transcriptional level, further confirming CREB transcriptional regulation of multiple processes in prostate cancer.

The CREB family consists of CREB, CREM and ATF1. Given the high structural similarity between CREB1 and ATF1, this study also addressed the issue of whether ATF1 and CREB have overlapping functions. Previous studies focusing on early mouse embryonic development have indicated compensatory roles between CREB1 and ATF1^{273, 274}. Specifically, CREB1 and ATF1 in certain stages co-regulate cell survival to sustain early embryonic development. However, they are not equivalent as CREB1-deficient mice exhibited perinatal lethality while ATF1 deleted mice were fertile, suggesting they may have both redundant and non-redundant functions²⁷³. Here, I first investigated CREB1's and ATF1's functional roles by establishing single and double KO prostate cancer cell models. Both CREB1 and ATF1 in prostate cancer serve as transcriptional activators as a large number of genes were downregulated following knockout of either gene. When comparing two single KO downregulated gene lists, I further found CREB1 and ATF1 single KOs shared a diverse set of downstream targets but downregulated them to distinct extents (Figure 33). Moreover, double knockout of *CREB1* and *ATF1* led to a substantial increase in the number of downregulated genes and greater cell growth inhibition (Figure 34). Therefore, the cell growth mechanism associated with CREB1 and ATF1 might not only depend on the regulation of phosphorylation as previously described²⁷⁵, but also on their shared and unique transcriptional regulation. Of note, CREB-dependent transcriptional activity also requires other coactivators

like CBP/P300 and CRTC and their cooperation with CREB1 and/or ATF1 in prostate cancer remains unclear; therefore, further validation focusing on the co-regulation of CREB1/ATF1 and their cooperation with other co-factors in prostate cancer is needed to understand the common and distinct transcriptional targets and how they are regulated.

Besides pathways linked to proliferation, I also uncovered a profound effect of CREB on extracellular matrix degradation, a process highly correlated with cancer invasion and metastasis²⁷⁶. *MMP16* was consistently identified as one of the top CREB-regulated genes (Figure 40). This finding is in line with two previous microarray analyses that indicated *MMP16* was increased either by CREB1 induction with transgenic Tet-Off system or under forskolin stimulation^{277, 278}. As a membrane-localized matrix metalloproteinase, *MMP16* bears proteolytic activity for extracellular matrix degradation such as being involved in the cleavage of *MMP2* for cell invasion. Indeed, the important contribution of *MMP16* in migration, invasion and metastasis has been established in several cancer types²⁷⁹⁻²⁸¹. *MMP16* promoted tumor metastasis by inducing epithelial-mesenchymal transition (EMT) in hepatocellular carcinoma and augmented migration and invasion in colon cancer cells. In melanoma, *MMP16* was suggested to serve as a key driver of lymphatic vessel invasion²⁷⁹. Therefore, I anticipate that impaired expression of *MMP16* via CREB inhibition may also benefit patients at risk of developing metastatic prostate cancer. Moreover, the prognostic significance of *MMP16* has been previously reported in many cancer types including hepatocellular carcinoma, prostate cancer, colorectal carcinoma and melanoma²⁷⁹⁻²⁸². Likewise, *MMP16* genetic amplifications were observed in multiple prostate cancer clinical cohorts, where *MMP16* amplification also predicted poor prognosis (Figure 42). These data suggest that *MMP16* could also be a prognostic marker for prostate cancer. Interestingly, *MMP16*'s role in cell growth may depend on the cancer subtype. In melanoma, knockdown of *MMP16* by shRNA increased tumor growth in xenograft models²⁷⁹ while in prostate cancer and hepatocellular carcinoma, there

was no significant change of cell growth when MMP16 expression level was altered²⁸⁰⁻²⁸². However, in gastric cancer, shRNAs targeting *MMP16* suppressed cell proliferation and colony formation²⁸³.

The vulnerability of cells to *CREB1/ATF1* double knockout led us to test the efficacy of a recently developed CREB inhibitor that inhibits both CREB1 and ATF1 isoforms *in vitro* and *in vivo*. The CREB inhibitor, 666-15, disrupts the interaction between CREB and CREBBP¹⁷⁴. Prior studies demonstrated that 666-15 significantly decreased CREB-dependent transcriptional activity²⁵⁷. Multiple groups have confirmed the anti-proliferation and metastatic effect of 666-15 *in vitro* and *in vivo*^{39, 177, 179, 257}. *In vitro* proliferation assays showed that a range of prostate cancer cell lines were inhibited by 666-15, with IC50s ranging from 200 nM to 1 μ M (Figure 36B). Further, I found CRPC C4-2 cells to be more sensitive to 666-15 than their HSPC LNCaP parental cells from which they were derived (Figure 36E). In C4-2 xenograft nude mice, treatment of 666-15 significantly reduced tumor growth rate and showed no significant side effects (Figure 37). These results are consistent with previous studies in breast cancer and AML^{179, 257}. Importantly, 666-15 impaired the growth of enzalutamide-resistant PDX tumor (Figure 38). However, I found that two PDXs with equally high p-CREB basal levels had different responses to 666-15 treatment, indicating that p-CREB levels alone likely cannot predict 666-15 sensitivity. Given that I did see different responses to 666-15 between C4-2 and 22Rv1 cells (Figures 30&35), I anticipate that, not surprisingly, the genetic background of the tumor may influence drug efficacy. Thus, other biomarkers will need to be identified in the future to help select the most appropriate patient population. Through the RNA-seq analyses, I also identified *FOLH1* (PSMA) as one of the most significantly CREB-regulated genes in prostate cancer (Figure 39). Though it is expressed in both benign and prostate cancer, PSMA, a cell surface protein is markedly upregulated in more aggressive prostate cancers²⁸⁴. As a consequence, two PSMA-targeted PETs have already been recently

approved by the FDA for use in the detection of advancing prostate cancer^{285, 286}. Therefore, future studies will investigate whether PSMA-PET can be used as a pharmacodynamic biomarker of CREB activity/inhibition and a possible predictive biomarker for future patient selection should CREB inhibitors even reach the clinic.

Collectively, I elucidated a signaling axis that originates from AR, triggers CAMKK2-CAMKI-CREB mediated transcription and prostate cancer progression. As such, I proposed that CREB and other components of this signaling cascade will emerge as novel, viable and druggable targets for the treatment of advanced prostate cancer. Further, since overexpression and/or activation of CREB has been observed in other cancers, data generated from this research will likely have broader relevance for the treatment of other cancers.

Chapter 5

Discussion and Future Directions

Despite the discovery and development of novel therapeutic strategies for targeting AR, effective treatments are still lacking for CRPC. The pressing need to block reactive AR and identification of CAMKK2 as a vital effector of AR signaling in CRPC propels us to investigate AR-CAMKK2 signaling pathway and look for an alternative treatment strategy for CRPC. In the present study, I identified two independent downstream effectors, ULK1 and CREB, of AR-CAMKK2 signaling in CRPC (Figure 43). Through distinct regulation mechanisms, AR-CAMKK2 can phosphorylate and activate both to promote cancer progression, which inspires us to apply them as potential viable therapeutic targets for CRPC treatment.

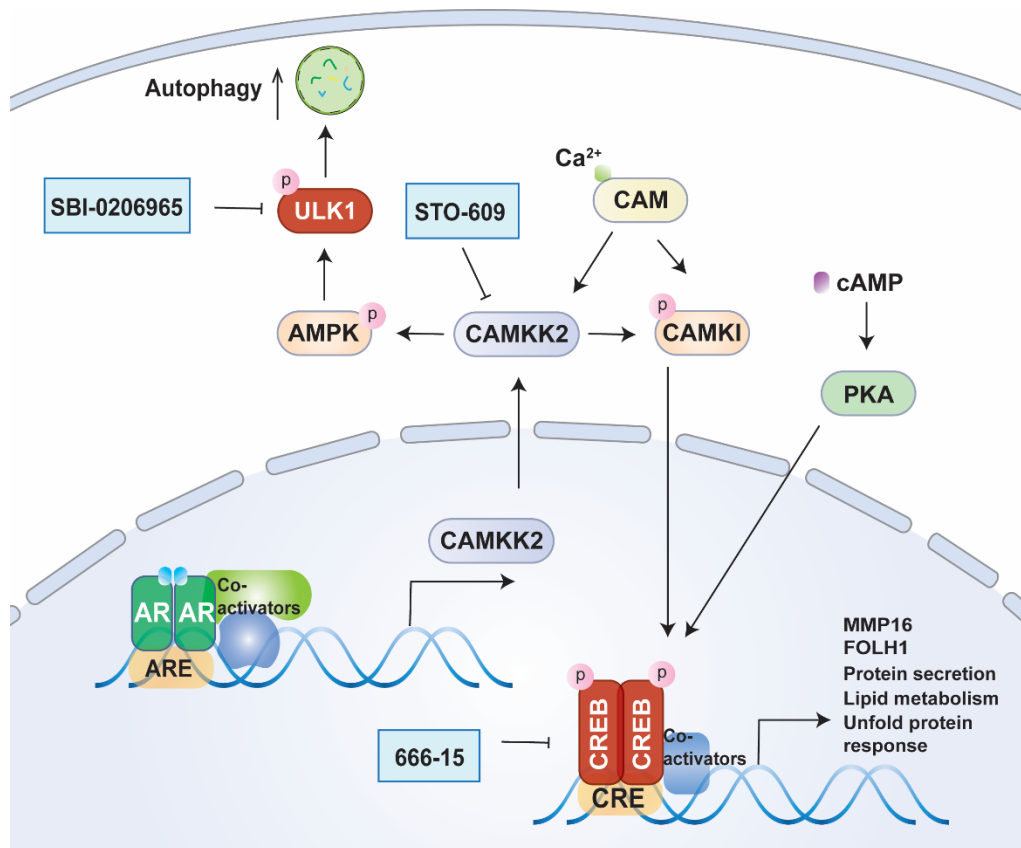


Figure 43. A schematic representation of AR-CAMKK2-AMPK-ULK1 and AR-CAMKK2-CAMKI-CREB signaling pathways.

AR-induced CAMKK2 phosphorylates both AMPK and CAMKI. Increased AMPK and CAMKI activity promote the activation of ULK1 and CREB respectively and eventually drive the prostate cancer progression. Targeting the key molecules in this oncogenic signaling cascade represents alternative therapeutic strategies for CRPC.

In chapter 3, I elucidated that AR-CAMKK2-AMPK-mediated phosphorylation of ULK1 at Ser555 plays an essential role in autophagy activation, which provides a survival mechanism for tumor cells to overcome a stressful environment. My data showed that CAMKK2 deficiency impaired CRPC cell viability and proliferation in a harsh microenvironment such as castration and low serum media, indicating a protective role of CAMKK2 under nutrient scarcity. Prior studies have documented AMPK as a primary downstream target of AR-CAMKK2 to execute their roles in the metabolic alteration. Several metabolic proteins including TBC1D4, PGC1 α and PFKFB2/3 can be directly phosphorylated by AMPK and promote glucose uptake and glycolysis as well as maintain the mitochondrial biogenesis⁴⁶. In addition, AMPK was found to increase the phosphorylation of p38, resulting in the stability of AR to protect cells from enzalutamide treatment⁴⁹. My data herein, provides a new mechanistic insight into AR-CAMKK2-AMPK's regulation in prostate cancer cell survival through ULK1-mediated autophagy. Indeed, a high correlation between ULK1 mRNA/protein levels and poor prognosis has been observed in previous studies^{231, 232}. As a result, targeting such protective autophagy might be beneficial for CRPC treatment. Previous clinical trials have investigated the efficacy of chloroquine derivatives in prostate cancer patients²⁴⁴. However, limited information has been produced on patient response and survival benefits in part due to the side effect. As chloroquine inhibits the late lysosomal step of autophagy, inevitably, it interferes with some normal cellular processes like lysosomal function and endocytosis and thus lacks the specificity to autophagy activity^{244, 287}. To this regard, targeting early and specific autophagy processes like ULK1-initiated autophagosome biogenesis is preferable. I indicated here, SBI-0206965, a ULK1 inhibitor, not only blocked AR-induced autophagy initiation, but exhibited a strong anti-proliferation effect in both HSPC and CRPC cell growth. Therefore, CAMKK2-AMPK-ULK1 represents a potential druggable cascade for CRPC. A recent study has also reported a new ULK1 inhibitor ULK101, which is more potent and selective than SBI-0206965²⁴⁶. ULK101 has been demonstrated effective in U2OS cells with nutrient deficiency and lung cancer with KRAS mutant. Testing and comparing available ULK1

inhibitors in the prostate cancer context will be the next step. Moreover, all current studies of ULK1 inhibitors are based on cell models, hence, the knowledge of pharmacokinetics and safety of these compounds are completely devoid. Preclinical animal data will be required to provide more information and further validation.

In chapter 4, I identified AR-CAMKK2 as one of upstream regulators of CREB through phosphorylation at Ser133 (ATF1, S63). Unlike ULK1, CAMKK2 regulates CREB through CAMKI instead of AMPK. Though previous studies have suggested the pro-cancer role of CAMKI in other cancer types^{39, 45, 288}, this is the first time, to my knowledge, CAMKI was elucidated to be involved in AR-CAMKK2-mediated cell growth in prostate cancer. In addition to AR-CAMKK2-CAMKI signaling, interestingly, p-CREB can be regulated by other upstream kinases. CAMKK2 seems to only contribute to androgen induced p-CREB but is dispensable for AR antagonist stimulated p-CREB. The latter modification might be primarily regulated by PKA as previous documented¹²¹, though it has not been validated in my experiment since the effort to inhibit PKA activity by PKI (protein kinase inhibitor) failed in LNCaP cells, possibly due to the poor take-up rate in my cells. I also cannot rule out the function of other kinases on p-CREB. For instance, MAPK, another classical CREB upstream kinase, has been reported to be activated by antiandrogens^{262, 289}, and it is unclear whether there is any connection to p-CREB. In this regard, future work to delineate a comprehensive map of upstream regulators of CREB will provide a better understanding of the complexities of CREB in prostate cancer development and facilitate to effectively modify the targeting strategy. For example, to block AR induced p-CREB, CAMKK2 inhibition will be preferred while PKA inhibitor will be considered to avert enzalutamide resistant occurrence. Functionally, I demonstrated that CREB1 is not only required for AR induced HSPC cell proliferation but also important for CRPC survival *in vitro* and *in vivo*. Ser133 appears to be essential for this regulation as S133A mutant fails to support the cell growth in CRPC. I also found CREB1 and ATF1 exhibit functional redundancy, as such, dual deletion or pharmacological

inhibition by 666-15, displayed a greater tumor suppressive effect, highlighting the potential value of CREB as a promising therapeutic target. Recently, a synergistic Inhibitor of CREB inhibitor, 653-47 has been developed. Although 653-47 cannot directly target CREB dependent transcriptional activity, it potentiates anti-tumor activity when combined with 666-15¹⁸⁰. This combination has not been tested *in vivo*. Future work will focus on testing more potent and selective CREB inhibitors especially in PDX models which have a relatively weaker response to the current CREB inhibitor. Moreover, identification of friendly monitored biomarkers for responsive patient populations will also be a pressing need during drug development. In the present study, FOLH1 (PSMA) has been identified as a CREB downstream target. As the successful application of PSMA-PET for advanced prostate cancer in clinic, it is worth determining whether PSMA-PET scanning can be used as a biomarker to access CREB inhibitor response.

Another interesting aspect for further exploration is the metastatic role of CAMKK2-CREB signaling in prostate cancer. In this study, I observed that genes involved in extracellular matrix organization were preferentially decreased in CREB-defective CRPC. MMP16, as one of the leading-edge genes, was most significantly changed in all SKO, DKO and 666-15 treatment groups, indicating the potential role of CREB in extracellular matrix regulation. Degradation of extracellular matrix by proteases like matrix metalloproteinases is one of the essential steps for prostate cancer cells to intravasate into nearby vascular and lymphatic system²¹⁹. Similar to these findings, MMP2 and MMP9 in breast and renal cancers have also been observed increase by CREB, leading to the disruption of the extracellular matrix and thus driving metastasis^{290, 291}. In addition to the invasion and intravasation step, CREB can also promote angiogenesis through expression of VEGF and/or epigenetic regulation by HDAC2 and EZH2^{121, 150, 166}. In fact, CREB has been linked with metastasis in several cancers including renal cancer, breast cancer, laryngeal cancer, prostate cancer and melanoma⁹⁶. As a consequence, recent studies have highlighted the efficacy of CREB inhibitors to block metastasis in breast cancer and KRAS and

p53 mutant pancreatic cancer^{179, 292}. Although I have described a decrease of migration of C4-2 cells under 666-15 by wound healing assay, the role of CAMKK2-CREB, especially the application of CREB inhibitors in prostate cancer metastasis is still needed to be further investigated *in vivo*. One critical concern is the extrinsic CAMKK2-CREB role in osteoclasts²¹⁹. Inhibition of CAMKK2-CREB decreased differentiation of osteoclasts which might provide a favorable bone microenvironment for prostate cancer survival. To answer this question, we are developing a new prostate cancer metastatic model which can monitor the micrometastatic lesions in major organs from orthotopically injection (Figure 44). Once the model is fully validated, it will be useful to produce a convincing conclusion about CAMKK2 and CREB inhibitors in prostate cancer metastasis.

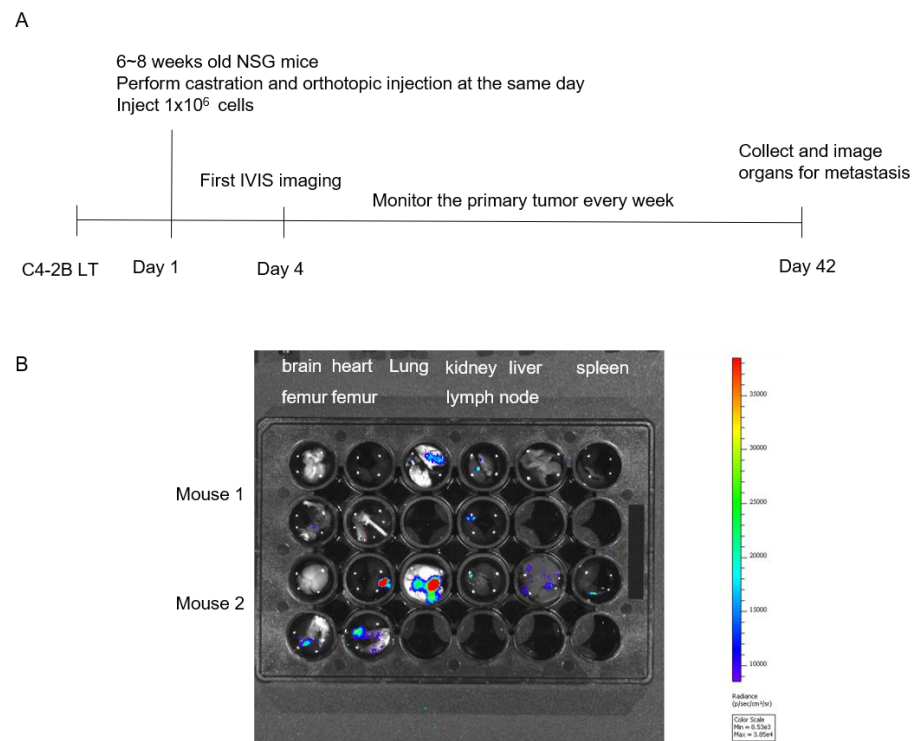


Figure 44. A mouse model of prostate cancer metastasis.

(A) A schematic of a mouse model of prostate cancer metastasis using C4-2B-LT cells.

(B) Bioluminescence imaging of major organs in the sixth week after orthotopic injection.

Taken together, this study delineated two new mechanisms by which AR-CAMKK2 promotes prostate cancer progression. On one hand, AR-CAMKK2 mediates AMPK to participate in the initiation of autophagy and provides a survival advantage for tumorigenesis. On the other hand, AR-CAMKK2-CAMKI serves as one of the key upstreams of CREB to maintain the proliferation and migration of CRPC. These findings not only extend our understanding of AR-CAMKK2 dependent signaling events that drive prostate cancer but highlight new therapeutic targets for cancer therapy. Admittedly, CAMKK2 is still a favorable attractive therapeutic target given its function as a central hub to regulate multiple oncogenic pathways. Thus far, STO-609 remains as the most frequently used CAMKK2 inhibitor in the literature. Though it did not show systemic toxicity and exhibited an acceptable anti-cancer activity in preclinical experiments^{24, 55, 293, 294}, some limitations such as off-target effect and poor pharmacokinetic property preclude it from being further developed for clinical application^{221, 222, 250}. Therefore, to develop novel potent and selective CAMKK2 inhibitors will be an attractive future direction for research.

Appendix

Lin,Chenchu

From: Journalpermissions <journalpermissions@springernature.com>
Sent: Tuesday, May 25, 2021 8:36 AM
To: Lin,Chenchu
Subject: [EXT] RE: Permission letter for thesis

WARNING: This email originated from outside of MD Anderson. Please validate the sender's email address before clicking on links or attachments as they may not be safe.

Dear Chenchu Lin,

Thank you for your recent Springer Nature permissions request.

As an author, you retain certain non-exclusive rights over the 'Published Version' for which no permissions are necessary as long as you acknowledge and reference the first publication. These include:

- The right to reuse graphic elements contained in the Article and created by you in presentations or other works you author
- The right of you and your academic institution to reproduce the Article for course teaching. Note, this does not include the right to include in course packs for resale by libraries or by the institution
- To reproduce, or allow a third party to reproduce the Article in whole or in part in any printed volume (book or thesis) authored by you.

You may also wish to refer to our 'Reprints and Permissions' FAQs on Springer.com:
<https://www.springernature.com/gp/partners/rights-permissions-third-party-distribution>

Best wishes,
Paloma

Paloma Hammond
(she/her/hers - [more information why](#))
Rights Executive

SpringerNature
The Campus, 4 Crinan Street, London N1 9XW, United Kingdom

E paloma.hammond@springernature.com

<https://www.macmillanihe.com/>
<http://www.nature.com>
<http://www.springer.com>
<https://www.palgrave.com/gp/>

BLACK LIVES MATTER

Bibliography

1. Society. TAC. Cancer facts & figures 2021. . Atlanta: American Cancer Society. 2021.
2. Chaturvedi AP, Dehm SM. Androgen receptor dependence. *Adv Exp Med Biol.* 2019;1210: 333-350.
3. Society TAC. Hormone therapy for prostate cancer. <https://www.cancer.org/cancer/prostate-cancer/treating/hormone-therapy.html>. 2020.
4. Knudsen KE, Scher HI. Starving the addiction: New opportunities for durable suppression of ar signaling in prostate cancer. *Clin Cancer Res.* 2009;15: 4792-4798.
5. Saranyutanon S, Srivastava SK, Pai S, Singh S, Singh AP. Therapies targeted to androgen receptor signaling axis in prostate cancer: Progress, challenges, and hope. *Cancers (Basel).* 2019;12.
6. Shore ND, Saad F, Cookson MS, George DJ, Saltzstein DR, Tutrone R, Akaza H, Bossi A, van Veenhuyzen DF, Selby B, Fan X, Kang V, Walling J, Tombal B, Investigators HS. Oral relugolix for androgen-deprivation therapy in advanced prostate cancer. *N Engl J Med.* 2020;382: 2187-2196.
7. Foley C, Mitsiades N. Moving beyond the androgen receptor (AR): Targeting AR-interacting proteins to treat prostate cancer. *Horm Cancer.* 2016;7: 84-103.
8. Higano C. Enzalutamide, apalutamide, or darolutamide: Are apples or bananas best for patients? *Nat Rev Urol.* 2019;16: 335-336.
9. Fizazi K, Albiges L, Lortol Y, Massard C. Odm-201: A new-generation androgen receptor inhibitor in castration-resistant prostate cancer. *Expert Rev Anticancer Ther.* 2015;15: 1007-1017.
10. Moilanen AM, Riikonen R, Oksala R, Ravanti L, Aho E, Wohlfahrt G, Nykanen PS, Tormakangas OP, Palvimo JJ, Kallio PJ. Discovery of ODM-201, a new-generation androgen receptor inhibitor targeting resistance mechanisms to androgen signaling-directed prostate cancer therapies. *Sci Rep.* 2015;5: 12007.

11. Kregel S, Wang C, Han X, Xiao L, Fernandez-Salas E, Bawa P, McCollum BL, Wilder-Romans K, Apel IJ, Cao X, Speers C, Wang S, Chinnaiyan AM. Androgen receptor degraders overcome common resistance mechanisms developed during prostate cancer treatment. *Neoplasia*. 2020;22: 111-119.
12. Stone L. UT-34: A promising new ar degrader. *Nat Rev Urol*. 2019;16: 640.
13. Venkadakrishnan VB, Ben-Salem S, Heemers HV. AR-dependent phosphorylation and phospho-proteome targets in prostate cancer. *Endocr Relat Cancer*. 2020;27: R193-R210.
14. Frigo DE, Howe MK, Wittmann BM, Brunner AM, Cushman I, Wang Q, Brown M, Means AR, McDonnell DP. CaM kinase kinase beta-mediated activation of the growth regulatory kinase AMPK is required for androgen-dependent migration of prostate cancer cells. *Cancer Res*. 2011;71: 528-537.
15. Racioppi L, Means AR. Calcium/calmodulin-dependent protein kinase kinase 2: Roles in signaling and pathophysiology. *J Biol Chem*. 2012;287: 31658-31665.
16. Huang W, Racioppi L. Calcium calmodulin kinase kinase 2. In: Choi S, editor. *Encyclopedia of signaling molecules*. Cham: Springer International Publishing, 2018:655-661.
17. O'Brien MT, Oakhill JS, Ling NX, Langendorf CG, Hoque A, Dite TA, Means AR, Kemp BE, Scott JW. Impact of genetic variation on human CaMKK2 regulation by Ca^{2+} -calmodulin and multisite phosphorylation. *Sci Rep*. 2017;7: 43264.
18. Tokumitsu H, Hatano N, Fujimoto T, Yurimoto S, Kobayashi R. Generation of autonomous activity of Ca^{2+} /calmodulin-dependent protein kinase kinase beta by autophosphorylation. *Biochemistry*. 2011;50: 8193-8201.
19. Green MF, Scott JW, Steel R, Oakhill JS, Kemp BE, Means AR. Ca^{2+} /calmodulin-dependent protein kinase kinase beta is regulated by multisite phosphorylation. *J Biol Chem*. 2011;286: 28066-28079.

20. Sharma NL, Massie CE, Ramos-Montoya A, Zecchini V, Scott HE, Lamb AD, MacArthur S, Stark R, Warren AY, Mills IG, Neal DE. The androgen receptor induces a distinct transcriptional program in castration-resistant prostate cancer in man. *Cancer Cell*. 2013;23: 35-47.
21. Massie CE, Lynch A, Ramos-Montoya A, Boren J, Stark R, Fazli L, Warren A, Scott H, Madhu B, Sharma N, Bon H, Zecchini V, Smith DM, Denicola GM, Mathews N, Osborne M, Hadfield J, Macarthur S, Adryan B, Lyons SK, Brindle KM, Griffiths J, Gleave ME, Rennie PS, Neal DE, Mills IG. The androgen receptor fuels prostate cancer by regulating central metabolism and biosynthesis. *EMBO J*. 2011;30: 2719-2733.
22. Karacosta LG, Foster BA, Azabdaftari G, Feliciano DM, Edelman AM. A regulatory feedback loop between Ca^{2+} /calmodulin-dependent protein kinase kinase 2 (CaMKK2) and the androgen receptor in prostate cancer progression. *J Biol Chem*. 2012;287: 24832-24843.
23. Fu H, He HC, Han ZD, Wan YP, Luo HW, Huang YQ, Cai C, Liang YX, Dai QS, Jiang FN, Zhong WD. MicroRNA-224 and its target CAMKK2 synergistically influence tumor progression and patient prognosis in prostate cancer. *Tumour Biol*. 2015;36: 1983-1991.
24. Penfold L, Woods A, Muckett P, Nikitin AY, Kent TR, Zhang S, Graham R, Pollard A, Carling D. CaMKK2 promotes prostate cancer independently of AMPK via increased lipogenesis. *Cancer Res*. 2018;78: 6747-6761.
25. White MA, Tsouko E, Lin C, Rajapakshe K, Spencer JM, Wilkenfeld SR, Vakili SS, Pulliam TL, Awad D, Nikolos F, Katreddy RR, Kaiparettu BA, Sreekumar A, Zhang X, Cheung E, Coarfa C, Frigo DE. GLUT12 promotes prostate cancer cell growth and is regulated by androgens and CaMKK2 signaling. *Endocr Relat Cancer*. 2018;25: 453-469.
26. Brzozowski JS, Skelding KA. The multi-functional calcium/calmodulin stimulated protein kinase (CaMK) family: Emerging targets for anti-cancer therapeutic intervention. *Pharmaceuticals (Basel)*. 2019;12.

27. Chin D, Winkler KE, Means AR. Characterization of substrate phosphorylation and use of calmodulin mutants to address implications from the enzyme crystal structure of calmodulin-dependent protein kinase i. *J Biol Chem.* 1997;272: 31235-31240.
28. Haribabu B, Hook SS, Selbert MA, Goldstein EG, Tomhave ED, Edelman AM, Snyderman R, Means AR. Human calcium-calmodulin dependent protein kinase i: cDNA cloning, domain structure and activation by phosphorylation at threonine-177 by calcium-calmodulin dependent protein kinase i kinase. *EMBO J.* 1995;14: 3679-3686.
29. Verploegen S, Lammers JW, Koenderman L, Coffey PJ. Identification and characterization of CKLiK, a novel granulocyte Ca(++)/calmodulin-dependent kinase. *Blood.* 2000;96: 3215-3223.
30. Ishikawa Y, Tokumitsu H, Inuzuka H, Murata-Hori M, Hosoya H, Kobayashi R. Identification and characterization of novel components of a Ca²⁺/calmodulin-dependent protein kinase cascade in hela cells. *FEBS Lett.* 2003;550: 57-63.
31. Kang X, Cui C, Wang C, Wu G, Chen H, Lu Z, Chen X, Wang L, Huang J, Geng H, Zhao M, Chen Z, Muschen M, Wang HY, Zhang CC. CAMKs support development of acute myeloid leukemia. *J Hematol Oncol.* 2018;11: 30.
32. Lei Y, Yu T, Li C, Li J, Liang Y, Wang X, Chen Y, Wang X. Expression of CAMK1 and its association with clinicopathologic characteristics in pancreatic cancer. *J Cell Mol Med.* 2020.
33. Deb TB, Zuo AH, Barndt RJ, Sengupta S, Jankovic R, Johnson MD. PNCK overexpression in HER-2 gene-amplified breast cancer causes trastuzumab resistance through a paradoxical PTEN-mediated process. *Breast Cancer Res Treat.* 2015;150: 347-361.
34. Xu Y, Wang J, Cai S, Chen G, Xiao N, Fu Y, Chen Q, Qiu S. PNCK depletion inhibits proliferation and induces apoptosis of human nasopharyngeal carcinoma cells in vitro and in vivo. *J Cancer.* 2019;10: 6925-6932.
35. Wu S, Lv Z, Wang Y, Sun L, Jiang Z, Xu C, Zhao J, Sun X, Li X, Hu L, Tang A, Gui Y, Zhou F, Cai Z, Wang R. Increased expression of pregnancy up-regulated non-ubiquitous calmodulin

kinase is associated with poor prognosis in clear cell renal cell carcinoma. PLoS One. 2013;8: e59936.

36. Gardner HP, Ha SI, Reynolds C, Chodosh LA. The CAM kinase, PNCK, is spatially and temporally regulated during murine mammary gland development and may identify an epithelial cell subtype involved in breast cancer. Cancer Res. 2000;60: 5571-5577.

37. Cho YA, Choi S, Park S, Park CK, Ha SY. Expression of pregnancy up-regulated non-ubiquitous calmodulin kinase (PNCK) in hepatocellular carcinoma. Cancer Genomics Proteomics. 2020;17: 747-755.

38. Bergamaschi A, Kim YH, Kwei KA, La Choi Y, Bocanegra M, Langerod A, Han W, Noh DY, Huntsman DG, Jeffrey SS, Borresen-Dale AL, Pollack JR. CAM1D amplification implicated in epithelial-mesenchymal transition in basal-like breast cancer. Mol Oncol. 2008;2: 327-339.

39. Kang X, Lu Z, Cui C, Deng M, Fan Y, Dong B, Han X, Xie F, Tyner JW, Coligan JE, Collins RH, Xiao X, You MJ, Zhang CC. The ITIM-containing receptor LAIR1 is essential for acute myeloid leukaemia development. Nat Cell Biol. 2015;17: 665-677.

40. Volpin V, Michels T, Sorrentino A, Menevse AN, Knoll G, Ditz M, Milenkovic VM, Chen CY, Rathinasamy A, Griewank K, Boutros M, Haferkamp S, Berneburg M, Wetzel CH, Seckinger A, Hose D, Goldschmidt H, Ehrenschrwender M, Witzens-Harig M, Szoor A, Vereb G, Khandelwal N, Beckhove P. CAMK1D triggers immune resistance of human tumor cells refractory to anti-PD-L1 treatment. Cancer Immunol Res. 2020;8: 1163-1179.

41. Davare MA, Saneyoshi T, Soderling TR. Calmodulin-kinases regulate basal and estrogen stimulated medulloblastoma migration via Rac1. J Neurooncol. 2011;104: 65-82.

42. Sang LJ, Ju HQ, Liu GP, Tian T, Ma GL, Lu YX, Liu ZX, Pan RL, Li RH, Piao HL, Marks JR, Yang LJ, Yan Q, Wang W, Shao J, Zhou Y, Zhou T, Lin A. LncRNA Camk-A regulates Ca(2+)-signaling-mediated tumor microenvironment remodeling. Mol Cell. 2018;72: 71-83 e77.

43. Deb TB, Coticchia CM, Barndt R, Zuo H, Dickson RB, Johnson MD. Pregnancy-upregulated nonubiquitous calmodulin kinase induces ligand-independent EGFR degradation. *Am J Physiol Cell Physiol*. 2008;295: C365-377.
44. Wang L, Lin Y, Meng H, Liu C, Xue J, Zhang Q, Li C, Zhang P, Cui F, Chen W, Jiang A. Long non-coding RNA LOC283070 mediates the transition of Incap cells into androgen-independent cells possibly via CAMK1D. *Am J Transl Res*. 2016;8: 5219-5234.
45. Liu R, Chen Z, Wang S, Zhao G, Gu Y, Han Q, Chen B. Screening of key genes associated with RCHOP immunochemotherapy and construction of a prognostic risk model in diffuse large bcell lymphoma. *Mol Med Rep*. 2019;20: 3679-3690.
46. Khan AS, Frigo DE. A spatiotemporal hypothesis for the regulation, role, and targeting of AMPK in prostate cancer. *Nat Rev Urol*. 2017;14: 164-180.
47. Xiao B, Sanders MJ, Carmena D, Bright NJ, Haire LF, Underwood E, Patel BR, Heath RB, Walker PA, Hallen S, Giordanetto F, Martin SR, Carling D, Gamblin SJ. Structural basis of AMPK regulation by small molecule activators. *Nat Commun*. 2013;4: 3017.
48. Willows R, Sanders MJ, Xiao B, Patel BR, Martin SR, Read J, Wilson JR, Hubbard J, Gamblin SJ, Carling D. Phosphorylation of AMPK by upstream kinases is required for activity in mammalian cells. *Biochem J*. 2017;474: 3059-3073.
49. Saxena N, Beraldi E, Fazli L, Somasekharan SP, Adomat H, Zhang F, Molokwu C, Gleave A, Nappi L, Nguyen K, Brar P, Nikesitch N, Wang Y, Collins C, Sorensen PH, Gleave M. Androgen receptor (AR) antagonism triggers acute succinate-mediated adaptive responses to reactivate ar signaling. *EMBO Mol Med*. 2021: e13427.
50. Tennakoon JB, Shi Y, Han JJ, Tsouko E, White MA, Burns AR, Zhang A, Xia X, Ilkayeva OR, Xin L, Ittmann MM, Rick FG, Schally AV, Frigo DE. Androgens regulate prostate cancer cell growth via an AMPK-PGC-1alpha-mediated metabolic switch. *Oncogene*. 2014;33: 5251-5261.
51. Domenech E, Maestre C, Esteban-Martinez L, Partida D, Pascual R, Fernandez-Miranda G, Seco E, Campos-Olivas R, Perez M, Megias D, Allen K, Lopez M, Saha AK, Velasco G, Rial E,

- Mendez R, Boya P, Salazar-Roa M, Malumbres M. AMPK and PFKFB3 mediate glycolysis and survival in response to mitophagy during mitotic arrest. *Nat Cell Biol.* 2015;17: 1304-1316.
52. Moon JS, Jin WJ, Kwak JH, Kim HJ, Yun MJ, Kim JW, Park SW, Kim KS. Androgen stimulates glycolysis for de novo lipid synthesis by increasing the activities of hexokinase 2 and 6-phosphofructo-2-kinase/fructose-2,6-bisphosphatase 2 in prostate cancer cells. *Biochem J.* 2011;433: 225-233.
53. Park HU, Suy S, Danner M, Dailey V, Zhang Y, Li H, Hyduke DR, Collins BT, Gagnon G, Kallakury B, Kumar D, Brown ML, Fornace A, Dritschilo A, Collins SP. AMP-activated protein kinase promotes human prostate cancer cell growth and survival. *Mol Cancer Ther.* 2009;8: 733-741.
54. Chow FA, Anderson KA, Noeldner PK, Means AR. The autonomous activity of Calcium/calmodulin-dependent protein kinase IV is required for its role in transcription. *J Biol Chem.* 2005;280: 20530-20538.
55. Lin F, Marcelo KL, Rajapakshe K, Coarfa C, Dean A, Wilganowski N, Robinson H, Sevcik E, Bissig KD, Goldie LC, Means AR, York B. The CaMKK2/CAMKIV relay is an essential regulator of hepatic cancer. *Hepatology.* 2015;62: 505-520.
56. Wen L, Chen Z, Zhang F, Cui X, Sun W, Geary GG, Wang Y, Johnson DA, Zhu Y, Chien S, Shyy JY. Ca^{2+} /calmodulin-dependent protein kinase kinase beta phosphorylation of sirtuin 1 in endothelium is atheroprotective. *Proc Natl Acad Sci U S A.* 2013;110: E2420-2427.
57. Gocher AM, Azabdaftari G, Euscher LM, Dai S, Karacosta LG, Franke TF, Edelman AM. AKT activation by $Ca(2+)$ /calmodulin-dependent protein kinase kinase 2 (CAMKK2) in ovarian cancer cells. *J Biol Chem.* 2017;292: 14188-14204.
58. Lin C, Blessing AM, Pulliam TL, Shi Y, Wilkenfeld SR, Han JJ, Murray MM, Pham AH, Duong K, Brun SN, Shaw RJ, Ittmann MM, Frigo DE. Inhibition of CAMKK2 impairs autophagy and castration-resistant prostate cancer via suppression of AMPK-ULK1 signaling. *Oncogene.* 2021;40: 1690-1705.

59. Li X, He S, Ma B. Autophagy and autophagy-related proteins in cancer. *Mol Cancer*. 2020;19: 12.
60. Liang C. Negative regulation of autophagy. *Cell Death Differ*. 2010;17: 1807-1815.
61. Zachari M, Ganley IG. The mammalian ULK1 complex and autophagy initiation. *Essays Biochem*. 2017;61: 585-596.
62. Joo JH, Dorsey FC, Joshi A, Hennessy-Walters KM, Rose KL, McCastlain K, Zhang J, Iyengar R, Jung CH, Suen DF, Steeves MA, Yang CY, Prater SM, Kim DH, Thompson CB, Youle RJ, Ney PA, Cleveland JL, Kundu M. Hsp90-Cdc37 chaperone complex regulates Ulk1- and Atg13-mediated mitophagy. *Mol Cell*. 2011;43: 572-585.
63. Birgisdottir AB, Mouilleron S, Bhujabal Z, Wirth M, Sjøttem E, Evjen G, Zhang W, Lee R, O'Reilly N, Tooze SA, Lamark T, Johansen T. Members of the autophagy class III phosphatidylinositol 3-kinase complex I interact with GABARAP and GABARAPL1 via LIR motifs. *Autophagy*. 2019;15: 1333-1355.
64. Russell RC, Tian Y, Yuan H, Park HW, Chang YY, Kim J, Kim H, Neufeld TP, Dillin A, Guan KL. ULK1 induces autophagy by phosphorylating Beclin-1 and activating VPS34 lipid kinase. *Nat Cell Biol*. 2013;15: 741-750.
65. Wold MS, Lim J, Lachance V, Deng Z, Yue Z. ULK1-mediated phosphorylation of ATG14 promotes autophagy and is impaired in huntington's disease models. *Mol Neurodegener*. 2016;11: 76.
66. Zhou C, Ma K, Gao R, Mu C, Chen L, Liu Q, Luo Q, Feng D, Zhu Y, Chen Q. Regulation of mATG9 trafficking by Src- and ULK1-mediated phosphorylation in basal and starvation-induced autophagy. *Cell Res*. 2017;27: 184-201.
67. Li TY, Sun Y, Liang Y, Liu Q, Shi Y, Zhang CS, Zhang C, Song L, Zhang P, Zhang X, Li X, Chen T, Huang HY, He X, Wang Y, Wu YQ, Chen S, Jiang M, Chen C, Xie C, Yang JY, Lin Y, Zhao S, Ye Z, Lin SY, Chiu DT, Lin SC. ULK1/2 constitute a bifurcate node controlling glucose metabolic fluxes in addition to autophagy. *Mol Cell*. 2016;62: 359-370.

68. Shang L, Chen S, Du F, Li S, Zhao L, Wang X. Nutrient starvation elicits an acute autophagic response mediated by ULK1 dephosphorylation and its subsequent dissociation from AMPK. *Proc Natl Acad Sci U S A*. 2011;108: 4788-4793.
69. Holczer M, Hajdu B, Lorincz T, Szarka A, Banhegyi G, Kapuy O. Fine-tuning of AMPK-ULK1-mTORC1 regulatory triangle is crucial for autophagy oscillation. *Sci Rep*. 2020;10: 17803.
70. Dite TA, Ling NXY, Scott JW, Hoque A, Galic S, Parker BL, Ngoei KRW, Langendorf CG, O'Brien MT, Kundu M, Viollet B, Steinberg GR, Sakamoto K, Kemp BE, Oakhill JS. The autophagy initiator ULK1 sensitizes AMPK to allosteric drugs. *Nat Commun*. 2017;8: 571.
71. Bach M, Larance M, James DE, Ramm G. The serine/threonine kinase ULK1 is a target of multiple phosphorylation events. *Biochem J*. 2011;440: 283-291.
72. Kim J, Kundu M, Viollet B, Guan KL. AMPK and mTOR regulate autophagy through direct phosphorylation of ULK1. *Nat Cell Biol*. 2011;13: 132-141.
73. Egan DF, Shackelford DB, Mihaylova MM, Gelino S, Kohnz RA, Mair W, Vasquez DS, Joshi A, Gwinn DM, Taylor R, Asara JM, Fitzpatrick J, Dillin A, Viollet B, Kundu M, Hansen M, Shaw RJ. Phosphorylation of ULK1 (hATG1) by amp-activated protein kinase connects energy sensing to mitophagy. *Science*. 2011;331: 456-461.
74. Mack HI, Zheng B, Asara JM, Thomas SM. AMPK-dependent phosphorylation of ULK1 regulates ATG9 localization. *Autophagy*. 2012;8: 1197-1214.
75. Tian W, Li W, Chen Y, Yan Z, Huang X, Zhuang H, Zhong W, Chen Y, Wu W, Lin C, Chen H, Hou X, Zhang L, Sui S, Zhao B, Hu Z, Li L, Feng D. Phosphorylation of ULK1 by AMPK regulates translocation of ULK1 to mitochondria and mitophagy. *FEBS Lett*. 2015;589: 1847-1854.
76. Liu CC, Lin YC, Chen YH, Chen CM, Pang LY, Chen HA, Wu PR, Lin MY, Jiang ST, Tsai TF, Chen RH. Cul3-KLHL20 ubiquitin ligase governs the turnover of ULK1 and VPS34 complexes to control autophagy termination. *Mol Cell*. 2016;61: 84-97.

77. Lin SY, Li TY, Liu Q, Zhang C, Li X, Chen Y, Zhang SM, Lian G, Liu Q, Ruan K, Wang Z, Zhang CS, Chien KY, Wu J, Li Q, Han J, Lin SC. GSK3-TIP60-ULK1 signaling pathway links growth factor deprivation to autophagy. *Science*. 2012;336: 477-481.
78. Nazio F, Carinci M, Valacca C, Bielli P, Strappazzon F, Antonioli M, Ciccocanti F, Rodolfo C, Campello S, Fimia GM, Sette C, Bonaldo P, Cecconi F. Fine-tuning of ULK1 mRNA and protein levels is required for autophagy oscillation. *J Cell Biol*. 2016;215: 841-856.
79. Nazio F, Strappazzon F, Antonioli M, Bielli P, Cianfanelli V, Bordi M, Gretzmeier C, Dengjel J, Piacentini M, Fimia GM, Cecconi F. mTOR inhibits autophagy by controlling ULK1 ubiquitylation, self-association and function through ambra1 and traf6. *Nat Cell Biol*. 2013;15: 406-416.
80. Gabriele F, Martinelli C, Comincini S. Prostate cancer cells at a therapeutic gunpoint of the autophagy process. *Journal of Cancer Metastasis and Treatment*. 2018;4: 17.
81. Zeng J, Liu W, Fan YZ, He DL, Li L. PrLZ increases prostate cancer docetaxel resistance by inhibiting LKB1/AMPK-mediated autophagy. *Theranostics*. 2018;8: 109-123.
82. He Z, Mangala LS, Theriot CA, Rohde LH, Wu H, Zhang Y. Cell killing and radiosensitizing effects of atorvastatin in PC3 prostate cancer cells. *J Radiat Res*. 2012;53: 225-233.
83. Santanam U, Banach-Petrosky W, Abate-Shen C, Shen MM, White E, DiPaola RS. Atg7 cooperates with Pten loss to drive prostate cancer tumor growth. *Genes Dev*. 2016;30: 399-407.
84. Lamoureux F, Thomas C, Crafter C, Kumano M, Zhang F, Davies BR, Gleave ME, Zoubeidi A. Blocked autophagy using lysosomotropic agents sensitizes resistant prostate tumor cells to the novel AKT inhibitor AZD5363. *Clin Cancer Res*. 2013;19: 833-844.
85. Shi Y, Han JJ, Tennakoon JB, Mehta FF, Merchant FA, Burns AR, Howe MK, McDonnell DP, Frigo DE. Androgens promote prostate cancer cell growth through induction of autophagy. *Mol Endocrinol*. 2013;27: 280-295.
86. Blessing AM, Rajapakshe K, Reddy Bollu L, Shi Y, White MA, Pham AH, Lin C, Jonsson P, Cortes CJ, Cheung E, La Spada AR, Bast RC, Jr., Merchant FA, Coarfa C, Frigo DE.

Transcriptional regulation of core autophagy and lysosomal genes by the androgen receptor promotes prostate cancer progression. *Autophagy*. 2017;13: 506-521.

87. Coffey K, Rogerson L, Ryan-Munden C, Alkharaif D, Stockley J, Heer R, Sahadevan K, O'Neill D, Jones D, Darby S, Staller P, Mantilla A, Gaughan L, Robson CN. The lysine demethylase, KDM4B, is a key molecule in androgen receptor signalling and turnover. *Nucleic Acids Res*. 2013;41: 4433-4446.

88. Sha J, Han Q, Chi C, Zhu Y, Pan J, Dong B, Huang Y, Xia W, Xue W. Upregulated KDM4B promotes prostate cancer cell proliferation by activating autophagy. *J Cell Physiol*. 2020;235: 2129-2138.

89. Bennett HL, Stockley J, Fleming JT, Mandal R, O'Prey J, Ryan KM, Robson CN, Leung HY. Does androgen-ablation therapy (AAT) associated autophagy have a pro-survival effect in Incap human prostate cancer cells? *BJU Int*. 2013;111: 672-682.

90. Nguyen HG, Yang JC, Kung HJ, Shi XB, Tilki D, Lara PN, Jr., DeVere White RW, Gao AC, Evans CP. Targeting autophagy overcomes enzalutamide resistance in castration-resistant prostate cancer cells and improves therapeutic response in a xenograft model. *Oncogene*. 2014;33: 4521-4530.

91. Kaini RR, Hu CA. Synergistic killing effect of chloroquine and androgen deprivation in LNCaP cells. *Biochem Biophys Res Commun*. 2012;425: 150-156.

92. Shaywitz AJ, Greenberg ME. CREB: A stimulus-induced transcription factor activated by a diverse array of extracellular signals. *Annu Rev Biochem*. 1999;68: 821-861.

93. Altarejos JY, Montminy M. CREB and the CRTC co-activators: Sensors for hormonal and metabolic signals. *Nat Rev Mol Cell Biol*. 2011;12: 141-151.

94. Carlezon WA, Jr., Duman RS, Nestler EJ. The many faces of CREB. *Trends Neurosci*. 2005;28: 436-445.

95. Sapio L, Salzillo A, Ragone A, Illiano M, Spina A, Naviglio S. Targeting CREB in cancer therapy: A key candidate or one of many? An update. *Cancers (Basel)*. 2020;12.

96. Steven A, Friedrich M, Jank P, Heimer N, Budczies J, Denkert C, Seliger B. What turns CREB on? And off? And why does it matter? *Cell Mol Life Sci.* 2020;77: 4049-4067.
97. Xiao X, Li BX, Mitton B, Ikeda A, Sakamoto KM. Targeting CREB for cancer therapy: Friend or foe. *Curr Cancer Drug Targets.* 2010;10: 384-391.
98. Tyson DR, Swarthout JT, Jefcoat SC, Partridge NC. PTH induction of transcriptional activity of the cAMP response element-binding protein requires the serine 129 site and glycogen synthase kinase-3 activity, but not casein Kinase II sites. *Endocrinology.* 2002;143: 674-682.
99. Swarthout JT, Tyson DR, Jefcoat SC, Jr., Partridge NC. Induction of transcriptional activity of the cyclic adenosine monophosphate response element binding protein by parathyroid hormone and epidermal growth factor in osteoblastic cells. *J Bone Miner Res.* 2002;17: 1401-1407.
100. Wang H, Xu J, Lazarovici P, Quirion R, Zheng W. cAMP response element-binding protein (CREB): A possible signaling molecule link in the pathophysiology of schizophrenia. *Front Mol Neurosci.* 2018;11: 255.
101. Trinh AT, Kim SH, Chang HY, Mastrocola AS, Tibbetts RS. Cyclin-dependent kinase 1-dependent phosphorylation of cAMP response element-binding protein decreases chromatin occupancy. *J Biol Chem.* 2013;288: 23765-23775.
102. Shnitkind S, Martinez-Yamout MA, Dyson HJ, Wright PE. Structural basis for graded inhibition of CREB:DNA interactions by multisite phosphorylation. *Biochemistry.* 2018;57: 6964-6972.
103. Mayr BM, Guzman E, Montminy M. Glutamine rich and basic region/leucine zipper (bZIP) domains stabilize cAMP-response element-binding protein (CREB) binding to chromatin. *J Biol Chem.* 2005;280: 15103-15110.
104. Quinn PG. Distinct activation domains within cAMP response element-binding protein (CREB) mediate basal and camp-stimulated transcription. *J Biol Chem.* 1993;268: 16999-17009.

105. Felinski EA, Quinn PG. The coactivator dTAF(II)110/h(TAF(II)135 is sufficient to recruit a polymerase complex and activate basal transcription mediated by CREB. *Proc Natl Acad Sci U S A*. 2001;98: 13078-13083.
106. Sakamoto K, Karelina K, Obrietan K. Creb: A multifaceted regulator of neuronal plasticity and protection. *J Neurochem*. 2011;116: 1-9.
107. Yun YD, Dumoulin M, Habener JF. DNA-binding and dimerization domains of adenosine 3',5'- cyclic monophosphate-responsive protein CREB reside in the carboxyl-terminal 66 amino acids. *Mol Endocrinol*. 1990;4: 931-939.
108. Zhang X, Odom DT, Koo SH, Conkright MD, Canettieri G, Best J, Chen H, Jenner R, Herbolsheimer E, Jacobsen E, Kadam S, Ecker JR, Emerson B, Hogenesch JB, Unterman T, Young RA, Montminy M. Genome-wide analysis of cAMP-response element binding protein occupancy, phosphorylation, and target gene activation in human tissues. *Proc Natl Acad Sci U S A*. 2005;102: 4459-4464.
109. Berdeaux R, Hutchins C. Anabolic and pro-metabolic functions of CREB-CRTC in skeletal muscle: Advantages and obstacles for type 2 diabetes and cancer cachexia. *Front Endocrinol (Lausanne)*. 2019;10: 535.
110. Luo Q, Viste K, Urdy-Zaa JC, Senthil Kumar G, Tsai WW, Talai A, Mayo KE, Montminy M, Radhakrishnan I. Mechanism of CREB recognition and coactivation by the CREB-regulated transcriptional coactivator CRTC2. *Proc Natl Acad Sci U S A*. 2012;109: 20865-20870.
111. Sadamoto H, Saito K, Muto H, Kinjo M, Ito E. Direct observation of dimerization between different CREB1 isoforms in a living cell. *PLoS One*. 2011;6: e20285.
112. Borlikova G, Endo S. Inducible cAMP early repressor (ICER) and brain functions. *Mol Neurobiol*. 2009;40: 73-86.
113. Foulkes NS, Borrelli E, Sassone-Corsi P. CREM gene: Use of alternative DNA-binding domains generates multiple antagonists of camp-induced transcription. *Cell*. 1991;64: 739-749.

114. Zhang H, Kong Q, Wang J, Jiang Y, Hua H. Complex roles of cAMP-PKA-CREB signaling in cancer. *Exp Hematol Oncol*. 2020;9: 32.
115. Chen AE, Ginty DD, Fan CM. Protein kinase a signalling via CREB controls myogenesis induced by Wnt proteins. *Nature*. 2005;433: 317-322.
116. James MA, Lu Y, Liu Y, Vikis HG, You M. RGS17, an overexpressed gene in human lung and prostate cancer, induces tumor cell proliferation through the cyclic AMP-PKA-CREB pathway. *Cancer Res*. 2009;69: 2108-2116.
117. Xiong J, Zhou X, Gong Z, Wang T, Zhang C, Xu X, Liu J, Li W. PKA/CREB regulates the constitutive promoter activity of the USP22 gene. *Oncol Rep*. 2015;33: 1505-1511.
118. Xia Y, Zhan C, Feng M, Leblanc M, Ke E, Yeddula N, Verma IM. Targeting CREB pathway suppresses small cell lung cancer. *Mol Cancer Res*. 2018;16: 825-832.
119. Sun RF, Zhao CY, Chen S, Yu W, Zhou MM, Gao CR. Androgen receptor stimulates hexokinase 2 and induces glycolysis by PKA/CREB signaling in hepatocellular carcinoma. *Dig Dis Sci*. 2021;66: 802-813.
120. Yu T, Yang G, Hou Y, Tang X, Wu C, Wu XA, Guo L, Zhu Q, Luo H, Du YE, Wen S, Xu L, Yin J, Tu G, Liu M. Cytoplasmic GPER translocation in cancer-associated fibroblasts mediates cAMP/PKA/CREB/glycolytic axis to confer tumor cells with multidrug resistance. *Oncogene*. 2017;36: 2131-2145.
121. Zhang Y, Zheng D, Zhou T, Song H, Hulsurkar M, Su N, Liu Y, Wang Z, Shao L, Ittmann M, Gleave M, Han H, Xu F, Liao W, Wang H, Li W. Androgen deprivation promotes neuroendocrine differentiation and angiogenesis through CREB-EZH2-TSP1 pathway in prostate cancers. *Nat Commun*. 2018;9: 4080.
122. Reh fuss RP, Walton KM, Loriaux MM, Goodman RH. The cAMP-regulated enhancer-binding protein ATF-1 activates transcription in response to cAMP-dependent protein kinase A. *J Biol Chem*. 1991;266: 18431-18434.

123. Guo YJ, Pan WW, Liu SB, Shen ZF, Xu Y, Hu LL. ERK/MAPK signalling pathway and tumorigenesis. *Exp Ther Med*. 2020;19: 1997-2007.
124. Zhang W, Liu HT. MAPK signal pathways in the regulation of cell proliferation in mammalian cells. *Cell Res*. 2002;12: 9-18.
125. Zhao N, Peacock SO, Lo CH, Heidman LM, Rice MA, Fahrenholtz CD, Greene AM, Magani F, Copello VA, Martinez MJ, Zhang Y, Daaka Y, Lynch CC, Burnstein KL. Arginine vasopressin receptor 1a is a therapeutic target for castration-resistant prostate cancer. *Sci Transl Med*. 2019;11.
126. Cheng Y, Zhu Y, Xu J, Yang M, Chen P, Xu W, Zhao J, Geng L, Gong S. PKN2 in colon cancer cells inhibits M2 phenotype polarization of tumor-associated macrophages via regulating DUSP6-Erk1/2 pathway. *Mol Cancer*. 2018;17: 13.
127. Sen T, Gupta R, Kaiser H, Sen N. Activation of PERK elicits memory impairment through inactivation of CREB and downregulation of PSD95 after traumatic brain injury. *J Neurosci*. 2017;37: 5900-5911.
128. Zhao Y, Wu H, Xing X, Ma Y, Ji S, Xu X, Zhao X, Wang S, Jiang W, Fang C, Zhang L, Yan F, Wang X. CD13 induces autophagy to promote hepatocellular carcinoma cell chemoresistance through the p38/Hsp27/CREB/ATG7 pathway. *J Pharmacol Exp Ther*. 2020;374: 512-520.
129. Cho JH, Hong WG, Jung YJ, Lee J, Lee E, Hwang SG, Um HD, Park JK. Gamma-ionizing radiation-induced activation of the EGFR-p38/ERK-STAT3/CREB-1-EMT pathway promotes the migration/invasion of non-small cell lung cancer cells and is inhibited by podophyllotoxin acetate. *Tumour Biol*. 2016;37: 7315-7325.
130. Hui K, Yang Y, Shi K, Luo H, Duan J, An J, Wu P, Ci Y, Shi L, Xu C. The p38 MAPK-regulated PKD1/CREB/Bcl-2 pathway contributes to selenite-induced colorectal cancer cell apoptosis in vitro and in vivo. *Cancer Lett*. 2014;354: 189-199.

131. Wan Y, Yang M, Kolattukudy S, Stark GR, Lu T. Activation of cAMP-responsive-element-binding protein by PI3 kinase and p38 MAPK is essential for elevated expression of transforming growth factor beta2 in cancer cells. *J Interferon Cytokine Res.* 2010;30: 677-681.
132. Corona G, Deiana M, Incani A, Vauzour D, Dessi MA, Spencer JP. Inhibition of p38/CREB phosphorylation and Cox-2 expression by olive oil polyphenols underlies their anti-proliferative effects. *Biochem Biophys Res Commun.* 2007;362: 606-611.
133. Chuderland D, Seger R. Calcium regulates ERK signaling by modulating its protein-protein interactions. *Commun Integr Biol.* 2008;1: 4-5.
134. Marambaud P, Dreses-Werringloer U, Vingtdoux V. Calcium signaling in neurodegeneration. *Mol Neurodegener.* 2009;4: 20.
135. Mao LM, Tang Q, Wang JQ. Protein kinase C-regulated cAMP response element-binding protein phosphorylation in cultured rat striatal neurons. *Brain Res Bull.* 2007;72: 302-308.
136. Wang P, Huang S, Wang F, Ren Y, Hehir M, Wang X, Cai J. Cyclic AMP-response element regulated cell cycle arrests in cancer cells. *PLoS One.* 2013;8: e65661.
137. Shankar E, Krishnamurthy S, Paranandi R, Basu A. PKCepsilon induces Bcl-2 by activating CREB. *Int J Oncol.* 2010;36: 883-888.
138. Kimura Y, Corcoran EE, Eto K, Gengyo-Ando K, Muramatsu MA, Kobayashi R, Freedman JH, Mitani S, Hagiwara M, Means AR, Tokumitsu H. A CAMK cascade activates CRE-mediated transcription in neurons of *Caenorhabditis elegans*. *EMBO Rep.* 2002;3: 962-966.
139. Liu X, Yu X, Xie J, Zhan M, Yu Z, Xie L, Zeng H, Zhang F, Chen G, Yi X, Zheng J. ANGPTL2/LILRB2 signaling promotes the propagation of lung cancer cells. *Oncotarget.* 2015;6: 21004-21015.
140. Shao H, Ma L, Jin F, Zhou Y, Tao M, Teng Y. Immune inhibitory receptor LILRB2 is critical for the endometrial cancer progression. *Biochem Biophys Res Commun.* 2018;506: 243-250.

141. Zhou X, Li J, Yang W. Calcium/calmodulin-dependent protein kinase II regulates cyclooxygenase-2 expression and prostaglandin E2 production by activating camp-response element-binding protein in rat peritoneal macrophages. *Immunology*. 2014;143: 287-299.
142. Sun P, Enslen H, Myung PS, Maurer RA. Differential activation of CREB by Ca^{2+} /calmodulin-dependent protein kinases type II and type IV involves phosphorylation of a site that negatively regulates activity. *Genes Dev*. 1994;8: 2527-2539.
143. Shimomura A, Ogawa Y, Kitani T, Fujisawa H, Hagiwara M. Calmodulin-dependent protein kinase II potentiates transcriptional activation through activating transcription factor 1 but not cAMP response element-binding protein. *J Biol Chem*. 1996;271: 17957-17960.
144. Ma H, Groth RD, Cohen SM, Emery JF, Li B, Hoedt E, Zhang G, Neubert TA, Tsien RW. Gamma CaMKII shuttles Ca^{2+} /CAM to the nucleus to trigger CREB phosphorylation and gene expression. *Cell*. 2014;159: 281-294.
145. Du K, Montminy M. CREB is a regulatory target for the protein kinase AKT/PKB. *J Biol Chem*. 1998;273: 32377-32379.
146. Devi TS, Singh LP, Hosoya K, Terasaki T. GSK-3 beta/CREB axis mediates IGF-1-induced ECM/adhesion molecule expression, cell cycle progression and monolayer permeability in retinal capillary endothelial cells: Implications for diabetic retinopathy. *Biochim Biophys Acta*. 2011;1812: 1080-1088.
147. Steven A, Seliger B. Control of CREB expression in tumors: From molecular mechanisms and signal transduction pathways to therapeutic target. *Oncotarget*. 2016;7: 35454-35465.
148. Phuong NT, Lim SC, Kim YM, Kang KW. Aromatase induction in tamoxifen-resistant breast cancer: Role of phosphoinositide 3-kinase-dependent CREB activation. *Cancer Lett*. 2014;351: 91-99.
149. Ma X, Wu D, Zhou S, Wan F, Liu H, Xu X, Xu X, Zhao Y, Tang M. The pancreatic cancer secreted Reg4 promotes macrophage polarization to M2 through EGFR/AKT/CREB pathway. *Oncol Rep*. 2016;35: 189-196.

150. Wu D, Zhau HE, Huang WC, Iqbal S, Habib FK, Sartor O, Cvitanovic L, Marshall FF, Xu Z, Chung LW. cAMP-responsive element-binding protein regulates vascular endothelial growth factor expression: Implication in human prostate cancer bone metastasis. *Oncogene*. 2007;26: 5070-5077.
151. Kumar AP, Bhaskaran S, Ganapathy M, Crosby K, Davis MD, Kochunov P, Schoolfield J, Yeh IT, Troyer DA, Ghosh R. Akt/cAMP-responsive element binding protein/cyclin D1 network: A novel target for prostate cancer inhibition in transgenic adenocarcinoma of mouse prostate model mediated by nexrutine, a phellodendron amurense bark extract. *Clin Cancer Res*. 2007;13: 2784-2794.
152. Calvo A, Perez-Stable C, Segura V, Catena R, Guruceaga E, Nguewa P, Blanco D, Parada L, Reiner T, Green JE. Molecular characterization of the Ggamma-globin-Tag transgenic mouse model of hormone refractory prostate cancer: Comparison to human prostate cancer. *Prostate*. 2010;70: 630-645.
153. Deng X, Elzey BD, Poulson JM, Morrison WB, Ko SC, Hahn NM, Ratliff TL, Hu CD. Ionizing radiation induces neuroendocrine differentiation of prostate cancer cells in vitro, in vivo and in prostate cancer patients. *Am J Cancer Res*. 2011;1: 834-844.
154. Suarez CD, Deng X, Hu CD. Targeting CREB inhibits radiation-induced neuroendocrine differentiation and increases radiation-induced cell death in prostate cancer cells. *Am J Cancer Res*. 2014;4: 850-861.
155. Deng X, Liu H, Huang J, Cheng L, Keller ET, Parsons SJ, Hu CD. Ionizing radiation induces prostate cancer neuroendocrine differentiation through interplay of CREB and ATF2: Implications for disease progression. *Cancer Res*. 2008;68: 9663-9670.
156. Park MH, Lee HS, Lee CS, You ST, Kim DJ, Park BH, Kang MJ, Heo WD, Shin EY, Schwartz MA, Kim EG. P21-activated kinase 4 promotes prostate cancer progression through CREB. *Oncogene*. 2013;32: 2475-2482.

157. Wang M, Gao W, Lu D, Teng L. MiR-1271 inhibits cell growth in prostate cancer by targeting ERG. *Pathol Oncol Res.* 2018;24: 385-391.
158. Tong Q, Weaver MR, Kosmacek EA, O'Connor BP, Harmacek L, Venkataraman S, Oberley-Deegan RE. MnTE-2-PyP reduces prostate cancer growth and metastasis by suppressing p300 activity and p300/HIF-1/CREB binding to the promoter region of the PAI-1 gene. *Free Radic Biol Med.* 2016;94: 185-194.
159. Mallappa S, Neeli PK, Karnewar S, Kotamraju S. Doxorubicin induces prostate cancer drug resistance by upregulation of ABCG4 through gsh depletion and CREB activation: Relevance of statins in chemosensitization. *Mol Carcinog.* 2019;58: 1118-1133.
160. Garcia GE, Nicole A, Bhaskaran S, Gupta A, Kyprianou N, Kumar AP. AKT-and CREB-mediated prostate cancer cell proliferation inhibition by nexrutine, a phellodendron amurense extract. *Neoplasia.* 2006;8: 523-533.
161. Jin L, Zhang Q, Guo R, Wang L, Wang J, Wan R, Zhang R, Xu Y, Li S. Different effects of corticotropin-releasing factor and urocortin 2 on apoptosis of prostate cancer cells in vitro. *J Mol Endocrinol.* 2011;47: 219-227.
162. Huang H, Cheville JC, Pan Y, Roche PC, Schmidt LJ, Tindall DJ. PTEN induces chemosensitivity in PTEN-mutated prostate cancer cells by suppression of Bcl-2 expression. *J Biol Chem.* 2001;276: 38830-38836.
163. Sang M, Hulsurkar M, Zhang X, Song H, Zheng D, Zhang Y, Li M, Xu J, Zhang S, Ittmann M, Li W. GRK3 is a direct target of CREB activation and regulates neuroendocrine differentiation of prostate cancer cells. *Oncotarget.* 2016;7: 45171-45185.
164. Meng XY, Zhang HZ, Ren YY, Wang KJ, Chen JF, Su R, Jiang JH, Wang P, Ma Q. Pinin promotes tumor progression via activating CREB through PI3K/AKT and ERK/MAPK pathway in prostate cancer. *Am J Cancer Res.* 2021;11: 1286-1303.
165. Wang L, Whitlatch LW, Flanagan JN, Holick MF, Chen TC. Vitamin d autocrine system and prostate cancer. *Recent Results Cancer Res.* 2003;164: 223-237.

166. Hulsurkar M, Li Z, Zhang Y, Li X, Zheng D, Li W. Beta-adrenergic signaling promotes tumor angiogenesis and prostate cancer progression through HDAC2-mediated suppression of thrombospondin-1. *Oncogene*. 2017;36: 1525-1536.
167. Yang Y, Bai Y, He Y, Zhao Y, Chen J, Ma L, Pan Y, Hinten M, Zhang J, Karnes RJ, Kohli M, Westendorf JJ, Li B, Zhu R, Huang H, Xu W. PTEN loss promotes intratumoral androgen synthesis and tumor microenvironment remodeling via aberrant activation of RUNX2 in castration-resistant prostate cancer. *Clin Cancer Res*. 2018;24: 834-846.
168. Ghosh R, Garcia GE, Crosby K, Inoue H, Thompson IM, Troyer DA, Kumar AP. Regulation of COX-2 by cyclic AMP response element binding protein in prostate cancer: Potential role for nexrutine. *Neoplasia*. 2007;9: 893-899.
169. Malaguarnera R, Sacco A, Morcavallo A, Squatrito S, Migliaccio A, Morrione A, Maggiolini M, Belfiore A. Metformin inhibits androgen-induced IGF-IR up-regulation in prostate cancer cells by disrupting membrane-initiated androgen signaling. *Endocrinology*. 2014;155: 1207-1221.
170. Rishi V, Potter T, Laudeman J, Reinhart R, Silvers T, Selby M, Stevenson T, Krosky P, Stephen AG, Acharya A, Moll J, Oh WJ, Scudiero D, Shoemaker RH, Vinson C. A high-throughput fluorescence-anisotropy screen that identifies small molecule inhibitors of the DNA binding of b-zip transcription factors. *Anal Biochem*. 2005;340: 259-271.
171. Heyerdahl SL, Rozenberg J, Jamtgaard L, Rishi V, Varticovski L, Akah K, Scudiero D, Shoemaker RH, Karpova TS, Day RN, McNally JG, Vinson C. The arylstibonic acid compound NSC13746 disrupts b-zip binding to DNA in living cells. *Eur J Cell Biol*. 2010;89: 564-573.
172. Rishi V, Oh WJ, Heyerdahl SL, Zhao J, Scudiero D, Shoemaker RH, Vinson C. 12 arylstibonic acids that inhibit the DNA binding of five b-zip dimers. *J Struct Biol*. 2010;170: 216-225.
173. Zhao J, Stagno JR, Varticovski L, Nimako E, Rishi V, McKinnon K, Akee R, Shoemaker RH, Ji X, Vinson C. P6981, an arylstibonic acid, is a novel low nanomolar inhibitor of cAMP response element-binding protein binding to DNA. *Mol Pharmacol*. 2012;82: 814-823.

174. Best JL, Amezcua CA, Mayr B, Flechner L, Murawsky CM, Emerson B, Zor T, Gardner KH, Montminy M. Identification of small-molecule antagonists that inhibit an activator: coactivator interaction. *Proc Natl Acad Sci U S A*. 2004;101: 17622-17627.
175. Li BX, Xiao X. Discovery of a small-molecule inhibitor of the KIX-KID interaction. *Chembiochem*. 2009;10: 2721-2724.
176. Li BX, Yamanaka K, Xiao X. Structure-activity relationship studies of naphthol AS-E and its derivatives as anticancer agents by inhibiting CREB-mediated gene transcription. *Bioorg Med Chem*. 2012;20: 6811-6820.
177. Xie F, Li BX, Kassenbrock A, Xue C, Wang X, Qian DZ, Sears RC, Xiao X. Identification of a potent inhibitor of CREB-mediated gene transcription with efficacious in vivo anticancer activity. *J Med Chem*. 2015;58: 5075-5087.
178. Srinivasan S, Totiger T, Shi C, Castellanos J, Lamichhane P, Dosch AR, Messaggio F, Kashikar N, Honnenahally K, Ban Y, Merchant NB, VanSaun M, Nagathihalli NS. Tobacco carcinogen-induced production of GM-CSF activates CREB to promote pancreatic cancer. *Cancer Res*. 2018;78: 6146-6158.
179. Kim MP, Li X, Deng J, Zhang Y, Dai B, Allton KL, Hughes TG, Siangco C, Augustine JJ, Kang Y, McDaniel JM, Xiong S, Koay EJ, McAllister F, Bristow CA, Heffernan TP, Maitra A, Liu B, Barton MC, Wasylshen AR, Fleming JB, Lozano G. Oncogenic KRAS recruits an expansive transcriptional network through mutant p53 to drive pancreatic cancer metastasis. *Cancer Discov*. 2021.
180. Xie F, Fan Q, Li BX, Xiao X. Discovery of a synergistic inhibitor of camp-response element binding protein (CREB)-mediated gene transcription with 666-15. *J Med Chem*. 2019;62: 11423-11429.
181. Anderson KA, Ribar TJ, Lin F, Noeldner PK, Green MF, Muehlbauer MJ, Witters LA, Kemp BE, Means AR. Hypothalamic CaMKK2 contributes to the regulation of energy balance. *Cell Metab*. 2008;7: 377-388.

182. Hurwitz AA, Foster BA, Allison JP, Greenberg NM, Kwon ED. The TRAMP mouse as a model for prostate cancer. *Curr Protoc Immunol*. 2001;Chapter 20: Unit 20 25.
183. Lesche R, Groszer M, Gao J, Wang Y, Messing A, Sun H, Liu X, Wu H. Cre/loxp-mediated inactivation of the murine Pten tumor suppressor gene. *Genesis*. 2002;32: 148-149.
184. Wu X, Wu J, Huang J, Powell WC, Zhang J, Matusik RJ, Sangiorgi FO, Maxson RE, Sucov HM, Roy-Burman P. Generation of a prostate epithelial cell-specific cre transgenic mouse model for tissue-specific gene ablation. *Mech Dev*. 2001;101: 61-69.
185. Chen R, Liang X, Murray MM, Karasik E, Han JJ, Zhu M, Foster BA, Frigo DE, Wang G. A simple quantitative PCR assay to determine TRAMP transgene zygosity. *Prostate Cancer Prostatic Dis*. 2020.
186. Navone NM, van Weerden WM, Vessella RL, Williams ED, Wang Y, Isaacs JT, Nguyen HM, Culig Z, van der Pluijm G, Rentsch CA, Marques RB, de Ridder CMA, Bubendorf L, Thalmann GN, Brennen WN, Santer FR, Moser PL, Shepherd P, Efstathiou E, Xue H, Lin D, Buijs J, Bosse T, Collins A, Maitland N, Buzza M, Kouspou M, Achtman A, Taylor RA, Risbridger G, Corey E. Movember gap1 pdx project: An international collection of serially transplantable prostate cancer patient-derived xenograft (PDX) models. *Prostate*. 2018;78: 1262-1282.
187. Ruifrok AC, Johnston DA. Quantification of histochemical staining by color deconvolution. *Anal Quant Cytol Histol*. 2001;23: 291-299.
188. Blessing AM, Ganesan S, Rajapakshe K, Ying Sung Y, Reddy Bollu L, Shi Y, Cheung E, Coarfa C, Chang JT, McDonnell DP, Frigo DE. Identification of a novel coregulator, SH3YL1, that interacts with the androgen receptor n-terminus. *Mol Endocrinol*. 2015;29: 1426-1439.
189. Wang T, Wei JJ, Sabatini DM, Lander ES. Genetic screens in human cells using the CRISPR-Cas9 system. *Science*. 2014;343: 80-84.
190. Bolger AM, Lohse M, Usadel B. Trimmomatic: A flexible trimmer for illumina sequence data. *Bioinformatics*. 2014;30: 2114-2120.

191. Dobin A, Davis CA, Schlesinger F, Drenkow J, Zaleski C, Jha S, Batut P, Chaisson M, Gingeras TR. Star: Ultrafast universal RNA-seq aligner. *Bioinformatics*. 2013;29: 15-21.
192. Anders S, Pyl PT, Huber W. HTseq--a python framework to work with high-throughput sequencing data. *Bioinformatics*. 2015;31: 166-169.
193. Love MI, Huber W, Anders S. Moderated estimation of fold change and dispersion for RNA-seq data with DESeq2. *Genome Biol*. 2014;15: 550.
194. Subramanian A, Tamayo P, Mootha VK, Mukherjee S, Ebert BL, Gillette MA, Paulovich A, Pomeroy SL, Golub TR, Lander ES, Mesirov JP. Gene set enrichment analysis: A knowledge-based approach for interpreting genome-wide expression profiles. *Proc Natl Acad Sci U S A*. 2005;102: 15545-15550.
195. Norris J, Fan D, Aleman C, Marks JR, Futreal PA, Wiseman RW, Iglehart JD, Deininger PL, McDonnell DP. Identification of a new subclass of Alu DNA repeats which can function as estrogen receptor-dependent transcriptional enhancers. *J Biol Chem*. 1995;270: 22777-22782.
196. Cerami E, Gao J, Dogrusoz U, Gross BE, Sumer SO, Aksoy BA, Jacobsen A, Byrne CJ, Heuer ML, Larsson E, Antipin Y, Reva B, Goldberg AP, Sander C, Schultz N. The cBio cancer genomics portal: An open platform for exploring multidimensional cancer genomics data. *Cancer Discov*. 2012;2: 401-404.
197. Gao J, Aksoy BA, Dogrusoz U, Dresdner G, Gross B, Sumer SO, Sun Y, Jacobsen A, Sinha R, Larsson E, Cerami E, Sander C, Schultz N. Integrative analysis of complex cancer genomics and clinical profiles using the cbiportal. *Sci Signal*. 2013;6: p11.
198. Klionsky DJ, Abdelmohsen K, Abe A, Abedin MJ, Abeliovich H, Acevedo Arozena A, Adachi H, Adams CM, Adams PD, Adeli K, Adhihetty PJ, Adler SG, Agam G, Agarwal R, Aghi MK, Agnello M, Agostinis P, Aguilar PV, Aguirre-Ghiso J, Airoidi EM, Ait-Si-Ali S, Akematsu T, Akporiaye ET, Al-Rubeai M, Albaiceta GM, Albanese C, Albani D, Albert ML, Aldudo J, Algul H, Alirezai M, Alloza I, Almasan A, Almonte-Beceril M, Alnemri ES, Alonso C, Altan-Bonnet N, Altieri DC, Alvarez S, Alvarez-Erviti L, Alves S, Amadoro G, Amano A, Amantini C, Ambrosio S, Amelio I,

Amer AO, Amessou M, Amon A, An Z, Anania FA, Andersen SU, Andley UP, Andreadi CK, Andrieu-Abadie N, Anel A, Ann DK, Anoopkumar-Dukie S, Antonioli M, Aoki H, Apostolova N, Aquila S, Aquilano K, Araki K, Arama E, Aranda A, Araya J, Arcaro A, Arias E, Arimoto H, Ariosia AR, Armstrong JL, Arnould T, Arsov I, Asanuma K, Askanas V, Asselin E, Atarashi R, Atherton SS, Atkin JD, Attardi LD, Auburger P, Auburger G, Aurelian L, Autelli R, Avagliano L, Avantagegiati ML, Avrahami L, Awale S, Azad N, Bachetti T, Backer JM, Bae DH, Bae JS, Bae ON, Bae SH, Baehrecke EH, Baek SH, Baghdiguian S, Bagniewska-Zadworna A, Bai H, Bai J, Bai XY, Bailly Y, Balaji KN, Balduini W, Ballabio A, Balzan R, Banerjee R, Banhegyi G, Bao H, Barbeau B, Barrachina MD, Barreiro E, Bartel B, Bartolome A, Bassham DC, Bassi MT, Bast RC, Jr., Basu A, Batista MT, Batoko H, Battino M, Bauckman K, Baumgarner BL, Bayer KU, Beale R, Beaulieu JF, Beck GR, Jr., Becker C, Beckham JD, Bedard PA, Bednarski PJ, Begley TJ, Behl C, Behrends C, Behrens GM, Behrns KE, Bejarano E, Belaid A, Belleudi F, Benard G, Berchem G, Bergamaschi D, Bergami M, Berkhout B, Berliocchi L, Bernard A, Bernard M, Bernassola F, Bertolotti A, Bess AS, Besteiro S, Bettuzzi S, Bhalla S, Bhattacharyya S, Bhutia SK, Biagosch C, Bianchi MW, Biard-Piechaczyk M, Billes V, Bincoletto C, Bingol B, Bird SW, Bitoun M, Bjedov I, Blackstone C, Blanc L, Blanco GA, Blomhoff HK, Boada-Romero E, Bockler S, Boes M, Boesze-Battaglia K, Boise LH, Bolino A, Boman A, Bonaldo P, Bordi M, Bosch J, Botana LM, Botti J, Bou G, Bouche M, Bouchecareilh M, Boucher MJ, Boulton ME, Bouret SG, Boya P, Boyer-Guittaut M, Bozhkov PV, Brady N, Braga VM, Brancolini C, Braus GH, Bravo-San Pedro JM, Brennan LA, Bresnick EH, Brest P, Bridges D, Bringer MA, Brini M, Brito GC, Brodin B, Brookes PS, Brown EJ, Brown K, Broxmeyer HE, Bruhat A, Brum PC, Brumell JH, Brunetti-Pierri N, Bryson-Richardson RJ, Buch S, Buchan AM, Budak H, Bulavin DV, Bultman SJ, Bultynck G, Bumbasirevic V, Burelle Y, Burke RE, Burmeister M, Butikofer P, Caberlotto L, Cadwell K, Cahova M, Cai D, Cai J, Cai Q, Calatayud S, Camougrand N, Campanella M, Campbell GR, Campbell M, Campello S, Candau R, Caniggia I, Cantoni L, Cao L, Caplan AB, Caraglia M, Cardinali C, Cardoso SM, Carew JS, Carleton LA, Carlin CR, Carloni S, Carlsson SR, Carmona-Gutierrez D,

Carneiro LA, Carnevali O, Carra S, Carrier A, Carroll B, Casas C, Casas J, Cassinelli G, Castets P, Castro-Obregon S, Cavallini G, Ceccherini I, Cecconi F, Cederbaum AI, Cena V, Cenci S, Cerella C, Cervia D, Cetrullo S, Chaachouay H, Chae HJ, Chagin AS, Chai CY, Chakrabarti G, Chamilos G, Chan EY, Chan MT, Chandra D, Chandra P, Chang CP, Chang RC, Chang TY, Chatham JC, Chatterjee S, Chauhan S, Che Y, Cheetham ME, Cheluvappa R, Chen CJ, Chen G, Chen GC, Chen G, Chen H, Chen JW, Chen JK, Chen M, Chen M, Chen P, Chen Q, Chen Q, Chen SD, Chen S, Chen SS, Chen W, Chen WJ, Chen WQ, Chen W, Chen X, Chen YH, Chen YG, Chen Y, Chen Y, Chen Y, Chen YJ, Chen YQ, Chen Y, Chen Z, Chen Z, Cheng A, Cheng CH, Cheng H, Cheong H, Cherry S, Chesney J, Cheung CH, Chevet E, Chi HC, Chi SG, Chiacchiera F, Chiang HL, Chiarelli R, Chiariello M, Chieppa M, Chin LS, Chiong M, Chiu GN, Cho DH, Cho SG, Cho WC, Cho YY, Cho YS, Choi AM, Choi EJ, Choi EK, Choi J, Choi ME, Choi SI, Chou TF, Chouaib S, Choubey D, Choubey V, Chow KC, Chowdhury K, Chu CT, Chuang TH, Chun T, Chung H, Chung T, Chung YL, Chwae YJ, Cianfanelli V, Ciarcia R, Ciechomska IA, Ciriolo MR, Cirone M, Claerhout S, Clague MJ, Claria J, Clarke PG, Clarke R, Clementi E, Cleyrat C, Cnop M, Coccia EM, Cocco T, Codogno P, Coers J, Cohen EE, Colecchia D, Coletto L, Coll NS, Colucci-Guyon E, Comincini S, Condello M, Cook KL, Coombs GH, Cooper CD, Cooper JM, Coppens I, Corasaniti MT, Corazzari M, Corbalan R, Corcelle-Termeau E, Cordero MD, Corral-Ramos C, Corti O, Cossarizza A, Costelli P, Costes S, Cotman SL, Coto-Montes A, Cottet S, Couve E, Covey LR, Cowart LA, Cox JS, Coxon FP, Coyne CB, Cragg MS, Craven RJ, Crepaldi T, Crespo JL, Criollo A, Crippa V, Cruz MT, Cuervo AM, Cuezva JM, Cui T, Cutillas PR, Czaja MJ, Czyzyk-Krzeska MF, Dagda RK, Dahmen U, Dai C, Dai W, Dai Y, Dalby KN, Dalla Valle L, Dalmaso G, D'Amelio M, Damme M, Darfeuille-Michaud A, Dargemont C, Darley-Usmar VM, Dasarathy S, Dasgupta B, Dash S, Dass CR, Davey HM, Davids LM, Davila D, Davis RJ, Dawson TM, Dawson VL, Daza P, de Belleruche J, de Figueiredo P, de Figueiredo RC, de la Fuente J, De Martino L, De Matteis A, De Meyer GR, De Milito A, De Santi M, de Souza W, De Tata V, De Zio D, Debnath J, Dechant R, Decuypere JP, Deegan S, Dehay B, Del Bello B, Del Re DP,

Delage-Mourroux R, Delbridge LM, Deldicque L, Delorme-Axford E, Deng Y, Dengjel J, Denizot M, Dent P, Der CJ, Deretic V, Derrien B, Deutsch E, Devarenne TP, Devenish RJ, Di Bartolomeo S, Di Daniele N, Di Domenico F, Di Nardo A, Di Paola S, Di Pietro A, Di Renzo L, DiAntonio A, Diaz-Araya G, Diaz-Laviada I, Diaz-Meco MT, Diaz-Nido J, Dickey CA, Dickson RC, Diederich M, Digard P, Dikic I, Dinesh-Kumar SP, Ding C, Ding WX, Ding Z, Dini L, Distler JH, Diwan A, Djavaheri-Mergny M, Dmytruk K, Dobson RC, Doetsch V, Dokladny K, Dokudovskaya S, Donadelli M, Dong XC, Dong X, Dong Z, Donohue TM, Jr., Doran KS, D'Orazi G, Dorn GW, 2nd, Dosenko V, Dridi S, Drucker L, Du J, Du LL, Du L, du Toit A, Dua P, Duan L, Duann P, Dubey VK, Duchen MR, Duchosal MA, Duez H, Dugail I, Dumit VI, Duncan MC, Dunlop EA, Dunn WA, Jr., Dupont N, Dupuis L, Duran RV, Durcan TM, Duvezin-Caubet S, Duvvuri U, Eapen V, Ebrahimi-Fakhari D, Echard A, Eckhart L, Edelstein CL, Edinger AL, Eichinger L, Eisenberg T, Eisenberg-Lerner A, Eissa NT, El-Deiry WS, El-Khoury V, Elazar Z, Eldar-Finkelman H, Elliott CJ, Emanuele E, Emmenegger U, Engedal N, Engelbrecht AM, Engeler S, Enserink JM, Erdmann R, Erenpreisa J, Eri R, Eriksen JL, Erman A, Escalante R, Eskelinen EL, Espert L, Esteban-Martinez L, Evans TJ, Fabri M, Fabrias G, Fabrizi C, Facchiano A, Faergeman NJ, Faggioni A, Fairlie WD, Fan C, Fan D, Fan J, Fang S, Fanto M, Fanzani A, Farkas T, Faure M, Favier FB, Fearnhead H, Federici M, Fei E, Felizardo TC, Feng H, Feng Y, Feng Y, Ferguson TA, Fernandez AF, Fernandez-Barrena MG, Fernandez-Checa JC, Fernandez-Lopez A, Fernandez-Zapico ME, Feron O, Ferraro E, Ferreira-Halder CV, Fesus L, Feuer R, Fiesel FC, Filippi-Chiela EC, Filomeni G, Fimia GM, Fingert JH, Finkbeiner S, Finkel T, Fiorito F, Fisher PB, Flajolet M, Flamigni F, Florey O, Florio S, Floto RA, Folini M, Follo C, Fon EA, Fornai F, Fortunato F, Fraldi A, Franco R, Francois A, Francois A, Frankel LB, Fraser ID, Frey N, Freyssenet DG, Frezza C, Friedman SL, Frigo DE, Fu D, Fuentes JM, Fueyo J, Fujitani Y, Fujiwara Y, Fujiya M, Fukuda M, Fulda S, Fusco C, Gabryel B, Gaestel M, Gailly P, Gajewska M, Galadari S, Galili G, Galindo I, Galindo MF, Gallicciotti G, Galluzzi L, Galluzzi L, Galy V, Gammoh N, Gandy S, Ganesan AK, Ganesan S, Ganley IG, Gannage M, Gao FB, Gao F, Gao JX, Garcia Nannig L, Garcia Vescovi E, Garcia-

Macia M, Garcia-Ruiz C, Garg AD, Garg PK, Gargini R, Gassen NC, Gatica D, Gatti E, Gavard J, Gavathiotis E, Ge L, Ge P, Ge S, Gean PW, Gelmetti V, Genazzani AA, Geng J, Genschik P, Gerner L, Gestwicki JE, Gewirtz DA, Ghavami S, Ghigo E, Ghosh D, Giammarioli AM, Giampieri F, Giampietri C, Giatromanolaki A, Gibbings DJ, Gibellini L, Gibson SB, Ginet V, Giordano A, Giorgini F, Giovannetti E, Girardin SE, Gispert S, Giuliano S, Gladson CL, Glavic A, Gleave M, Godefroy N, Gogal RM, Jr., Gokulan K, Goldman GH, Goletti D, Goligorsky MS, Gomes AV, Gomes LC, Gomez H, Gomez-Manzano C, Gomez-Sanchez R, Goncalves DA, Goncu E, Gong Q, Gongora C, Gonzalez CB, Gonzalez-Alegre P, Gonzalez-Cabo P, Gonzalez-Polo RA, Goping IS, Gorbea C, Gorbunov NV, Goring DR, Gorman AM, Gorski SM, Goruppi S, Goto-Yamada S, Gotor C, Gottlieb RA, Gozes I, Gozuacik D, Graba Y, Graef M, Granato GE, Grant GD, Grant S, Gravina GL, Green DR, Greenhough A, Greenwood MT, Grimaldi B, Gros F, Grose C, Groulx JF, Gruber F, Grumati P, Grune T, Guan JL, Guan KL, Guerra B, Guillen C, Gulshan K, Gunst J, Guo C, Guo L, Guo M, Guo W, Guo XG, Gust AA, Gustafsson AB, Gutierrez E, Gutierrez MG, Gwak HS, Haas A, Haber JE, Hadano S, Hagedorn M, Hahn DR, Halayko AJ, Hamacher-Brady A, Hamada K, Hamai A, Hamann A, Hamasaki M, Hamer I, Hamid Q, Hammond EM, Han F, Han W, Handa JT, Hanover JA, Hansen M, Harada M, Harhaji-Trajkovic L, Harper JW, Harrath AH, Harris AL, Harris J, Hasler U, Hasselblatt P, Hasui K, Hawley RG, Hawley TS, He C, He CY, He F, He G, He RR, He XH, He YW, He YY, Heath JK, Hebert MJ, Heinzen RA, Helgason GV, Hensel M, Henske EP, Her C, Herman PK, Hernandez A, Hernandez C, Hernandez-Tiedra S, Hetz C, Hiesinger PR, Higaki K, Hilfiker S, Hill BG, Hill JA, Hill WD, Hino K, Hofius D, Hofman P, Hoglinger GU, Hohfeld J, Holz MK, Hong Y, Hood DA, Hoozemans JJ, Hoppe T, Hsu C, Hsu CY, Hsu LC, Hu D, Hu G, Hu HM, Hu H, Hu MC, Hu YC, Hu ZW, Hua F, Hua Y, Huang C, Huang HL, Huang KH, Huang KY, Huang S, Huang S, Huang WP, Huang YR, Huang Y, Huang Y, Huber TB, Huebbe P, Huh WK, Hulmi JJ, Hur GM, Hurley JH, Husak Z, Hussain SN, Hussain S, Hwang JJ, Hwang S, Hwang TI, Ichihara A, Imai Y, Imbriano C, Inomata M, Into T, Iovane V, Iovanna JL, Iozzo RV, Ip NY, Irazoqui JE, Iribarren P, Isaka Y, Isakovic AJ, Ischiropoulos H, Isenberg JS,

Ishaq M, Ishida H, Ishii I, Ishmael JE, Isidoro C, Isobe K, Isono E, Issazadeh-Navikas S, Itahana K, Itakura E, Ivanov AI, Iyer AK, Izquierdo JM, Izumi Y, Izzo V, Jaattela M, Jaber N, Jackson DJ, Jackson WT, Jacob TG, Jacques TS, Jagannath C, Jain A, Jana NR, Jang BK, Jani A, Janji B, Jannig PR, Jansson PJ, Jean S, Jendrach M, Jeon JH, Jessen N, Jeung EB, Jia K, Jia L, Jiang H, Jiang H, Jiang L, Jiang T, Jiang X, Jiang X, Jiang X, Jiang Y, Jiang Y, Jimenez A, Jin C, Jin H, Jin L, Jin M, Jin S, Jinwal UK, Jo EK, Johansen T, Johnson DE, Johnson GV, Johnson JD, Jonasch E, Jones C, Joosten LA, Jordan J, Joseph AM, Joseph B, Joubert AM, Ju D, Ju J, Juan HF, Juenemann K, Juhasz G, Jung HS, Jung JU, Jung YK, Jungbluth H, Justice MJ, Jutten B, Kaakoush NO, Kaarniranta K, Kaasik A, Kabuta T, Kaeffer B, Kagedal K, Kahana A, Kajimura S, Kakhlon O, Kalia M, Kalvakolanu DV, Kamada Y, Kambas K, Kaminskyy VO, Kampinga HH, Kandouz M, Kang C, Kang R, Kang TC, Kanki T, Kanneganti TD, Kanno H, Kanthasamy AG, Kantorow M, Kaparakis-Liaskos M, Kapuy O, Karantza V, Karim MR, Karmakar P, Kaser A, Kaushik S, Kawula T, Kaynar AM, Ke PY, Ke ZJ, Kehrl JH, Keller KE, Kemper JK, Kenworthy AK, Kepp O, Kern A, Kesari S, Kessel D, Ketteler R, Kettelhut Ido C, Khambu B, Khan MM, Khandelwal VK, Khare S, Kiang JG, Kiger AA, Kihara A, Kim AL, Kim CH, Kim DR, Kim DH, Kim EK, Kim HY, Kim HR, Kim JS, Kim JH, Kim JC, Kim JH, Kim KW, Kim MD, Kim MM, Kim PK, Kim SW, Kim SY, Kim YS, Kim Y, Kimchi A, Kimmelman AC, Kimura T, King JS, Kirkegaard K, Kirkin V, Kirshenbaum LA, Kishi S, Kitajima Y, Kitamoto K, Kitaoka Y, Kitazato K, Kley RA, Klimecki WT, Klinkenberg M, Klucken J, Knaevelsrud H, Knecht E, Knuppertz L, Ko JL, Kobayashi S, Koch JC, Koechlin-Ramonatxo C, Koenig U, Koh YH, Kohler K, Kohlwein SD, Koike M, Komatsu M, Kominami E, Kong D, Kong HJ, Konstantakou EG, Kopp BT, Korcsmaros T, Korhonen L, Korolchuk VI, Koshkina NV, Kou Y, Koukourakis MI, Koumenis C, Kovacs AL, Kovacs T, Kovacs WJ, Koya D, Kraft C, Krainc D, Kramer H, Kravic-Stevovic T, Krek W, Kretz-Remy C, Krick R, Krishnamurthy M, Kriston-Vizi J, Kroemer G, Kruer MC, Kruger R, Ktistakis NT, Kuchitsu K, Kuhn C, Kumar AP, Kumar A, Kumar A, Kumar D, Kumar D, Kumar R, Kumar S, Kundu M, Kung HJ, Kuno A, Kuo SH, Kuret J, Kurz T, Kwok T, Kwon TK, Kwon YT, Kyrmizi I, La Spada AR, Lafont

F, Lahm T, Lakkaraju A, Lam T, Lamark T, Lancel S, Landowski TH, Lane DJ, Lane JD, Lanzi C, Lapaquette P, Lapierre LR, Laporte J, Laukkanen J, Laurie GW, Lavandero S, Lavie L, LaVoie MJ, Law BY, Law HK, Law KB, Layfield R, Lazo PA, Le Cam L, Le Roch KG, Le Stunff H, Leardkamolkarn V, Lecuit M, Lee BH, Lee CH, Lee EF, Lee GM, Lee HJ, Lee H, Lee JK, Lee J, Lee JH, Lee JH, Lee M, Lee MS, Lee PJ, Lee SW, Lee SJ, Lee SJ, Lee SY, Lee SH, Lee SS, Lee SJ, Lee S, Lee YR, Lee YJ, Lee YH, Leeuwenburgh C, Lefort S, Legouis R, Lei J, Lei QY, Leib DA, Leibowitz G, Lekli I, Lemaire SD, Lemasters JJ, Lemberg MK, Lemoine A, Leng S, Lenz G, Lenzi P, Lerman LO, Lettieri Barbato D, Leu JI, Leung HY, Levine B, Lewis PA, Lezoualc'h F, Li C, Li F, Li FJ, Li J, Li K, Li L, Li M, Li M, Li Q, Li R, Li S, Li W, Li W, Li X, Li Y, Lian J, Liang C, Liang Q, Liao Y, Liberal J, Liberski PP, Lie P, Lieberman AP, Lim HJ, Lim KL, Lim K, Lima RT, Lin CS, Lin CF, Lin F, Lin F, Lin FC, Lin K, Lin KH, Lin PH, Lin T, Lin WW, Lin YS, Lin Y, Linden R, Lindholm D, Lindqvist LM, Lingor P, Linkermann A, Liotta LA, Lipinski MM, Lira VA, Lisanti MP, Liton PB, Liu B, Liu C, Liu CF, Liu F, Liu HJ, Liu J, Liu JJ, Liu JL, Liu K, Liu L, Liu L, Liu Q, Liu RY, Liu S, Liu S, Liu W, Liu XD, Liu X, Liu XH, Liu X, Liu X, Liu X, Liu Y, Liu Y, Liu Z, Liu Z, Liuzzi JP, Lizard G, Ljubic M, Lodhi IJ, Logue SE, Lokeshwar BL, Long YC, Lonial S, Loos B, Lopez-Otin C, Lopez-Vicario C, Lorente M, Lorenzi PL, Lorincz P, Los M, Lotze MT, Lovat PE, Lu B, Lu B, Lu J, Lu Q, Lu SM, Lu S, Lu Y, Luciano F, Luckhart S, Lucocq JM, Ludovico P, Lugea A, Lukacs NW, Lum JJ, Lund AH, Luo H, Luo J, Luo S, Luparello C, Lyons T, Ma J, Ma Y, Ma Y, Ma Z, Machado J, Machado-Santelli GM, Macian F, MacIntosh GC, MacKeigan JP, Macleod KF, MacMicking JD, MacMillan-Crow LA, Madeo F, Madesh M, Madrigal-Matute J, Maeda A, Maeda T, Maegawa G, Maellaro E, Maes H, Magarinos M, Maiese K, Maiti TK, Maiuri L, Maiuri MC, Maki CG, Malli R, Malorni W, Maloyan A, Mami-Chouaib F, Man N, Mancias JD, Mandelkow EM, Mandell MA, Manfredi AA, Manie SN, Manzoni C, Mao K, Mao Z, Mao ZW, Marambaud P, Marconi AM, Marelja Z, Marfe G, Margeta M, Margittai E, Mari M, Mariani FV, Marin C, Marinelli S, Marino G, Markovic I, Marquez R, Martelli AM, Martens S, Martin KR, Martin SJ, Martin S, Martin-Acebes MA, Martin-Sanz P, Martinand-Mari C, Martinet W, Martinez J, Martinez-Lopez N, Martinez-Outschoorn U,

Martinez-Velazquez M, Martinez-Vicente M, Martins WK, Mashima H, Mastrianni JA, Matarese G, Matarrese P, Mateo R, Matoba S, Matsumoto N, Matsushita T, Matsuura A, Matsuzawa T, Mattson MP, Matus S, Maugeri N, Mauvezin C, Mayer A, Maysinger D, Mazzolini GD, McBrayer MK, McCall K, McCormick C, McInerney GM, McIver SC, McKenna S, McMahon JJ, McNeish IA, Mechta-Grigoriou F, Medema JP, Medina DL, Megyeri K, Mehrpour M, Mehta JL, Mei Y, Meier UC, Meijer AJ, Melendez A, Melino G, Melino S, de Melo EJ, Mena MA, Meneghini MD, Menendez JA, Menezes R, Meng L, Meng LH, Meng S, Menghini R, Menko AS, Menna-Barreto RF, Menon MB, Meraz-Rios MA, Merla G, Merlini L, Merlot AM, Meryk A, Meschini S, Meyer JN, Mi MT, Miao CY, Micale L, Michaeli S, Michiels C, Migliaccio AR, Mihailidou AS, Mijaljica D, Mikoshiba K, Milan E, Miller-Fleming L, Mills GB, Mills IG, Minakaki G, Minassian BA, Ming XF, Minibayeva F, Minina EA, Mintern JD, Minucci S, Miranda-Vizuete A, Mitchell CH, Miyamoto S, Miyazawa K, Mizushima N, Mnich K, Mograbi B, Mohseni S, Moita LF, Molinari M, Molinari M, Moller AB, Mollereau B, Mollinedo F, Mongillo M, Monick MM, Montagnaro S, Montell C, Moore DJ, Moore MN, Mora-Rodriguez R, Moreira PI, Morel E, Morelli MB, Moreno S, Morgan MJ, Moris A, Moriyasu Y, Morrison JL, Morrison LA, Morselli E, Moscat J, Moseley PL, Mostowy S, Motori E, Mottet D, Mottram JC, Moussa CE, Mpakou VE, Mukhtar H, Mulcahy Levy JM, Muller S, Munoz-Moreno R, Munoz-Pinedo C, Munz C, Murphy ME, Murray JT, Murthy A, Mysorekar IU, Nabi IR, Nabissi M, Nader GA, Nagahara Y, Nagai Y, Nagata K, Nagelkerke A, Nagy P, Naidu SR, Nair S, Nakano H, Nakatogawa H, Nanjundan M, Napolitano G, Naqvi NI, Nardacci R, Narendra DP, Narita M, Nascimbeni AC, Natarajan R, Navegantes LC, Nawrocki ST, Nazarko TY, Nazarko VY, Neill T, Neri LM, Netea MG, Netea-Maier RT, Neves BM, Ney PA, Nezis IP, Nguyen HT, Nguyen HP, Nicot AS, Nilsen H, Nilsson P, Nishimura M, Nishino I, Niso-Santano M, Niu H, Nixon RA, Njar VC, Noda T, Noegel AA, Nolte EM, Norberg E, Norga KK, Noureini SK, Notomi S, Notterpek L, Nowikovsky K, Nukina N, Nurnberger T, O'Donnell VB, O'Donovan T, O'Dwyer PJ, Oehme I, Oeste CL, Ogawa M, Ogretmen B, Ogura Y, Oh YJ, Ohmuraya M, Ohshima T, Ojha R, Okamoto K, Okazaki T, Oliver FJ, Ollinger K, Olsson S, Orban DP, Ordonez P, Orhon I, Orosz L, O'Rourke

EJ, Orozco H, Ortega AL, Ortona E, Osellame LD, Oshima J, Oshima S, Osiewacz HD, Otomo T, Otsu K, Ou JH, Outeiro TF, Ouyang DY, Ouyang H, Overholtzer M, Ozbun MA, Ozdinler PH, Ozpolat B, Pacelli C, Paganetti P, Page G, Pages G, Pagnini U, Pajak B, Pak SC, Pakos-Zebrucka K, Pakpour N, Palkova Z, Palladino F, Pallauf K, Pallet N, Palmieri M, Paludan SR, Palumbo C, Palumbo S, Pampliega O, Pan H, Pan W, Panaretakis T, Pandey A, Pantazopoulou A, Papackova Z, Papademetrio DL, Papassideri I, Papini A, Parajuli N, Pardo J, Parekh VV, Parenti G, Park JI, Park J, Park OK, Parker R, Parlato R, Parys JB, Parzych KR, Pasquet JM, Pasquier B, Pasumarthi KB, Patschan D, Patterson C, Pattingre S, Pattison S, Pause A, Pavenstadt H, Pavone F, Pedrozo Z, Pena FJ, Penalva MA, Pende M, Peng J, Penna F, Penninger JM, Pensalfini A, Pepe S, Pereira GJ, Pereira PC, Perez-de la Cruz V, Perez-Perez ME, Perez-Rodriguez D, Perez-Sala D, Perier C, Perl A, Perlmutter DH, Perrotta I, Pervaiz S, Pesonen M, Pessin JE, Peters GJ, Petersen M, Petrache I, Petrof BJ, Petrovski G, Phang JM, Piacentini M, Pierdominici M, Pierre P, Pierrefite-Carle V, Pietrocola F, Pimentel-Muinos FX, Pinar M, Pineda B, Pinkas-Kramarski R, Pinti M, Pinton P, Piperdi B, Piret JM, Plataniias LC, Platta HW, Plowey ED, Poggeler S, Poirot M, Polcic P, Poletti A, Poon AH, Popelka H, Popova B, Poprawa I, Poulose SM, Poulton J, Powers SK, Powers T, Pozuelo-Rubio M, Prak K, Prange R, Prescott M, Priault M, Prince S, Proia RL, Proikas-Cezanne T, Prokisch H, Promponas VJ, Przyklenk K, Puertollano R, Pugazhenth S, Puglielli L, Pujol A, Puyal J, Pyeon D, Qi X, Qian WB, Qin ZH, Qiu Y, Qu Z, Quadrilatero J, Quinn F, Raben N, Rabinowich H, Radogna F, Ragusa MJ, Rahmani M, Raina K, Ramanadham S, Ramesh R, Rami A, Randall-Demllo S, Randow F, Rao H, Rao VA, Rasmussen BB, Rasse TM, Ratovitski EA, Rautou PE, Ray SK, Razani B, Reed BH, Reggiori F, Rehm M, Reichert AS, Rein T, Reiner DJ, Reits E, Ren J, Ren X, Renna M, Reusch JE, Revuelta JL, Reyes L, Rezaie AR, Richards RI, Richardson DR, Richetta C, Riehle MA, Rihn BH, Rikihisa Y, Riley BE, Rimbach G, Rippo MR, Ritis K, Rizzi F, Rizzo E, Roach PJ, Robbins J, Roberge M, Roca G, Roccheri MC, Rocha S, Rodrigues CM, Rodriguez CI, de Cordoba SR, Rodriguez-Muela N, Roelofs J, Rogov VV, Rohn TT, Rohrer B, Romanelli D, Romani L, Romano PS, Roncero MI,

Rosa JL, Rosello A, Rosen KV, Rosenstiel P, Rost-Roszkowska M, Roth KA, Roue G, Rouis M, Rouschop KM, Ruan DT, Ruano D, Rubinsztein DC, Rucker EB, 3rd, Rudich A, Rudolf E, Rudolf R, Ruegg MA, Ruiz-Roldan C, Ruparelia AA, Rusmini P, Russ DW, Russo GL, Russo G, Russo R, Rusten TE, Ryabovol V, Ryan KM, Ryter SW, Sabatini DM, Sacher M, Sachse C, Sack MN, Sadoshima J, Saftig P, Sagi-Eisenberg R, Sahni S, Saikumar P, Saito T, Saitoh T, Sakakura K, Sakoh-Nakatogawa M, Sakuraba Y, Salazar-Roa M, Salomoni P, Saluja AK, Salvaterra PM, Salvioli R, Samali A, Sanchez AM, Sanchez-Alcazar JA, Sanchez-Prieto R, Sandri M, Sanjuan MA, Santaguida S, Santambrogio L, Santoni G, Dos Santos CN, Saran S, Sardiello M, Sargent G, Sarkar P, Sarkar S, Sarrias MR, Sarwal MM, Sasakawa C, Sasaki M, Sass M, Sato K, Sato M, Satriano J, Savaraj N, Saveljeva S, Schaefer L, Schaible UE, Scharl M, Schatzl HM, Schekman R, Scheper W, Schiavi A, Schipper HM, Schmeisser H, Schmidt J, Schmitz I, Schneider BE, Schneider EM, Schneider JL, Schon EA, Schonenberger MJ, Schonthal AH, Schorderet DF, Schroder B, Schuck S, Schulze RJ, Schwarten M, Schwarz TL, Sciarretta S, Scotto K, Scovassi AI, Screatton RA, Screen M, Seca H, Sedej S, Segatori L, Segev N, Seglen PO, Segui-Simarro JM, Segura-Aguilar J, Seki E, Sell C, Seiliez I, Semenkovich CF, Semenza GL, Sen U, Serra AL, Serrano-Puebla A, Sesaki H, Setoguchi T, Settembre C, Shacka JJ, Shajahan-Haq AN, Shapiro IM, Sharma S, She H, Shen CK, Shen CC, Shen HM, Shen S, Shen W, Sheng R, Sheng X, Sheng ZH, Shepherd TG, Shi J, Shi Q, Shi Q, Shi Y, Shibutani S, Shibuya K, Shidoji Y, Shieh JJ, Shih CM, Shimada Y, Shimizu S, Shin DW, Shinohara ML, Shintani M, Shintani T, Shioi T, Shirabe K, Shiri-Sverdlov R, Shirihai O, Shore GC, Shu CW, Shukla D, Sibirny AA, Sica V, Sigurdson CJ, Sigurdsson EM, Sijwali PS, Sikorska B, Silveira WA, Silvente-Poirot S, Silverman GA, Simak J, Simmet T, Simon AK, Simon HU, Simone C, Simons M, Simonsen A, Singh R, Singh SV, Singh SK, Sinha D, Sinha S, Sinicrope FA, Sirko A, Sirohi K, Sishi BJ, Sittler A, Siu PM, Sivridis E, Skwarska A, Slack R, Slaninova I, Slavov N, Smaili SS, Smalley KS, Smith DR, Soenen SJ, Soleimanpour SA, Solhaug A, Somasundaram K, Son JH, Sonawane A, Song C, Song F, Song HK, Song JX, Song W, Soo KY, Sood AK, Soong TW, Soontornniyomkij V, Sorice M, Sotgia F,

Soto-Pantoja DR, Sotthibundhu A, Sousa MJ, Spaink HP, Span PN, Spang A, Sparks JD, Speck PG, Spector SA, Spies CD, Springer W, Clair DS, Stacchiotti A, Staels B, Stang MT, Starczynowski DT, Starokadomskyy P, Steegborn C, Steele JW, Stefanis L, Steffan J, Stellrecht CM, Stenmark H, Stepkowski TM, Stern ST, Stevens C, Stockwell BR, Stoka V, Storchova Z, Stork B, Stratoulis V, Stravopodis DJ, Strnad P, Strohecker AM, Strom AL, Stromhaug P, Stulik J, Su YX, Su Z, Subauste CS, Subramaniam S, Sue CM, Suh SW, Sui X, Sukserree S, Sulzer D, Sun FL, Sun J, Sun J, Sun SY, Sun Y, Sun Y, Sun Y, Sundaramoorthy V, Sung J, Suzuki H, Suzuki K, Suzuki N, Suzuki T, Suzuki YJ, Swanson MS, Swanton C, Sward K, Swarup G, Sweeney ST, Sylvester PW, Szatmari Z, Szegezdi E, Szlosarek PW, Taegtmeyer H, Tafani M, Taillebourg E, Tait SW, Takacs-Vellai K, Takahashi Y, Takats S, Takemura G, Takigawa N, Talbot NJ, Tamagno E, Tamburini J, Tan CP, Tan L, Tan ML, Tan M, Tan YJ, Tanaka K, Tanaka M, Tang D, Tang D, Tang G, Tanida I, Tanji K, Tannous BA, Tapia JA, Tasset-Cuevas I, Tatar M, Tavassoly I, Tavernarakis N, Taylor A, Taylor GS, Taylor GA, Taylor JP, Taylor MJ, Tchetina EV, Tee AR, Teixeira-Clerc F, Telang S, Tencomnao T, Teng BB, Teng RJ, Terro F, Tettamanti G, Theiss AL, Theron AE, Thomas KJ, Thome MP, Thomes PG, Thorburn A, Thorner J, Thum T, Thumm M, Thurston TL, Tian L, Till A, Ting JP, Titorenko VI, Toker L, Toldo S, Tooze SA, Topisirovic I, Torgersen ML, Torosantucci L, Torriglia A, Torrisi MR, Tournier C, Towns R, Trajkovic V, Travassos LH, Triola G, Tripathi DN, Trisciuglio D, Troncoso R, Trougakos IP, Truttmann AC, Tsai KJ, Tschan MP, Tseng YH, Tsukuba T, Tsung A, Tsvetkov AS, Tu S, Tuan HY, Tucci M, Tumbarello DA, Turk B, Turk V, Turner RF, Tveita AA, Tyagi SC, Ubukata M, Uchiyama Y, Udelnow A, Ueno T, Umekawa M, Umemiya-Shirafuji R, Underwood BR, Ungermann C, Ureshino RP, Ushioda R, Uversky VN, Uzcategui NL, Vaccari T, Vaccaro MI, Vachova L, Vakifahmetoglu-Norberg H, Valdor R, Valente EM, Vallette F, Valverde AM, Van den Berghe G, Van Den Bosch L, van den Brink GR, van der Goot FG, van der Klei IJ, van der Laan LJ, van Doorn WG, van Egmond M, van Golen KL, Van Kaer L, van Lookeren Campagne M, Vandenabeele P, Vandenberghe W, Vanhorebeek I, Varela-Nieto I, Vasconcelos MH, Vasko R,

Vavvas DG, Vega-Naredo I, Velasco G, Velentzas AD, Velentzas PD, Vellai T, Vellenga E, Vendelbo MH, Venkatachalam K, Ventura N, Ventura S, Veras PS, Verdier M, Vertessy BG, Viale A, Vidal M, Vieira HL, Vierstra RD, Vigneswaran N, Vij N, Vila M, Villar M, Villar VH, Villarroja J, Vindis C, Viola G, Viscomi MT, Vitale G, Vogl DT, Voitsekhovskaja OV, von Haefen C, von Schwarzenberg K, Voth DE, Vouret-Craviari V, Vuori K, Vyas JM, Waeber C, Walker CL, Walker MJ, Walter J, Wan L, Wan X, Wang B, Wang C, Wang CY, Wang C, Wang C, Wang C, Wang D, Wang F, Wang F, Wang G, Wang HJ, Wang H, Wang HG, Wang H, Wang HD, Wang J, Wang J, Wang M, Wang MQ, Wang PY, Wang P, Wang RC, Wang S, Wang TF, Wang X, Wang XJ, Wang XW, Wang X, Wang X, Wang Y, Wang Y, Wang Y, Wang YJ, Wang Y, Wang Y, Wang YT, Wang Y, Wang ZN, Wappner P, Ward C, Ward DM, Warnes G, Watada H, Watanabe Y, Watase K, Weaver TE, Weekes CD, Wei J, Weide T, Wehl CC, Weindl G, Weis SN, Wen L, Wen X, Wen Y, Westermann B, Weyand CM, White AR, White E, Whitton JL, Whitworth AJ, Wiels J, Wild F, Wildenberg ME, Wileman T, Wilkinson DS, Wilkinson S, Willbold D, Williams C, Williams K, Williamson PR, Winklhofer KF, Witkin SS, Wohlgemuth SE, Wollert T, Wolvetang EJ, Wong E, Wong GW, Wong RW, Wong VK, Woodcock EA, Wright KL, Wu C, Wu D, Wu GS, Wu J, Wu J, Wu M, Wu M, Wu S, Wu WK, Wu Y, Wu Z, Xavier CP, Xavier RJ, Xia GX, Xia T, Xia W, Xia Y, Xiao H, Xiao J, Xiao S, Xiao W, Xie CM, Xie Z, Xie Z, Xilouri M, Xiong Y, Xu C, Xu C, Xu F, Xu H, Xu H, Xu J, Xu J, Xu J, Xu L, Xu X, Xu Y, Xu Y, Xu ZX, Xu Z, Xue Y, Yamada T, Yamamoto A, Yamanaka K, Yamashina S, Yamashiro S, Yan B, Yan B, Yan X, Yan Z, Yanagi Y, Yang DS, Yang JM, Yang L, Yang M, Yang PM, Yang P, Yang Q, Yang W, Yang WY, Yang X, Yang Y, Yang Y, Yang Z, Yang Z, Yao MC, Yao PJ, Yao X, Yao Z, Yao Z, Yasui LS, Ye M, Yedvobnick B, Yeganeh B, Yeh ES, Yeyati PL, Yi F, Yi L, Yin XM, Yip CK, Yoo YM, Yoo YH, Yoon SY, Yoshida K, Yoshimori T, Young KH, Yu H, Yu JJ, Yu JT, Yu J, Yu L, Yu WH, Yu XF, Yu Z, Yuan J, Yuan ZM, Yue BY, Yue J, Yue Z, Zacks DN, Zacksenhaus E, Zaffaroni N, Zaglia T, Zakeri Z, Zecchini V, Zeng J, Zeng M, Zeng Q, Zervos AS, Zhang DD, Zhang F, Zhang G, Zhang GC, Zhang H, Zhang H, Zhang H, Zhang H, Zhang J, Zhang J, Zhang J, Zhang J, Zhang JP, Zhang L, Zhang L,

Zhang L, Zhang L, Zhang MY, Zhang X, Zhang XD, Zhang Y, Zhang Y, Zhang Y, Zhang Y, Zhang Y, Zhao M, Zhao WL, Zhao X, Zhao YG, Zhao Y, Zhao YX, Zhao Z, Zhao ZJ, Zheng D, Zheng XL, Zheng X, Zhivotovsky B, Zhong Q, Zhou GZ, Zhou G, Zhou H, Zhou SF, Zhou XJ, Zhu H, Zhu H, Zhu WG, Zhu W, Zhu XF, Zhu Y, Zhuang SM, Zhuang X, Ziparo E, Zois CE, Zoladek T, Zong WX, Zorzano A, Zughaier SM. Guidelines for the use and interpretation of assays for monitoring autophagy (3rd edition). *Autophagy*. 2016;12: 1-222.

199. Yang Y, Klionsky DJ. Autophagy and disease: Unanswered questions. *Cell Death Differ*. 2020;27: 858-871.

200. Galluzzi L, Pietrocola F, Bravo-San Pedro JM, Amaravadi RK, Baehrecke EH, Cecconi F, Codogno P, Debnath J, Gewirtz DA, Karantza V, Kimmelman A, Kumar S, Levine B, Maiuri MC, Martin SJ, Penninger J, Piacentini M, Rubinsztein DC, Simon HU, Simonsen A, Thorburn AM, Velasco G, Ryan KM, Kroemer G. Autophagy in malignant transformation and cancer progression. *EMBO J*. 2015;34: 856-880.

201. Amaravadi RK, Kimmelman AC, Debnath J. Targeting autophagy in cancer: Recent advances and future directions. *Cancer Discov*. 2019;9: 1167-1181.

202. Levy JMM, Towers CG, Thorburn A. Targeting autophagy in cancer. *Nat Rev Cancer*. 2017;17: 528-542.

203. Fabio Gabrielle CM, Sergio Comincini. Prostate cancer cells at a therapeutic gunpoint of the autophagy process. *Journal of Cancer Metastasis and Treatment*. 2018;4.

204. Mizushima N, Levine B, Cuervo AM, Klionsky DJ. Autophagy fights disease through cellular self-digestion. *Nature*. 2008;451: 1069-1075.

205. Green DR, Galluzzi L, Kroemer G. Mitochondria and the autophagy-inflammation-cell death axis in organismal aging. *Science*. 2011;333: 1109-1112.

206. Karsli-Uzunbas G, Guo JY, Price S, Teng X, Laddha SV, Khor S, Kalaany NY, Jacks T, Chan CS, Rabinowitz JD, White E. Autophagy is required for glucose homeostasis and lung tumor maintenance. *Cancer Discov*. 2014;4: 914-927.

207. Levy JM, Thompson JC, Griesinger AM, Amani V, Donson AM, Birks DK, Morgan MJ, Mirsky DM, Handler MH, Foreman NK, Thorburn A. Autophagy inhibition improves chemosensitivity in BRAF(V600E) brain tumors. *Cancer Discov.* 2014;4: 773-780.
208. Tan Q, Wang M, Yu M, Zhang J, Bristow RG, Hill RP, Tannock IF. Role of autophagy as a survival mechanism for hypoxic cells in tumors. *Neoplasia.* 2016;18: 347-355.
209. Daskalaki I, Gkikas I, Tavernarakis N. Hypoxia and selective autophagy in cancer development and therapy. *Front Cell Dev Biol.* 2018;6: 104.
210. Wang L, Wang J, Xiong H, Wu F, Lan T, Zhang Y, Guo X, Wang H, Saleem M, Jiang C, Lu J, Deng Y. Co-targeting hexokinase 2-mediated warburg effect and ULK1-dependent autophagy suppresses tumor growth of PTEN- and TP53-deficiency-driven castration-resistant prostate cancer. *EBioMedicine.* 2016;7: 50-61.
211. Kranzbuhler B, Salemi S, Mortezaei A, Sulser T, Eberli D. Combined N-terminal androgen receptor and autophagy inhibition increases the antitumor effect in enzalutamide sensitive and enzalutamide resistant prostate cancer cells. *Prostate.* 2019;79: 206-214.
212. Amaravadi RK, Lippincott-Schwartz J, Yin XM, Weiss WA, Takebe N, Timmer W, DiPaola RS, Lotze MT, White E. Principles and current strategies for targeting autophagy for cancer treatment. *Clin Cancer Res.* 2011;17: 654-666.
213. Mauthe M, Orhon I, Rocchi C, Zhou X, Luhr M, Hijlkema KJ, Coppes RP, Engedal N, Mari M, Reggiori F. Chloroquine inhibits autophagic flux by decreasing autophagosome-lysosome fusion. *Autophagy.* 2018;14: 1435-1455.
214. Solomon VR, Lee H. Chloroquine and its analogs: A new promise of an old drug for effective and safe cancer therapies. *Eur J Pharmacol.* 2009;625: 220-233.
215. Alers S, Löffler AS, Wesselborg S, Stork B. Role of AMPK-mTOR-ULK1/2 in the regulation of autophagy: Cross talk, shortcuts, and feedbacks. *Mol Cell Biol.* 2012;32: 2-11.
216. Mihaylova MM, Shaw RJ. The AMPK signalling pathway coordinates cell growth, autophagy and metabolism. *Nat Cell Biol.* 2011;13: 1016-1023.

217. Marcelo KL, Means AR, York B. The Ca(2+)/calmodulin/CaMKK2 axis: Nature's metabolic camshaft. *Trends Endocrinol Metab.* 2016;27: 706-718.
218. Hardie DG. AMPK and autophagy get connected. *EMBO J.* 2011;30: 634-635.
219. Dadwal UC, Chang ES, Sankar U. Androgen receptor-CaMKK2 axis in prostate cancer and bone microenvironment. *Front Endocrinol (Lausanne).* 2018;9: 335.
220. Mizushima N, Yoshimori T. How to interpret LC3 immunoblotting. *Autophagy.* 2007;3: 542-545.
221. Bain J, Plater L, Elliott M, Shpiro N, Hastie CJ, McLauchlan H, Klevernic I, Arthur JS, Alessi DR, Cohen P. The selectivity of protein kinase inhibitors: A further update. *Biochem J.* 2007;408: 297-315.
222. O'Byrne SN, Scott JW, Pilotte JR, Santiago ADS, Langendorf CG, Oakhill JS, Eduful BJ, Counago RM, Wells CI, Zuercher WJ, Willson TM, Drewry DH. In depth analysis of kinase cross screening data to identify CaMKK2 inhibitory scaffolds. *Molecules.* 2020;25.
223. Kukimoto-Niino M, Yoshikawa S, Takagi T, Ohsawa N, Tomabeche Y, Terada T, Shirouzu M, Suzuki A, Lee S, Yamauchi T, Okada-Iwabu M, Iwabu M, Kadowaki T, Minokoshi Y, Yokoyama S. Crystal structure of the Ca²⁺/calmodulin-dependent protein kinase kinase in complex with the inhibitor STO-609. *J Biol Chem.* 2011;286: 22570-22579.
224. Kim J, Guan KL. Regulation of the autophagy initiating kinase ULK1 by nutrients: Roles of mTORC1 and AMPK. *Cell Cycle.* 2011;10: 1337-1338.
225. Lee JW, Park S, Takahashi Y, Wang HG. The association of AMPK with ULK1 regulates autophagy. *PLoS One.* 2010;5: e15394.
226. Laker RC, Drake JC, Wilson RJ, Lira VA, Lewellen BM, Ryall KA, Fisher CC, Zhang M, Saucerman JJ, Goodyear LJ, Kundu M, Yan Z. AMPK phosphorylation of ULK1 is required for targeting of mitochondria to lysosomes in exercise-induced mitophagy. *Nat Commun.* 2017;8: 548.

227. Berglund L, Bjorling E, Oksvold P, Fagerberg L, Asplund A, Szigartyo CA, Persson A, Ottosson J, Wernerus H, Nilsson P, Lundberg E, Sivertsson A, Navani S, Wester K, Kampf C, Hober S, Ponten F, Uhlen M. A gene-centric human protein atlas for expression profiles based on antibodies. *Mol Cell Proteomics*. 2008;7: 2019-2027.
228. Egan D, Kim J, Shaw RJ, Guan KL. The autophagy initiating kinase ULK1 is regulated via opposing phosphorylation by AMPK and mTOR. *Autophagy*. 2011;7: 643-644.
229. Hoadley KA, Yau C, Hinoue T, Wolf DM, Lazar AJ, Drill E, Shen R, Taylor AM, Cherniack AD, Thorsson V, Akbani R, Bowlby R, Wong CK, Wiznerowicz M, Sanchez-Vega F, Robertson AG, Schneider BG, Lawrence MS, Noushmehr H, Malta TM, Cancer Genome Atlas N, Stuart JM, Benz CC, Laird PW. Cell-of-origin patterns dominate the molecular classification of 10,000 tumors from 33 types of cancer. *Cell*. 2018;173: 291-304 e296.
230. Taylor BS, Schultz N, Hieronymus H, Gopalan A, Xiao Y, Carver BS, Arora VK, Kaushik P, Cerami E, Reva B, Antipin Y, Mitsiades N, Landers T, Dolgalev I, Major JE, Wilson M, Socci ND, Lash AE, Heguy A, Eastham JA, Scher HI, Reuter VE, Scardino PT, Sander C, Sawyers CL, Gerald WL. Integrative genomic profiling of human prostate cancer. *Cancer Cell*. 2010;18: 11-22.
231. Zhang HY, Ma YD, Zhang Y, Cui J, Wang ZM. Elevated levels of autophagy-related marker ULK1 and mitochondrion-associated autophagy inhibitor LRPPRC are associated with biochemical progression and overall survival after androgen deprivation therapy in patients with metastatic prostate cancer. *J Clin Pathol*. 2017;70: 383-389.
232. Liu B, Miyake H, Nishikawa M, Tei H, Fujisawa M. Expression profile of autophagy-related markers in localized prostate cancer: Correlation with biochemical recurrence after radical prostatectomy. *Urology*. 2015;85: 1424-1430.
233. Egan DF, Chun MG, Vamos M, Zou H, Rong J, Miller CJ, Lou HJ, Raveendra-Panickar D, Yang CC, Sheffler DJ, Teriete P, Asara JM, Turk BE, Cosford ND, Shaw RJ. Small molecule inhibition of the autophagy kinase ULK1 and identification of ULK1 substrates. *Mol Cell*. 2015;59: 285-297.

234. Loffler AS, Alers S, Dieterle AM, Keppeler H, Franz-Wachtel M, Kundu M, Campbell DG, Wesselborg S, Alessi DR, Stork B. Ulk1-mediated phosphorylation of AMPK constitutes a negative regulatory feedback loop. *Autophagy*. 2011;7: 696-706.
235. White E, DiPaola RS. The double-edged sword of autophagy modulation in cancer. *Clin Cancer Res*. 2009;15: 5308-5316.
236. Mathew R, White E. Autophagy, stress, and cancer metabolism: What doesn't kill you makes you stronger. *Cold Spring Harb Symp Quant Biol*. 2011;76: 389-396.
237. Chhipa RR, Wu Y, Ip C. AMPK-mediated autophagy is a survival mechanism in androgen-dependent prostate cancer cells subjected to androgen deprivation and hypoxia. *Cell Signal*. 2011;23: 1466-1472.
238. White E. Deconvoluting the context-dependent role for autophagy in cancer. *Nat Rev Cancer*. 2012;12: 401-410.
239. Niture S, Ramalinga M, Kedir H, Patacsil D, Niture SS, Li J, Mani H, Suy S, Collins S, Kumar D. TNFAIP8 promotes prostate cancer cell survival by inducing autophagy. *Oncotarget*. 2018;9: 26884-26899.
240. Mortezaei A, Salemi S, Kranzbuhler B, Gross O, Sulser T, Simon HU, Eberli D. Inhibition of autophagy significantly increases the antitumor effect of abiraterone in prostate cancer. *World J Urol*. 2019;37: 351-358.
241. Zhao F, Huang W, Zhang Z, Mao L, Han Y, Yan J, Lei M. Triptolide induces protective autophagy through activation of the CaMKK beta-AMPK signaling pathway in prostate cancer cells. *Oncotarget*. 2016;7: 5366-5382.
242. Munkley J, Rajan P, Lafferty NP, Dalgliesh C, Jackson RM, Robson CN, Leung HY, Elliott DJ. A novel androgen-regulated isoform of the TSC2 tumour suppressor gene increases cell proliferation. *Oncotarget*. 2014;5: 131-139.
243. Solitro AR, MacKeigan JP. Leaving the lysosome behind: Novel developments in autophagy inhibition. *Future Med Chem*. 2016;8: 73-86.

244. Verbaanderd C, Maes H, Schaaf MB, Sukhatme VP, Pantziarka P, Sukhatme V, Agostinis P, Bouche G. Repurposing drugs in oncology (redo)-chloroquine and hydroxychloroquine as anti-cancer agents. *Ecancermedicalscience*. 2017;11: 781.
245. Zhang Y, Luo P, Leng P. Effect of autophagy inhibitor hydroxychloroquine on chemosensitivity of castration-resistant prostate cancer. *Sichuan Da Xue Xue Bao Yi Xue Ban*. 2019;50: 323-327.
246. Martin KR, Celano SL, Solitro AR, Gunaydin H, Scott M, O'Hagan RC, Shumway SD, Fuller P, MacKeigan JP. A potent and selective ULK1 inhibitor suppresses autophagy and sensitizes cancer cells to nutrient stress. *iScience*. 2018;8: 74-84.
247. Petherick KJ, Conway OJ, Mpamhanga C, Osborne SA, Kamal A, Saxty B, Ganley IG. Pharmacological inhibition of ULK1 kinase blocks mammalian target of rapamycin (mTOR)-dependent autophagy. *J Biol Chem*. 2015;290: 11376-11383.
248. Dite TA, Langendorf CG, Hoque A, Galic S, Rebello RJ, Ovens AJ, Lindqvist LM, Ngoei KRW, Ling NXY, Furic L, Kemp BE, Scott JW, Oakhill JS. AMP-activated protein kinase selectively inhibited by the type ii inhibitor SBI-0206965. *J Biol Chem*. 2018;293: 8874-8885.
249. Price DJ, Drewry DH, Schaller LT, Thompson BD, Reid PR, Maloney PR, Liang X, Banker P, Buckholz RG, Selley PK, McDonald OB, Smith JL, Shearer TW, Cox RF, Williams SP, Reid RA, Tacconi S, Faggioni F, Piubelli C, Sartori I, Tessari M, Wang TY. An orally available, brain-penetrant CaMKK2 inhibitor reduces food intake in rodent model. *Bioorg Med Chem Lett*. 2018;28: 1958-1963.
250. Asquith CRM, Godoi PH, Counago RM, Laitinen T, Scott JW, Langendorf CG, Oakhill JS, Drewry DH, Zuercher WJ, Koutentis PA, Willson TM, Kalogirou AS. 1,2,6-thiadiazinones as novel narrow spectrum calcium/calmodulin-dependent protein kinase kinase 2 (CaMKK2) inhibitors. *Molecules*. 2018;23.
251. Profeta GS, Dos Reis CV, Santiago ADS, Godoi PHC, Fala AM, Wells CI, Sartori R, Salmazo APT, Ramos PZ, Massirer KB, Elkins JM, Drewry DH, Gileadi O, Counago RM. Binding and

structural analyses of potent inhibitors of the human Ca(2+)/calmodulin dependent protein kinase kinase 2 (CaMKK2) identified from a collection of commercially-available kinase inhibitors. *Sci Rep.* 2019;9: 16452.

252. Sakamoto KM, Frank DA. CREB in the pathophysiology of cancer: Implications for targeting transcription factors for cancer therapy. *Clin Cancer Res.* 2009;15: 2583-2587.

253. Takemoto-Kimura S, Suzuki K, Horigane SI, Kamijo S, Inoue M, Sakamoto M, Fujii H, Bito H. Calmodulin kinases: Essential regulators in health and disease. *J Neurochem.* 2017;141: 808-818.

254. Thomson DM, Herway ST, Fillmore N, Kim H, Brown JD, Barrow JR, Winder WW. AMP-activated protein kinase phosphorylates transcription factors of the CREB family. *J Appl Physiol* (1985). 2008;104: 429-438.

255. de Alexandre RB, Horvath AD, Szarek E, Manning AD, Leal LF, Kardauke F, Epstein JA, Carraro DM, Soares FA, Apanasovich TV, Stratakis CA, Faucz FR. Phosphodiesterase sequence variants may predispose to prostate cancer. *Endocr Relat Cancer.* 2015;22: 519-530.

256. Penfold L, Woods A, Muckett P, Nikitin AY, Kent TR, Zhang S, Graham R, Pollard A, Carling D. CaMKK2 promotes prostate cancer independently of AMPK via increased lipogenesis. *Cancer Res.* 2018.

257. Xie F, Li BX, Xiao X. Design, synthesis and biological evaluation of regioisomers of 666-15 as inhibitors of CREB-mediated gene transcription. *Bioorg Med Chem Lett.* 2017;27: 994-998.

258. Li BX, Gardner R, Xue C, Qian DZ, Xie F, Thomas G, Kazmierczak SC, Habecker BA, Xiao X. Systemic inhibition of CREB is well-tolerated in vivo. *Sci Rep.* 2016;6: 34513.

259. Genua M, Pandini G, Sisci D, Castoria G, Maggiolini M, Vigneri R, Belfiore A. Role of cyclic amp response element-binding protein in insulin-like growth factor-i receptor up-regulation by sex steroids in prostate cancer cells. *Cancer Res.* 2009;69: 7270-7277.

260. Wang Q, Wang HX, Shen JY, Zhang R, Hong JW, Li Z, Chen G, Li MX, Ding Z, Li J, Zhang JP, Zhang MR, Xu LC. The anti-androgenic effects of cypermethrin mediated by non-classical

testosterone pathway activation of mitogen-activated protein kinase cascade in mouse sertoli cells. *Ecotoxicol Environ Saf.* 2019;177: 58-65.

261. Dejima T, Imada K, Takeuchi A, Shiota M, Leong J, Tombe T, Tam K, Fazli L, Naito S, Gleave ME, Ong CJ. Suppression of lim and SH3 domain protein 1 (LASP1) negatively regulated by androgen receptor delays castration resistant prostate cancer progression. *Prostate.* 2017;77: 309-320.

262. Li S, Fong KW, Gritsina G, Zhang A, Zhao JC, Kim J, Sharp A, Yuan W, Aversa C, Yang XJ, Nelson PS, Feng FY, Chinnaiyan AM, de Bono JS, Morrissey C, Rettig MB, Yu J. Activation of MAPK signaling by CXCR7 leads to enzalutamide resistance in prostate cancer. *Cancer Res.* 2019;79: 2580-2592.

263. Adelaiye-Ogala R, Gryder BE, Nguyen YTM, Alilin AN, Grayson AR, Bajwa W, Jansson KH, Beshiri ML, Agarwal S, Rodriguez-Nieves JA, Capaldo B, Kelly K, VanderWeele DJ. Targeting the PI3K/AKT pathway overcomes enzalutamide resistance by inhibiting induction of the glucocorticoid receptor. *Mol Cancer Ther.* 2020;19: 1436-1447.

264. Fu M, Rao M, Wu K, Wang C, Zhang X, Hessien M, Yeung YG, Gioeli D, Weber MJ, Pestell RG. The androgen receptor acetylation site regulates cAMP and AKT but not ERK-induced activity. *J Biol Chem.* 2004;279: 29436-29449.

265. Langendorf CG, O'Brien MT, Ngoei KRW, McAloon LM, Dhagat U, Hoque A, Ling NXY, Dite TA, Galic S, Loh K, Parker MW, Oakhill JS, Kemp BE, Scott JW. CaMKK2 is inactivated by cAMP-PKA signaling and 14-3-3 adaptor proteins. *J Biol Chem.* 2020;295: 16239-16250.

266. Chung S, Furihata M, Tamura K, Uemura M, Daigo Y, Nasu Y, Miki T, Shuin T, Fujioka T, Nakamura Y, Nakagawa H. Overexpressing PKIB in prostate cancer promotes its aggressiveness by linking between PKA and AKT pathways. *Oncogene.* 2009;28: 2849-2859.

267. Xu S, Zhou W, Ge J, Zhang Z. Prostaglandin E2 receptor EP4 is involved in the cell growth and invasion of prostate cancer via the cAMP-PKA/PI3K-AKT signaling pathway. *Mol Med Rep.* 2018;17: 4702-4712.

268. Huang B, Song BL, Xu C. Cholesterol metabolism in cancer: Mechanisms and therapeutic opportunities. *Nat Metab.* 2020;2: 132-141.
269. Kong Y, Cheng L, Mao F, Zhang Z, Zhang Y, Farah E, Bosler J, Bai Y, Ahmad N, Kuang S, Li L, Liu X. Inhibition of cholesterol biosynthesis overcomes enzalutamide resistance in castration-resistant prostate cancer (CRPC). *J Biol Chem.* 2018;293: 14328-14341.
270. Lemberger T, Parkitna JR, Chai M, Schutz G, Engblom D. CREB has a context-dependent role in activity-regulated transcription and maintains neuronal cholesterol homeostasis. *FASEB J.* 2008;22: 2872-2879.
271. Cui A, Ding D, Li Y. Regulation of hepatic metabolism and cell growth by the ATF/CREB family of transcription factors. *Diabetes.* 2021;70: 653-664.
272. Song YF, Xu YH, Zhuo MQ, Wu K, Luo Z. CREB element is essential for unfolded protein response (UPR) mediating the Cu-induced changes of hepatic lipogenic metabolism in chinese yellow catfish (*pelteobagrus fulvidraco*). *Aquat Toxicol.* 2018;203: 69-79.
273. Bleckmann SC, Blendy JA, Rudolph D, Monaghan AP, Schmid W, Schutz G. Activating transcription factor 1 and CREB are important for cell survival during early mouse development. *Mol Cell Biol.* 2002;22: 1919-1925.
274. Hummler E, Cole TJ, Blendy JA, Ganss R, Aguzzi A, Schmid W, Beermann F, Schutz G. Targeted mutation of the CREB gene: Compensation within the CREB/ATF family of transcription factors. *Proc Natl Acad Sci U S A.* 1994;91: 5647-5651.
275. Shanware NP, Zhan L, Hutchinson JA, Kim SH, Williams LM, Tibbetts RS. Conserved and distinct modes of CREB/ATF transcription factor regulation by PP2A/B56gamma and genotoxic stress. *PLoS One.* 2010;5: e12173.
276. Walker C, Mojares E, Del Rio Hernandez A. Role of extracellular matrix in development and cancer progression. *Int J Mol Sci.* 2018;19.
277. McClung CA, Nestler EJ. Regulation of gene expression and cocaine reward by CREB and deltaFosB. *Nat Neurosci.* 2003;6: 1208-1215.

278. Wang G, Jones SJ, Marra MA, Sadar MD. Identification of genes targeted by the androgen and PKA signaling pathways in prostate cancer cells. *Oncogene*. 2006;25: 7311-7323.
279. Tatti O, Gucciardo E, Pekkonen P, Holopainen T, Louhimo R, Repo P, Maliniemi P, Lohi J, Rantanen V, Hautaniemi S, Alitalo K, Ranki A, Ojala PM, Keski-Oja J, Lehti K. MMP16 mediates a proteolytic switch to promote cell-cell adhesion, collagen alignment, and lymphatic invasion in melanoma. *Cancer Res*. 2015;75: 2083-2094.
280. Shen Z, Wang X, Yu X, Zhang Y, Qin L. MMP16 promotes tumor metastasis and indicates poor prognosis in hepatocellular carcinoma. *Oncotarget*. 2017;8: 72197-72204.
281. Wu S, Ma C, Shan S, Zhou L, Li W. High expression of matrix metalloproteinases 16 is associated with the aggressive malignant behavior and poor survival outcome in colorectal carcinoma. *Sci Rep*. 2017;7: 46531.
282. Jiang C, Wang J, Dong C, Wei W, Li J, Li X. Membranous type matrix metalloproteinase 16 induces human prostate cancer metastasis. *Oncol Lett*. 2017;14: 3096-3102.
283. Cao L, Chen C, Zhu H, Gu X, Deng D, Tian X, Liu J, Xiao Q. MMP16 is a marker of poor prognosis in gastric cancer promoting proliferation and invasion. *Oncotarget*. 2016;7: 51865-51874.
284. Chang SS. Overview of prostate-specific membrane antigen. *Rev Urol*. 2004;6 Suppl 10: S13-18.
285. Administration USFD. FDA approves first psma-targeted pet imaging drug for men with prostate cancer2020.
286. Administration USFD. FDA approves second psma-targeted pet imaging drug for men with prostate cancer2021.
287. Kimura T, Takabatake Y, Takahashi A, Isaka Y. Chloroquine in cancer therapy: A double-edged sword of autophagy. *Cancer Res*. 2013;73: 3-7.

288. Lei Y, Yu T, Li C, Li J, Liang Y, Wang X, Chen Y, Wang X. Expression of CAMK1 and its association with clinicopathologic characteristics in pancreatic cancer. *J Cell Mol Med*. 2021;25: 1198-1206.
289. Leung JK, Sadar MD. Non-genomic actions of the androgen receptor in prostate cancer. *Front Endocrinol (Lausanne)*. 2017;8: 2.
290. Wang X, Cui H, Lou Z, Huang S, Ren Y, Wang P, Weng G. Cyclic AMP responsive element-binding protein induces metastatic renal cell carcinoma by mediating the expression of matrix metalloproteinase-2/9 and proteins associated with epithelial-mesenchymal transition. *Mol Med Rep*. 2017;15: 4191-4198.
291. Son J, Lee JH, Kim HN, Ha H, Lee ZH. cAMP-response-element-binding protein positively regulates breast cancer metastasis and subsequent bone destruction. *Biochem Biophys Res Commun*. 2010;398: 309-314.
292. Jiang M, Yan Y, Yang K, Liu Z, Qi J, Zhou H, Qian N, Zhou Q, Wang T, Xu X, Xiao X, Deng L. Small molecule nAS-E targeting cAMP response element binding protein (CREB) and CREB-binding protein interaction inhibits breast cancer bone metastasis. *J Cell Mol Med*. 2019;23: 1224-1234.
293. York B, Li F, Lin F, Marcelo KL, Mao J, Dean A, Gonzales N, Gooden D, Maity S, Coarfa C, Putluri N, Means AR. Pharmacological inhibition of CaMKK2 with the selective antagonist STO-609 regresses NAFLD. *Sci Rep*. 2017;7: 11793.
294. Racioppi L, Nelson ER, Huang W, Mukherjee D, Lawrence SA, Lento W, Masci AM, Jiao Y, Park S, York B, Liu Y, Baek AE, Drewry DH, Zuercher WJ, Bertani FR, Businaro L, Geradts J, Hall A, Means AR, Chao N, Chang CY, McDonnell DP. CaMKK2 in myeloid cells is a key regulator of the immune-suppressive microenvironment in breast cancer. *Nat Commun*. 2019;10: 2450.

Vita

Chenchu Lin was born in Fuzhou, Fujian, China. She attended the Affiliated High School of Fujian Normal University, Fujian, China in 2003. After graduating from high school in 2006, She attended the China Pharmaceutical University, China, graduating in 2010 with a Bachelor of Science degree in Basic Pharmaceutical Science Base Class and in 2013 with a Master of Science degree in Pharmacology. She then worked in Shanghai Institute of Materia Medica Chinese Academy of Sciences before she entered the University of Houston. In 2018, she transferred to The University of Texas MD Anderson Cancer Center UTHealth Graduate School of Biomedical Sciences.

Permanent address:

10310 Wylde Point Lane, Missouri City, TX